UNIVERZITA KARLOVA V PRAZE

PŘÍRODOVĚDECKÁ FAKULTA

KATEDRA EXPERIMENTÁLNÍ BIOLOGIE ROSTLIN

Studijní program: Anatomie a fyziologie rostlin

Mgr. Jan Fíla

Úloha fosforylace proteinů v progamické fázi vývoje samčího gametofytu tabáku

The role of protein phosphorylation during progamic phase of tobacco male gametophyte development

Disertační práce

Školitel: doc. RNDr. David Honys, Ph.D.

Praha 2016

Prohlášení:

Prohlašuji, že jsem závěrečnou práci zpracoval samostatně a že jsem uvedl všechny použité informační zdroje a literaturu. Tato práce ani její podstatná část nebyla předložena k získání jiného nebo stejného akademického titulu.

V Praze, 17.5.2016

…………………………………………

Mgr. Jan Fíla

Prohlášení školitele o podílu na publikacích:

Jménem spoluautorů souhlasím s tím, že uvedené publikace jsou součástí této disertační práce. Publikace vznikly kolektivním úsilím uvedených autorů, přičemž podíl Mgr. Jana Fíly na uvedených publikacích je specifikován níže.

V Praze, 17.5.2016

……………………………………………

doc. RNDr. David Honys, Ph.D.

Poděkování

Na tomto místě bych chtěl poděkovat svému školiteli doc. RNDr. Davidu Honysovi, Ph.D. za vedení a diskuse v průběhu celého studia. Velké díky patří RNDr. Věře Čapkové, CSc., se kterou mi bylo přáno několik let provádět experimenty a naučit se od ní spousty dovedností. RNDr. Nikoletě Dupľákové, Ph.D. bych chtěl poděkovat za naučení se základním laboratorním návykům během mých prvních experimentů konaných v rámci projektu Otevřená věda a v průběhu mého bakalářského studia. V neposlední řadě bych rád poděkoval Saidu Hafidhovi, Ph.D., kterému vděčím za možnost práce se sekretomickými daty a za mnohé diskuse v průběhu přípravy textu této disertační práce. Díky patří i zbývajícím členům Laboratoře biologie pylu za to, že vytvářeli tvůrčí a příjemné prostředí po celou dobu studia.

Dále bych chtěl poděkovat našim dvěma partnerským německým laboratořím, které se podílely na hmotnostně-spektrometrické identifikaci fosfopeptidů. Prvně jde o Skupinu aplikované biochemie z IPK v Gaterslebenu pod vedením Dr. Hanse-Petera Mocka. Z této skupiny patří velké díky Dr. Andree Matros za poskytnutí tabákových sekvenčních databází a pomoc s analýzou fosfoproteomických dat. Druhými německými spolupracovníky jsou Dr. René Peiman Zahedi a Sonja Radau z ISAS v Dortmundu, kterým děkujeme za obohacení vzorků o fosfopeptidy a identifikaci fosforylovaných peptidů pomocí hmotnostní spektrometrie.

V neposlední řadě patří poděkování mé manželce Markétě, která mi byla oporou v průběhu celého studia i v době psaní disertační práce.

Abstrakt

Zralý pyl tabáku obsahuje silně dehydratovanou cytoplazmu a je metabolicky neaktivní. Po rehydrataci cytoplazmy je jeho metabolizmus nastartován a po dokončení aktivace vyrůstá pylovou aperturou pylová láčka. Změny v zavodnění cytoplazmy spolu s nastartováním metabolizmu jsou doprovázeny regulací translace i post-translačních modifikací (zejména fosforylace) přítomných proteinů. V této disertační práci jsou prezentovány fosfopeptidy ze zralého pylu tabáku virginského *(Nicotiana tabacum)*, pylu aktivovaného *in vitro* 5 min a pylu aktivovaného *in vitro* 30 min. Z každého stádia byl získán celkový proteinový extrakt, jenž byl naštěpen trypsinem a získaná peptidová směs byla obohacena metodou MOAC (afinitní chromatografie s využitím kovového oxidu/hydroxidu) s matricí z oxidu titaničitého. Fosfopeptidy v obohaceném eluátu byly identifikovány kapalinovou chromatografií v kombinaci s tandemovou hmotnostní spektrometrií (LC–MS/MS).

Celkem bylo identifikováno 471 fosfopeptidů, nesoucích 432 přesně lokalizovaných fosforylačních míst. Získané fosfopeptidy pocházely z 301 fosfoproteinů, které spadaly do třinácti funkčních kategorií. Převládajícími funkcemi se staly transkripce, syntéza proteinů, cílení a skladování proteinů a přenos signálu. Mnohé fosfopeptidy podléhaly koncentračním změnám mezi třemi studovanými stádii samčího gametofytu; 209 regulovaných fosforylovaných peptidů vykázalo sedm regulačních trendů, z nichž většina patřila do skupiny zahrnující fosfopeptidy identifikované exkluzivně ve zralém pylu. Navíc bylo v získaném fosfoproteomickém datovém souboru nalezeno pět kinázových motivů obsahujících fosforylovaný serin a jeden fosfothreoninový motiv. V pylovém proteomu a v sekretomu pylových láček tabáku pak byly vyhledány kinázy, jež mají podle predikce rozpoznávat nalezené sekvenční motivy.

Souhrnně vzato se jedná o první fosfoprotemickou studii aktivovaného pylu krytosemenných rostlin (Angiospermae) a o studii značně rozšiřující identifikovanou část fosfoproteomu zralého pylu tabáku virginského *(Nicotiana tabacum)*.

Klíčová slova: samčí gametofyt, aktivace pylu, oxid titaničitý, obohacování o fosfopeptidy, fosfoproteomika, kináza, fosforylační motiv

Abstrakt v angličtině (English abstract)

Tobacco male gametophyte has a strongly dehydrated cytoplasm and represents a metabolically inactive stage. Upon cytoplasm rehydration, pollen grain becomes metabolically active and after the activation is finished, the pollen tube growth through a selected pollen aperture starts. The rehydration together with metabolic activation are accompanied by the regulation of translation and post-translational modifications (mainly phosphorylation) of the existing proteins. In this Ph.D. thesis, there were identified phosphopeptides from tobacco *(Nicotiana tabacum)* mature pollen, pollen activated *in vitro* 5 min and pollen activated *in vitro* 30 min. The total proteins from the above male gametophyte stages were extracted. The protein extract was trypsinized and the acquired peptide mixture was enriched by MOAC (metal oxide/hydroxide affinity chromatography) with titanium dioxide matrix. The enriched fraction was subjected to liquid chromatography coupled with tandem mass spectrometry (LC–MS/MS).

Totally, there were identified 471 phosphopeptides, carrying 432 exactly localized phosphorylation sites. The acquired peptide identifications were mapped to 301 phosphoproteins that were placed into 13 functional categories, dominant of which were transcription, protein synthesis, protein destination and storage, and signal transduction. Notable part of phosphorylated peptides were shown to be regulated during pollen activation; 209 regulated phosphorylated peptides were listed into seven groups based on their regulatory trends, majority of which were identified exclusively in mature pollen. Moreover, there were found five phosphorylation motifs with a central phosphoserine and one phosphothreonine motif, which were predicted to be recognized by several kinase families. The members of these kinase families were then found in tobacco pollen proteome and pollen tube secretome.

Collectively, this Ph.D. thesis represents the first phosphoproteomic study of any angiosperm (Angiospermae) activated pollen, and notably broadens the identified part of tobacco *(Nicotiana tabacum)* male gametophyte phosphoproteome.

Key words: male gametophyte, pollen activation, titanium dioxide, phosphopeptide enrichment, phosphoproteomics, kinase, phosphorylation motif

Seznam použitých zkratek

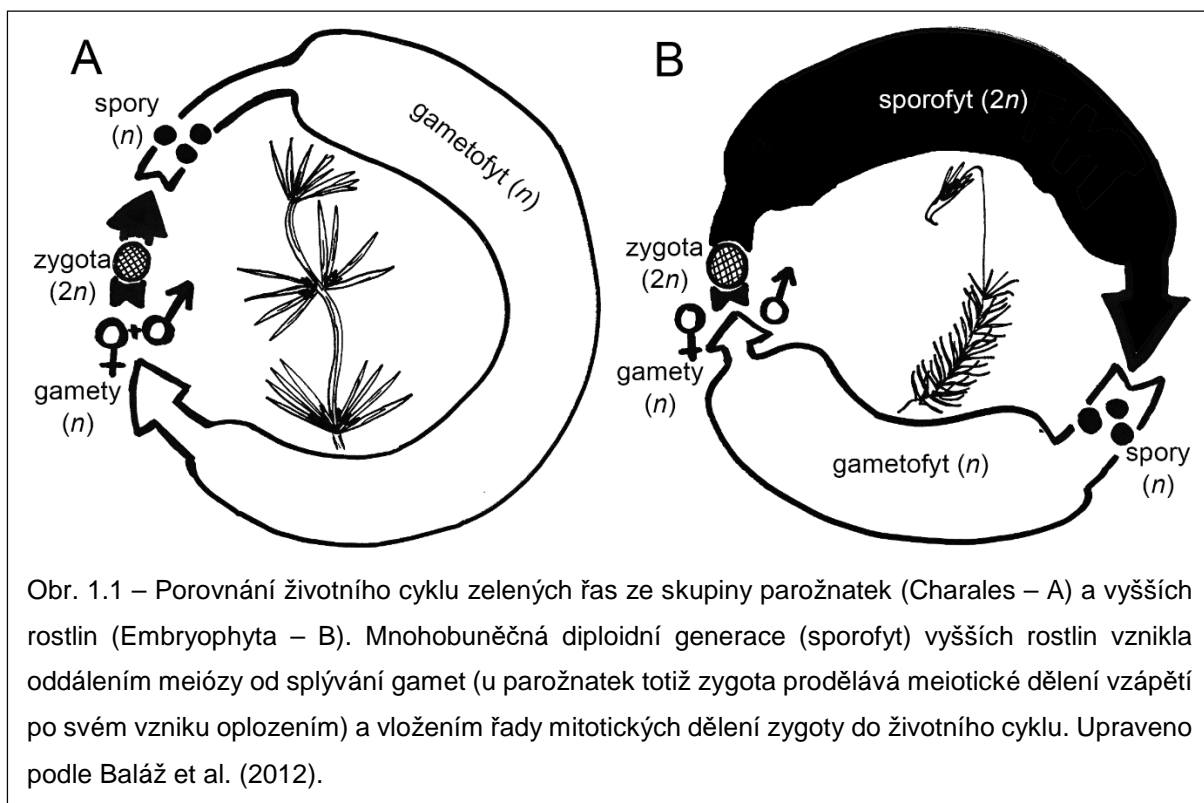|	
2D DIGE	– dvojrozměrná diferenční gelová elektroforéza
2D IEF–PAGE	– dvojrozměrná proteinová elektroforéza kombinující isoelektrickou fokusaci a polyakrylamidovou gelovou elektroforézu
CAMK2	– Ca^{2+}/kalmodulin-dependentní proteinová kináza 2
CDK	– cyklin-dependentní proteinová kináza
CDPK–SnRK	– Ca^{2+}-dependentní proteinové kinázy–příbuzné kinázám nefermentujícím sacharózu (angl. Ca^{2+}-dependent protein kinase–sucrose-non-fermenting-related kinase)
CK2	– kaseinová kináza 2
EDTA	– kyselina ethylendiamintetraoctová
EPP	– EDTA/puromycin-rezistentní částice
EST	– *angl.* expressed sequence tag
HILIC	– chromatografie s hydrofilními interakcemi
IDA	– kyselina iminodioctová
IMAC	– chelatační afinitní chromatografie
MAPK	– mitogenem aktivovaná proteinová kináza
MOAC	– afinitní chromatografie s využitím kovového oxidu/hydroxidu
NTA	– kyselina nitrilotrioctová
PMI	– pylová mitóza I
PMII	– pylová mitóza II
SAX	– aniontová ionexová chromatografie
SCX	– kationtová ionexová chromatografie
SDS–PAGE	– polyakrylamidová gelová elektroforéza v přítomnosti dodecylsíranu sodného
SIMAC	– postupná eluce metody IMAC (*angl.* sequentional elution from IMAC)

Obsah

1. Úvod do problematiky

1.1. Evoluce životního cyklu rostlin (Archaeplastida)

Rozmnožování je jednou z význačných vlastností živých organizmů na Zemi. Pro rozmnožování rostlin (Archaeplastida) je typické střídání pohlavní a nepohlavní generace, tzv. rodozměna (metageneze). Tato kapitola se bude dále věnovat zeleným rostlinám (Viridiplantae), mezi něž se řadí klasické zelené řasy (Chlorophyta) a vyšší rostliny společně s parožnatkami a příbuznými zelenými řasami (Streptophyta). Původně nejspíše trávily zelené řasy (např. parožnatky – Charales; viz Haig, 2010), které jsou předky vyšších rostlin (Embryophyta), většinu svého životního cyklu v podobě haploidního gametofytu (viz Qiu et al., 2012). Dospělá řasa (tedy gametofyt) tvoří mitotickým dělením haploidní gamety, na rozdíl od živočichů, u kterých se vytvářejí gamety meiotickým dělením. Splynutím rostlinných gamet vzniká diploidní zygota. V případě parožnatek nepodléhá zygota žádnému mitotickému dělení, ale naopak ihned dává vzniknout meiotickým dělením čtyřem haploidním sporám. Ze spor pak vyrůstá další generace haploidního gametofytu (zahrnující mimo jiné dospělou řasu) a celý životní cyklus se opakuje. Diploidní vícebuněčná generace pak v evoluci nejspíše vznikla

Obr. 1.1 – Porovnání životního cyklu zelených řas ze skupiny parožnatek (Charales – A) a vyšších rostlin (Embryophyta – B). Mnohobuněčná diploidní generace (sporofyt) vyšších rostlin vznikla oddálením meiózy od splývání gamet (u parožnatek totiž zygota prodělává meiotické dělení vzápětí po svém vzniku oplozením) a vložením řady mitotických dělení zygoty do životního cyklu. Upraveno podle Baláž et al. (2012).

oddálením meiózy od splývání gamet, zygota tak podstupuje řadu mitotických dělení a takto vzniklé diploidní buňky pak společně dávají vzniknout diploidnímu mnohobuněčnému sporofytu (viz Qiu et al., 2012; Obr. 1.1).

V případě mechů (Bryophyta *sensu stricto*), játrovek (Marchantiophyta) a hlevíků (Anthocerotophyta) zůstává gametofyt dominující generací životního cyklu, na němž je výživou závislý diploidní sporofyt. Sporofyt hlevíků se však od nezeleného sporofytu mechů a játrovek liší. Za povšimnutí stojí samotná velikost sporofytu hlevíků, který dosahuje téměř takové velikosti jako jejich gametofyt. Kromě toho jsou sporofyty hlevíků zelené a fotosyntetizují, dokonce byl prokázán přenos asimilátů ze sporofytu do gametofytu (Stewart a Rodgers, 1977). Hlevíky by se tak s jistou měrou nadsázky daly označit za první rostlinnou skupinu, kde dochází k jisté redukci gametofytu a nabývání velikosti a životaschopnosti sporofytu. S touto hypotézou by krásně souzněly evoluční stromy, z nichž plyne, že hlevíky by měly být sesterskou skupinou cévnatých rostlin (Tracheophyta) (Qiu et al., 2006; Chang a Graham, 2011). Nicméně takovéto příbuzenské vztahy mezi hlevíky a cévnatými byly některými autory recentně zpochybněny (Liu et al., 2014; Wickett et al., 2014), takže na definitivní rozuzlení příbuzenských vztahů mezi mechy, játrovkami a hlevíky si ještě budeme muset počkat (viz Villarreal a Renzaglia, 2015).

Sporofyt se dočkal své samostatnosti až u cévnatých rostlin (Tracheophyta). U přesliček a kapradin (Monilophyta) spolu s plavuněmi (Lycophyta) již sporofyt v životním cyklu dominuje, nicméně gametofyt zpravidla zůstává zachován jako samostatná generace, často bývá zelený, autotrofní, i když u některých skupin je mykotrofní (viz Qiu et al., 2012). Za zmínku stojí vranečky (Selaginella), kde došlo ke značné redukci samčího i samičího gametofytu; vranečky totiž mají gametofyty odděleného pohlaví na rozdíl od ostatních plavuní, jež mají oboupohlavný gametofyt. Gametofyty vranečků se zpravidla vyvíjejí uvnitř spory, jejíž obal praská až v době zralosti gametofytů (viz Schulz et al., 2010). U semenných rostlin (Spermatophyta) se gametofyt již stává zcela závislým na sporofytu a postupně dochází k jeho značné redukci. Zatímco u nahosemenných (Gymnospermae) samičí gametofyt sestává z několika tisíc buněk a samčí ze 4–40, u krytosemenných (Angiospermae) nejčastěji zbylo ze samičího gametofytu pouhých osm buněk a tři buňky ze samčího gametofytu (viz Qiu et al., 2012).

1.2. Životní cyklus krytosemenných rostlin (Angiospermae)

V této kapitole bude detailněji rozebrán životní cyklus krytosemenných rostlin (Angiospermae), protože se mezi ně řadí mimo jiné modelový tabák virginský *(Nicotiana tabacum)*, na němž byla provedena většina experimentů, zahrnutých do této disertační práce (Obr. 1.2).

Začněme dospělými rostlinami, které náleží k diploidnímu sporofytu. Generativním orgánem rostlin je květ, jenž bývá tvořen květními obaly spolu s tyčinkami a pestíky. Krytosemenné rostliny mají obvykle jak spory, tak gametofyty a potažmo gamety odděleného pohlaví.

Nejprve se zaměřme na vývoj **samičích spor a gametofytu**, podívejme se tedy do nitra semeníku, spodní části pestíku, v níž jsou uložena vajíčka (Obr. 1.3). Na úvod je vhodné
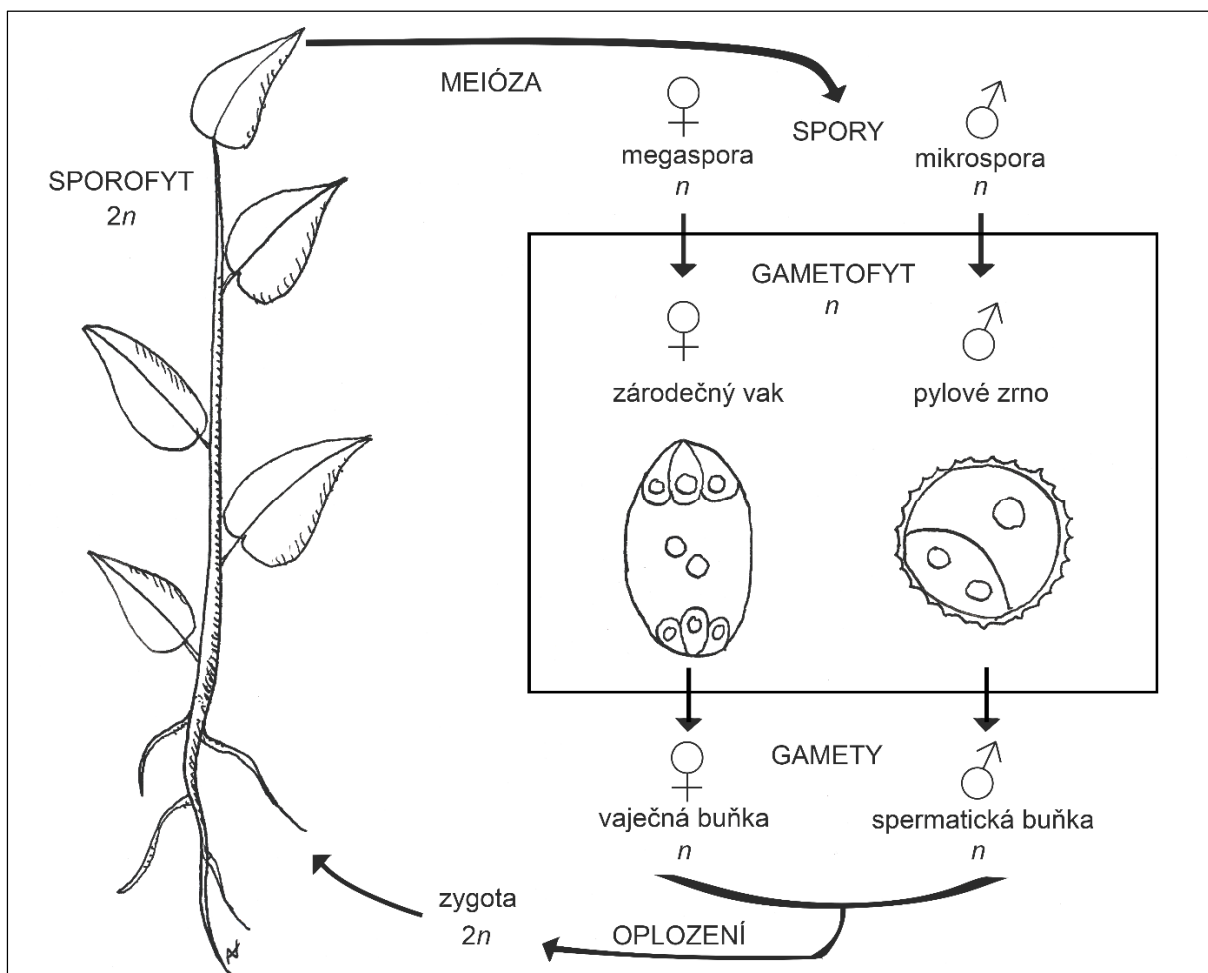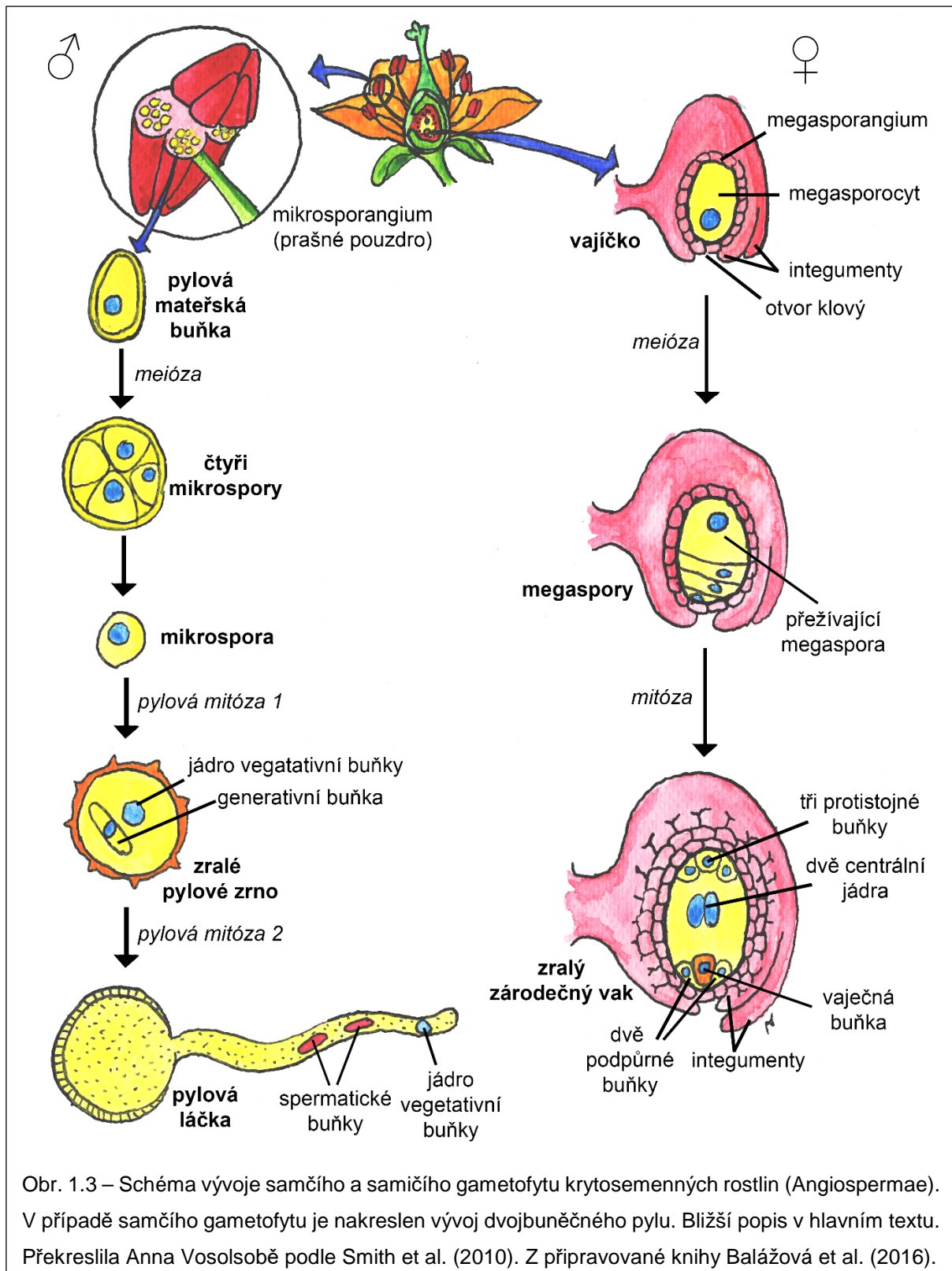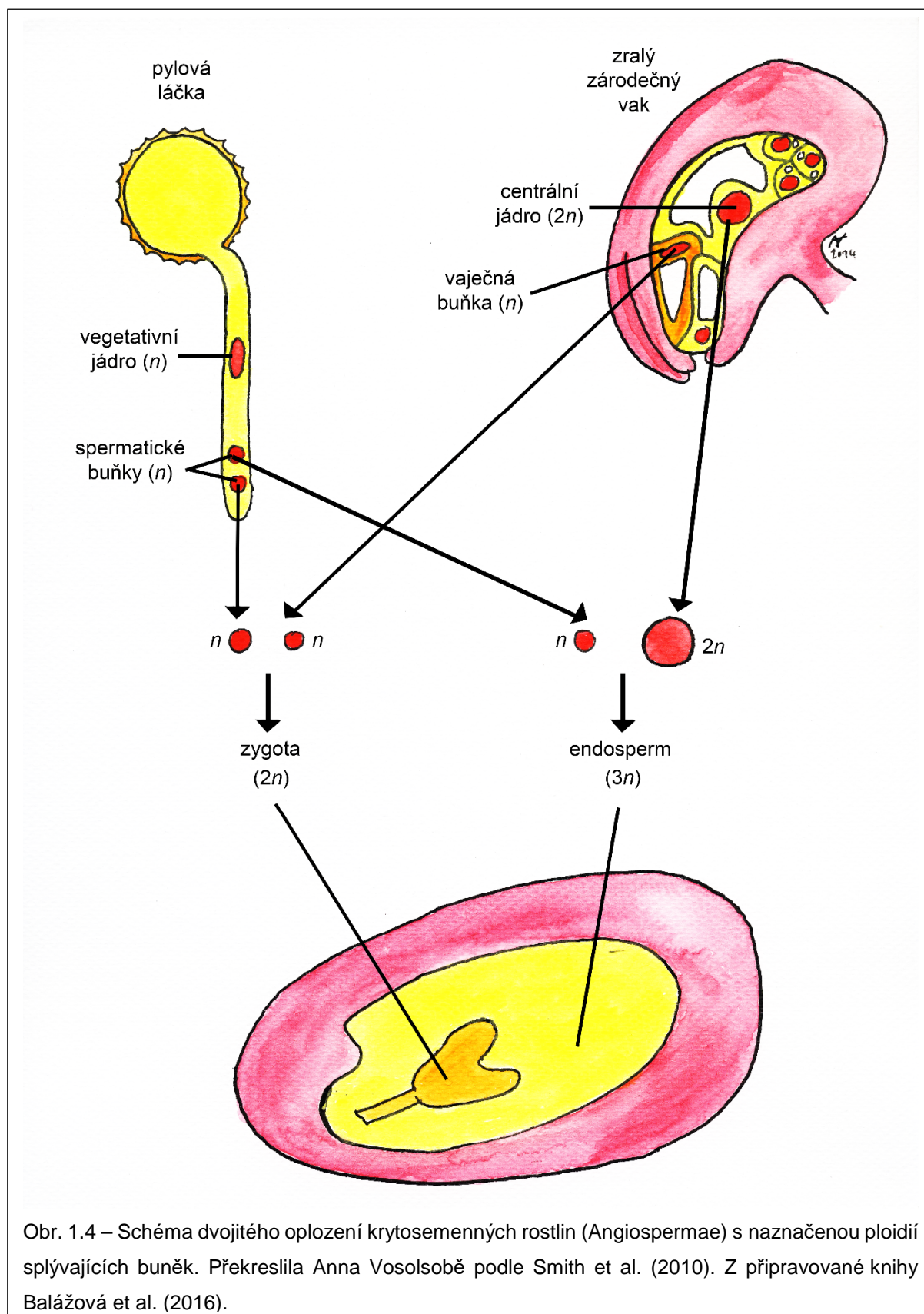

Obr. 1.2 – Schéma životního cyklu krytosemenných rostlin (Angiospermae). Diploidní fáze gametofytu je označena jako *2n*, zatímco haploidní fáze nese označení *n*. Překreslila Anna Vosolsobě podle Smith et al. (2010). Z připravované knihy Balážová et al. (2016).

připomenout, že rostlinné vajíčko není samotnou gametou, jak je tomu u živočichů, nýbrž mnohobuněčnou strukturou, z níž samotná gameta (u rostlin zvaná vaječná buňka) teprve vznikne. Vajíčko, vyplněné základním pletivem (zvaným nucellus), je obklopeno dvěma obaly, integumenty (viz Huang a Russell, 1992). Integumenty však vajíčko neobalují po celém obvodu, na jednom pólu vajíčka bývá otvor klový (mikropyle). Vraťme se ale k samotnému vzniku vajíčka; z buňky nucellu se diferencuje stále ještě diploidní megasporocyt (někdy také označovaný jako mateřská buňka zárodečného vaku), který je podroben meióze, při níž vznikají čtyři haploidní megaspory (viz Christensen et al., 1998). Zpravidla tři z nich procházejí apoptózou a dále se vyvíjí jen jediná. Vyvolená megaspora se dále vyvíjí za vzniku samičího gametofytu; prochází mitotickými děleními, která nejsou bezprostředně následována vznikem buněčných stěn. Dojde tedy nejprve k rozdělení původního jádra na osm a až následně dochází k oddělení jednotlivých buněk, jichž je ale pouze sedm (viz Christensen et al., 1998; Drews a Yadegari, 2002). Tato sedmibuněčná struktura s osmi jádry je samičí gametofyt, jenž se u krytosemenných častěji nazývá zárodečný vak. Uvnitř zárodečného vaku nalezneme samičí gametu (vaječnou buňku), obklopenou dvěma synergidami. Proti těmto buňkám jsou umístěny tři antipody a uprostřed se nachází centrální jádro zárodečného vaku, jež vzniká splynutím dvou původně haploidních jader, tudíž je diploidní (viz Drews a Yadegari, 2002). Tento typ zárodečného vaku se nazývá Polygonum, na počest rdesna, u něhož byl prvně objeven. Jedná se o nejrozšířenější typ zárodečného vaku u krytosemenných, jenž se vyskytuje u asi 70 % rostlinných druhů, včetně tabáku virginského (Enaleeva, 1997). Existuje však několik alternativních typů vývoje zárodečného vaku, které vedou k jinému počtu a uspořádání jader ve zralém zárodečném vaku (viz Reiser a Fischer, 1993).

Ponechme nyní zralý zárodečný vak i s připravenou samičí gametou (vaječnou buňkou) stranou a podívejme se do nitra prašníků, kde dochází k vývoji **samčích spor a posléze gametofytu** (viz McCormick, 1993; Obr. 1.3). Ze sporofytního pletiva se diferencují dvě iniciály – tapetální iniciála, jejíž dělením vzniká vyživovací pletivo pylových zrn (tapetum) a mikrosporycyt (též zvaný pylová mateřská buňka; viz McCormick, 1993). Diploidní mikrosporocyty se meioticky dělí za vzniku tetrády mikrospor (viz Borg a Twell, 2010). Tetrády jsou zprvu propojeny kalózou a k jejich uvolnění napomáhají enzymy uvolněné z tapeta (viz McCormick, 1993). Uvolněné mikrospory se zvětšují, utvářejí se v nich vakuoly a jejich jádro putuje k periferii buňky. Nastává čas na první mitotické dělení, zvané pylová mitóza I (PMI). Toto dělení je typické svojí asymetrií – dochází ke vzniku velké buňky vegetativní a

menší buňky generativní (viz Borg a Twell, 2010). Pro vznik funkčních pylových zrn je správný průběh pylové mitózy I klíčový, při jejím narušení u huseníčku rolního, například u mutantů *gemini pollen 1* (Park et al., 1998) nebo *two-in-one* (Oh et al., 2005), dochází k vážným feno-

Obr. 1.3 – Schéma vývoje samčího a samičího gametofytu krytosemenných rostlin (Angiospermae). V případě samčího gametofytu je nakreslen vývoj dvojbuněčného pylu. Bližší popis v hlavním textu. Překreslila Anna Vosolsobě podle Smith et al. (2010). Z připravované knihy Balážová et al. (2016).

pylová láčka

zralý zárodečný vak

centrální jádro (2n)

vaječná buňka (n)

vegetativní jádro (n)

spermatické buňky (n)

n n

n 2n

zygota (2n)

endosperm (3n)

Obr. 1.4 – Schéma dvojitého oplození krytosemenných rostlin (Angiospermae) s naznačenou ploidií splývajících buněk. Překreslila Anna Vosolsobě podle Smith et al. (2010). Z připravované knihy Balážová et al. (2016).

typovým projevům. Malá generativní buňka je po PMI následně obklopena větší buňkou vegetativní a dostává se do jejího nitra. Jádro vegetativní buňky obsahuje rozvolněný chromatin a buněčný cyklus opouští v G1 fázi, oproti tomu generativní buňka s kondenzovaným chromatinem prochází ještě jedním mitotickým dělením (zvaným pylová mitóza II; PMII) za vzniku dvou buněk spermatických, které jsou samčími gametami. Pylová mitóza II může probíhat ještě před vznikem zralých pylových zrn, pak bude zralý pyl trojbuněčný, nebo k ní může docházet až po vyklíčení pylu na blizně a zralý byl tak bude tvořen pouhými dvěma buňkami. Dvojbuněčný pyl je uvolňován zástupci asi 70 % rostlinných čeledí, mimo jiné tabákem virginským *(Nicotiana tabacum)* a ostatními lilkovitými *(Solanaceae)* a liliovitými *(Liliaceae*; Brewbaker, 1967). Naopak trojbuněčný pyl nalezneme u zbývajících zástupců krytosemenných, příkladně u huseníčku rolního *(Arabidopsis thaliana)* a ostatních brukvovitých *(Brassicaceae)* a lipnicovitých *(Poaceae*; Brewbaker, 1967). Za evolučně původní znak krytosemenných bývá považován dvojbuněčný pyl s tím, že ke vzniku trojbuněčného pylu došlo několikrát nezávisle na sobě. Nedávno bylo ale zjištěno, že se určité rostlinné druhy navrátily od tvorby trojbuněčného pylu zpět k dvojbuněčnému pylu (Williams et al., 2014). Cytoplazma zralého pylu je silně dehydratovaná a pyl je v metabolicky klidovém stádiu. Zpravidla obsahuje více dehydratovanou cytoplazmu dvojbuněčný pyl, díky čemuž je méně připravený k nastartování růstu pylové láčky než trojbuněčný pyl. Naopak trojbuněčná pylová zrna jsou méně dehydratovaná a rychleji z nich vyrůstají pylové láčky (Brewbaker, 1967).

Po dopadu na papilární buňky blizny (tedy opylení) se pylová cytoplazma zavodňuje a dochází k aktivaci pylu, v prostředí *in vitro* trvaly tyto procesy minimálně 21 minut od vystavení pylu růstovému médiu. Během této doby ještě nedocházelo k růstu pylové láčky, ale docházelo pouze k rehydrataci a aktivaci pylu (Vogler et al., 2015). Po aktivaci začne pylová láčka klíčit jednou z pylových apertur a prorůstá bliznou dále k semeníku. K počátku klíčení dochází po 24 minutách od počátku pylové aktivace (Vogler et al., 2015). Pylová láčka vzniká z vegetativní buňky a během svého růstu oboustranně komunikuje s vodícími pletivy čnělky (Hafidh et al., 2014). Úkolem pylové láčky je dopravit obě spermatické buňky (tedy samčí gamety) do zárodečného vaku. Zde dochází ke splynutí jedné spermatické buňky s vaječnou buňkou, čímž vzniká diploidní zygota, jež představuje počátek další sporofytické generace (Obr. 1.4). Druhá spermatická buňka splývá s centrálním jádrem zárodečného vaku, čímž je utvořen základ triploidního vyživovacího pletiva (endospermu, Obr. 1.4). Vzhledem k tomu, že
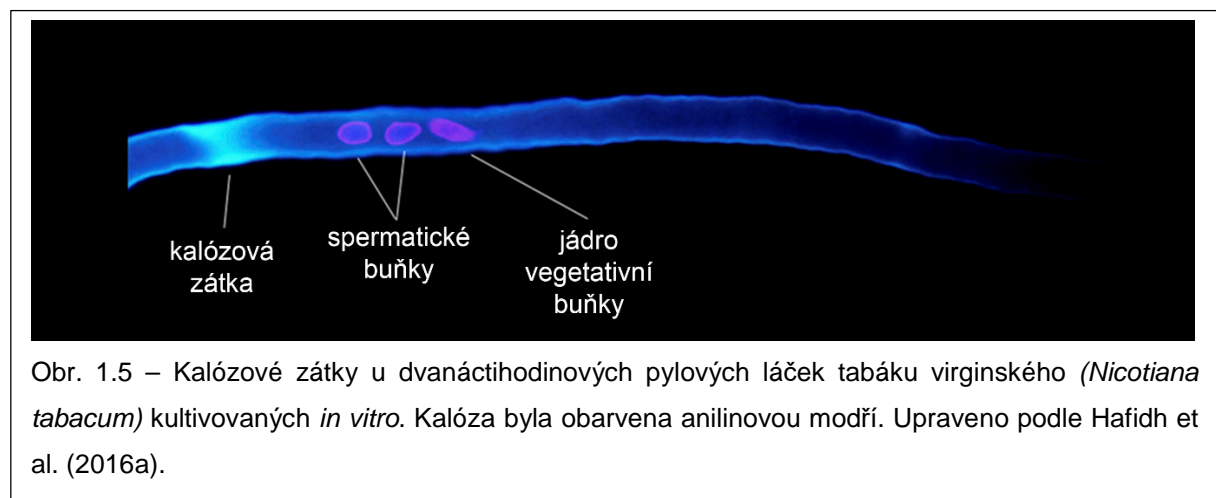
pro zdárný vznik zygoty a vyživovacího pletiva jsou zapotřebí dvě splynutí buněk, hovoříme u krytosemenných o tzv. dvojitém oplození (viz Raghavan, 2003).

Po oplození se z vajíčka s oplozeným zárodečným vakem vyvíjí semeno, uvnitř něhož dochází k vývoji embrya a vyživovacího pletiva (endospermu) a u některých rostlin navíc zůstávají zachovány buňky nucellu, jež se také podílejí na výživě embrya. Vyživovací pletivo odvozené z nucellu se pak nazývá perisperm. Při zrání semene je embryo v klidovém stavu a vyčkává na příhodné podmínky, aby mohlo vyklíčit a dát vzniknout nové dospělé rostlině, tedy další generaci sporofytu, v jehož květech se celý cyklus opakuje.

1.3. Aktivace pylu a její regulace

Vraťme se nyní k aktivaci pylu a počáteční fázi růstu pylové láčky. Jak již bylo zmíněno výše, zralý pyl je klidovým stádiem vývoje samčího gametofytu. Vzhledem k tomu, že je jeho úkolem přenést genetickou informaci vnějším prostředím (mnohdy nepříliš příznivým), obsahuje dehydratovanou cytoplazmu, je obklopen pevnou buněčnou stěnou a je metabolicky neaktivní.

Po dopadu na bliznu dochází k rehydrataci pylové cytoplazmy, aktivaci pylu a posléze k růstu pylové láčky. Dvojbuněčný a trojbuněčný pyl se liší v rychlosti nastartování růstu pylové láčky a v tom, do jaké míry spoléhají v počáteční fázi růstu na zásoby živin uložených ve zralém pylu (Mulcahy a Mulcahy, 1988). Růst pylové láčky u rostlin se zralým dvojbuněčným pylem sestává ze dvou fází: první část růstu je pomalejší a netvoří se při ní kalózové zátky. Naopak druhá fáze zahrnuje tvorbu kalózových zátek a růst pylové láčky probíhá rychleji (Obr. 1.5). V první fázi byly k růstu využity živiny z pylového zrna, zatímco

Obr. 1.5 – Kalózové zátky u dvanáctihodinových pylových láček tabáku virginského *(Nicotiana tabacum)* kultivovaných *in vitro*. Kalóza byla obarvena anilinovou modří. Upraveno podle Hafidh et al. (2016a).

druhá fáze využívá výživy z čnělky. Oproti tomu trojbuněčný pyl začne nedlouho po dopadu na blizmu růst rychleji, k čemuž využívá živin z čnělky od samotného počátku svého růstu.

Růst pylové láčky není isodiametrický, ale podobně jako u kořenových vlásků, houbových hyf a obratlovčích neuronů je vrcholový (viz Palanivelu a Preuss, 2000; Šamaj et al., 2006). Dochází tedy pouze k prodlužování vegetativní buňky, k jejímu dalšímu buněčnému dělení v průběhu růstu pylové láčky nedochází. Nejdelší pylové láčky dosahují úctyhodných 50 centimetrů (Mascarenhas, 1993). Vrcholový růst závisí na následujících buněčných mechanizmech: správné orientaci cytoskeletálních vláken, transportu sekretorických váčků, signalizaci pomocí malých GTPáz a tvorbě iontových gradientů (viz Palanivelu a Preuss, 2000; Šamaj et al., 2006).
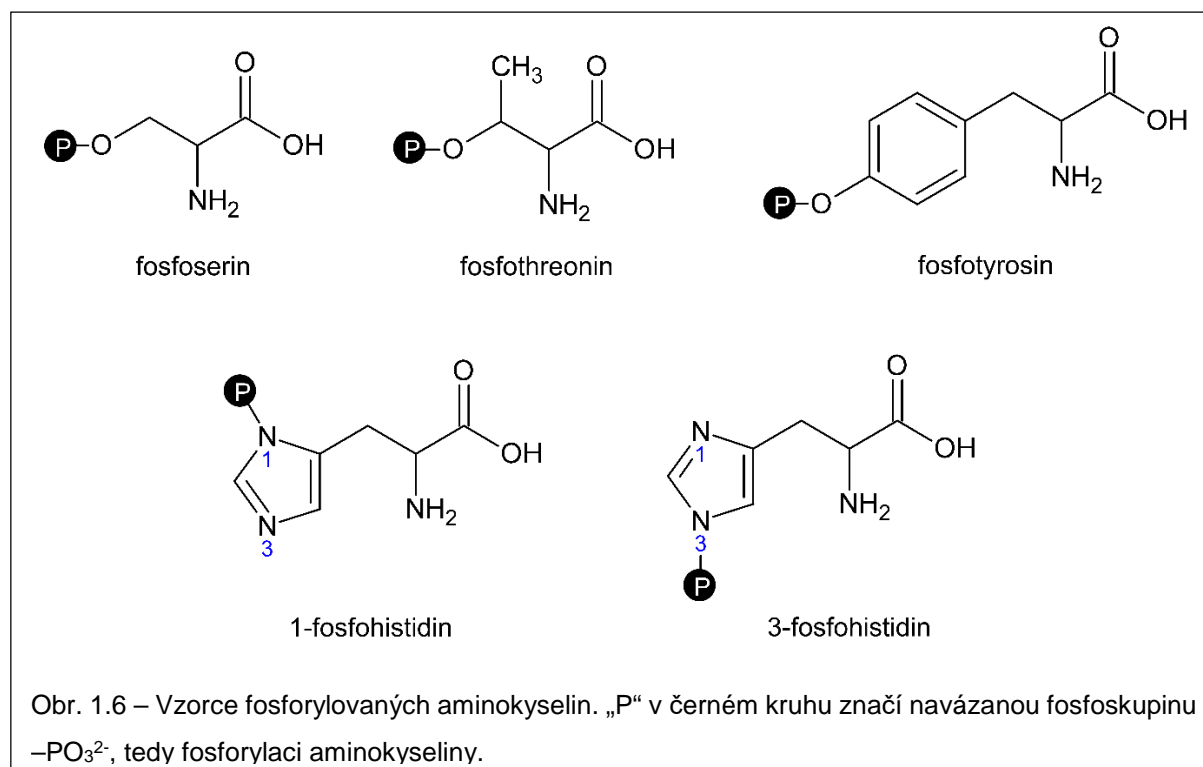
Kromě toho je aktivace zralého pylu modelem pro studium translačních regulací. U tabáku byla transkripce detekována pouze během několika prvních hodin růstu pylové láčky, tudíž se původně došlo k závěru, že růst pylové láčky je životně závislý na translaci, ale téměř nezávislý na transkripci (Čapková et al., 1988). Nedávno však byly objeveny transkripty, které byly nově syntetizovány i po čtyřiadvacetihodinové kultivaci pylových láček *in vitro* (Hafidh et al., 2012a; 2012b; 2016a). Značné množství regulovaných transkriptů, které jsou v pylových zrnech skladovány, jsou uskladněny v translačně neaktivních EDTA/puromycin-rezistentních částicích (angl. EDTA/puromycine-resistant particles; EPPs; Honys et al., 2000). V EPP komplexech byly nalezeny mRNA, rRNA i celé ribosomální podjednotky spolu s celou řadou proteinů regulujících translaci přítomných transkriptů (Honys et al., 2009). Skladované transkripty jsou připraveny ve zralém pylu, aby v rostoucí pylové láčce byla ukončena jejich represe a mohlo dojít k jejich translaci. Regulace genové exprese ve stádiu translace umožňuje pružněji reagovat na růstové signály v souvislostí s nastartováním růstu pylové láčky. Kromě správného načasování startu translace skladovaných mRNA, je nutná i správná lokalizace syntézy těchto proteinů, a tou je vrchol pylové láčky. EPP komplexy jsou tudíž v průběhu růstu dopravovány nejspíše právě směrem k vrcholu pylové láčky (Honys et al., 2009). Podobné částice obsahující skladované transkripty byly objeveny například v embryích ježovky (Spirin a Nemer, 1965) nebo v savčích neuronech (Carson a Barbarese, 2005).

Translace však není jedinou úrovní genové exprese, při níž dochází v rostoucích pylových láčkách k regulaci. Proteiny jsou regulovány mimo jiné posttranslačními modifikacemi. K nejdynamičtějším modifikacím využívaným k regulaci funkce proteinů patří fosforylace proteinů, jež se uplatňuje mimo jiné při regulaci rehydratace a aktivace samčího

gametofytu (Fíla et al., 2012; Mayank et al., 2012). Podobně jako v případě pylu, dochází i u jiných rostlinných modelů k rehydrataci. Pouštní xerofyt *Craterostigma plantagineum* přežívá nepřízeň podmínek v dehydratovaném stádiu. V období dešťů dochází k jeho rehydrataci a obnovení růstu. I v případě této rostliny je rehydratace doprovázena změnou ve fosforylaci proteinů (Röhrig et al., 2006; 2008). Jenže k fosforylaci proteinů v souvislosti s rehydratací nedochází jen u vysychajících xerofytů, ale i u běžných druhů rostlin, například u kukuřice seté *(Zea mays)*, kde byly zkoumány fosforylované proteiny hrající úlohu při vysychání a rehydrataci růstové zóny listů (Bonhomme et al., 2012).

1.4. Fosforylace proteinů

K fosforylaci proteinů zpravidla dochází posttranslačně. Fosfátová skupina je navázána na postranní řetězec určitých aminokyselin, a to buď přes atom kyslíku, nebo přes atom dusíku. Fosforylaci proteinů obstarávají proteiny zvané kinázy, naopak za defosforylaci cílových proteinů zodpovídají fosfatázy (viz Krebs a Beavo, 1979). Aminokyseliny nesoucí fosfátovou skupinu na atomu kyslíku jsou serin, threonin a tyrosin (Obr. 1.6). Na atomech dusíku je pak fosforylován histidin, přičemž existují dvě jeho fosforylované isoformy, 1–fosfohistidin a 3–fosfohistidin (Obr. 1.6). Dvojité fosforylace jediného histidinu je možné v laboratoři dosáhnout, avšak v živých organizmech doposud objevena nebyla (Besant a Attwood, 2009). Konvenčními

Obr. 1.6 – Vzorce fosforylovaných aminokyselin. „P" v černém kruhu značí navázanou fosfoskupinu $-PO_3^{2-}$, tedy fosforylaci aminokyseliny.

fosfoproteomickými technikami se obvykle dospěje k identifikaci aminokyselin fosforylovaných na atomech kyslíku, což je způsobené odlišnými chemickými vlastnostmi (Attwood et al., 2007) a odlišnou stabilitou obou isoforem fosfohistidinu a *O*–fosforylovaných aminokyselin v kyselém prostředí, jemuž zpravidla bývají vzorky vystaveny v některém z kroků konvenčních fosfoproteomických technik (Dunn et al., 2010; Fíla a Honys, 2012). Zatímco fosfoserin, fosfothreonin a fosfotyrosin v kyselém prostředí 1 M kyseliny chlorovodíkové (HCl) dosahují hodinových poločasů rozpadu – fosfoserin a fosfothreonin 18 h, fosfotyrosin 5 h (Plimmer, 1941), obě isoformy histidinu dosahují v 1 M HCl při 49 °C několikasekundového poločasu rozpadu – 1–fosfohistidin 18 s a 3–fosfohistidin 24,5 s (Hultquist, 1968).

Aminokyseliny mají dvě ionizovatelné skupiny navázané na α–uhlíku, karboxylovou a amino skupinu (viz Wagner a Musso, 1983). Tyto skupiny se spolu propojují za vzniku peptidické vazby (viz Bashan et al., 2003). Vlastnosti postranních skupin jednotlivých aminokyselin se liší. Postranní polární skupina serinu, threoninu a tyrosinu se za fyziologického pH mění fosforylací ve skupinu záporně nabitou. Kyselá disociační konstanta fosfátu je asi 2,1 (Kokubu et al., 2005), takže při fyziologickém pH 7,2 (Roos a Boron, 1981) je proton z fosfátu odštěpen a skupina tak nabývá záporného náboje. Díky tomuto zápornému náboji se posouvá isoelektrický bod celého fosforylovaného proteinu do kyselejších hodnot než v případě nefosforylovaného proteinu (Darewicz et al., 2005). Jeden protein může být fosforylován i vícekrát, takže získaný záporný náboj je o to silnější. Fosforylace proteinů proto může měnit interakce jednotlivých polypeptidových řetězců téhož proteinu (Lapko et al., 1996; Groban et al., 2006), nebo dokonce meziproteinové interakce (Bauer et al., 2003; Kim et al., 2004). Alternativní možností vlivu fosforylované skupiny na aktivitu proteinu je zablokování aktivního místa enzymu, díky čemuž je znemožněn vstup substrátu do aktivního místa. Příkladem enzymu s tímto způsobem regulace je isocitrát dehydrogenáza (Garnak a Reeves, 1979), která katalyzuje druhou reakci citrátového cyklu, tedy přeměnu isocitrátu na α–ketoglutarát.

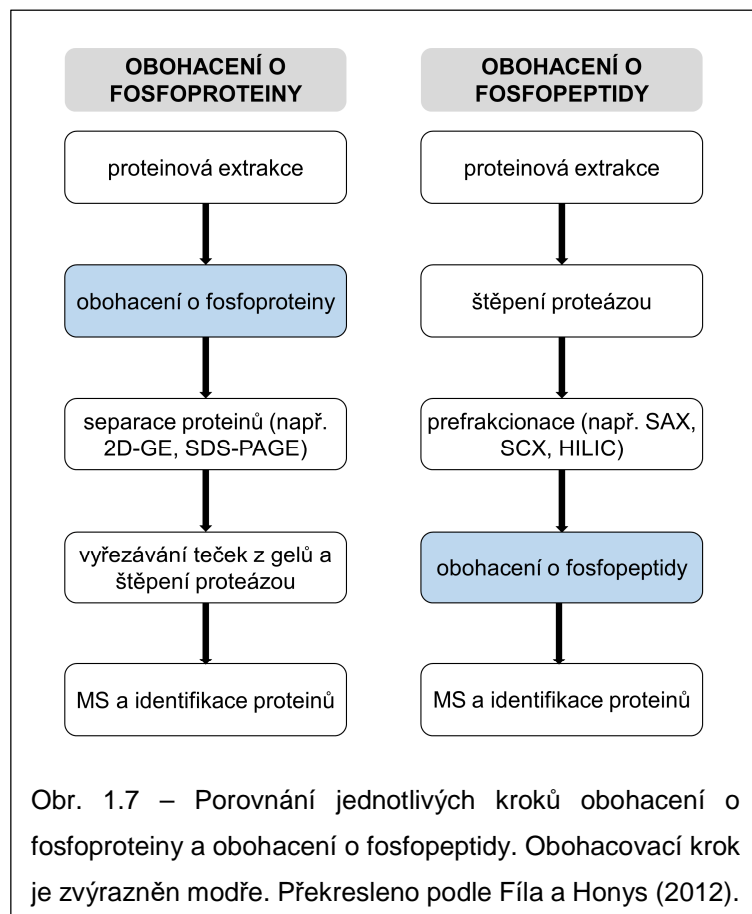## 1.5. Metody studia fosforylace proteinů

Fosforylace proteinů představuje velmi dynamickou posttranslační modifikaci. Studium role fosforylace se dá započít buď od odhalování role jednotlivých kináz a fosfatáz nebo od odhalování lokalizace fosforylačních míst na cílových proteinech.

První přístup je výhodný zejména v situacích, kdy byla jasně odhalena kináza nebo fosfatáza zodpovědná za příslušný buněčný proces, popř. aktivní v určitých pletivech. Z pylových studií stojí za zmínku například pokusy dokazující klíčovou roli dvou AGC kináz (AGC 1.5 a AGC 1.7; Zhang et al., 2009) a Ca^{2+}-dependentní kinázy (CPK32; Zhou et al., 2014) potřebných pro polarizovaný růst pylové láčky huseníčku rolního nebo práce odhalující roli serin/threonin proteinové kinázy v samčím gametofytu tabáku (Dissanayake et al., 2004). Vytipovávání kináz hrajících důležitou signalizační úlohu v samčím gametofytu poněkud komplikuje fakt, že v pylovém transkriptomu a proteomu huseníčku rolního byla detekována celá řada proteinových kináz (Hafidh et al., 2016a). U proteomu tabáku je navíc situace méně přehledná, protože genomické sekvence tabáku nebyly plně anotovány (Sierro et al., 2014), ačkoli i v pylovém proteomu (Ischebeck et al., 2014) a transkriptomu (Hafidh et al., 2012b) bylo identifikováno množství proteinových kináz.

Druhým přístupem je odhalování fosforylačních míst v cílových proteinech, kterého se nejčastěji dosahuje fosfoproteomickými přístupy. První krok fosfoproteomických studií představuje důkladná homogenizace a extrakce proteinů (Sheoran et al., 2009; Fíla et al., 2011). Zejména zralá pylová zrna jsou poněkud obtížněji homogenizovatelná, protože jejich dehydratovaná cytoplazma je obklopena tvrdou buněčnou stěnou. Homogenizaci je tak potřeba věnovat patřičnou pozornost. Extrakční činidlo aplikované v následném extrakčním protokolu určuje, jaké spektrum proteomu bude z pletiva izolováno (Sheoran et al., 2009). Zejména v případech, kdy se užívají extrakční pufry bez silného extrakčního činidla, bývá nutné zablokovat aktivitu přítomných proteáz patřičnými inhibitory (např. leupeptin, pepstatin A a fenylmethansulfonyl fluorid; Sabotič a Kos, 2012) a v případě studia fosfoproteinů je zapotřebí ještě přidat inhibitory fosfatáz a kináz (Edmead et al., 1999). Je dobré připomenout, že přítomnost inhibitorů ve vzorku při obohacení může znatelně snižovat specifitu obohacovacího protokolu (Aryal a Ross, 2010).

V průběhu fosfoproteomického experimentu bývá nevyhnutelné aplikovat některý obohacovací protokol, popř. kombinaci několika z nich (Dunn et al., 2010; Fíla a Honys, 2012), a to ze tří hlavních důvodů: (1) Mnohé fosfoproteiny nejsou v buňce příliš hojně zastoupeny, takže je jejich detekce méně pravděpodobná než v případě abundantnějších proteinů. (2) Jeden protein nemusí být úplně fosforylovaný nebo defosforylovaný, ale v jediné buňce lze najít několik forem lišících se ve stupni fosforylace (Obaya a Sedivy, 2002). (3) Detekce fosfopeptidů ve směsi s nefosforylovanými peptidy naráží na technické limitace hmotnostní

spektrometrie – fosfopeptidy se ve směsi s nefosforylovanými peptidy hůře ionizují, tudíž zůstávají v pozitivním skenovacím módu obtížně detekovatelné a některé dokonce nedetekovatelné (Janek et al., 2001). Po fosfopeptidovém obohacení, při němž jsou nefosforylované peptidy odstraněny, pak mohou být fosforylované peptidy snáze detekovány (Jensen a Larsen, 2007). Obohacovací krok ve fosfoproteomických protokolech může být aplikován ve dvou stádiích (Obr. 1.7). Buď k obohacení dochází na úrovni intaktních fosfoproteinů a k proteolytickému štěpení (nejčastěji trypsinem) se přistupuje až po rozdělení celých proteinů, nebo naopak, celkový proteinový extrakt je podroben proteolytickému štěpení za vzniku směsi peptidů a obohacovací protokol tak vychytává fosforylované peptidy (Fíla a Honys, 2012).

OBOHACENÍ O FOSFOPROTEINY	OBOHACENÍ O FOSFOPEPTIDY
proteinová extrakce	proteinová extrakce
obohacení o fosfoproteiny	štěpení proteázou
separace proteinů (např. 2D-GE, SDS-PAGE)	prefrakcionace (např. SAX, SCX, HILIC)
vyřezávání teček z gelů a štěpení proteázou	obohacení o fosfopeptidy
MS a identifikace proteinů	MS a identifikace proteinů

Obr. 1.7 – Porovnání jednotlivých kroků obohacení o fosfoproteiny a obohacení o fosfopeptidy. Obohacovací krok je zvýrazněn modře. Překresleno podle Fíla a Honys (2012).

Oba přístupy, tedy obohacování o fosfoproteiny i o fosfopeptidy, přinášejí jisté výhody, zatímco jinde narážejí na určité limity. Protokol spoléhající na **obohacování o fosfoproteiny** (Obr. 1.7) je obvykle následován jednorozměrnou polyakrylamidovou gelovou elektroforézou v přítomnosti dodecylsíranu sodného (SDS–PAGE; Collins et al., 2005; Wolschin a Weckwerth, 2005; Wolschin et al., 2005) nebo dvojrozměrnou proteinovou elektroforézou (kombinující isoelektrickou fokusaci a SDS–PAGE, tedy 2D IEF–PAGE; Röhrig et al., 2008; Fíla et al., 2012; Rocchetti et al., 2014). Namísto konvenční dvojrozměrné elektroforézy lze využít dvojrozměrnou diferenční gelovou elektroforézu (2D DIGE; Machida et al., 2007; Tian et al., 2014). Díky tomu je možné na gelu oddělit jednotlivé isoformy daného proteinu, popřípadě také různé formy téhož fosfoproteinu lišící se stupněm fosforylace. Z gelu je možno určit molekulární hmotnost daného proteinu a v případě dvojrozměrné separace také jeho

isoelektrický bod. Pozitivem je také přispění nefosforylovaných peptidů k určení identity daného proteinu. Naopak značnou limitací těchto protokolů je zpravidla výrazně nižší úspěšnost při určování přesné lokalizace fosforylačních míst daného proteinu (Röhrig et al., 2008; Fíla a Honys, 2012). Bez přesného určení místa fosforylace zůstává bílkovina pouhým kandidátem na fosforylaci a při následných analýzách se dá těžko usuzovat, kolik fosforylačních míst protein obsahuje a v jakém motivu se fosforylovaná aminokyselina vyskytuje. Tato nevýhoda souvisí s další komplikací, a tou je nespecifita. Stává se, že i protokoly obohacující o fosfopeptidy trpí jistou měrou nespecifity, celé fosfoproteiny jsou však tímto rizikem postiženy mnohem více, neboť intaktní bílkovina může zachovávat části své trojrozměrné struktury, díky nimž se může snadněji nespecificky vázat na chromatografickou matrici při obohacovacím kroku.

Nejčastějším protokolem užívaným pro obohacení fosfoproteinů je afinitní chromatografie s využitím kovového oxidu/hydroxidu (angl. metal-oxide/hydroxide affinity chromatography, zkr. MOAC). Nejčastěji jako matrice sloužil hydroxid hlinitý (Wolschin et al., 2005) nebo oxid titaničitý (Lenman et al., 2008). Další možnost představuje chelatační afinitní chromatografie (angl. immobilized metal affinity chromatography, zkr. IMAC), která na rozdíl od metody MOAC užívá v matrici nosič, na nějž jsou navázány kovové ionty (Collins et al., 2005) – u metody MOAC se jedná pouze o samotný kovový oxid/hydroxid. Poslední zmiňovanou metodou je imunoprecipitace proteinů obsahujících fosfotyrosin (Pandey et al., 2000).

Naopak **obohacení o fosfopeptidy** (Obr. 1.7) se provádí až po štěpení celkového extraktu na peptidy, opět se konvenčně užívají specifické proteázy (nejčastěji trypsin). Vzorek, se kterým se pracuje, je tudíž komplexnější a všechny peptidy ve vzorku jsou smíchány. Peptidy se však snadněji než intaktní proteiny dělí chromatografickými metodami. Aby se fosfopeptidovému obohacení podroboval méně komplexní vzorek, často se provádí prefrakcionace chromatografickými metodami, nejčastěji aniontovou ionexovou chromatografií (angl. strong anionic ion-exchange chromatography, SAX; Nühse et al., 2004), kationtovou ionexovou chromatografií (angl. strong cationic ion-exchange chromatography, SCX; Beausoleil et al., 2004) nebo chromatografií s hydrofilními interakcemi (HILIC; McNulty a Annan, 2008). Kromě toho jsou peptidy kratší a zpravidla nenabývají komplexních trojrozměrných struktur, jako je tomu v případě intaktních proteinů. Nespecifita obohacení o fosfopeptidy je tak menší, i když pořád jisté riziko nespecifity hrozí (Negroni et al., 2012). Často se však stává, že vyšší specifita obohacení za daných podmínek je doprovázena nižší

senzitivitou, takže slaběji se vázající fosfopeptidy jsou za takovýchto obohacovacích podmínek ztraceny. Tudíž při optimalizaci protokolu záleží na tom, zda chceme detekovat také slaběji se vázající fosfopeptidy a jakou míru nespecifity si můžeme dovolit (Tsai et al., 2008). Velkou výhodou obohacování o fosfopeptidy je identifikace přesného místa fosforylace, k níž se ve většině případů dospěje. Na druhou stranu, nefosforylované peptidy nepomohou s identifikací fosforylovaného proteinu, protože byly odstraněny v průběhu obohacovacího kroku a někdy je nemožné fosfopeptid jednoznačně přiřadit k jednomu proteinu, protože je sdílen dvěma nebo více proteiny.

Hlavní principy metod užívaných pro fosfopeptidové obohacení jsou obdobné jako v případě obohacení o fosfoproteiny. Často se užívají zejména afinitní chromatografie s využitím kovového oxidu/hydroxidu (MOAC) a chelatační afinitní chromatografie (IMAC). Nejčastěji užívanými matricemi při metodě MOAC se staly oxid titaničitý (Pinkse et al., 2004) a oxid zirkoničitý (Kweon a Håkansson, 2006). Metoda IMAC užívá nejčastěji jako nosiče kovových oxidů kyselinu iminodioctovou (IDA) a kyselinu nitrilotrioctovou (NTA) (Neville et al., 1997). Nesenými kovovými kationty se staly například Fe^{3+} (Neville et al., 1997), Ga^{3+} (Posewitz a Tempst, 1999), Zr^{4+} (Feng et al., 2007) a Ti^{4+} (Zhou et al., 2008). Z dalších protokolů stojí za zmínku imunoprecipitace fosfopeptidů obsahujících fosfotyrosin (Rush et al., 2005) a metody obohacující fosfopeptidy na základě chemických modifikací, jež byly shrnuty v Dunnově přehledovém článku (Dunn et al., 2010).

Různé obohacovací protokoly odhalují jinou část fosfoproteomu, takže pro pokrytí co největší části fosfoproteomu je zapotřebí aplikovat několik paralelních fosfoproteomických obohacovacích technik (Bodenmiller et al., 2007; Ito et al., 2009). Kombinace několika fosfoproteomických přístupů nemusí být pouze paralelní, ale lze ji provést i postupně – takže první obohacení slouží spíše jako prefrakcionace a druhé obohacení pak navyšuje specifitu metody.

První možností je kombinovat obohacení na obou úrovních. Nejprve dojde k obohacení o fosfoproteiny a posléze je obohacený eluát naštěpen specifickou proteázou a na peptidové směsi je proveden další obohacovací krok, tentokrát na úrovni fosfopeptidů. Takto byla využita kombinace metody MOAC s matricí z hydroxidu hlinitého pro obohacení fosfoproteinů a metody MOAC s matricí z oxidu titaničitého pro obohacení fosfopeptidů z naštěpeného eluátu získaného první metodou obohacení (Hoehenwarter et al., 2013; Beckers et al., 2014).

Kombinaci protokolů však není nutné provádět pouze na obou úrovních, lze kombinovat protokoly pouze na úrovni fosfopeptidů. První možností je opakované obohacení supernatantu, pocházejícího z obohacení, stejným protokolem. Takto byla aplikována metoda IMAC. V prvním kole obohacení se zachytily zejména peptidy vícekrát fosforylované (a tedy vázající se k chromatografické matrici silněji), zatímco jednou fosforylované (a slaběji se vázající k matrici) končily také v supernatantu a až druhým obohacením byly zachyceny (Ye et al., 2010). Tandemová aplikace metody IMAC tedy zvyšovala senzitivitu, takže došlo k identifikaci fosfopeptidů, které by jinak nebyly matricí zachyceny, a došlo by tak k jejich nenávratné ztrátě. Druhou možností je kombinace dvou různých protokolů obohacujících o fosfopeptidy, protokolu se říká SIMAC (z angl. zkratky sequentional elution from IMAC; Thingholm et al., 2008). V prvním kole se obohacuje metodou IMAC s tím, že se vytvářejí dva eluáty – první se získává kyselým elučním činidlem a druhý zásaditým elučním roztokem. V kyselém pufru jsou uvolněny zejména jednou fosforylované peptidy, zatímco vícekrát fosforylované peptidy se dostanou především do zásaditého pufru. Kyselý eluát spolu se supernatantem s nezachycenými peptidy pak byl ještě podroben druhému kolu obohacení, tentokrát metodou MOAC s matricí tvořenou oxidem titaničitým. Spektrum identifikovaných fosfopeptidů se díky dvojímu obohacení rozšířilo.

1.6. Studie pylového fosfoproteomu

První publikovanou fosfoproteomemickou studií zralého pylu krytosemenných rostlin (Angiospermae) se stal fosfoproteom huseníčku rolního (*Arabidopsis thaliana*; Mayank et al., 2012). Tato práce doplnila dostupná proteomická data, která byla v případě huseníčku nejprve získána konvenčními gelovými technikami (Holmes-Davis et al., 2005; Noir et al., 2005; Sheoran et al., 2006) a až poté byl negelovým přístupem počet identifikovaných proteinů znatelně rozšířen (Grobei et al., 2009). Mayankova studie využila kombinaci přístupů obohacujících o fosfopeptidy – IMAC, MOAC a SIMAC – a vedla k identifikaci 962 fosfopeptidů, které náležely k 598 fosfoproteinům. Z hlediska funkce fosforylovaných proteinů převládaly následující kategorie: regulace metabolizmu a funkce proteinů, metabolizmus, osud proteinů, vazba dalších proteinů, přenos signálu a buněčný transport. Taktéž byly mezi identifikovanými fosfoproteiny různé kinázy, hlavně AGC proteinové kinázy, Ca^{2+}-dependentní proteinové kinázy a sacharózu nefermentující (angl. sucrose non-fermenting) proteinové kinázy 1.

Dalším krytosemenným druhem s publikovaným fosfoproteomem zralého pylu se stal tabák virginský *(Nicotiana tabacum*; Fíla et al., 2012). Není bez zajímavosti, že pylový proteom tabáku (publikovaný spolu s proteomy dalších sedmi stádií vývoje samčího gametofytu od mikrosporocytů po pylové láčky) byl publikován později, tentokrát byl však odhalen přímo pomocí negelových technik (Ischebeck et al., 2014). K odhalení fosfoproteomu zralého pylu a pylu aktivovaného *in vitro* 30 min byla nejprve aplikována metoda MOAC obohacující o fosfoproteiny, užívající matrici z hydroxidu hlinitého. Eluát obohacený o fosfoproteiny byl podroben jednak dělení na dvojrozměrné gelové elektroforéze, vyříznutí teček (angl. *spot*) z gelu a jejich naštěpení trypsinem, jednak přímému štěpení trypsinem a negelovému dělení peptidů bez dalšího obohacení. Celkem bylo identifikováno 139 fosfoproteinových kandidátů, jenže přesnou pozici se podařilo identifikovat u pouhého jednoho fosforylačního místa. Z tohoto důvodu byl na zralém pylu proveden paralelní experiment, v němž byl celkový proteinový extrakt přímo naštěpen trypsinem a získaná peptidová směs byla obohacena o fosfopeptidy metodou MOAC s matricí tvořenou oxidem titaničitým. Tímto přístupem se podařilo určit pozici dalších 51 fosforylačních míst v již identifikovaných fosfoproteinových kandidátech. Detailnější studie odhalující přesnou pozici většího množství fosforylačních míst ze zralého pylu a regulaci fosforylace v průběhu aktivace pylu tak u tabáku doposud provedena nebyla.

Třetí fosfoproteomická studie provedená na samčím gametofytu se od předchozích dvou odlišuje ve dvou hlavních ohledech (Chen et al., 2012). Prvně byl zkoumaným druhem smrk Wilsonův *(Picea wilsonii)*, zástupce skupiny nahosemenných (Gymnospermae), zatímco tabák i huseníček patří mezi krytosemenné (Angiospermae). Druhou odlišností je, že proteom a fosfoproteom tohoto druhu byl zkoumán z odlišného pohledu. Zatímco u huseníčku i tabáku se mělo jednat o proteiny, jejichž fosforylace zodpovídá za správný vývoj samčího gametofytu, smrkový fosfoproteom se zabýval fosforylací proteinů v pylových láčkách kultivovaných na růstovém médiu s nedostatkem sacharózy a vápenatých iontů (Ca^{2+}), jednalo se tedy o fosforylaci proteinů v odpovědi na nedostatek živin v médiu. Celkem v této studii bylo identifikováno 166 proteinů a 42 fosfoproteinů.

U zralého pylu tabáku a pylu aktivovaného *in vitro* tak doposud chyběla fosfoproteomická studie, která by odhalila přesná místa fosforylace. V našem předchozím fosfoproteomickém výzkumu (Fíla et al., 2012), který tvořil podstatnou část mé diplomové práce, byla identifikována přesná pozice fosforylačních míst pouze u několika kandidátů, a to

výhradně v kandidátních proteinech identifikovaných po obohacení o fosfoproteiny z proteinového extraktu zralého pylu. Navíc jsme se v této práci vůbec nezabývali dynamikou fosforylace v průběhu pylové aktivace. Z tohoto důvodu byla mezi stádia samčího gametofytu zkoumaná v této disertační práci přidána také pylová zrna aktivovaná *in vitro* 5 min. Tato práce tak zcela logicky navazuje na náš předchozí výzkum a velmi podstatnou měrou jej doplňuje a rozšiřuje.

2. Cíle práce

Tato disertační práce sestává z následujících dílčích cílů:

(1) Přesná lokalizace fosforylačních míst u fosfoproteinů identifikovaných ze zralého pylu tabáku virginského *(Nicotiana tabacum)*, pylu aktivovaného *in vitro* 5 min a pylu aktivovaného *in vitro* 30 min.

(2) Zachycení změn ve fosforylaci proteinů v průběhu aktivace pylu tabáku virginského *(Nicotiana tabacum)*.

(3) Vyhledání hojně zastoupených kinázových motivů v získaném datovém souboru a porovnání nalezených motivů se zastoupenými kinázovými motivy v pylovém fosfopeoteomu huseníčku rolního *(Arabidopsis thaliana)*.

(4) Vyhledání kináz rozpoznávajících nalezené sekvenční motivy v pylovém proteomu a fosfoproteomu huseníčku rolního *(Arabidopsis thaliana)* a tabáku virginského *(Nicotiana tabacum)*.

(5) Vyhledání proteinových kináz v publikovaném souboru sekretomických dat tabáku virginského *(Nicotiana tabacum)*, a to v sekretomu pylových láček kultivovaných 24 hodin *semi in vivo* a *in vitro*.

3. Souhrn publikovaných výsledků

Výsledky naplňující výše vytyčené cíle byly publikovány celkem ve čtyřech publikacích, z toho dvě publikace jsou původními vědeckými články a dvě publikace přehledovými články.

Fosfoproteom zralého pylu tabáku virginského *(Nicotiana tabacum)* spolu se studií dynamiky fosforylace během aktivace pylu tabáku po pěti a třiceti minutách aktivace *in vitro* byl publikován v časopise Molecular & Cellular Proteomics s $IF_{2014} = 6,564$ (Fíla et al., 2016). Celkem bylo identifikováno 471 fosfopeptidů, které odhalily přesnou pozici 432 fosforylačních míst. Identifikované fosfoproteiny náležely do třinácti funkčních kategorií, z nichž nejvíce fosforylovaných bílkovin spadalo do následujících kategorií: transkripce, proteosyntéza, skladování a cílení proteinů a přenos signálu. Navíc kvantitativní data umožnila identifikaci fosfopeptidů reagujících na aktivaci pylu. Regulované fosfopeptidy byly rozděleny do sedmi skupin podle regulačního trendu, přičemž nejvíce fosfopeptidů bylo identifikováno exkluzivně ve zralém pylu.

Získaná fosfoproteomická data byla dále analyzována, takže již v původním fosfoproteomickém článku (Fíla et al., 2016) byly vyhledány kinázové motivy. Fosfoproteomická data získaná u tabáku virginského *(Nicotiana tabacum)* byla porovnána s fosfoproteomem huseníčku rolního *(Arabidopsis thaliana*; Mayank et al., 2012). Protože tehdy ještě nebyl nejnovější fosfoproteom tabáku virginského publikován, byl fosfoproteom huseníčku porovnán s našimi předchozími daty, získanými v rámci mé diplomové práce (Fíla et al., 2014). Tento přehledový článek byl publikován v časopise Biochemical Society Transactions s $IF_{2014} = 3,194$. Dále byly dosavadní poznatky o fosforylaci proteinů v průběhu vývoje samčího gametofytu shrnuty v přehledovém článku publikovaném v časopise Plant Reproduction s $IF_{2014} = 2,607$ (Hafidh et al., 2016a). Součástí této publikace je tabulka s kinázami identifikovanými v transkriptomu, proteomu a fosfoproteomu huseníčku rolního *(Arabidopsis thaliana)*.

V neposlední řadě jsem se podílel na klonování konstruktů a analýze dat týkajících se sekretomu pylových láček tabáku virginského *(Nicotiana tabacum)* kultivovaných metodou *semi in vivo* a *in vitro*, publikovaném v časopise Genome Biology s $IF_{2014} = 10,810$ (Hafidh et al., 2016b).

4. Diskuse

4.1. Tabákový pylový fosfoproteom

V publikovaném fosfoproteomu zralého pylu, pylu aktivovaném *in vitro* 5 min a pylu aktivovaném *in vitro* 30 min získaném po fosfopeptidovém obohacení metodou MOAC s matricí z oxidu titaničitého bylo celkem nelezeno 471 fosfopeptidů, které vedly k identifikaci 432 fosforylačních míst (Fíla et al., 2016; Tab. 4.1). Tyto fosforylované peptidy byly přítomny v 301 různých proteinech. Počet proteinů je o něco nižší než počet identifikovaných fosfopeptidů, protože jeden protein mohl být reprezentován více fosfopeptidy s větším počtem fosforylačních míst. Takovýto počet identifikovaných fosfoproteinů i fosforylačních míst představuje značné rozšíření fosfoproteomu získaného po obohacování o fosfoproteiny metodou MOAC s matricí z hydroxidu hlinitého, kdy bylo identifikováno pouhých 139 fosfoproteinových kandidátů s jedním fosforylačním místem a dalších 51 fosforylačních míst bylo odhaleno po obohacení fosfopeptidů oxidem titaničitým ze zralého pylu (Fíla et al., 2012; Tab. 4.1). Fosfoproteom tabáku tak byl rozšířen o nově identifikovaná fosforylační místa a počtem známých fosfopeptidů se tak přiblížil pylovému fosfoproteomu huseníčku rolního, v němž bylo identifikováno několika metodami fosfopeptidového obohacení celkem 962 fosfopeptidů odhalujících 609 fosforylačních míst v 598 fosfoproteinech (Mayank et al., 2012; Tab. 4.1).

Nižší počet fosfopeptidů identifikovaných v tabákovém fosfoproteomu může být způsoben dvěma příčinami: (1) Pro identifikaci tabákových fosfoproteinů byly využity EST sekvence tabáku (získané vesměs ze sporofytických pletiv), kde nemusí být obsaženy transkripty specifické pro samčí gametofyt. Tabákový genom je sice osekvenován, ale není plně anotován (Sierro et al., 2014), tudíž genomové sekvence tabáku byly pro identifikaci fosfopeptidů méně vhodné než EST sekvence. Díky chybějícím sekvencím tak nemusela být některá identifikovaná spektra přiřazena k fosfoproteinům. Oproti tomu genomové sekvence huseníčku rolního jsou k dispozici již od roku 2000 (Arabidopsis Genome Initiative, 2000) a od té doby byly jeho anotace postupně vylepšovány. (2) V našem případě byl aplikován jediný protokol obohacující o fosfopeptidy, zatímco Mayank s kolektivem využili kombinaci tří protokolů. Často se totiž stává, že aplikace několika různých protokolů rozšiřuje identifikovanou část fosfoproteomu, protože různé obohacovací protokoly odhalují nepřekrývající se části fosfoproteomu (Bodenmiller et al., 2007; Ito et al., 2009).

Tab. 4.1 – Srovnání fosfoproteomických studií samčího gametofytu tabáku virginského *(Nicotiana tabacum)* a huseníčku rolního *(Arabidopsis thaliana)*. Poměr jednotlivých fosforylovaných aminokyselin v případě prvního tabákového fosfoprotemu není příliš vypovídající, protože byl určen jen na základě 52 fosforylačních míst.

Parametr	První pylový tabákový fosfoproteom (Fíla et al., 2012)	Druhý pylový tabákový fosfoproteom (Fíla et al., 2016)	Pylový fosfoproteom huseníčku (Mayank et al., 2012)
Studie zahrnovala aktivovaný pyl	Ano	Ano	Ne
Užitá obohacovací technika	Al(OH)$_3$–MOAC obohacení o fosfoproteiny + TiO$_2$–MOAC obohacení o fosfopeptidy u již identifikovaných proteinů	TiO$_2$–MOAC obohacení o fosfopeptidy	3 metody obohacování o fosfopeptidy: IMAC, TiO$_2$–MOAC a SIMAC
Počet identifikovaných fosfoproteinů	139	301	598
Počet identifikovaných fosfopeptidů	1 + 51	471	962
Počet přesně identifikovaných fosforylačních míst	1 + 51	432	609
Poměr fosforylačních míst na serinu : threoninu : tyrosinu	67,3 % : 32.7 % : 0 %	86,4 % : 13,4 % : 0,2 %	86 % : 14 % : 0,16 %

S prvně jmenovanou příčinou nižšího počtu fosforylačních míst identifikovaných v pylovém tabákovém fosfoproteomu souvisí i další skutečnost. Asi pětina identifikovaných fosfopeptidů byla zařazena do kategorií „nejasná klasifikace" (angl. unclear classification) a „neznámá funkce" (angl. unknown). Mnohé z těchto proteinů budou nejspíše pylově specifické nebo zastoupeny v pylu hojněji než ve sporofytických pletivech, zatímco jejich funkce zůstává neznámá. V tabákovém proteomu bylo 837 z celkových 2135 identifikovaných proteinů gametofyticky specifických (nebo přinejmenším v samčím gametofytu signifikantně abundantnějších; Ischebeck et al., 2014). Z těchto 837 proteinů jich 120 mělo nejasnou funkci. Z tohoto je zřejmé, že mnoho pylově specifických proteinů stále čeká na odhalení své funkce.

4.2. Zastoupení jednotlivých fosforylovaných aminokyselin

Vzhledem k tomu, že konvenční fosfoproteomické techniky vedou k odhalení *O–fosforylovaných* aminokyselin, jsme našli v pylovém tabákovém fosfoproteomu pouze fosforylovaný serin, threonin a tyrosin, ale žádný fosforylovaný histidin (Fíla et al., 2016). Ve většině fosfoproteomických studií, které zahrnují dostatečný počet identifikovaných fosfoproteinů, dosahovalo zastoupení fosforylovaného serinu 80–90 %, zatímco na fosforylovaný threonin připadalo asi 10–15 %. Fosfotyrosinových fosforylačních míst je nejméně, obvykle maximálně pouhých několik jednotek procent.

V pylovém fosfoproteomu tabáku připadalo 86,4 % na fosfoserin, 13,4 % na fosforylovaný threonin a jediné fosforylační místo na tyrosinu odpovídalo 0,2 % (Fíla et al., 2016). Poměr fosforylačních míst ve fosfoproteomu zralého pylu huseníčku rolního byl velmi podobný: bylo zde identifikováno 86 % míst na fosfoserinu, 14 % na fosfothreoninu a 0,16 % na fosfotyrosinu. V případě živočišných buněčných kultur dosahoval podíl fosfotyrosinu několika jednotek procent, 1,8 % (Olsen et al., 2006), 2,3 % (Molina et al., 2007) nebo 3,8 % (Beausoleil et al., 2004). Je ale potřeba přihlédnout k faktu, že se zpravidla jednalo o lidské nádorové buněčné linie s celkově vysokou měrou fosforylace. V rostlinných fosfoproteomech býval podíl fosfotyrosinu zpravidla výrazně menší, a tak poměr pS : pT : pY v buněčných kulturách huseníčku rolního dosahoval 91,8 : 7,5 : 0,7 (van Bentem et al., 2008) nebo 83,81 : 16,18 : 0,01 (Benschop et al., 2007). Na druhou stranu existují i studie s vyšším podílem fosfotyrosinu – 4,3 % (Sugiyama et al., 2008) a 4,2 % u buněčných kultur huseníčku rolního (Nakagami et al., 2010) a 2,9 % u buněčných kultur rýže seté *(Oryza sativa*; Nakagami et al., 2010). Z těchto dat je zřejmé, že doposud není jasně vyřešeno, jak často se u rostlin fosforylace tyrosinu vyskytuje (van Bentem a Hirt, 2009; Mithoe a Menke, 2011).

Fosforylace tyrosinu hraje důležitou roli v klíčových procesech během života rostliny, například byla objevena fosforylace brassinosteroidového receptoru BRI1 (Oh et al., 2009) nebo ve fytochromové signalizační dráze (Nito et al., 2013). V případě pylových láček je fosforylace tyrosinu klíčová pro správný růst, protože pylové láčky pod vlivem inhibitorů fosforylace tyrosinu (fenylarsin oxidu a genisteinu) signifikantně zpomalily růstovou rychlost. Přesné cílové proteiny fosforylované na tyrosinu však doposud identifikovány nebyly, i když byla pravděpodobně narušena dynamika aktinového cytoskeletu (Zi et al., 2007). Jediné fosforylační místo na tyrosinu v pylovém fosfoproteomu tabáku bylo neseno peptidem
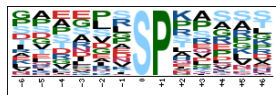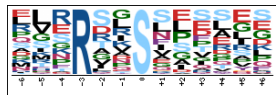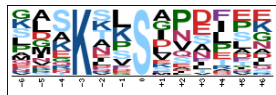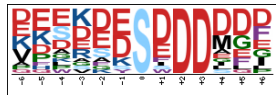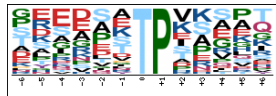
GVSY*GGGQSSLGYLFGGGEAPK v proteinu podobnému SPIRAL1 1 (angl. SPIRAL1-like 1 protein; Fíla et al., 2016).

4.3. Nalezené kinázové motivy v pylovém fosfoproteomu huseníčku a tabáku

Jak v pylovém fosfoproteomu tabáku (Fíla et al., 2016), tak v pylovém fosfoproteomu huseníčku (Mayank et al., 2012) byly vyhledány kinázové motivy programem Motif-X (Schwartz a Gygi, 2005; Chou a Schwartz, 2011). Hledání spočívalo v porovnání získaného souboru dat s kontrolními daty, díky čemuž se vybraly motivy, kde se vyskytovala fosforylace častěji, než by odpovídalo náhodě. Znalost fosforylačních motivů rostlin je poněkud omezená, tudíž mnohé motivy byly odvozeny z dat získaných na ostatních modelových organizmech, hlavně na člověku (Lee et al., 2011a). V případě pylového fosfoproteomu tabáku bylo objeveno pět kinázových motivů s centrálním serinem a jeden motiv s centrální pozicí obsazenou threoninem (Fíla et al., 2016). Pylový fosfoproteom huseníčku rolního obsahoval pouhé dva kinázové motivy, oba s centrálním serinem (Mayank et al., 2012).

Prvním fosforylačním motivem sdíleným pylovými fosfoproteomy obou druhů byl xxxxxxS*Pxxxxx (Tab. 4.2), tedy motiv, kde je fosforylovaný serin následován prolinem (písmeno následované hvězdičkou symbolizuje fosforylovanou aminokyselinu). U tabáku byl ještě identifikován obdobný motiv s centrálním threoninem, tedy xxxxxxT*Pxxxxx (Tab. 4.2). Fosforylační místo (nerozhoduje, zdali na serinu nebo threoninu) následované prolinem je rozpoznáváno dvěma velkými skupinami kináz – mitogenem aktivovanými proteinovými kinázami (MAPK) a cyklin-dependentními proteinovými kinázami (CDK; Lee et al., 2011b). Zástupci MAP kináz byli identifikováni jak v pylovém proteomu huseníčku (Grobei et al., 2009; Hafidh et al., 2016a; Tab. 4.4), tak v pylovém proteomu tabáku (Ischebeck et al., 2014; Tab. 4.3). MAP kinázy hrají důležitou úlohu při rehydrataci pylových zrn (Wilson et al., 1997), zatímco cyklin-dependentní proteinové kinázy jsou známy pro svoji regulaci buněčného cyklu. Jejich přítomnost v samčím gametofytu by mohla být důležitá pro regulaci v průběhu obou pylových mitotických dělení (PMI a PMII; Hafidh et al., 2012b). Alternativní úlohou cyklin-dependentní proteinové kinázy G1 specifickou pro pylové láčky je regulace sestřihu pre-mRNA kódující kalóza syntázu, čímž reguluje syntézu buněčné stěny (Huang et al., 2013).

Tab. 4.2 – Fosforylační motivy identifikované v pylovém fosfoproteomu tabáku virginského *(Nicotiana tabacum)*. Tabulka připravena s využitím dat z publikace Fíla et al. (2016).

Motiv	Schéma motivu	Skóre motivu	Počet peptidů s fosforylovaným motivem ve zkoumaném vzorku	Celkový počet peptidů ve zkoumaném vzorku	Počet peptidů s motivem v referenčním vzorku	Celkový počet peptidů v referenčním vzorku	Kolikrát byl výskyt motivu ve zkoumaném vzorku častější	Identifikace v pylovém fosfoproteomu huseníčku rolního (Mayank et al., 2012)
xxxxxxS*Pxxxxxx		16,00	118	350	3081	57130	6,25	Ano
xxxRxxS*xxxxxx		11,38	37	194	2733	53642	3,74	Ano
xxxKxxS*xxxxxx		7,48	30	157	3148	50909	3,09	Ne
xxxxxxS*DxExxx		26,76	23	232	221	54049	24,25	Ne
xxxxxxS*xDDxxx		20,05	15	209	186	53828	20,77	Ne
xxxxxxT*Pxxxxx		16,00	31	52	2033	36035	10,57	Ne

Dalším fosfoserinovým motivem sdíleným fosfoproteomy obou druhů je xxxRxxS*xxxxxx (Tab. 4.2), tedy arginin následován dvěma jakýmikoliv aminokyselinami a fosforylovaným serinem. Tento alkalický motiv měl v tabákovém fosfoproteomu ještě jednu obdobu: na pozici argininu byl navázán lysin, tedy xxxKxxS*xxxxxx (Tab. 4.2). Oba alkalické motivy jsou rozpoznávány Ca^{2+}/kalmodulin-dependentními proteinovými kinázami (CAMK2; Lee et al., 2011b). Chimerická CAMK se dvěma doménami, jednou reagující na volné vápenaté ionty a druhou vázající kalmodulin s navázaným Ca^{2+}, byla exprimována v samčím gametofytu

lilie *(Lilium longiflorum)* a tabáku virginského *(Nicotiana tabacum)* (Poovaiah et al., 1999) – exprese této kinázy začínala v mateřské buňce samčího gametofytu a pak pokračovala v dalších stádiích s tím, že vrcholila ve stádiu tetrády mikrospor. Druhou skupinou kináz rozeznávající výše zmiňované alkalické motivy jsou Ca^{2+}-dependentní proteinové kinázy–příbuzné kinázám nefermentujícím sacharózu (angl. Ca^{2+}-dependent protein kinase–sucrose-non-fermenting-related kinase; CDPK–SnRK; Lee et al., 2011b). Dvě kinázy z rodin rozeznávajících tento mo-

Tab. 4.3 – Kinázy rozpoznávající nalezené kinázové motivy, které byly identifikovány v proteomu (Ischebeck et al., 2014) a fosfoproteomu (Fíla et al., 2016) samčího gametofytu tabáku virginského.

Kód proteinu (accession)	Název proteinu	% identifikované sekvence	Počet proteinů ve skupině	Počet peptidů celkem (unikátních)
Mitogenem aktivované proteinové kinázy (motivy xxxxxxS*Pxxxxx a xxxxxxT*Pxxxxx)				
EH665702	MAP kináza *(Nicotiana tabacum)*	17,43	1	1 (1)
TC122915	MAP kináza Ntf4-2 *(Nicotiana tabacum)*	16,81	31	2 (1)
TC145219	MAP kináza 9 *(Arabidopsis thaliana)*	14,17	1	3 (3)
TC145276	MAP kináza 8 *(Arabidopsis thaliana)*	21,79	2	2 (1)
A5H7H4	MAP kináza 4 *(Nicotiana attenuata)*	10,53	18	2 (1)
TC139884	MAP kináza 15 *(Oryza sativa)*	32,12	7	4 (1)
AM782478	serin/threonin proteinová kináza *(Medicago truncatula)*	8,67	1	1 (1)
TC142329	CDK-aktivační kináza *(Nicotiana tabacum)*	3,78	2	1 (1)
NT_TC90910	MAP kináza	–	1	1 (1)
NT_TC92460	MAP kináza	–	1	1 (1)
Cyklin-dependentní proteinové kinázy (motivy xxxxxxS*Pxxxxx a xxxxxxT*Pxxxxx)				
TC144307	cyklin-dependentní kináza B1-1 *(Nicotiana tabacum)*	9,35	6	2 (2)
TC135847	cyklin-dependentní kináza B2 *(Solanum lycopersicum)*	4,55	3	1 (1)
NP917540; Q40483	cyklin-dependentní kináza A *(Nicotiana tabacum)*	5,12	4	1 (1)
Ca^{2+}-dependentní proteinové kinázy (motivy xxxRxxS*xxxxxx a xxxKxxS*xxxxxx)				
NT_TC96252	Ca^{2+}-dependentní kináza 4 *(Solanum tuberosum)*	–	1	1 (1)
Ca^{2+}-dependentní proteinové kinázy–příbuzné kinázám nefermentujícím sacharózu; CDPK–SnRK (motivy xxxRxxS*xxxxxx a xxxKxxS*xxxxxx)				
TC155405	serin/threonin kináza SAPK8-like *(Solanum tuberosum)*	8,70	14	1 (1)
TC123960	kináza příbuzná SNF1 *(Nicotiana benthamiana)*	5,17	3	1 (1)
Kaseinové kinázy (motivy xxxxxxS*DxExxx a xxxxxxS*xDDxxx)				
TC122922	kaseinová kináza 2 alfa *(Nicotiana tabacum)*	14,47	17	3 (1)
TC161480	kaseinová kináza 2 *(Nicotiana tabacum)*	7,41	7	1 (1)

tiv byly identifikovány v pylovém proteomu tabáku virginského (Ischebeck et al., 2014; Tab. 4.3) a čtyři homology byly nalezeny v proteomu huseníčku rolního (Grobei et al., 2009; Hafidh et al., 2016a; Tab. 4.4). Taktéž ve fosfoproteomu prašníku rýže byly SnRK nejhojnějšími kinázami, u nichž se podařilo predikovat cílový protein (Ye et al., 2015).

Zbývající dva fosforylační motivy byly identifikovány pouze v pylovém fosfoproteomu tabáku virginského. Oba jsou kyselé a obsahují na prostřední pozici fosfoserin, který je následován (1) kyselinou asparagovou, jakoukoliv aminokyselinou a kyselinou glutamovou nebo (2) libovolnou aminokyselinou a dvěma molekulami kyseliny asparagové. Jedná se tedy o motivy xxxxxxS*DxExxx a xxxxxxS*xDDxxx (Tab 4.2), které se dají shrnout do jediného motivu, xxxxxxS*(D/E)(D/E)(D/E)xxx, kde je fosforylovaný serin následován třemi kyselými aminokyselinami (vždy buď kyselinou asparagovou, nebo kyselinou glutamovou), jenž je rozpoznáván kaseinovou kinázou 2 (CK2; Lee et al., 2011b). V pylovém proteomu tabáku virginského byly identifikovány dvě kaseinové kinázy (Ischebeck et al., 2014; Tab. 4.3).

Tab. 4.4 – Kinázy rozpoznávající nalezené kinázové motivy z pylového proteomu (Grobei et al., 2009) a fosfoproteomu (Mayank et al., 2012) huseníčku rolního *(Arabidopsis thaliana)*.

Kód proteinu (Arabidopsis gene identifier)	Název proteinu	Důkaz v pylovém transkriptomu	Důkaz na 2D gelu	Nalezen v pylovém fosfoproteomu
AT1G18150	MAP kináza 8	Ano	Ne	Ano
AT1G73670	MAP kináza 15	Ano	Ne	Ano
AT2G43790	MAP kináza 6	Ano	Ne	Ne
AT3G18040	MAP kináza 9	Ano	Ne	Ne
AT4G28980	cyklin-dependentní kináza F1	Ano	Ne	Ano
AT1G35670	Ca^{2+}-dependentní kináza 2	Ano	Ne	Ano
AT2G38910	Ca^{2+}-dependentní kináza 20	Ano	Ne	Ne
AT4G09570	Ca^{2+}-dependentní kináza 4	Ano	Ne	Ano
AT5G19360	Ca^{2+}-dependentní kináza 34	Ano	Ne	Ne

Ve všech uvedených případech se jedná o *in silico* data a ne experimentálně prokázané přiřazení jednotlivých proteinových kináz k jejich cílovým proteinům. Nadále tedy zůstává spekulací, která konkrétní kináza zodpovídá za konkrétní fosforylaci daného proteinu. Ke

zjištění takovýchto informací by bylo zapotřebí provést další experimenty studující vztahy mezi jednotlivými fosforylačními událostmi cílových proteinů a kinázami.
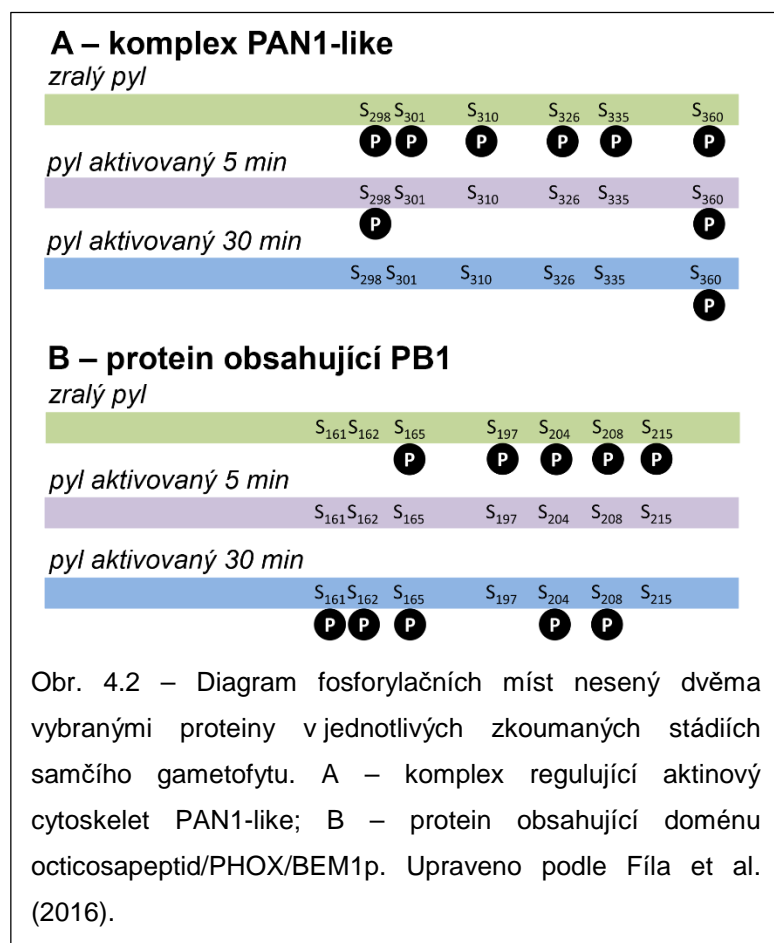
4.4. Dynamika fosforylace mezi jednotlivými stádii samčího gametofytu

Regulované fosfopeptidy nalezené ve fosfoproteomu samčího gametofytu tabáku virginského byly rozděleny do sedmi skupin podle svého regulačního trendu. Skupiny I, II a III zahrnovaly fosfopeptidy přítomné výlučně v příslušném stádiu – tedy ve zralém pylu, pylu aktivovaném *in vitro* 5 min a pylu aktivovaném *in vitro* 30 min. Skupiny IV, V a VI obsahovaly fosfopeptidy, které byly identifikovány ve dvou stádiích a ve třetím chyběly, ve skupině IV tak byly fosfopeptidy ze zralého pylu a pylu aktivovaného 5 min, skupina V zahrnovala fosfopeptidy výhradně z aktivovaných stádií a nakonec skupina VI obsahovala fosfopeptidy s nejdynamičtější změnou fosforylace – byly přítomny ve zralém pylu, po pětiminutové aktivaci se staly nedetekovatelnými a znovu se objevily po třiceti minutách aktivace. V poslední, sedmé skupině byly zařazeny regulované fosfopeptidy identifikované ve všech třech studovaných stádiích. Z celkových 209 regulovaných fosfopeptidů jich bylo nejvíce zařazeno do skupiny I (135), kterou následovaly skupiny IV a VI s 21, resp. 19 fosfopeptidy (Obr. 4.1). Ve zbývajících skupinách už bylo méně než 10 fosfopeptidů, shodně po devíti peptidech

Obr. 4.1 – Vennův diagram znázorňující zastoupení regulovaných fosfopeptidů mezi jednotlivými zkoumanými stádii – zralý pyl, pyl aktivovaný *in vitro* 5 min a pyl aktivovaný *in vitro* 30 min. Upraveno podle Fíla et al. (2016).

bylo zařazeno do skupin II, III a V. Poslední skupina VII pak obsahovala nejméně fosfopeptidů, konkrétně sedm.
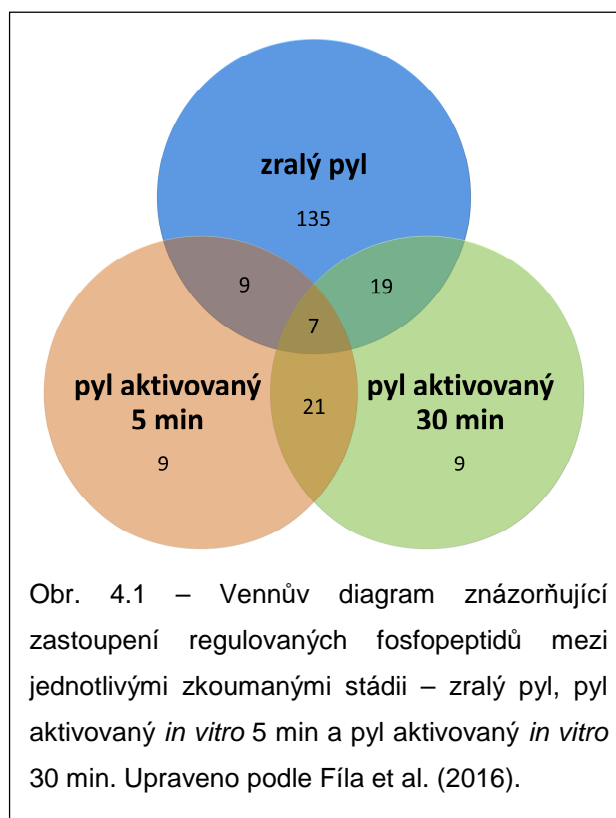
I u regulovaných fosfopeptidů byly určeny převažující funkce proteinů. Nejvíce zastoupenými kategoriemi se staly transkripce, translace a také syntéza a skladování proteinů. Do těchto tří kategorií patřila obvykle dohromady asi třetina až polovina fosfopeptidů v dané regulační skupině. Časté zastoupení měly podobně jako v celkovém souboru

fosfoproteomických dat proteiny s nejistou klasifikací (angl. unclear classification), na něž připadala ve většině regulačních skupin asi čtvrtina identifikovaných fosfopeptidů (skupiny I, II, III, IV), přičemž ve skupině VI dosahovala dokonce téměř poloviny. V poslední skupině VII byly fosfopeptidy s nejasnou klasifikací funkce zastoupeny fosfopeptidy s neznámou funkcí, které dosahovaly asi čtvrtiny všech fosfopeptidů skupiny VII. Právě mezi proteiny s neurčenou funkcí mohou spadat zajímaví kandidáti, kteří zodpovídají za regulaci rehydratace a aktivace pylových zrn a zaslouží si tedy pozornost v dalším výzkumu.

Obr. 4.2 – Diagram fosforylačních míst nesený dvěma vybranými proteiny v jednotlivých zkoumaných stádiích samčího gametofytu. A – komplex regulující aktinový cytoskelet PAN1-like; B – protein obsahující doménu octicosapeptid/PHOX/BEM1p. Upraveno podle Fíla et al. (2016).

Změny fosforylace mezi jednotlivými studovanými stádii samčího gametofytu mohou být značně komplexní, protože každé z fosforylačních míst může podléhat změnám ve fosforylaci nezávisle, přičemž některá fosforylační místa mohou být fosforylována konstitutivně (Wang et al., 2001; McCoy et al., 2005). Příklady proteinů s větším počtem různě regulovaných fosforylačních míst jsou komplex regulující aktinový cytoskelet PAN1-like a protein obsahující doménu octicosapeptid/PHOX/BEM1p. PAN1-like komplex obsahoval šest fosforylačních míst (Obr. 4.2A). Fosfopeptidy NSPFGFEDSVPGS*PLS*R a NSPFGFEDSVPGSPLS*R (hvězdička značí fosforylovanou aminokyselinu) byly identifikovány výhradně ve zralém pylu. Na základě těchto dat můžeme spekulovat, že první fosforylovaný atom serinu by mohl být fosforylován ve zralém pylu, po pětiminutové aktivaci dosáhnout vrcholu své aktivace a po třiceti minutách už být defosforylován. Je dále možné, že ve zralém pylu koexistoval protein ve dvou formách, jednou a dvakrát fosforylované. Druhý vybraný kandidát, protein obsahující doménu octicosapeptid/PHOX/BEM1p nesl v prezentovaném souboru dat sedm fosforylačních

míst (Obr. 4.2B). Fosfopeptidy FVDALNSGPIHASPAGAVAS*PAGSADFLFGS*EK a FVDALNSGPIHAS*PAGAVASPAGS*ADFLFGSEK byly společně přítomny výhradně ve zralém pylu, zatímco peptid FVDALNSGPIHASPAGAVAS*PAGS*ADFLFGSEK byl identifikován jak ve zralém pylu, tak v pylu po třicetiminutové aktivaci. Pravděpodobně je tedy ve zralém pylu fosforylován na všech čtyřech zmiňovaných serinech, po pěti minutách aktivace pylu dochází k defosforylaci všech fosforylačních míst, ale po třiceti minutách k opětovné fosforylaci dvou vybraných fosforylačních míst. Defosforylace po pěti minutách aktivace by tak mohla být spjata s rehydratací a aktivací pylových zrn. Navíc byly u tohoto proteinu identifikovány fosfopeptidy LFLFPANPPS*S*VGSGVPQSR a LFLFPANPPSS*VGS*G-VPQSR, které se objevily výhradně v pylu aktivovaném 30 min, zatímco fosfopeptid LFLFPANPPSSVGS*GVPQSR byl identifikován také ve zralém pylu. Je tak možné, že třetí serin byl fosforylován ve zralém pylu, po aktivaci defosforylován a opět fosforylován až po třiceti minutách aktivace. Oproti tomu první dvě fosforylační místa (obě na serinu) byla detekována exkluzivně v pylu aktivovaném 30 min. Všechny tyto možné fosforylační změny však zůstávají spekulacemi. Navíc nelze vyloučit, že některá fosforylační místa se mohla vyskytovat i v dalších stádiích, jen byla pod detekčními limity použitých metod. Z uvedených příkladů plyne, že jeden protein může být fosforylován na více místech, a ta mohou podléhat různým regulacím.

4.5. Sekretované proteinové kinázy

Vzhledem k tomu, že je fosforylace proteinů pravděpodobně důležitá i při vzájemné komunikaci pylové láčky s vodícími pletivy čnělky, byly vyhledány proteinové kinázy v sekretomu pylových láček kultivovaných *semi in vivo* po dobu 24 hodin a v sekretomu pylových láček kultivovaných *in vitro* 24 hodin (Hafidh et al., 2016b).

V následující podkapitole bude řeč o každé proteinové skupině jako o jednotlivém proteinu. Proteinová skupina slučuje homologické proteiny, které se hledacím algoritmem nepodařilo od sebe odlišit (Tab. 4.5). V *semi in vivo* sekretomu byly identifikovány dvě kinázy, z nichž jedna proteinová skupina byla nalezena zároveň v *in vitro* sekretomu (Tab. 4.5). Kromě toho byly exkluzivně v *in vitro* sekretomu nalezeny další čtyři proteinové kinázy.

Prvé dvě kinázy ze *semi in vivo* sekretomu jsou homology genů At4g39110 a At2g21480 z huseníčku rolního *(Arabidopsis thaliana)*, jež kódují proteinové kinázy z rodiny malectin/receptorových proteinových kináz. Proteiny z této kinázové rodiny jsou silně

exprimovány právě v květech a pylu, kde hrají důležitou úlohu při navádění pylové láčky směrem k zárodečnému vaku (Lindner et al., 2012). Do této kinázové rodiny patří například FERONIA, která reguluje prasknutí pylové láčky zárodečném vaku a uvolnění spermatických buněk (Huck et al., 2003) nebo ANXUR1 (ANX1) a ANXUR2 (ANX2), které naopak blokují předčasné prasknutí pylové láčky a uvolnění spermatických jader (Boisson-Dernier et al., 2009). Funkce homologů identifikovaných proteinů a důvod jejich sekrece je však doposud neznámý, zatím byla prokázána pouze fosforylace proteinu At2g21480 (Mayank et al., 2012).

Tab. 4.5 – Proteinové kinázy identifikované v sekretomu pylových láček tabáku virginského *(Nicotiana tabacum)* kultivovaných *semi in vivo* a *in vitro* (Hafidh et al., 2016b). Do tabulky byly umístěny pouze proteiny identifikované minimálně ve třech ze čtyř replikátů na základě alespoň dvou peptidů.

Proteinová skupina	Kód proteinu (accession)	Název proteinu	Molekulární hmotnost (kDa)	Isoelektrický bod (pI)	Počet peptidů (unikátních peptidů)	Identifikace v *semi-in-vivo* sekretomu	Identifikace v *in vitro* sekretomu
1.	K4D103	Necharakterizovaný protein *(Solanum lycopersicum)*	88	6,5	3 (1)	Ano	Ano
1.	UPI0002BCB164	Kináza podobná receptorové kináze At4g39110 *(Solanum lycopersicum)*	96	6,5	3 (1)	Ano	Ano
2.	M0ZV21	Necharakterizovaný protein *(Solanum tuberosum)*	97	6,4	3 (1)	Ano	Ne
3.	V7BAK9	Necharakterizovaný protein *(Phaseolus vulgaris)*	59	5,9	2 (1)	Ne	Ano
3.	I1JIW4	Necharakterizovaný protein *(Glycine max)*	59	5,8	2 (1)	Ne	Ano
3.	I1KMJ1	Necharakterizovaný protein *(Glycine max)*	60	5,6	2 (1)	Ne	Ano
3.	I1M756	Necharakterizovaný protein *(Glycine max)*	59	6,0	2 (1)	Ne	Ano
3.	I1NDX2	Necharakterizovaný protein *(Glycine max)*	61	5,8	2 (1)	Ne	Ano
3.	UPI0002336CEB	Ca^{2+}-dependentní kináza 17-like *(Glycine max)*	60	6,0	2 (1)	Ne	Ano
3.	UPI00032A7548	Ca^{2+}-dependentní kináza 17-like *(Cicer arietinum)*	60	5,8	2 (1)	Ne	Ano
3.	V7BM70	Necharakterizovaný protein *(Phaseolus vulgaris)*	61	5,2	2 (1)	Ne	Ano
4.	Q6KC53	Ca^{2+}-dependentní kináza *(Nicotiana plumbaginifolia)*	60	6,1	2 (1)	Ne	Ano
5.	H6UM40	Ca^{2+}-dependentní kináza *(Nicotiana tabacum)*	57	5,7	4 (4)	Ne	Ano
6.	M1CGN1	Necharakterizovaný protein *(Solanum tuberosum)*	56	6,1	4 (1)	Ne	Ano
6.	K4C7G7	Necharakterizovaný protein *(Solanum lycopersicum)*	57	6,1	4 (1)	Ne	Ano
6.	UPI0002BC828F	Ca^{2+}-dependentní kináza 4-like *(Solanum lycopersicum)*	56	6,0	4 (1)	Ne	Ano

Zbývající kinázy identifikované v *in vitro* sekretomu náleží do rodiny Ca^{2+}-dependentních proteinových kináz. Proteinové skupiny 3 a 4 jsou homology genu At5g12180 z huseníčku rolního, zatímco proteinové skupiny 5 a 6 jsou homology genů At4g09570 a

At1g35670, přičemž nebylo možné odlišit identitu jednotlivých homologů. Ca^{2+}-dependentní kinázy reagují na změny v gradientu vápenatých iontů, které byly popsány mimo jiné u pylových láček (Holdaway-Clarke et al., 1997; Holdaway-Clarke a Hepler, 2003). Gen At5g12180 kóduje Ca^{2+}-dependentní kinázu 17, která má zásadní úlohu při růstu a cílení pylové láčky směrem k zárodečným vakům (Myers et al., 2009). Druhé dva lokusy kódují další dvě Ca^{2+}-dependentní proteinové kinázy, konkrétně Ca^{2+}-dependentní kinázu 4 (At4g09570) a Ca^{2+}-dependentní kinázu 11 (At1g35670). Obě tyto kinázy se účastní signalizace reagující na přítomnost kyseliny abscisové, protože fosforylovaly transkripční faktory spouštějící odpověď na kyselinu abscisovou (Zhu et al., 2007). Kromě toho fosforylují syntázu 1–amino-cyklopropan–1–karboxylové kyseliny, čímž zvyšují stabilitu tohoto enzymu, díky čemuž podporují syntézu ethylenu (Luo et al., 2014). V neposlední řadě byl popsán interaktom těchto kináz (Uno et al., 2009). Obě byly identifikovány v pylovém proteomu huseníčku rolního (Grobei et al., 2009) a Ca^{2+}-dependentní kináza 11 spolu s Ca^{2+}-dependentní kinázou 24 regulovala aktivitu draselných kanálů v pylové láčce (Zhao et al., 2013). Studium funkce Ca^{2+}-dependentních proteinových kináz spolu s jejich sekrecí pylovými láčkami by mohlo přinést další důležité informace o jejich funkci v samčím gametofytu.

4.6. Plánované budoucí experimenty

Získaný fosfoproteom zralého pylu tabáku, pylu aktivovaného *in vitro* 5 min a pylu aktivovaného *in vitro* 30 min vedl k identifikaci značného množství fosfopeptidů. V prezentovaném datovém souboru byly nalezeny kinázové motivy a některé fosfopeptidy předvedly dynamickou povahu svojí fosforylace. Tato data však neprozrazují, jakou funkci mají jednotlivá fosforylační místa. K odhalení přesné funkce identifikovaných fosfoproteinů a k jejich provázání s kinázami zodpovědnými za dané fosforylační události bude zapotřebí provést další experimenty.

Ze získaného datového souboru budou vybrány fosfoproteiny z kategorie s neznámou nebo nejasnou klasifikací, popřípadě proteiny zodpovědné za regulaci syntézy proteinů. K vybraným kandidátům budou nalezeny homology u huseníčku rolního a poté budou ke genům nalezeny T-DNA inzerční linie v dostupných internetových databázích. S mutanty budou prováděny fenotypické analýzy, aby se odhalilo, zda vyřazení genu z funkce vykazuje u zkoumaných rostlin změnu fenotypu, z čehož zvláštní důraz bude kladen na fenotyp obou gametofytů. Kromě toho bude určena lokalizace proteinu, bude provedena analýza ektopické

exprese (angl. overexpression) a také promotorová analýza. Po získání základních informací o daném fosfoproteinu se přejde k analýze funkce konkrétních fosforylačních míst.

5. Závěry práce

Experimenty v rámci této disertační práce vedly k identifikaci fosforylovaných peptidů ze tří stádií samčího gametofytu tabáku virginského *(Nicotiana tabacum)*: ze zralého pylu, pylu aktivovaného *in vitro* 5 minut a pylu aktivovaného *in vitro* 30 minut. Tabák virginský se tak stal první krytosemennou rostlinou (Angiospermae) s identifikovaným fosfoproteomem z aktivovaného pylu; u prvního fosfoproteomu samčího gametofytu získaného z huseníčku rolního byl analýzám podroben pouze zralý pyl (Mayank et al., 2012). Jedinými dalšími pylovými láčkami, jež byly podrobeny fosfoproteomickým experimentům, byly pylové láčky smrku Wilsonova *(Picea wilsonii*; Chen et al., 2012), který ale patří mezi nahosemenné rostliny (Gymnospermae). Fosfopeptidy s regulačními trendy v průběhu pylové aktivace byly rozděleny do sedmi skupin v závislosti na vykázaném regulačním trendu, s tím, že nejpočetnější skupina zahrnovala fosfopeptidy identifikované výhradně ve zralém pylu.

Celkově bylo identifikováno 471 fosforylovaných peptidů, v jejichž sekvencích byla určena přesná pozice 432 fosforylačních míst. Znatelně se tak rozšířil počet fosfopeptidů oproti předchozí fosfoproteomické studii, jež tvořila značnou část mé diplomové práce a v níž bylo přesně lokalizováno pouhých 52 fosforylačních míst (Fíla et al., 2012). Identifikované peptidy pocházely z 301 fosforylovaných proteinů, které byly rozděleny do třinácti funkčních kategorií. Nejhojněji zastoupenými kategoriemi se staly transkripce, translace, cílení a skladování proteinů a přenos signálu. Za zmínku rovněž stojí fosfoproteiny s neznámou funkcí nebo nejasnou klasifikací, které souhrnně dosáhly pětiny identifikovaných fosfoproteinů. Značný podíl těchto proteinů poukazuje na fakt, že mnohé pylově specifické proteiny doposud nejsou prozkoumány. Právě tyto proteiny by v budoucnu mohly být žhavými kandidáty zastávajícími životně důležité funkce při vývoji samčího gametofytu.

Kromě toho byly identifikované fosfopeptidy podrobeny vyhledávání fosforylačních sekvenčních motivů. V průběhu těchto analýz bylo nalezeno pět sekvenčních motivů s centrálním fosfoserinem (tedy xxxxxxS*Pxxxxx, xxxRxxS*xxxxxx, xxxKxxS*xxxxxx, xxxxxxS*DxExxx a xxxxxxS*xDDxxx), z nichž dva motivy byly společné s fosfoproteomem pylového fosfoproteomu huseníčku rolního, konkrétně xxxxxxS*Pxxxxx a xxxRxxS*xxxxxx. Jeden motiv pak nesl v centrální pozici fosfothreonin (xxxxxxT*Pxxxxx), ale byl nalezen pouze v pylovém fosfoproteomu tabáku virginského. K nalezeným sekvenčním motivům byly predikcí vytipovány proteinové kinázy, které mají zodpovídat za fosforylaci příslušných

motivů. Členové těchto kinázových rodin byli vyhledáni v pylovém proteomu tabáku virginského a huseníčku rolního. Jednalo se o mitogenem aktivované proteinové kinázy a cyklin-dependentní proteinové kinázy (rozpoznávající motivy xxxxxxS*Pxxxxx a xxxxxxT*Pxxxxx), Ca^{2+}-dependentní proteinové kinázy a Ca^{2+}-dependentní proteinové kinázy–příbuzné kinázám nefermentujícím sacharózu (s cílovými motivy xxxRxxS*xxxxxx a xxxKxxS*xxxxxx) a kaseinové kinázy (fosforylující motivy xxxxxxS*DxExxx a xxxxxxS*xDDxxx). Kromě kináz nalezených ve fosfoproteomu byl prohledán soubor sekretomických dat pylových láček tabáku virginského (Hafidh et al., 2016b), kde byly nalezeny kinázy ze dvou rodin – malectin/receptorové proteinové kinázy a Ca^{2+}-dependentní proteinové kinázy.

Tato práce tak přispěla k odhalení nových fosforylačních míst ze zralého pylu tabáku virginského *(Nicotiana tabacum)*, která doposud nebyla identifikována a jako první podrobila fosfoproteomickým technikám dvě stádia aktivovaného pylu tabáku, coby první krytosemenné rostliny. I když provázání jednotlivých substrátů a kináz nebylo experimentálně podloženo, jedná se o zajímavý startovací soubor dat, díky němuž se snadněji budou vybírat fosfoproteinoví kandidáti i samotné proteinové kinázy pro následné funkční studie.

6. Závěry práce v angličtině (English summary)

The experiments presented within the scope of this Ph.D. thesis led to the identification of phosphorylated peptides from three stages of tobacco *(Nicotiana tabacum)* male gametophyte: mature pollen grains, pollen activated *in vitro* 5 min, and pollen activated *in vitro* 30 min. Tobacco became the first angiosperm species (Angiospermae) with phosphoproteome identified from activated pollen since the first angiosperm phosphoproteomic studies on male gametophyte were carried out exclusively on mature pollen (Mayank et al., 2012). The only alternative study performed on activated pollen or pollen tubes is the analysis of *Picea wilsonii* (Chen et al., 2012), which belongs to gymnosperms (Gymnospermae). Phosphopeptides regulated during pollen activation were put into seven groups according to their regulatory trend, making the mature pollen-specific phosphopeptides the most abundant category.

In total, there were identified 471 phosphorylated peptides with 432 unambiguously positioned phosphorylation sites. The number of unambiguous phosphorylation sites identified in mature pollen increased notably since in the previous tobacco phosphoproteomic study that represented a notable part of my diploma thesis, there were identified only 52 phosphosites (Fíla et al., 2012). The identified phosphopeptides originated from 301 phosphorylated proteins, which were divided into 13 functional categories. The most prominent categories were transcription, translation, protein destination and storage, and signal transduction. The proteins with unknown or unclear classification were also worth mentioning since they collectively occupied nearly one fifth of the presented phosphoproteome. It tends to speculate that these candidates represent the pollen-specific proteins, function of which remains still unknown. These proteins might represent hot candidates playing an essential role during male gametophyte development.

Furthermore, the identified phosphopeptides were searched for the phosphorylation motifs. There were identified five motifs with a central phosphoserine (namely xxxxxxS*Pxxxxx, xxxRxxS*xxxxxx, xxxKxxS*xxxxxx, xxxxxxS*DxExxx, and xxxxxxS*xDDxxx), two of which were common with *Arabidopsis thaliana* mature pollen phosphoproteome (xxxxxxS*Pxxxxx, and xxxRxxS*xxxxxx in particular). Only one motif carried in its central position a phosphorylated threonine (xxxxxxT*Pxxxxx) but it was identified exclusively in tobacco male gametophyte phosphoproteome. There were predicted kinases that should recognize these sequence motifs. Members of these kinase families were

then found in pollen proteomes of *Nicotiana tabacum* and *Arabidopsis thaliana*: mitogen-activated protein kinases, and cyclin-dependent protein kinases (recognizing motifs xxxxxxS*Pxxxxx, and xxxxxxT*Pxxxxx), Ca^{2+}-dependent protein kinases, and Ca^{2+}-dependent protein kinase–sucrose-non-fermenting-related kinases (with target motifs xxxRxxS*xxxxxx, and xxxKxxS*xxxxxx), and casein kinases (phosphorylating motifs xxxxxxS*DxExxx, and xxxxxxS*xDDxxx). The other dataset subjected to kinase search was tobacco pollen tube secretome (Hafidh et al., 2016b) where two kinase families were identified, namely malectin/receptor protein kinases, and Ca^{2+}-dependent protein kinases.

This thesis presents data that strongly contributed to the identification of novel phosphorylation sites from tobacco mature pollen, and moreover it subjected two activated stages of tobacco male gametophyte as the first angiosperm species to the phosphoproteomics studies. Although the associations of kinases and their substrates was not experimentally proven, it represents an interesting data set, which will assist in selection of proper phosphoprotein candidates and protein kinases for the subsequent functional studies.

7. Publikované články

Součástí této disertační práce jsou výsledky publikované celkem ve čtyřech impaktovaných publikacích, a to ve dvou původních článcích (z nichž na jednom jsem prvním autorem) a dvou přehledových článcích (z nichž jsem opět na jednom prvním autorem).

7.1. Fosfoproteom samčího gametofytu tabáku virginského

Fíla, J., Radau, S., Matros, A., Hartmann, A., Scholz, U., Feciková, J., Mock, H.-P., Čapková, V., Zahedi, R. P., Honys, D. (2016). Phosphoproteomics profiling of tobacco mature pollen and pollen activated *in vitro*. Molecular & Cellular Proteomics 15, 1338–1350. doi: 10.1074/mcp.M115.051672. $IF_{2014} = 6{,}564$

V této publikaci jsem se podílel na samotných experimentech – sběru pylu, aktivaci pylu a extrakci proteinů. Posléze jsem analyzoval dodaná fosfoproteomická data – vyhledával jsem kinázové motivy, třídil proteiny do funkčních kategorií a výraznou měrou jsem dotvářel finální tabulky. Taktéž jsem se podílel na psaní manuskriptu této publikace.

Phosphoproteomics Profiling of Tobacco Mature Pollen and Pollen Activated *in vitro**[S]

Jan Fíla‡ ‡‡, Sonja Radau§‡‡, Andrea Matros¶‡‡, Anja Hartmann¶, Uwe Scholz‖, Jana Fecíková‡, Hans-Peter Mock¶, Věra Čapková‡, René Peiman Zahedi§, and David Honys‡**

Tobacco mature pollen has extremely desiccated cytoplasm, and is metabolically quiescent. Upon re-hydration it becomes metabolically active and that results in later emergence of rapidly growing pollen tube. These changes in cytoplasm hydration and metabolic activity are accompanied by protein phosphorylation. In this study, we subjected mature pollen, 5-min-activated pollen, and 30-min-activated pollen to TCA/acetone protein extraction, trypsin digestion and phosphopeptide enrichment by titanium dioxide. The enriched fraction was subjected to nLC-MS/MS. We identified 471 phosphopeptides that carried 432 phosphorylation sites, position of which was exactly matched by mass spectrometry. These 471 phosphopeptides were assigned to 301 phosphoproteins, because some proteins carried more phosphorylation sites. Of the 13 functional groups, the majority of proteins were put into these categories: transcription, protein synthesis, protein destination and storage, and signal transduction. Many proteins were of unknown function, reflecting the fact that male gametophyte contains many specific proteins that have not been fully functionally annotated. The quantitative data highlighted the dynamics of protein phosphorylation during pollen activation; the identified phosphopeptides were divided into seven groups based on the regulatory trends. The major group comprised mature pollen-specific phosphopeptides that were dephosphorylated during pollen activation. Several phosphopeptides representing the same phosphoprotein had different regulation, which pinpointed the complexity of protein phosphorylation and its clear functional context. Collectively, we showed the first phosphoproteomics data on activated pollen where the position of phosphorylation sites was clearly demonstrated and regulatory kinetics was resolved. *Molecular & Cellular Proteomics 15: 10.1074/mcp.M115.051672, 1338–1350, 2016.*

From the ‡Laboratory of Pollen Biology, Institute of Experimental Botany ASCR, v.v.i., Rozvojova 263, 165 00 Praha 6, Czech Republic; §Leibniz-Institut für Analytische Wissenschaften-ISAS-e.V., Otto-Hahn-Straβe 6b, 44227 Dortmund, Germany; ¶Department of Physiology and Cell Biology, Leibniz Institute of Plant Genetic and Crop Plant Research, Corrensstraβe 3, 06466 Gatersleben, Germany; ‖Department of Breeding Research, Leibniz Institute of Plant Genetic and Crop Plant Research, Corrensstraβe 3, 06466 Gatersleben, Germany

Tobacco mature pollen represents an extremely resistant structure filled with a desiccated cytoplasm that is surrounded by an extremely tough cell wall. This metabolically quiescent stage of male gametophyte has to reach stigma tissue in a viable state. After pollination, the rehydration and metabolic activation of a pollen grain starts. The pollen activation is represented by a time period when there is no pollen tube growth, and only metabolic processes within the original volume of cytoplasm occur together with cytoplasm hydration (1). Within this period, the pollen aperture later used for pollen tube outgrowth is selected. After that, a rapid pollen tube tip growth starts in order to deliver the genetic information carried by two sperm cells to the ovaries. Desiccated mature pollen of many angiosperm species can be also rehydrated and activated *in vitro* (2). Here we aim to elucidate the regulation processes of pollen grain re-hydration and activation mediated by protein phosphorylation.

Protein phosphorylation, representing one of the most frequent regulatory mechanisms, was shown to control a number of cellular processes, such as signal transduction, regulation of transcription and translation, regulation of cytoskeleton dynamics, cell cycle regulation, metabolism regulation, regulation of protein stability, and protein targeting (3–5). Similar to pollen activation, the rehydration of African xerophyte *Craterostigma plantagineum* was accompanied by changes in protein phosphorylation (6). Attachment of a phosphate group to the polypeptide chain shifts the pI of a protein to more acidic range (7). Such pI shift usually causes changes of protein conformation within a single domain (8) or even influences domain-domain interactions (9). In case of enzymes, phosphorylation sometimes inhibits activity by occupying the active site of the protein, as was documented for instance for isocitrate dehydrogenase (10).

In order to be able to identify phosphorylated proteins, it is inevitable to apply some of the various enrichment protocols (11, 12) because of several reasons: (i) Phosphoproteins are mostly low abundant so they are overwhelmed by the excess

of nonphosphorylated proteins. (ii) A given protein is expressed in many copies and contains many potential phosphorylation sites (Ser/Thr/Tyr residues), but individual phosphorylation sites are usually only partly phosphorylated— *i.e.* only a small share of the present protein molecules will be phosphorylated at a given position whereas the majority will be nonphosphorylated. (iii) The identification of phosphopeptides by mass spectrometry is still challenging from the technical point of view. The enrichment can be performed at two levels. The first possibility is to fish the intact phosphoproteins out of a protein mixture whereas the second approach relies on the enrichment of phosphorylated peptides of the protease-digested protein sample. A plethora of protocols are meanwhile available for both approaches, whereas for both advantages as well as disadvantages have been reported (11). In order to broaden the phosphoproteome coverage, a tandem procedure applying first the former approach and then after protease cleavage also the latter one was suggested (13, 14).

The first angiosperm pollen phosphoproteome published was that of *Arabidopsis thaliana* (15), which completed the pollen proteomic data because before that, three Arabidopsis pollen proteomic data sets achieved by the conventional in-gel approach (16–18) and one high-throughput proteomic study (19) were published. Mayank and colleagues identified many phosphopeptides, notable number of which played their roles in regulation of metabolism and protein function, metabolism, protein fate, binding other proteins, signal transduction, and cellular transport. Many kinases were identified in the data set, showing that these were indeed subject to phosphorylation, for instance AGC protein kinases, calcium-dependent protein kinases, and sucrose non-fermenting 1-related protein kinases (15).

The tobacco pollen proteome was studied directly by a high-throughput approach but appeared only recently (20). In this study, Ischebeck and colleagues compared the proteome of eight male gametophyte stages ranging from diploid microsporocytes to pollen tubes. Interestingly, the first tobacco pollen phosphoproteomic paper appeared earlier than the whole proteome was published (21). In order to identify phosphoproteins in tobacco mature pollen and pollen activated *in vitro* for 30 min, metal oxide/hydroxide affinity chromatography phosphoprotein enrichment employing an aluminum hydroxide matrix (Al(OH)$_3$) was carried out (22). This approach led to the identification of only one phosphorylation site, so that additionally titanium dioxide (TiO$_2$)[1] enrichment was ap-

plied, identifying 51 more phosphorylation sites in the already-identified proteins from mature pollen. Among those proteins were for instance various translation initiation and elongation factors, metabolic proteins (for instance fructose bisphosphate-aldolase, glyceraldehyde-3-phosphate dehydrogenase, and alcohol dehydrogenase), Rho guanine nucleotide dissociation inhibitor, and several ribosomal proteins. However, not many signaling proteins were identified in this study. The third male gametophyte phosphoproteome revealed to date was that of a gymnosperm *Picea wilsonii*. However, the proteome of this species was studied from the perspective of deficient growth media, and several phosphoproteins linked to Ca^{2+} and sucrose deficiency were identified (23).

The present study is a continuation of our male gametophyte phosphoproteomic studies. Herein, we employed phosphopeptide enrichment by metal oxide/hydroxide affinity chromatography with TiO$_2$ matrix (24) on three stages of male gametophyte, this time including two stages of activated pollen (5 min and 30 min) as well as mature pollen. Collectively, 471 phosphopeptides carrying 432 phosphorylation sites (phosphoRS probabilities >90%) have been identified in the three stages of male gametophyte. These phosphorylation sites belonged to 301 phosphoproteins that were classified into 13 functional categories; with transcription, protein synthesis, destination and storage, as well as signal transduction being the dominant functional groups. A phosphorylation motif search revealed 5 motifs with a central phosphoserine and one motif with a central phosphothreonine. Quantitative data led to the discovery of regulated phosphopeptides, which were grouped into seven categories based on their regulatory trends throughout the studied developmental stages.

EXPERIMENTAL PROCEDURES

Plant Material and Pollen Activation In Vitro—Tobacco plants (*Nicotiana tabacum* cv. Samsun) were grown in a greenhouse from April to September. Flower buds shortly before anthesis were collected between June and September. Anthers were removed from the buds and let dehisce at room temperature on a filtration paper overnight. Then, mature pollen was sieved by a stocking and stored at −20 °C (25) until it was further used. The collected pollen represented bulk samples originating from three groups of 15 plants that were grown in separate parts of the greenhouse. These bulk samples were further referred to as the three biological replicates.

Mature pollen was activated *in vitro* as a shaken suspension for 5 min, and 30 min, respectively, each stage in three biological replicates

---

[1] The abbreviations used are: page: TiO$_2$, titanium dioxide; Al(OH)$_3$, aluminium hydroxide; bZIP, basic leucine zipper; CAMK2, Ca^{2+}/calmodulin-dependent protein kinase; CDK, cyclin-dependent protein kinase; CDPK—SnRK, Ca^{2+}-dependent protein kinase–sucrose-non-fermenting-related kinase; CK2, casein kinase 2; Cys, cysteine; DCN1, defective in cullin neddylation protein 1; DHB, 2,5–dihydroxybenzoic acid; EPP, EDTA/puromycine-resistant particle; GO, gene ontology; IMAC, immobilized metal affinity chromatography;
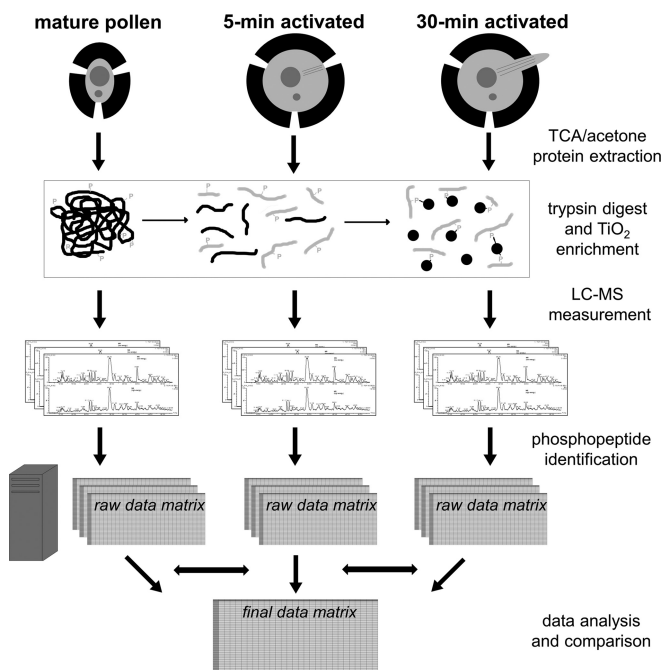
LEA, late embryogenesis abundant; MAPK, mitogen-activated protein kinase; Met, methionine; MS/MS, tandem mass spectrometry; nLC, nano liquid chromatography; PB1, octicosapeptide/PHOX/BEM1p; PPI1, peptidyl-prolyl cis-trans isomerase 1; Rho GAP, Rho GTPase activation protein; Rho GDI2, Rho guanine nucleotide dissociation inhibitor 2; RNF4, RING FINGER PROTEIN 4; Ser, serine; SIMAC, sequential elution from IMAC; SMM-MES, sucrose-mineral medium buffered with MES; SNC1, SUPRESSOR OF NPR1–1, CONSTITUTIVE 1; Thr, threonine; Tyr, tyrosine; UBA, ubiquitin-associated; UBX, ubiquitin-like; UNC-89, UNCOORDINATED-89; WVD2, WAVE-DAMPENED 2.

FIG. 1. **A schematic workflow of the performed experiments.** The three stages of tobacco male gametophyte (particularly mature pollen, pollen activated *in vitro* for 5 min and pollen activated *in vitro* for 30 min) were subjected to TCA/acetone protein extraction, trypsin digest and phosphopeptide enrichment by TiO_2. The obtained phosphopeptide-enriched eluate was fractionated by nLC and measured by MS/MS. The present phosphopeptides were identified (if possible with the unambiguous position of the phosphosite) and the results further analyzed.

as mentioned above, at 27 °C in sucrose-mineral medium buffered with MES (SMM-MES; 175 mM sucrose, 1.6 mM boric acid, 3 mM $Ca(NO_3)_2 \cdot 4H_2O$, 0.8 mM $MgSO_4 \cdot H_2O$, 1 mM KNO_3, 25 mM MES, pH 5.9) (26). The activated pollen was then harvested by filtration on a vacuum pump-driven apparatus, and immediately frozen in liquid nitrogen. The three stages differ from each other as follows: mature pollen represents an oval-shaped structure with a desiccated cytoplasm. Upon re-hydration, 5-min activated pollen becomes round-shaped with a hydrated cytoplasm. Furthermore, one pollen aperture is usually chosen for pollen tube outgrowth after 30-min imbibition (see supplemental Fig. S1).

Protein Extraction and Phosphopeptide Enrichment—The total proteins were extracted from all the above stages by TCA/acetone precipitation (27) with slight modifications (21) in three biological replicates as mentioned above (see Fig. 1 for workflow overview). In detail, mature or activated pollen was homogenized by a pestle in a mortar. The acquired fine powder was resuspended in 10 volumes of 10% w/v TCA in acetone supplemented with 1% w/v DTT. After 5 min sonication in an ultrasonic bath, the samples were briefly frozen in liquid nitrogen, incubated at −20 °C for 45 min, and centrifuged (23,000 × *g*, 15 min, 4 °C). After the removal of the supernatant, the samples were washed by 1.5 ml acetone with 1% w/v DTT, sonicated for 5 min, briefly frozen in liquid nitrogen, and kept at −20 °C for 30 min. After the centrifugation under the above conditions, the washing step was repeated. Finally, the pellet was dried and stored at −20 °C.

The total protein extracts from all stages were resuspended in 0.2 M guanidinium chloride and 50 mM ammonium bicarbonate supplemented with PhosStop phosphatase inhibitor mixture (Roche, Penzberg, Germany), carbamidomethylated as described elsewhere (28)

and subsequently trypsin-digested (trypsin-to-protein ratio 1:50; 37 °C, 12 h).

There were three biological replicates for each studied stage. For each of the triplicates, 500 μg peptides were dissolved in loading buffer (80% v/v ACN, 6% v/v TFA, saturated with phthalic acid) and subjected to phosphopeptide enrichment by TiO_2. Seven synthetic peptides were spiked to the peptide mixture in order to check the reproducibility of the replicates. The phosphopeptides bound to TiO_2 beads were washed and eluted as described previously (21, 29).

nLC-MS/MS Measurement and Phosphopeptide Identification—The phosphopeptide-enriched samples were analyzed by nLC-MS/MS on an LTQ Orbitrap Elite (Thermo Fisher Scientific, Bremen, Germany) mass spectrometer coupled to an Ultimate 3000 nLC (Thermo Fisher Scientific). Peptides were pre-concentrated on a self-packed Synergi HydroRP trapping column (100 μm ID, 4 μm particle size, 10 nm pore size, 2 cm length) and separated on a self-packed Synergi HydroRP main column (75 μm ID, 2.5 μm particle size, 10 nm pore size, 30 cm length) at 60 °C and a flow rate of 270 nl·min^{-1} using a binary gradient (A: 0.1% formic acid, B: 0.1% formic acid, 84% ACN) ranging from 3% to 45% B in 240 min.

MS survey scans were acquired from 350–2000 *m/z* in the Orbitrap at a resolution of 60,000 using the polysiloxane m/z 445.120030 as lock mass. The ten most intense ions were subjected to collision-induced dissociation and MS/MS using normalized collision energy of 35% and an activation time of 30 ms and MS/MS were acquired in the LTQ. AGC values were set to 10^6 for MS and 10^4 for MS/MS scans.

The acquired spectra were searched against the TIGR EST sequence database for Tobacco (ftp://occams.dfci.harvard.edu/pub/bio/tgi/data/; release version 10/04/2011, 48961 entries) using Proteome Discoverer 1.3 with Mascot. Quantification, false discovery assessment and phosphorylation site localization were performed using the following nodes: Precursor Ions Area Detector, Peptide Validator, and phoshoRS (30). Searches were conducted with the following settings: 10 ppm MS tolerance, 0.5 Da MS/MS tolerance, trypsin as a cleaving enzyme with max. two missed cleavage sites, carbamidomethylation (Cys) as fixed, and oxidation (Met) together with phosphorylation (Ser, Thr, Tyr) as variable modifications. Finally, the results were subjected to the filtering criteria of mass deviation ≤ 4 ppm and high confidence (corresponding to a false discovery rate <1% on the peptide-spectrum match level). The standard deviation of the peak areas of the synthetic peptides was below 25% so the results were considered reproducible. Peak areas were considered per peptide, *i.e.* different charge states were combined. Of all identified phosphopeptides, only the ones that showed a standard deviation <30% of the abundance between the biological replicates of the same stage, and that were identified in all of the replicates were listed in the result tables. Moreover, only phosphopeptides with an unambiguously assigned phosphorylation site with a probability higher than 90% (phoshoRS) were considered. All raw data and search results have been deposited in proteomeXchange (31) with the accession PXD003042.

nLC-MS/MS of the Trypsinized Crude Protein Extract—For each sample ~1 μg of the trypsin digest was analyzed by nLC-MS/MS prior to TiO_2 enrichment, using the same conditions as above. Data analysis was also conducted as above, however, omitting phosphorylation as variable modification. Only proteins meeting the following criteria were quantified: (1) at least 2 unique peptides quantified in at least 2 out of 3 biological replicates, (2) for all conditions standard deviations between biological replicates had to be <40%. Proteins that differed among any of two studied stages at least twofold in abundance were considered as regulated.

Protein Categories and Motif Search—The gene ontology (GO) and enzyme codes were originally acquired by Blast2GO ver 2.7.2 (https://www.blast2go.com); the identified tobacco ESTs translated in the

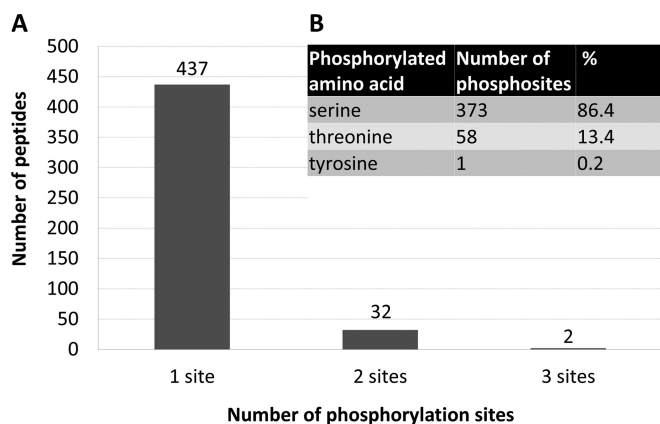| Phosphorylated amino acid	Number of phosphosites	%
serine	373	86.4
threonine	58	13.4
tyrosine	1	0.2

Fig. 2. **The statistics of identified phosphopeptides.** *A*, Column diagram showing the number of phosphopeptides according to the number of unambiguously identified phosphorylation sites in a single peptide. If a phosphorylation site was identified in more than one peptide, it was counted repeatedly every time on every peptide. *B*, Number of phosphorylation sites according to the phosphorylated amino acid (serine, threonine, or tyrosine) identified. If a phosphorylation site was identified in more than one peptide, it was counted only once.

longest reading frame were searched against the Arabidopsis proteome. For many of the sequences, the GO terms (divided into three groups: molecular function, biological process, and cellular compartment) together with the EC enzyme codes were assigned according to the homologous Arabidopsis sequences. However, some of the tobacco sequences lacked their Arabidopsis homologue in the proteome database and/or the gene ontology was not informative enough. So finally, the acquired GO terms were manually converted to protein categories and subcategories according to Bevan *et al.* (32) to enable better categorization of the data. In case a protein had more functions, it was catalogued according to the prevailing function.

All unambiguous phosphopeptides (supplemental Table S2) were analyzed for the significant phosphorylation motifs by Motif-X software (33, 34). Two searches were performed, one looking up phosphorylated serine and the other one searching for phosphorylated threonine (phosphotyrosine motifs were not searched because there was only one phosphorylated tyrosine in the phosphopeptide data set). The width of a phosphorylation motif was set to 13 (where the phosphoamino acid was placed into the central position), number of occurrences to 15, and significance score to 0.000001. As a background, data set of tobacco Uniprot sequences was uploaded.

The regulated phosphopeptides were manually divided into seven categories according to their regulatory trends. The motif search was not performed on the regulated phosphopeptide data set because it contained only a limited number of phosphopeptides. The graphical representation of the peptide abundances in the various stages was performed by the VANTED software package (http://www.vanted.org, ref. 35).

RESULTS

Phosphopeptide Enrichment and Identification—In this study, 471 phosphopeptides were identified with an unambiguously assigned position of the phosphorylation site (supplemental Tables S1 and S2). The vast majority of the identified phosphopeptides was singly phosphorylated (437), whereas only a minority was doubly (32) or triply phosphorylated (2), see Fig. 2*A*. These 471 identified phosphopeptides

contained collectively 432 unique unambiguous phosphorylation sites. The number of unique phosphorylation sites is lower than the number of phosphosites identified in all phosphopeptides because some of the identified phosphorylation sites were redundant. Such a redundancy was observed for instance in case of couples of peptides, where one of which was completely cleaved whereas the other carried one missed-cleaved trypsin site (*e.g.* represented by the peptides KQLVSVAS*AVK and QLVSVAS*AVK from adenine nucleotide α hydrolases-like protein or peptides S*WDDADLK and S*WDDADLKLPGK from eukaryotic translation initiation factor 5B-like protein; an asterisk represents the phosphorylation site) or alternatively in case of two peptides, one of which was oxidized on a methionine whereas the other was not modified in that way (*e.g.* peptides KENVGPMVNLENPTS*PK and KENVGPmVNLENPTS*PK from low-temperature-induced 65 kDa protein or peptides EES*DDDMGFSLFD and EES*DDDm-GFSLFD from acidic ribosomal protein P1a-like protein; an asterisk represents phosphorylation site, and lowercase "m" represents an oxidized methionine).

Because conventional phosphoproteomic workflows were applied, only *O*-phosphorylated amino acids were identified, particularly serine, threonine, and tyrosine (Fig. 2*B*). The dominant phosphorylated amino acid was phosphoserine with 373 phosphorylation sites (86.4%), followed by phosphothreonine represented by 58 phosphorylation sites (13.4%). Only one phosphorylation site (corresponding to 0.2%) was detected on a tyrosine making it the rarest phosphorylated amino acid in the data set.

Identified Phosphoprotein Categories—The 471 identified phosphopeptides revealing 432 unique phosphorylation sites were assigned to 301 proteins as several proteins contained more than one phosphorylation site. A protein was defined throughout the article as a sequence identified either with a single accession number or with a unique combination of accession numbers. The combination of accession numbers was applied in case of one peptide being assigned to two or more identifiers, *e.g.* the couple NT_TC85822_1 and NT_TC87771_1 or the pair NT_TC82971_1 and NT_TC77872_1). Also, some accession numbers were assigned to more than one peptide, either as an exclusive number (*e.g.* NT_TC95936_1 or NT_TC83486_1), or in combination with another accession (*e.g.* NT_TC95936_1 and NT_FG166442_1, or NT_TC83486_1 and NT_FG175056_1). Thus, a row in supplemental Table S1 represents a single protein; the phosphopeptides belonging to one phosphoprotein are put together into one cell. The proteins were annotated according to the original TIGR protein descriptions. However, many of these annotations were not explanatory enough so in case of some phosphoproteins, the annotation was improved using the homologues found by tblastx in the GenBank database (http://blast.ncbi.nlm.nih.gov).

The annotated proteins were sorted according to their prevailing function. The GO search was performed by blast2GO

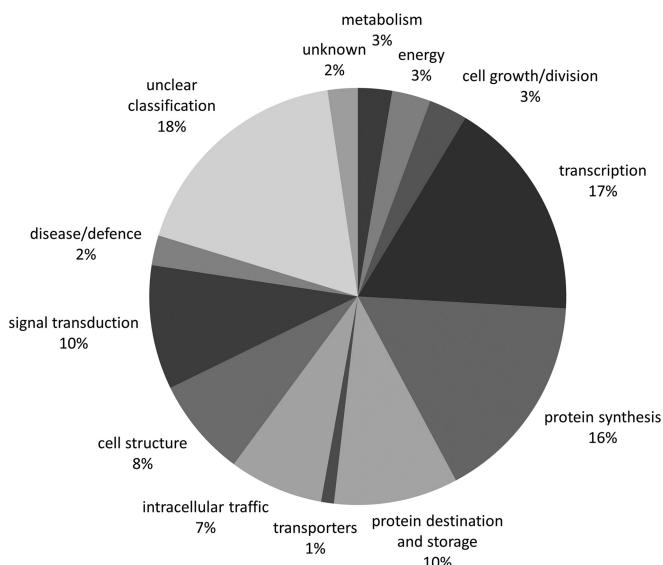FIG. 3. **Pie chart showing the percentage of the individual phosphoprotein categories.**

software (https://www.blast2go.com). Because the obtained results did not allow an easy categorization according to protein function, the gene ontology assignment was further performed manually into the categories according to Bevan *et al.* (32). Every protein was catalogued into just one category. In case one protein had more distinct functions, it was sorted into the category with the dominant function. The difference between "unclear classification" and "unknown" was as follows: the proteins with a known homologue and/or annotation (characterizing them only to some extent) with an unclear function were catalogued as "unclear classification" whereas the proteins without a known homologue and/or functional annotation were classified as "unknown." The protein categories are summarized by a pie chart in Fig. 3. The main category cataloguing almost one fifth of the phosphoproteins was represented by species with "unclear classification." Over one quarter of proteins (falling into two separate categories, protein synthesis, and protein destination and storage) was connected with translation. More than 10% belonged also to transcription (17%), and exactly 10% to signal transduction. Cell structure and intracellular traffic reached 8% or 7%, respectively. The other categories were represented only by a few percent: metabolism, energy, cell growth/division, disease/defense, unknown, and transporters. For enzymes, the EC numbers are given in supplemental Table S2.

Motif Analysis—Protein phosphorylation occurs usually on particular short amino acid motifs rather than on random sequences. Some of these motifs can be kinase-specific so their knowledge can reveal cellular regulatory networks in more detail. The dominant phosphorylation motifs in our data set compared with the random background based on the tobacco sequences from Uniprot protein (http://www.uniprot.org) database were identified by Motif-X software (supple-

mental Fig. S2). Two independent searches were performed - one focused on phosphoserine motifs and the other one looking up phosphothreonine motifs. The phosphotyrosine was not subjected to this analysis because only one phosphorylated tyrosine was present in the entire data set. The phosphorylation motifs had to be found at least 15 times in the experimental data set to be considered. The most abundant phosphoserine motif and the only phosphothreonine motif were represented by the phosphorylation site that was followed by a prolin: xxxxxxS*Pxxxxx, and xxxxxxT*Pxxxxx (where phosphorylation site is marked by an asterisk and the position that can be occupied by any amino acid is shown as "x"). The proline motif with a serine was detected 118 times, whereas proline following a threonine was found only 31 times. The remaining phosphoserine motifs were two basic and two acidic ones. The basic motifs were represented by a phosphorylated serine, preceded by a lysine or an arginine followed by any two amino acids. In particular, the motif xxxRxxS*xxxxxx was detected 37 times, whereas the slightly less abundant xxxKxxS*xxxxxx was carried by 30 phosphorylated peptides. The acidic motifs were composed of a serine followed either by a glutamic acid, one any amino acid, and a glutamic acid or by one any amino acid with two glutamic acids. The motif xxxxxxS*DxExxx was found 23 times whereas the second acidic motif xxxxxxS*xDDxxx was present in 15 phosphopeptides (supplemental Fig. S2). The kinase families that usually recognize such motifs are referred to more in detail in the discussion.

Regulated Phosphopeptides—In order to determine whether substantial changes on the level of protein expression occurred between the different time points, additional nLC-MS/MS measurements were performed on the complex peptide mixture without prior TiO_2 enrichment.

The concentration of the nonphosphorylated peptides from this analysis served as a reference (protein abundance), and the abundance of the phosphopeptides was compared with this reference. Some of the phosphorylated peptides changed their concentration in accordance with the abundance changes of the whole protein. The global abundance ratios of these phosphoproteins are shown in supplemental Table S3 in red. The concentration of such phosphorylated peptides changed likely because of the synthesis or degradation of the whole proteins rather than as a consequence of the sole phosphorylation or dephosphorylation. On the other hand, other phosphorylated peptides did not reflect the concentration changes of the corresponding proteins and showed either opposite abundance change or showed a changed abundance exclusively at the phosphopeptide level (and not on the level of the whole protein). The concentration ratio of such proteins is shown in supplemental Table S3 in black. Such changes in phosphopeptide abundance that were not reflected by the concentration of the whole protein are likely to be caused exclusively by protein phosphorylation or dephosphorylation processes.

Because proteins were quantified based on at least two unique peptides leading to a reduced precision compared with single peptide-based phosphopeptide quantification, here the maximum standard deviation allowed among biological replicates was 40%, compared to 30% for phosphopeptides. Moreover, because of the increased complexity of the samples the identification in two out of three candidates was considered sufficient.

The proteins considered to be of a different abundance had to show twofold difference between at least two stages. If we consider these proteins and the phosphopeptides that belonged to them, we counted 209 phosphopeptides, which were sorted into seven regulatory groups (see Fig. 4 and supplemental Fig. S3). The first three groups presented phosphopeptides that were identified exclusively in one of the three studied stages. The highest number of phosphorylated peptides fell into the category unique for mature pollen—135 phosphopeptides (group I). Nine phosphopeptides were identified exclusively in both 5-min (group II), and 30-min activated pollen (group III). The other three groups contained phosphorylated peptides that were detected in two stages out of three. Twenty-one common phosphorylated peptides were detected in 5-min and 30-min activated pollen (group IV), and 19 common phosphopeptides were detected in mature pollen and 30-min activated pollen (group VI). Only nine phosphopeptides fell into the group that was missing in 30-min activated pollen (group V). The last regulation group was represented by the phosphopeptides common to all three stages, represented by seven phosphopeptides (group VII).

The main protein categories where the regulated phosphopeptides belong to were transcription, translation, and protein synthesis and storage (please refer to the pie charts in Fig. 4). These categories collectively accounted for one third to one half of phosphopeptides in the respective regulation group. Quite common were also phosphopeptides with "unclear classification" that accounted for about a quarter of the phosphopeptides in the regulatory groups exclusive to any of the stages (group I, II, and III), and in the group IV with the common regulation to the 5-min and the 30-min activated stage. Furthermore, it represented almost a half in the group VI (*i.e.* peptides that were absent from 5-min activated pollen). In the regulation group VII (common to all studied stages), the functional category "unclear classification" was supplemented with "unknown," which represented over a quarter of identified phosphopeptides.

Group I, and group V represented the phosphopeptides that were phosphorylated in mature pollen, and then were dephosphorylated upon pollen activation. Exclusive phosphosites in mature pollen, concentration changes of which were not reflected by changes on the protein level were represented for instance by eukaryotic initiation factor 4B, various RNA binding proteins, mini zinc finger protein, C2 domain-containing protein, ubiquitin-activating enzyme 2, vesicle-associated protein 25, MODIFIER OF SNC1 (SUPRESSOR OF NPR1–1, CONSTITUTIVE 1) 1-like protein, and a variety of proteins with unclear classification, such as muscle M-line assembly protein UNCOORDINATED-89-like (UNC-89-like), dentin sialophosphoprotein-like protein, and glycine-rich protein 2. The phosphosites that were shared by 5-min activated pollen and mature pollen were found for example in eukaryotic translation initiation factor 4γ-like protein, nucleic acid binding protein, UBA (ubiquitin associating) and UBX (ubiquitin-like) domain-containing protein At4g15410-like, auxilin-related protein 2-like, and pollen tube Rho guanine nucleotide dissociation inhibitor 2 (Rho GDI2). The groups II, III, and IV were composed of phosphorylation sites that appeared only upon pollen activation. There were detected for instance zinc finger CCCH domain-containing protein 31-like protein, ribosomal protein S6-like, protein phosphatase inhibitor 2-like protein, serine/arginine-rich splicing factor RS2Z32-like, E3 ubiquitin-protein ligase RING FINGER PROTEIN 4 (RNF4)-like, WD repeat-containing protein 24 homolog, cytochrome *c* oxidase subunit 5b-1 protein, methyl-CpG-binding domain 10 protein, histone deacetylase 1 (HDT 1). The most dynamic regulatory trend was documented by group VI, peptides of which showed phosphorylation in mature pollen, then temporary dephosphorylation immediately upon pollen activation and a re-phosphorylation later during pollen activation (30 min). Such a dynamic regulation was detected in these phosphoproteins: phospholipase A2/esterase, bZIP transcription factor bZIP100, acidic ribosomal protein P1a-like protein, late embryogenesis abundant (LEA) proteins, RNA binding proteins and transcription initiation factor IIF subunit α-like protein. Finally, group VII collected the proteins that were present in all stages and showed significant abundance changes throughout the development. These species were for example represented by serine/threonine-protein kinase DST2-like, calreticulin precursor, 2-phosphoglycerate kinase-related family protein, and RNA polymerase-associated protein LEO1-like.

Multiple Phosphorylation—A single protein can carry several phosphorylation sites that show different regulatory trends (36, 37). Examples of such proteins identified in our study were actin cytoskeleton-regulatory complex PAN1-like protein, and octicosapeptide/PHOX/BEM1p-domain-containing protein (PB1-containing protein). The former is characterized by six phosphorylation sites that showed three regulatory trends (Fig. 5*A*, and supplemental Table S4). The phosphopeptides NSPFGFEDSVPGS*PLS*R and NSPFGFEDSVPGSPLS*R were identified exclusively in mature pollen whereas the phosphopeptide NSPFGFEDSVPGS*PLSR was present in mature pollen and 5-min activated pollen. We can speculate that the first serine became phosphorylated in mature pollen, peaked in 5-min activated pollen, and in 30-min activated pollen remained undetectable. On the other hand, the second serine dominated in mature pollen whereas later on was undetectable. Furthermore, it is likely that in mature pollen both phosphorylation forms (a singly and a doubly phosphorylated) coexisted possibly each showing a different regulatory activ-
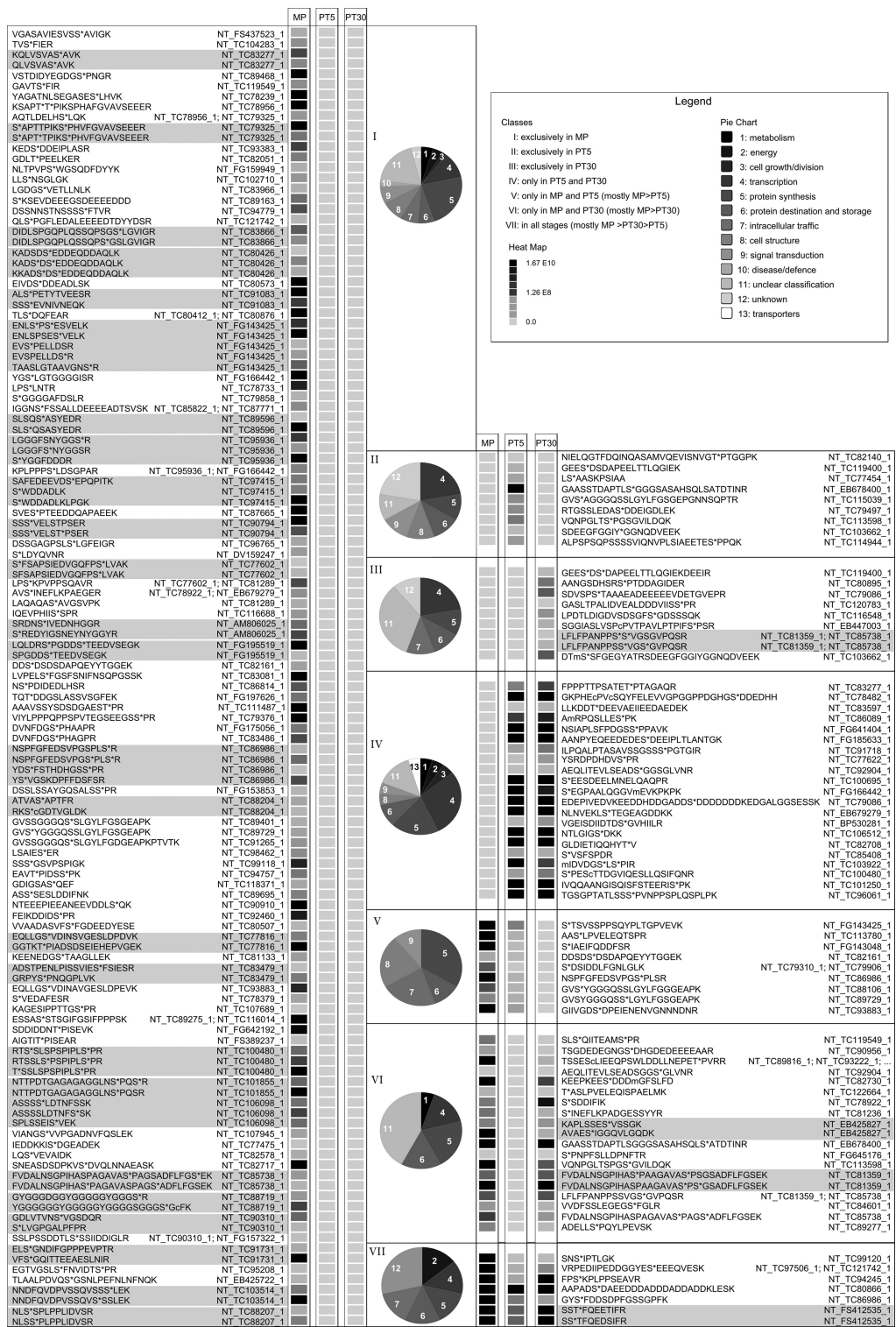
FIG. 4. **Expression profiles of the selected phosphopeptides with a different abundance in the studied male gametophyte stages.** The phosphopeptides were sorted into seven regulation groups based on their abundance differences in the three analyzed male gametophyte stages (group I - left panel; groups II–VII - right panel). The relative peptide abundance in each group is shown based on a gray scale (light gray - not detected; black - the highest concentration). Each column represents the average peptide abundance of the three independent LC-MS experiments. In the rows, the normalized abundance of peptides as extracted from the Proteome discoverer LC-MS software is presented. Peptides assigned to one and the same identifier are highlighted in gray. Gene ontology (GO) categories are presented for each group as a pie chart. The full presentation of the data set is provided in the supplemental Table S3.

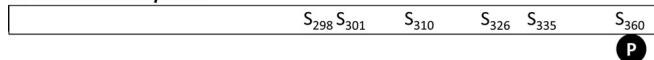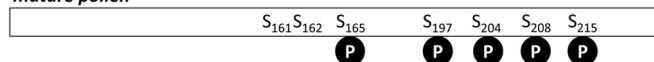**A – actin cytoskeleton-regulatory complex protein PAN1-like**
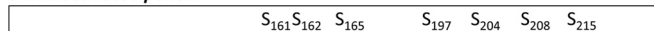
mature pollen
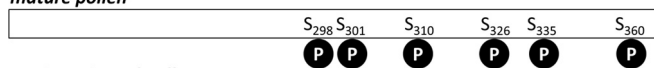
5-min activated pollen
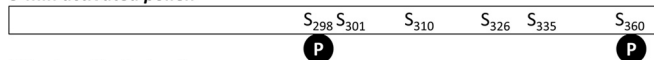
30-min activated pollen

B – PB1-containing protein

mature pollen

5-min activated pollen
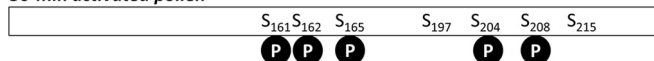
30-min activated pollen

FIG. 5. **Phosphorylation patterns of two selected phosphoproteins identified in our data set in three stages of male gametophyte.** *A*, Actin cytoskeleton-regulatory complex protein PAN1-like. *B*, PB1-containing protein. "S" stands for serine, the number indicates the position of the amino acid in the polypeptide chain, and phosphorylation site is depicted as a "P" in the black circle.

ity. The latter, PB1-containing protein is characterized by seven phosphorylation sites showing three regulatory trends (Fig. 5*B*, and supplemental Table S4). The phosphopeptides FVDALNSGPIHASPAGAVAS*PAGSADFLFGS*EK, and FVDALNSGPIHAS*PAGAVASPAGS*ADFLFGSEK coexisted exclusively in mature pollen, whereas the phosphopeptide FVDALNSGPIHASPAGAVAS*PAGS*ADFLFGSEK was present only in mature pollen and 30-min activated pollen. It is likely that phosphorylation of all these four serines occurs in mature pollen, it vanishes in 5-min activated pollen, and that two of the phosphorylation sites re-appear after 30 min of pollen activation. The dephosphorylation after 5 min of activation might be directly related to pollen activation/hydration. On the other hand, the phosphopeptides LFLFPANPPS*S*VGSG-VPQSR, and LFLFPANPPSS*VGS*GVPQSR were identified exclusively in 30-min activated pollen, whereas the phosphopeptide LFLFPANPPSSVGS*GVPQSR was found also in mature pollen. Possibly, the third phosphorylated serine appeared in mature pollen, vanished and re-appeared in 30-min activated pollen whereas the other two phosphoserines appeared only after 30 min of pollen activation. Collectively our results showed differential phosphorylation patterns for a large number of proteins likely involved in the early processes during tobacco pollen activation.

DISCUSSION

In the presented data set, 471 phosphopeptides have been identified in three stages of male gametophyte (mature pollen, pollen activated for 5 min and pollen activated for 30 min), which carried 432 unambiguous phosphorylation sites. The observed redundancy was caused by couples of phosphopeptides, one of which was "normal", and the other one was either missed-cleaved by trypsin or came from chemical modifications, such as methionine oxidation. These 432 unique phosphorylation sites have been assigned to 301 individual proteins. The number of phosphorylation sites identified represents a great improvement in comparison to our previous tobacco male gametophyte phosphoproteomic study that identified 52 unambiguous phosphorylation sites (21). In that study we applied Al(OH)$_3$- metal oxide/hydroxide affinity chromatography for phosphoprotein enrichment (allowing the annotation of only one phosphorylation site), and TiO$_2$ phosphopeptide enrichment for the analysis of phosphorylation sites of selected candidate proteins from mature pollen. Such improvement in the number of phosphorylation sites after phosphopeptide enrichment in the actual study compared with the phosphoprotein enrichment in the previous study is in accordance with several previous studies where phosphoprotein enrichment revealed only a limited number of phosphorylation sites (6, 38, 39). Moreover, a tandem approach enriching first for phosphoproteins and then after trypsin digest also for phosphopeptides was shown beneficial (13, 14).

The Proportion of the Phosphorylated Amino Acids in the Presented Phosphoproteome—The conventional phosphoproteomic techniques lead to the identification of *O*-phosphorylated amino acids: serine, threonine, and tyrosine because phosphorylated histidine (that carries phosphate attached to a nitrogen atom in its imidazole ring) is labile under acidic pH (that is usually applied during the conventional enrichment protocols and during conventional LC-MS; ref. 40). In most phosphoproteomics studies, the dominant phosphoamino acid is serine with 80–90%, followed by threonine occupying around 10–15%, and tyrosine reaching few percent. In our study, we observed the pSer/pThr/pTyr ratio of 86.4:13.4:0.2 that was astonishingly similar to the Arabidopsis mature pollen phosphoproteome with a ratio of 86:14:0.16 (15). In case of various human cell cultures, around 2–4% of phosphotyrosine were reported—particularly 1.8% (41), 2.3% (42), or 3.8% (43). Usually, there was less phosphotyrosine (<1%) observed in plants than in human cell cultures, although the human phosphoproteomic research was often conducted on cancer cell lines that have a huge phosphorylation level. The pSer/pThr/pTyr ratios in various Arabidopsis cell cultures ranged from 91.8:7.5:0.7 (44) to 83.81:16.18:0.01 (45). On the contrary, other studies reported a phosphotyrosine content comparable to the animal phosphoproteomes, such as 85:10.7:4.3 (46), and 82.7:13.1:4.2 (47) in Arabidopsis cell cultures, and 84.8:12.3:2.9 in a rice cell culture (47). From the differing contents of phosphotyrosine in the presented data sets, it is obvious that it still remains speculative how abundant phosphotyrosine phosphorylation in plants actually is (48, 49). Furthermore, the inhibitors of tyrosine phosphorylation (phenylarsine oxide and genistein) applied to the lily cultivated pollen strongly affected its growth rate, likely influencing the

dynamics of actin cytoskeleton (50). However, the exact position of phosphotyrosine phosphorylation in pollen proteins remains to be elucidated as well as any further possible role of tyrosine phosphorylation during pollen tube growth. Phosphotyrosine was shown to be carried by proteins playing an essential role throughout the life of a plant, such as brassinosteroid receptor BRI1 (51), or proteins involved in phytochrome signaling (52). The only phosphorylated tyrosine in our data set was identified in the peptide GVSY*GGGQSSLGYLF-GGGEAPK of the SPIRAL1-like 1 protein.

Phosphoproteins with Unknown Function—Among the identified phosphoproteins, the dominant functional category was "unclear classification." Collectively with "unknown," it counted for one fifth of the identified phosphoproteome (Fig. 3). It is likely that some of these "unknown" proteins are pollen-specific or pollen-enriched compared with sporophyte tissues, and that their role is still unknown. In tobacco proteome, it was clearly shown that gametophytic tissues contained specific proteins (837 out of 2135 proteins) that were not shared by sporophyte tissues, particularly leaves and roots (or were at least not as abundant as in gametophyte, and so remained below the detection limit of the proteomic techniques; ref. 20). Out of these 837 proteins, 120 fell into the GO category "not assigned", that represented approx. 14% of all pollen-specific proteins reported by Ischebeck and colleagues (20). From this point of view, our phosphoproteomic data set is consistent with the published tobacco male gametophyte proteome.

Phosphoproteins Involved in Translation and Protein Fate—Almost a quarter of the identified phosphoproteins have a likely role in translation; either in protein synthesis, or in protein destination and storage. Tobacco pollen activation and subsequent pollen tube growth was originally shown to be vitally dependent on translation but almost independent of transcription (53). Although our recent microarray transcriptomic analyses revealed a number of mRNAs being synthesized during pollen tube growth even after 24 h of cultivation (54, 55), many of the transcripts in the desiccated mature pollen are stored in EDTA/puromycine-resistant particles (EPPs). These particles contain parts of ribosomes and translation apparatus together with mRNAs (56, 57) and the translation of EPP-stored mRNAs starts after pollen activation. Translation initiation was shown to be regulated by protein phosphorylation of initiation factors and other regulatory proteins (5) so the presence of the translation initiation factors such as various forms of eukaryotic translation initiation factor 2, and eukaryotic translation initiation factors 3B, 4A-9, 4B, 4G, iso4F, 5B-like in our data set indicates ongoing translation regulation. The fate of proteins during cellular processes is also determined by their degradation via proteasome pathway, to which proteins labeled by polyubiquitine chain are subjected. Protein degradation is likely to have a key role during male gametophyte development. Recently, it was

demonstrated that defective in cullin neddylation protein 1 (DCN1) was crucial for proper pollen tube development (58).

Phosphoproteins Role During Transcription—We detected a remarkable proportion of phosphoproteins involved in transcription (17% in particular). On the contrary, there was no phosphoprotein candidate connected to transcription in our previous phosphoprotein-enriched data set (21), probably because of their generally low abundance and the limited dynamic range of protein visualization techniques used. Such a fact was already demonstrated for Arabidopsis mitochondrial phosphoproteome where phosphopeptide enrichment led to the identification of novel phosphorylation sites that were not previously identified by the alternative approaches (38). As mentioned above, active transcription in activated pollen grain as long as 24 h of pollen tube growth has been shown (54, 55). Here, we identified several transcription factors, most of which contained a zinc finger motif. One of them, ZAT10, was shown to be phosphorylated by two mitogen-activated protein kinases (MAPK3 and MAPK6) (59). Interestingly, most of our zinc finger transcription factors showed also prolyl-directed phosphorylation motif making them likely substrates of MAP kinases (60). Some MAP kinases were already identified in tobacco male gametophyte (20, 61, 62). However, experimental data directly linking these MAP kinases to their targets have yet to be established.

Signaling Phosphoproteins—Compared with the data achieved before (21), herein, we identified almost a twofold number of proteins connected with signaling (10% in this study compared to 6% after phosphoprotein enrichment). Some of the signaling molecules are of a low abundance and therefore likely below the detection limits of the phosphoprotein enrichment. From our data the pollen-specific Rho guanine nucleotide dissociation inhibitors (Rho GDIs) should be mentioned. Small GTPases from the Rho family play an essential role in a polarized tip cell growth of pollen tubes, and their activity is regulated by other interacting proteins, including Rho GDI among others. Rho GDI removes the prenylated Rho GTPase from the membrane and helps to maintain the cytoplasmic pool of this protein. Its activity was shown to be essential for pollen tube growth (63). The other signaling proteins from our data set were various protein kinases and phosphatases. Their presence was expected because the precise regulation accompanying the switch from the metabolically quiescent pollen grain to the rapidly-growing pollen tube is likely to involve the activity of kinases and phosphatases, phosphorylation of which was shown to regulate their activity (64). Many of the identified kinases showed low homology to the known sequences in the database making the specification of the appropriate kinase family hard or even impossible. This might be caused by the fact that they represented pollen-specific and/or tobacco-specific proteins, homologues of which were absent in recent databases.

Kinase Motifs—Many protein kinases show phosphorylation motif specificity or at least phosphorylation motif prefer-

ence. In order to find any possible up-regulated kinase motifs, we searched the presented data set using Motif-X algorithm. It should be noted that the information about linking a particular kinase to a phosphorylation motif is limited in plants and consequently the information is often extrapolated from other model organisms, mostly human (65). Two searches were performed looking up either for phosphoserine or for phosphothreonine (supplemental Fig. S2). Phosphorylated serine was shown to be present in five phosphorylation motifs whereas phosphothreonine occupied the central position of only one phosphorylation motif.

The first motif to be discussed is the prolyl-directed phosphorylation, *i.e.* a phosphorylated amino acid followed by a proline, regardless of the presence of phosphoserine (xxxx-xxS*Pxxxxx) or phosphothreonine (xxxxxxT*Pxxxxx). The prolyl-directed phosphorylation is typical for two big groups of protein kinases - mitogen-activated protein kinases (MAPK), and cyclin-dependent protein kinases (CDK; ref. 60). Both these large kinase families were identified in the tobacco male gametophyte proteome (20), supplemental Table S5. MAPKs play a key regulatory role in many physiological processes including stress reactions and pollen hydration (62). CDKs were originally shown to regulate cell cycle and their activity in male gametophyte was expected because both pollen mitoses are precisely regulated (54). The alternative function of CDKs is for example the regulation of pre-mRNA splicing of callose synthase in pollen tube that influences cell wall formation (66). Alkaline phosphorylation motifs xxxRxxS*xxxxxx, and xxxKxxS*xxxxxx are recognized by Ca^{2+}/calmodulin-dependent protein kinase (CAMK2; ref. 60). A chimeric CAMK with two distinct domains, one of which reacts to free Ca^{2+} and the other to Ca^{2+}/calmodulin, was shown to be expressed in male gametophyte of lily and tobacco (67). Its expression started in pollen mother cell and then continued to peak in the tetrad stage. Such an expression profile tends us to speculate that the expression of this kinase reacts to Ca^{2+} oscillations, and that precisely regulates the synchronous events during microsporogenesis. Besides, this alkaline motif is in plants also recognized by the Ca^{2+}-dependent protein kinase-sucrose-nonfermenting-related kinase (CDPK-SnRK) superfamily of protein kinases (68). Two kinases of this family were actually identified in tobacco male gametophyte proteome (Supplemental Table 5, and ref. 20). Last but not least, we identified two acidic kinase motifs with a central phosphoserine - xxxxxxS*DxExxx, and xxxxxxS*xDDxxx - corresponding in principle to the motif xxxxxxS*(D/E)(D/E)(D/E)xxx that is recognized by casein kinase 2 (CK2; ref. 60). Casein kinase 2 was shown to be activated by salicylic acid in tobacco (69), and two casein kinases were identified in tobacco male gametophyte proteome (supplemental Table S4, and ref. 20). We have to point out that although the corresponding kinases were identified in our data set, it still remains unproven whether they really interact with the phosphoproteins containing the corresponding motifs, and which of the kinases is actually responsible for a particular phosphorylation event.

Regulated Phosphopeptides and Their Function—There were established seven groups collecting the regulated phosphopeptides according to their regulatory trends. As mentioned above the groups I and V collected phosphopeptides that were phosphorylated in mature pollen. Because the phosphopeptides included in both group I and group V decreased in abundance after pollen activation, we assumed that the role of their phosphorylation is mainly required in dry mature pollen and/or their dephosphorylation represents the actual activation/de-repression. The dominant categories were protein synthesis and protein destination and storage, represented by many proteins for example by various translation initiation factors, LA-related protein like, among others. There was also identified protein Rho GDI that regulates the activity of Rho GTPases that are essential for tip growth of pollen tube (63). However, to our knowledge, the role of its phosphorylation site was not reported yet. According to our results, it can be assumed that its activity is switched on by dephosphorylation (at least of the particular phosphopeptide found in this regulatory group V) because the phosphates were attached to the protein exclusively in mature pollen and the concentration of the only phosphopeptide in group V decreased in pollen activated *in vitro* for 5 min. The other candidate specific to mature pollen was MAP kinase. MAP kinases were reported to play their roles upon pollen rehydration (62) so this phosphorylation might again be switching off the MAP kinase ready for pollen grain activation.

The groups II, III, and IV collected proteins phosphorylated strictly upon pollen activation. There appeared for example E3 ubiquitin-protein ligase RING FINGER 4 (RNF4)-like, the α-subunit of a nascent polypeptide-associated complex, protein phosphatase inhibitor 2, cytochrome oxidase c, histone deacetylase HDT1, villin and peptidyl-prolyl cis-trans isomerase 1 (PPI1), among others. Protein ubiquitination is likely to be initiated upon pollen activation in order to degrade the present proteins and to replace them with the newly synthesized species. Another E3 ubiquitin-protein ligase in Arabidopsis was reported to bind its target 14–3-3-proteins only upon phosphorylation of its particular amino acids (70). If the E3 ligase identified in our data set acts also after phosphorylation, we might speculate that this phosphorylation event represents an activation phosphorylation. The phosphorylated peptides from phosphatase inhibitor 2 appeared only upon protein phosphorylation. However, we might only speculate whether their phosphorylation promotes their activity or rather blocks it. Villin plays a role in actin cytoskeleton dynamics and it was shown to be phosphorylated on a tyrosine (71). The role of tyrosine phosphorylation during pollen tube growth was deduced from the pollen tube treatment by drugs influencing tyrosine phosphorylation that caused lower pollen germination rate and shorter pollen tubes (50). Because the treated pollen tubes showed a different arrangement of actin

filaments, it might be possible that not only actin itself but also actin-binding proteins (such as villin) have to be precisely tyrosine-phosphorylated.

The most dynamic regulation was shown for the group VI phosphopeptides. This category grouped phosphopeptides that were phosphorylated in mature pollen, then dephosphorylated in 5-min activated pollen and later after 30-min activation re-appeared again among phosphopeptides. Phosphopeptides of the following proteins were put exclusively to this category (*i.e.* they did not show any other phosphopeptides belonging to any other group of regulated phosphopeptides): transcription initiation factor IIF, acidic ribosomal protein P1a-like, LEA protein D34, and ARA4-interacting protein. The other phosphoproteins had their corresponding phosphopeptides also in other regulation groups. These phosphorylation sites might represent phosphoproteins that reflect with their phosphorylation/dephosphorylation cycles the ion signal pulses during pollen tube growth (72). However, we do not have the phosphoproteomics data regarding longer periods of pollen tube growth *in vitro*, so making any bold conclusion is beyond the scope of this article.

Group VII comprised the regulated phosphopeptides that appeared in all studied stages. There were only three proteins that fell with their phosphopeptides exclusively into this category—2-phosphoglycerate kinase-related family protein, nuclear RNA binding protein-like, and calreticulin precursor. The other proteins were identified by peptides that fell not only into this group but also in at least another one (mostly group I, see supplemental Table S3, and Fig. 4).

CONCLUSION

Collectively, we purified and identified phosphopeptides from mature pollen, 5-min activated pollen, and 30-min activated pollen, the three stages covering an early phase of male gametophyte activation. This study presents the first developmental phosphoproteomics data from angiosperm activated pollen including the dynamics of very early phosphorylation events during pollen re-hydration and activation (*i.e.* 5-min activated pollen). The only other studied pollen tubes were these of *Picea wilsonii*, a gymnosperm (23). We identified 471 phosphopeptides carrying 432 phosphorylation sites that were assigned to 301 phosphoproteins. Moreover, the quantitative data highlighted the dynamics of protein phosphorylation during pollen activation and the differential regulation of several phosphopeptides of the same phosphoprotein pinpointed the complexity of protein phosphorylation in its functional context. Such list of phosphorylated proteins also represents a good starting point for the selection of the most interesting candidates for subsequent studies revealing the function of their phosphorylation and its integration into the molecular processes underlying pollen tube growth and development. Thus, this study brought new insights into the activation of pollen because highlighted the phosphorylated proteins that are very likely candidates, which would take part in the regulation and processes of pollen tube activation.

** To whom correspondence should be addressed: Laboratory of Pollen Biology, Institute of Experimental Botany ASCR, v.v.i., Rozvojova 263, 165 00 Praha 6, Czech Republic. Tel.: +420 225 106 450; Fax: +420 225 106 456; E-mail: david@ueb.cas.cz.

REFERENCES

1. Vogler, F., Konrad, S. S. A., and Sprunck, S. (2015) Knockin' on pollen's door: live cell imaging of early polarization events in germinating Arabidopsis pollen. *Front. Plant Sci.* **6**, 246
2. Mascarenhas, J. P. (1993) Molecular mechanisms of pollen tube growth and differentiation. *Plant Cell* **5**, 1303–1314
3. Mishra, N. S., Tuteja, R., and Tuteja, N. (2006) Signaling through MAP kinase networks in plants. *Arch. Biochem. Biophys.* **452**, 55–68
4. Francis, D., and Halford, N. G. (1995) The plant cell cycle. *Physiol. Plant.* **93**, 365–374
5. van der Kelen, K., Beyaert, R., Inze, D., and de Veylder, L. (2009) Translational control of eukaryotic gene expression. *Crit. Rev. Biochem. Mol. Biol.* **44**, 143–168
6. Röhrig, H., Colby, T., Schmidt, J., Harzen, A., Facchinelli, F., and Bartels, D. (2008) Analysis of desiccation-induced candidate phosphoproteins from *Craterostigma plantagineum* isolated with a modified metal oxide affinity chromatography procedure. *Proteomics* **8**, 3548–3560
7. Darewicz, M., Dziuba, J., and Minkiewicz, P. (2005) Some properties of beta-casein modified via phosphatase. *Acta Alimentaria* **34**, 403–415
8. Fletterick, R. J., and Sprang, S. R. (1982) Glycogen-phosphorylase structures and function. *Acc. Chem. Res.* **15**, 361–369
9. Kim, J., Shen, Y., Han, Y. J., Park, J. E., Kirchenbauer, D., Soh, M. S., Nagy, F., Schafer, E., and Song, P. S. (2004) Phytochrome phosphorylation modulates light signaling by influencing the protein-protein interaction. *Plant Cell* **16**, 2629–2640
10. Garnak, M., and Reeves, H. C. (1979) Phosphorylation of isocitrate dehydrogenase of *Escherichia coli. Science* **203**, 1111–1112
11. Fíla, J., and Honys, D. (2012) Enrichment techniques employed in phosphoproteomics. *Amino Acids* **43**, 1025–1047
12. Dunn, J. D., Reid, G. E., and Bruening, M. L. (2010) Techniques for phosphopeptide enrichment prior to analysis by mass spectrometry. *Mass Spectrom. Rev.* **29**, 29–54
13. Hoehenwarter, W., Thomas, M., Nukarinen, E., Egelhofer, V., Röhrig, H., Weckwerth, W., Conrath, U., and Beckers, G. J. M. (2013) Identification of novel *in vivo* MAP kinase substrates in *Arabidopsis thaliana* through use of tandem metal oxide affinity chromatography. *Mol. Cell. Proteomics* **12**, 369–380
14. Beckers, G. J., Hoehenwarter, W., Röhrig, H., Conrath, U., and Weckwerth, W. (2014) Tandem metal-oxide affinity chromatography for enhanced depth of phosphoproteome analysis. *Methods Mol. Biol.* **1072**, 621–632
15. Mayank, P., Grossman, J., Wuest, S., Boisson-Dernier, A., Roschitzki, B., Nanni, P., Nuehse, T., and Grossniklaus, U. (2012) Characterization of the phosphoproteome of mature Arabidopsis pollen. *Plant J.* **72**, 89–101
16. Holmes-Davis, R., Tanaka, C. K., Vensel, W. H., Hurkman, W. J., and McCormick, S. (2005) Proteome mapping of mature pollen of *Arabidopsis thaliana. Proteomics* **5**, 4864–4884
17. Noir, S., Bräutigam, A., Colby, T., Schmidt, J., and Panstruga, R. (2005) A reference map of the *Arabidopsis thaliana* mature pollen proteome. *Biochem. Biophys. Res. Commun.* **337**, 1257–1266
18. Sheoran, I. S., Sproule, K. A., Olson, D. J. H., Ross, A. R. S., and Sawhney, V. K. (2006) Proteome profile and functional classification of proteins in *Arabidopsis thaliana* (Landsberg erecta) mature pollen. *Sex. Plant Reprod.* **19**, 185–196

19. Grobei, M. A., Qeli, E., Brunner, E., Rehrauer, H., Zhang, R., Roschitzki, B., Basler, K., Ahrens, C. H., and Grossniklaus, U. (2009) Deterministic protein inference for shotgun proteomics data provides new insights into Arabidopsis pollen development and function. *Genome Res.* **19,** 1786–1800

20. Ischebeck, T., Valledor, L., Lyon, D., Gingl, S., Nagler, M., Meijon, M., Egelhofer, V., and Weckwerth, W. (2014) Comprehensive cell-specific protein analysis in early and late pollen development from diploid microsporocytes to pollen tube growth. *Mol. Cell. Proteomics* **13,** 295–310

21. Fíla, J., Matros, A., Radau, S., Zahedi, R. P., Čapková, V., Mock, H.-P., and Honys, D. (2012) Revealing phosphoproteins playing role in tobacco pollen activated *in vitro. Proteomics* **12,** 3229–3250

22. Wolschin, F., Wienkoop, S., and Weckwerth, W. (2005) Enrichment of phosphorylated proteins and peptides from complex mixtures using metal oxide/hydroxide affinity chromatography (MOAC). *Proteomics* **5,** 4389–4397

23. Chen, Y., Liu, P., Hoehenwarter, W., and Lin, J. (2012) Proteomic and phosphoproteomic analysis of *Picea wilsonii* pollen development under nutrient limitation. *J. Proteome Res.* **11,** 4180–4190

24. Pinkse, M. W. H., Uitto, P. M., Hilhorst, M. J., Ooms, B., and Heck, A. J. R. (2004) Selective isolation at the femtomole level of phosphopeptides from proteolytic digests using 2D-nanoLC-ESI-MS/MS and titanium oxide precolumns. *Anal. Chem.* **76,** 3935–3943

25. Petrů, E., Hrabětová, E., and Tupý, J. (1964) The technique of obtaining germinating pollen without microbial contamination. *Biologia Plantarum* **6,** 68–69

26. Tupý, J., and Říhová, L. (1984) Changes and growth effect of pH in pollen tube culture. *J. Plant Physiol.* **115,** 1–10

27. Méchin, V., Damerval, C., and Zivy, M. (2006) Total protein extraction with TCA-acetone. In: Thiellement, H., Zivy, M., Damerval, C., and Méchin, V., eds. *Methods in Mol. Biol.*, pp. 1–8, Springer

28. Kollipara, L., and Zahedi, R. P. (2013) Protein carbamylation: *In vivo* modification or *in vitro* artefact? *Proteomics* **13,** 941–944

29. Beck, F., Lewandrowski, U., Wiltfang, M., Feldmann, I., Geiger, J., Sickmann, A., and Zahedi, R. P. (2011) The good, the bad, the ugly: Validating the mass spectrometric analysis of modified peptides. *Proteomics* **11,** 1099–1109

30. Taus, T., Koecher, T., Pichler, P., Paschke, C., Schmidt, A., Henrich, C., and Mechtler, K. (2011) Universal and confident phosphorylation site localization using phosphoRS. *J. Proteome Res.* **10,** 5354–5362

31. Vizcaino, J. A., Deutsch, E. W., Wang, R., Csordas, A., Reisinger, F., Rios, D., Dianes, J. A., Sun, Z., Farrah, T., Bandeira, N., Binz, P. A., Xenarios, I., Eisenacher, M., Mayer, G., Gatto, L., Campos, A., Chalkley, R. J., Kraus, H. J., Albar, J. P., Martinez-Bartolome, S., Apweiler, R., Omenn, G. S., Martens, L., Jones, A. R., and Hermjakob, H. (2014) ProteomeXchange provides globally coordinated proteomics data submission and dissemination. *Nature Biotechnol.* **32,** 223–226

32. Bevan, M., Bancroft, I., Bent, E., Love, K., Goodman, H., Dean, C., Bergkamp, R., Dirkse, W., Van Staveren, M., Stiekema, W., Drost, L., Ridley, P., Hudson, S. A., Patel, K., Murphy, G., Piffanelli, P., Wedler, H., Wedler, E., Wambutt, R., Weitzenegger, T., Pohl, T. M., Terryn, N., Gielen, J., Villarroel, R., De Clerck, R., Van Montagu, M., Lecharny, A., Auborg, S., Gy, I., Kreis, M., Lao, N., Kavanagh, T., Hempel, S., Kotter, P., Entian, K. D., Rieger, M., Schaeffer, M., Funk, B., Mueller-Auer, S., Silvey, M., James, R., Montfort, A., Pons, A., Puigdomenech, P., Douka, A., Voukelatou, E., Milioni, D., Hatzopoulos, P., Piravandi, E., Obermaier, B., Hilbert, H., Dusterhoft, A., Moores, T., Jones, J. D. G., Eneva, T., Palme, K., Benes, V., Rechman, S., Ansorge, W., Cooke, R., Berger, C., Delseny, M., Voet, M., Volckaert, G., Mewes, H. W., Klosterman, S., Schueller, C., Chalwatzis, N., and Project, E. U. A. G. (1998) Analysis of 1.9 Mb of contiguous sequence from chromosome 4 of *Arabidopsis thaliana. Nature* **391,** 485–488

33. Chou, M. F., and Schwartz, D. (2011) Biological sequence motif discovery using motif-x. *Curr. Protoc. Bioinformatics* Chapter 13, Unit 13.15–24

34. Schwartz, D., and Gygi, S. P. (2005) An iterative statistical approach to the identification of protein phosphorylation motifs from large-scale data sets. *Nature Biotechnol.* **23,** 1391–1398

35. Rohn, H., Junker, A., Hartmann, A., Grafahrend-Belau, E., Treutler, H., Klapperstueck, M., Czauderna, T., Klukas, C., and Schreiber, F. (2012) VANTED v2: a framework for systems biology applications. *BMC Syst. Biol.* **6**

36. McCoy, C. E., Campbell, D. G., Deak, M., Bloomberg, G. B., and Arthur, J. S. C. (2005) MSK1 activity is controlled by multiple phosphorylation sites. *Biochem. J.* **387,** 507–517

37. Wang, X. M., Paulin, F. E. M., Campbell, L. E., Gomez, E., O'Brien, K., Morrice, N., and Proud, C. G. (2001) Eukaryotic initiation factor 2B: identification of multiple phosphorylation sites in the epsilon-subunit and their functions *in vivo. EMBO J.* **20,** 4349–4359

38. Ito, J., Taylor, N. L., Castleden, I., Weckwerth, W., Millar, A. H., and Heazlewood, J. L. (2009) A survey of the *Arabidopsis thaliana* mitochondrial phosphoproteome. *Proteomics* **9,** 4229–4240

39. Luis Carrasco, J., Jose Castello, M., Naumann, K., Lassowskat, I., Navarrete-Gomez, M., Scheel, D., and Vera, P. (2014) Arabidopsis protein phosphatase DBP1 nucleates a protein network with a role in regulating plant defense. *Plos One* **9,** e90734

40. Hultquist, D. E. (1968) The preparation and characterization of phosphorylated derivatives of histidine. *Biochim Biophys Acta* **153,** 329–340

41. Olsen, J. V., Blagoev, B., Gnad, F., Macek, B., Kumar, C., Mortensen, P., and Mann, M. (2006) Global, *in vivo*, and site-specific phosphorylation dynamics in signaling networks. *Cell* **127,** 635–648

42. Molina, H., Horn, D. M., Tang, N., Mathivanan, S., and Pandey, A. (2007) Global proteomic profiling of phosphopeptides using electron transfer dissociation tandem mass spectrometry. *Proc. Natl. Acad. Sci. U.S.A.* **104,** 2199–2204

43. Beausoleil, S. A., Jedrychowski, M., Schwartz, D., Elias, J. E., Villén, J., Li, J. X., Cohn, M. A., Cantley, L. C., and Gygi, S. P. (2004) Large-scale characterization of HeLa cell nuclear phosphoproteins. *Proc. Natl. Acad. Sci. U.S.A.* **101,** 12130–12135

44. van Bentem, S. D., Anrather, D., Dohnal, I., Roitinger, E., Csaszar, E., Joore, J., Buijnink, J., Carreri, A., Forzani, C., Lorkovic, Z. J., Barta, A., Lecourieux, D., Verhounig, A., Jonak, C., and Hirt, H. (2008) Site-specific phosphorylation profiling of Arabidopsis proteins by mass spectrometry and peptide chip analysis. *J. Prot. Res.* **7,** 2458–2470

45. Benschop, J. J., Mohammed, S., O'Flaherty, M., Heck, A. J. R., Slijper, M., and Menke, F. L. H. (2007) Quantitative phosphoproteomics of early elicitor signaling in Arabidopsis. *Mol. Cell. Proteomics* **6,** 1198–1214

46. Sugiyama, N., Nakagami, H., Mochida, K., Daudi, A., Tomita, M., Shirasu, K., and Ishihama, Y. (2008) Large-scale phosphorylation mapping reveals the extent of tyrosine phosphorylation in Arabidopsis. *Mol. Syst. Biol.* **4,** 7

47. Nakagami, H., Sugiyama, N., Mochida, K., Daudi, A., Yoshida, Y., Toyoda, T., Tomita, M., Ishihama, Y., and Shirasu, K. (2010) Large-scale comparative phosphoproteomics identifies conserved phosphorylation sites in plants. *Plant Physiol.* **153,** 1161–1174

48. van Bentem, S. D., and Hirt, H. (2009) Protein tyrosine phosphorylation in plants: more abundant than expected? *Trends Plant Sci.* **14,** 71–76

49. Mithoe, S. C., and Menke, F. L. H. (2011) Phosphoproteomics perspective on plant signal transduction and tyrosine phosphorylation. *Phytochem.* **72,** 997–1006

50. Zi, H. J., Xiang, Y., Li, M., Wang, T., and Ren, H. Y. (2007) Reversible protein tyrosine phosphorylation affects pollen germination and pollen tube growth via the actin cytoskeleton. *Protoplasma* **230,** 183–191

51. Oh, M. H., Wang, X. F., Kota, U., Goshe, M. B., Clouse, S. D., and Huber, S. C. (2009) Tyrosine phosphorylation of the BRI1 receptor kinase emerges as a component of brassinosteroid signaling in Arabidopsis. *Proc. Natl. Acad. Sci. U.S.A.* **106,** 658–663

52. Nito, K., Wong, C. C. L., Yates, J. R., and Chory, J. (2013) Tyrosine phosphorylation regulates the activity of phytochrome photoreceptors. *Cell Rep.* **3,** 1970–1979

53. Čapková, V., Hrabětová, E., and Tupý, J. (1988) Protein synthesis in pollen tubes: preferential formation of new species independent of transcription. *Sex. Plant Reprod.* **1,** 150–155

54. Hafidh, S., Breznenová, K., Růžička, P., Feciková, J., Čapková, V., and Honys, D. (2012) Comprehensive analysis of tobacco pollen transcriptome unveils common pathways in polar cell expansion and underlying heterochronic shift during spermatogenesis. *BMC Plant Biol.* **12,** 24

55. Hafidh, S., Breznenová, K., and Honys, D. (2012) De novo post-pollen mitosis II tobacco pollen tube transcriptome. *Plant Signal. Behav.* **7,** 918–921

56. Honys, D., Combe, J. P., Twell, D., and Čapková, V. (2000) The translationally repressed pollen-specific ntp303 mRNA is stored in nonpolysomal mRNPs during pollen maturation. *Sex. Plant Reprod.* **13,** 135–144

57. Honys, D., Reňák, D., Feciková, J., Jedelský, P. L., Nebesářová, J., Dobrev, P., and Čapková, V. (2009) Cytoskeleton-associated large RNP complexes in tobacco male gametophyte (EPPs) are associated with ribosomes and are involved in protein synthesis, processing, and localization. *J. Proteome Res.* **8,** 2015–2031

58. Hosp, J., Ribarits, A., Retzer, K., Jin, Y. F., Tashpulatov, A., Resch, T., Friedmann, C., Ankele, E., Voronin, V., Palme, K., Heberle-Bors, E., and Touraev, A. (2014) A tobacco homolog of DCN1 is involved in pollen development and embryogenesis. *Plant Cell Rep.* **33,** 1187–1202

59. Nguyen, X. C., Kim, S. H., Lee, K., Kim, K. E., Liu, X. M., Han, H. J., My, H. T. H., Lee, S. W., Hong, J. C., Moon, Y. H., and Chung, W. S. (2012) Identification of a C2H2-type zinc finger transcription factor (ZAT10) from Arabidopsis as a substrate of MAP kinase. *Plant Cell Rep.* **31,** 737–745

60. Lee, T. Y., Bretana, N. A., and Lu, C. T. (2011) PlantPhos: using maximal dependence decomposition to identify plant phosphorylation sites with substrate site specificity. *BMC Bioinformatics* **12,** 13

61. Heberle-Bors, E., Voronin, V., Touraev, A., Testillano, P. S., Risueno, M. C., and Wilson, C. (2001) MAP kinase signaling during pollen development. *Sex. Plant Reprod.* **14,** 15–19

62. Wilson, C., Voronin, V., Touraev, A., Vicente, O., and Heberle-Bors, E. (1997) A developmentally regulated MAP kinase activated by hydration in tobacco pollen. *Plant Cell* **9,** 2093–2100

63. Klahre, U., Becker, C., Schmitt, A. C., and Kost, B. (2006) Nt-RhoGDI2 regulates Rac/Rop signaling and polar cell growth in tobacco pollen tubes. *Plant J.* **46,** 1018–1031

64. Payne, D. M., Rossomando, A. J., Martino, P., Erickson, A. K., Her, J. H., Shabanowitz, J., Hunt, D. F., Weber, M. J., and Sturgill, T. W. (1991) Identification of the regulatory phosphorylation sites in PP42/mitogen-activated protein kinase (MAP kinase). *EMBO J.* **10,** 885–892

65. Lee, T.-Y., Lin, Z.-Q., Hsieh, S.-J., Bretana, N. A., and Lu, C.-T. (2011) Exploiting maximal dependence decomposition to identify conserved motifs from a group of aligned signal sequences. *Bioinformatics* **27,** 1780–1787

66. Huang, X.-Y., Niu, J., Sun, M.-X., Zhu, J., Gao, J.-F., Yang, J., Zhou, Q., and Yang, Z.-N. (2013) Cyclin-dependent kinase G1 is associated with the spliceosome to regulate callose synthase 5 splicing and pollen wall formation in Arabidopsis. *Plant Cell* **25,** 637–648

67. Poovaiah, B. W., Xia, M., Liu, Z. H., Wang, W. Y., Yang, T. B., Sathyanarayanan, P. V., and Franceschi, V. R. (1999) Developmental regulation of the gene for chimeric calcium/calmodulin-dependent protein kinase in anthers. *Planta* **209,** 161–171

68. Hrabak, E. M., Chan, C. W. M., Gribskov, M., Harper, J. F., Choi, J. H., Halford, N., Kudla, J., Luan, S., Nimmo, H. G., Sussman, M. R., Thomas, M., Walker-Simmons, K., Zhu, J. K., and Harmon, A. C. (2003) The Arabidopsis CDPK-SnRK superfamily of protein kinases. *Plant Physiol.* **132,** 666–680

69. Hidalgo, P., Garreton, V., Berrios, C. G., Ojeda, H., Jordana, X., and Holuigue, L. (2001) A nuclear casein kinase 2 activity is involved in early events of transcriptional activation induced by salicylic acid in tobacco. *Plant Physiol.* **125,** 396–405

70. Yasuda, S., Sato, T., Maekawa, S., Aoyama, S., Fukao, Y., and Yamaguchi, J. (2014) Phosphorylation of Arabidopsis ubiquitin ligase ATL31 is critical for plant carbon/nitrogen nutrient balance response and controls the stability of 14–3-3 proteins. *J. Biol. Chem.* **289,** 15179–15193

71. Zhai, L. W., Zhao, P. L., Panebra, A., Guerrerio, A. L., and Khurana, S. (2001) Tyrosine phosphorylation of villin regulates the organization of the actin cytoskeleton. *J. Biol. Chem.* **276,** 36163–36167

72. Geitmann, A., and Cresti, M. (1998) Ca^{2+} channels control the rapid expansions in pulsating growth of *Petunia hybrida* pollen tubes. *J. Plant Physiol.* **152,** 439–447

7.2. Porovnání pylových fosfoproteomů tabáku virginského a huseníčku rolního

Fíla, J., Čapková, V., Honys, D. (2014). Phosphoproteomic studies in Arabidopsis and tobacco male gametophytes. Biochemical Society Transactions 42, 383–387. doi: 10.1042/BST20130249. $IF_{2014} = 3{,}194$

U tohoto přehledového článku jsem se podílel na analýze dat potřebných k jeho napsání i na samotném psaní manuskriptu.

Phosphoproteomic studies in *Arabidopsis* and tobacco male gametophytes

Jan Fíla*†, Věra Čapková* and David Honys*[1]

*Laboratory of Pollen Biology, Institute of Experimental Botany, Academy of Sciences of the Czech Republic, Rozvojová 263, Praha 6, Czech Republic
†Department of Plant Experimental Biology, Faculty of Science, Charles University in Prague, Viničná 5, Praha 2, Czech Republic

Abstract

Mature pollen represents an extremely resistant quiescent structure surrounded by a tough cell wall. After its hydration on stigma papillary cells, pollen tube growth starts rapidly. Massive metabolic changes are likely to be accompanied by changes in protein phosphorylation. Protein phosphorylation belongs among the most rapid post-translational modifications. To date, only *Arabidopsis thaliana* and tobacco (*Nicotiana tabacum*) mature pollen have been subjected to phosphoproteomic studies in order to identify the phosphoproteins present. In the present mini-review, *Arabidopsis* and tobacco datasets were compared with each other. The representation of the O-phosphorylated amino acids was compared between these two datasets, and the putative pollen-specific or pollen-abundant phosphopeptides were highlighted. Finally, the phosphorylation sites common for both *Arabidopsis* and tobacco phosphoproteins are listed as well as the phosphorylation motifs identified.

Introduction

Angiosperm mature pollen represents an extremely resistant tissue. Its desiccated cytoplasm is enveloped by a resistant cell wall. Mature pollen represents a quiescent stage that carries the genetic information of the donor plant, so it has to reach the stigma in a viable state. After the arrival on to the papillary cells on the stigma, the pollen cytoplasm rehydrates and pollen grain activates [1]. After a series of communication processes, rapid growth of a pollen tube starts.

To enable metabolic changes associated with the rapid growth of a pollen tube, the synthesis of novel proteins as well as post-translational modifications of the existing ones is of crucial importance. A number of transcripts is stored in complex mRNA storage granules called EPPs (EDTA/puromycin-resistant particles) [2,3]. Upon pollen rehydration, these transcripts are gradually activated and translated, and novel proteins are produced. After all, protein synthesis could not be flexible enough to enable rapid signalling, so post-translational modifications of proteins are performed, especially phosphorylation.

Protein phosphorylation represents one of the most dynamic post-translational modifications. It plays a key role in numerous cellular processes, such as protein synthesis, transcription regulation, cell cycle regulation, signal transduction, cytoskeleton dynamics and protein targeting to the nucleus [4–7]. Protein phosphorylation changes the properties of a modified protein. Because of its negative charge, the attachment of a phosphate group leads to

a decrease in the protein's pI [8]. Such pI changes are likely to change intramolecular and intermolecular interactions among individual domains. Alternatively, the attached phosphate can engage the active site of an enzyme and thus can block its activity (an example of this mechanism was discovered in isocitrate dehydrogenase [9]).

The male gametophyte and phosphoproteomics

Although pollen development, pollen activation and pollen tube growth are likely to be (co-)regulated by protein phosphorylation, only two large-scale pollen phosphoproteomic studies have been published to date. The first phosphoproteome published originated from *Arabidopsis thaliana* mature pollen [10], whereas the second study characterized phosphoproteins present in two time points in tobacco (*Nicotiana tabacum* cv. Samsun), mature pollen and germinating pollen after 30 min of activation *in vitro* [11].

To study the phosphorylated proteins on a large scale, the application of various enrichment techniques is of key importance since phosphoproteins represent only part of the cellular proteins and therefore are difficult to be detected in the mixture with the non-phosphorylated species (reviewed in [12,13]).

Each of the pollen phosphoproteomic studies applied a different set of methods for the identification of phosphorylated proteins present. In tobacco experiments, phosphoprotein enrichment was performed. The total proteins were extracted by TCA (trichloroacetic acid)/acetone, and enriched by MOAC (metal-oxide-affinity chromatography) with an Al(OH)$_3$ (aluminium hydroxide) matrix. The resulting phosphoprotein-enriched fraction was separated in two

distinct ways: by 2D gel electrophoresis and nano-LC–ESI–quadrupole TOF. Collectively, these two approaches led to the identification of 139 phosphoprotein candidates. The phosphoprotein enrichment led to the identification of only a limited number of phosphorylation sites; particularly one. Similar results were obtained in other studies applying phosphoprotein enrichment [14,15] and such results could be considered a disadvantage of phosphoprotein-enriching strategies (recently reviewed in [12]). To enable the identification of more phosphorylation sites, TiO_2 (titanium dioxide) phosphopeptide enrichment was performed on mature pollen protein crude extract in parallel. Such enrichment revealed the exact position of another 51 phosphosites, giving a total of 52 phosphorylation sites identified.

On the other hand, Mayank et al. [10] applied a combination of various phosphopeptide-enriching strategies: IMAC (immobilized metal-ion-affinity chromatography) [16], TiO_2-MOAC [17] and SIMAC (sequential elution from IMAC) [18]. Since direct phosphopeptide enrichment usually leads to a higher number of identified phosphopeptides with their exact phosphorylation sites, it is not surprising that 962 phosphopeptides corresponding to 598 phosphoproteins were identified.

Although the phosphopeptide enrichment usually results in a higher number of identified peptides, it was disadvantageous in the particular case of tobacco pollen since tobacco genomic sequences were not fully available in the public databases. The non-phosphorylated peptides identified upon phosphoprotein enrichment assisted in the proper identification of the phosphorylated proteins that very often relied on non-tobacco homologous sequences.

The conventional enrichment techniques led to the identification of phosphorylated serine, threonine and tyrosine residues. The proportion of all three phosphorylated amino acids was quite similar in both published male gametophyte phosphoproteomes. In *Arabidopsis*, there was 86% serine, 14% threonine and 0.16% tyrosine residues (represented by one phosphorylation site only) [10] (Figure 1A). In the less complex tobacco phosphoproteome, 67% phosphoserine and 33% phosphothreonine residues were identified. No phosphotyrosine was presented in this dataset [11] (Figure 1B). Tyrosine phosphorylation seems to be less abundant in plants, giving a phosphoserine/phosphothreonine/phosphotyrosine ratio of 91.8:7.5:0.7 [19] or 83.81:16.18:0.01 [20], depending on the material studied. This is likely to be caused by the absence of tyrosine-specific kinases from plants, where tyrosine phosphorylation appears to be carried out by dual-specificity kinases instead [21].

Although in most studies, phosphotyrosine was less abundant in plants compared with in animals, in some cases its proportion was comparable; for instance 4.3% phosphotyrosine in the study by Sugiyama et al. [22]. Thus it remains speculative whether tyrosine phosphorylation is really less abundant in plants compared with animals [23].

Phosphorylated histidine remains undetectable when the conventional phosphoproteomic techniques are applied since it is very labile under acidic pH. Thus special

Figure 1 | The proportion of O-phosphorylated amino acids in the published pollen phosphoproteomics data

(**A**) *Arabidopsis thaliana.* (**B**) *Nicotiana tabacum.*
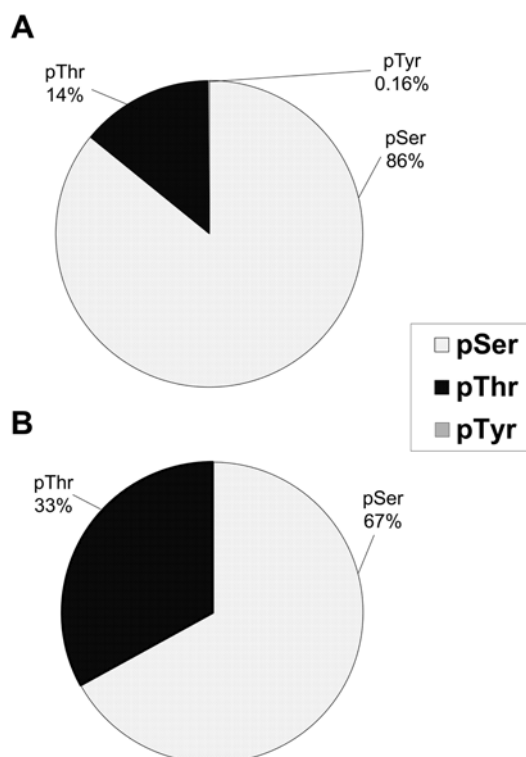
phosphoproteomic methods are required for studies of histidine phosphorylation [24].

Pollen-specific and unknown proteins identified

The phosphoproteomic data from both studies gave the number of phosphorylated proteins and, for some of them, the exact position of phosphorylation site was assigned. The most interesting candidates playing their roles in signalling were likely to be pollen-specific or with higher abundance in pollen. The intriguing unknown proteins can also play such a role.

The *Arabidopsis* phosphoproteome data were searched against the PhosPhAt database that summarizes phosphorylation sites identified in *Arabidopsis* [25,26]. The pollen phosphoproteome presented 240 novel phosphoproteins absent from the database at that time [10], because pollen had never been used as an experimental material for a phosphoproteomic study before. Thus the newly identified proteins were likely to be pollen-specific or at least to be phosphorylated in a pollen-specific manner. This hypothesis was supported at the transcriptomic level. The proteins already present in the database did not show any tissue-specific expression profile. On the contrary, most of the newly identified phosphoproteins showed high or enriched expression in the male gametophyte. Among these

pollen-specific or pollen-enriched proteins, there were several signalling proteins identified, such as protein kinases (e.g. AT1G16760, AT1G78940, AT2G24370 and AT4G31230) or protein phosphatases (e.g. AT1G17720, AT2G33700, AT3G15260 and AT5G10740). Moreover, there were also proteins identified that played a role during exocytosis, such as the members of the EXO70 family (AT5G13150 and AT5G13990). All of these proteins represent candidates for proteins with regulated expression in the male gametophyte. Furthermore, 18 proteins were classified as unknowns, for instance AT1G20770, AT1G30050, AT1G42480, AT2G32980, AT3G30320, AT4G31430, AT5G37550 and AT5G62750.

In contrast, similar information about pollen-specific and/or pollen-enriched proteins was less accessible for tobacco. The data published by Fíla et al. [11] presented the first tobacco phosphorylation sites to be deposited into the P3DB database [27,28], and they still represent the only tobacco data listed in this database. Consequently, on the basis of the P3DB data, it was not possible to distinguish whether there were pollen-specific phosphopeptides among the identified phosphoprotein candidates. Similar difficulties arose when searching for tobacco homologues since its genome sequence was not available in the public databases. It was necessary to identify the phosphopeptides according to homologous sequences from other species. Consequently, the identity of more protein isoforms remained often unclear since it could not be unambiguously stated whether distinctly identified isoforms reflected real isoforms also in tobacco. Moreover, many tobacco pollen-specific proteins may still be unknown and therefore not present in sequence databases. Eight phosphoprotein candidates played a signalling role: several isoforms of 14-3-3 proteins (which regulate many cellular processes [29]) and GDIs (guanine-nucleotide-dissociation inhibitors) of both Rab and Rho GTPases. Surprisingly, no phosphorylated kinases and/or phosphatases were detected. Furthermore, four uncharacterized proteins were identified among the tobacco phosphoprotein candidates.

Phosphorylation sites common to both tobacco and *Arabidopsis*

The intriguing question remained whether the two male gametophyte phosphoproteomic studies led to the identification of phosphorylation sites shared by both species. Again, it has to be kept in mind that both datasets were acquired by different sets of methods and that tobacco proteins were less successfully identified owing to the lack of tobacco sequences in public databases. Therefore the identification mostly relied on non-tobacco homologous sequences present in the database.

The phosphorylated peptides with a homologous phosphorylation site detected in both species are listed in Table 1. They were mostly associated with metabolism such as 2,3-bisphosphoglycerate-independent phosphoglycerate mutase, fructose-bisphosphate aldolase and plasma membrane AT-Pase. The other abundant category was translation regulation

represented by translation elongation factor EF1B/ripening-regulated protein and 60S acidic ribosomal protein. Last, but not least, homologous phosphorylation sites were identified in α-tubulin.

The phosphorylation sites shared in both published datasets did not belong to signalling proteins. This occurrence could be due to several reasons: (i) tobacco signalling proteins were not known and/or their degree of homology with known proteins was not high enough, (ii) many signalling proteins become phosphorylated only after pollen activation, but there was no phosphoproteomic study revealing exact phosphorylation sites in activated pollen, (iii) the homology of some tobacco and *Arabidopsis* signalling proteins could be quite low, so they do not share the conserved amino acids to be phosphorylated.

Phosphorylation motifs and kinases

The mature pollen phosphoproteomes were analysed for the phosphorylation motifs identified. The presence of particular motifs should highlight kinases responsible for the phosphorylation at given phosphosites.

The first set of motifs to be mentioned in both *Arabidopsis* and tobacco are MAPK (mitogen-activated protein kinase) or cyclin-dependent kinase motifs XXXS*PXXX and XXXT*PXXX. MAPKs were shown to play key regulatory roles during male gametophyte development [30]. These proline-directed phosphorylation sites were detected, for instance, in 60S ribosomal protein L12-2, eukaryotic initiation factor 4B, ripening-regulated protein, pollen tube RhoGDI2 in tobacco and, for example, RING/U-box superfamily protein, exocyst subunit EXO70 family protein H5 and ribosomal protein L19e in *Arabidopsis*.

The other kinase motifs common to both tobacco and *Arabidopsis* phosphoproteomes were basophilic motif RXXS*XX that is typical for non-plant CaMK2 (Ca^{2+}/calmodulin-dependent protein kinase 2) or 14-3-3 proteins. In *Arabidopsis*, this motif is recognized by other members of the CDPK (Ca^{2+}-dependent protein kinase)–SnRK (sucrose-non-fermenting-related kinase) superfamily since a typical CaMK is lacking [31]. Furthermore, in tobacco, a casein kinase motif S*XXD/E was detected.

Conclusion

The two phosphoproteomic studies presented provided an insight into the post-translational modifications in the male gametophyte. In tobacco, the phosphoproteomic study was limited by the fact that tobacco sequences were not fully available in public databases. So, the assembly of the sequenced contigs into annotated gene sequences will enable the identification of additional proteins from existing data. When the tobacco genome sequence becomes available in the databases, the identification of phosphopeptides will be easier and a combination of enrichment techniques could be applied in order to identify a broader spectrum of phosphorylated peptides [17].

Table 1 | List of homologous phosphopeptides identified in both *A. thaliana* and tobacco phosphoproteomes

After the protein name identified in tobacco, the species name of the sequence is given. The superscript after the accession number in tobacco indicates the database: a, TIGR EST *Nicotiana tabacum*; b, UniProt, 90% homology clusters, Viridiplantae. The asterisk (*) in the peptide sequences indicates the position of phosphorylation site. In cases where no amino acid with an asterisk is given, the exact position of the phosphorylation site could not be assigned.

Protein name: *Arabidopsis*	Protein name: tobacco	AGI: *Arabidopsis*	Accession number: tobacco	Peptide sequence: *Arabidopsis*	Peptide sequence: tobacco
H$^+$-ATPase 6	Plasma membrane ATPase 4 (*Nicotiana plumbaginifolia*)	AT2G07560.1	NT_TC82708_1[a]	GLDIDNLNQHY**T***V	GLDIETIQQHY**T***V
Phosphoglycerate mutase, 2,3-bisphosphoglycerate-independent	2,3-Bisphosphoglycerate-independent phosphoglycerate mutase (*Nicotiana tabacum*)	AT1G09780.1	NT_TC77653_1[a] NT_TC80529_1[a]	AHGTAVGLPSEDDMG-N**S***EVGHNALGA-GR	AHGNAVGLPTEDDM-GN**S***EVGHNALGA-GR
Translation elongation factor EF1B/ribosomal protein S6 family protein	Ripening-regulated protein DDTFR10-like (*Solanum tuberosum*)	AT2G18110.1	NT_TC77461_1[a]	ISGVSAEGSGVIVEGSS-PITEEAVATPPAAD-SK	ISGVSGEGAGVTVEGS-APITEEAVA**T***P-PAADTK
Glutathione transferase, C-terminal-like; translation elongation factor EF1B/ribosomal protein S6	Ripening-regulated protein DDTFR10-like (*Solanum tuberosum*)	AT1G30230.1	NT_TC77461_1[a]	ISGVSAEGSGVIVEGSA-PITEEAVATPPAA-DSK	ISGVSGEGAGVTVEGS-APITEEAVA**T***PP-AADTK
Tubulin *α*3	*α*-Tubulin, fragment (*Gossypium hirsutum*)	AT5G19770.1	Q9SQ71[b]	TVQFVDWCPTGFK	TVQFVDWCP**T***GFK
Tubulin *α*4 chain	*α*-Tubulin (*Nicotiana tabacum*)	AT1G04820.1	NT_TC77583_1[a] NT_TC77710_1[a] NT_TC78231_1[a] NT_TC80038_1[a]	TIQFVDWCPTGFK	RTIQFVDWCP**T***GFK
Tubulin *α*1	*α*-Tubulin (*Nicotiana tabacum*)	AT1G64740.1	NT_TC77583_1[a] NT_TC77710_1[a] NT_TC78231_1[a] NT_TC80038_1[a]	TIQFVDWCP**T***GFK	RTIQFVDWCP**T***GFK
Tubulin/FtsZ family protein	*α*-Tubulin (*Nicotiana tabacum*)	AT4G14960.2	NT_TC77583_1[a] NT_TC77710_1[a] NT_TC78231_1[a] NT_TC80038_1[a]	TIQFVDWCP**T***GFK	RTIQFVDWCP**T***GFK
Aldolase superfamily protein	Fructose-bisphosphate aldolase (*Solanum tuberosum*)	AT3G52930.1	NT_TC78239_1[a] NT_TC118911_1[a]	LA**S***INVENVETNR	RF**S***SINVENVESNR
Aldolase superfamily protein	Fructose-bisphosphate aldolase (*Solanum tuberosum*)	AT5G03690.1	NT_TC78239_1[a] NT_TC118911_1[a]	FV**S***INVENVESNR	RF**S***SINVENVESNR
60S acidic ribosomal protein family	60S acidic ribosomal protein-like protein (*Solanum tuberosum*)	AT2G27720.1	NT_TC91479_1[a]	LASVPSGGGGGGVAVA-SATSGGGGGGGAP-AAESK	LASVPCGGGGGGVA-VAAPAGGAAAA-A**S***AAEEKK

After the tobacco phosphoproteomic dataset is broadened, it will be possible to also compare the regulatory phosphoproteins present. Possibly, the differences could reflect different regulatory strategies in bicellular pollen (represented by tobacco) and tricellular pollen (represented by *Arabidopsis* [32]). However, in order to reveal such differences in a more general way, it will be necessary to perform phosphoprotein identification in other species (ideally with sequenced genome) shedding both bicellular and tricellular pollen as well.

Finally, '-omic' techniques can bring high-throughput data without knowing function and other details about any single identified protein. So, in order to reveal the function of the proteins themselves and of their phosphorylation sites, more detailed studies will be required.

Funding

References

1 Firon, N., Nepi, M. and Pacini, E. (2012) Water status and associated processes mark critical stages in pollen development and functioning. Ann. Bot. **109**, 1201–1213

2 Honys, D., Reňák, D., Feciková, J., Jedelský, P.L., Nebesářová, J., Dobrev, P. and Čapková, V. (2009) Cytoskeleton-associated large RNP complexes in tobacco male gametophyte (EPPs) are associated with ribosomes and are involved in protein synthesis, processing, and localization. J. Proteome Res. **8**, 2015–2031

3 Honys, D., Combe, J.P., Twell, D. and Čapková, V. (2000) The translationally repressed pollen-specific *ntp303* mRNA is stored in non-polysomal mRNPs during pollen maturation. Sex. Plant Reprod. **13**, 135–144

4 Komis, G., Illés, P., Beck, M. and Šamaj, J. (2011) Microtubules and mitogen-activated protein kinase signalling. Curr. Opin. Plant Biol. **14**, 650–657

5 Muench, D.G., Zhang, C. and Dahodwala, M. (2012) Control of cytoplasmic translation in plants. Wiley Interdiscip. Rev. RNA **3**, 178–194

6 Inze, D. and De Veylder, L. (2006) Cell cycle regulation in plant development. Annu. Rev. Genet. **40**, 77–105

7 Jensen, A.B., Goday, A., Figueras, M., Jessop, A.C. and Pagès, M. (1998) Phosphorylation mediates the nuclear targeting of the maize Rab17 protein. Plant J. **13**, 691–697

8 Gianazza, E. (1995) Isoelectric focusing as a tool for the investigation of posttranslational processing and chemical modifications of proteins. J. Chromatogr. A **705**, 67–87

9 Garnak, M. and Reeves, H.C. (1979) Phosphorylation of isocitrate dehydrogenase of *Escherichia coli*. Science **203**, 1111–1112

10 Mayank, P., Grossman, J., Wuest, S., Boisson-Dernier, A., Roschitzki, B., Nanni, P., Nühse, T. and Grossniklaus, U. (2012) Characterization of the phosphoproteome of mature *Arabidopsis* pollen. Plant J. **72**, 89–101

11 Fíla, J., Matros, A., Radau, S., Zahedi, R.P., Čapková, V., Mock, H.-P. and Honys, D. (2012) Revealing phosphoproteins playing role in tobacco pollen activated *in vitro*. Proteomics. **12**, 3229–3250

12 Fíla, J. and Honys, D. (2012) Enrichment techniques employed in phosphoproteomics. Amino Acids **43**, 1025–1047

13 Dunn, J.D., Reid, G.E. and Bruening, M.L. (2010) Techniques for phosphopeptide enrichment prior to analysis by mass spectrometry. Mass Spectrom. Rev. **29**, 29–54

14 Röhrig, H., Colby, T., Schmidt, J., Harzen, A., Facchinelli, F. and Bartels, D. (2008) Analysis of desiccation-induced candidate phosphoproteins from *Craterostigma plantagineum* isolated with a modified metal oxide affinity chromatography procedure. Proteomics **8**, 3548–3560

15 Machida, M., Kosako, H., Shirakabe, K., Kobayashi, M., Ushiyama, M., Inagawa, J., Hirano, J., Nakano, T., Bando, Y., Nishida, E. and Hattori, S. (2007) Purification of phosphoproteins by immobilized metal affinity chromatography and its application to phosphoproteome analysis. FEBS J. **274**, 1576–1587

16 Nühse, T.S., Stensballe, A., Jensen, O.N. and Peck, S.C. (2004) Phosphoproteomics of the *Arabidopsis* plasma membrane and a new phosphorylation site database. Plant Cell **16**, 2394–2405

17 Bodenmiller, B., Mueller, L.N., Mueller, M., Domon, B. and Aebersold, R. (2007) Reproducible isolation of distinct, overlapping segments of the phosphoproteome. Nat. Methods **4**, 231–237

18 Thingholm, T.E., Jensen, O.N., Robinson, P.J. and Larsen, M.R. (2008) SIMAC (sequential elution from IMAC), a phosphoproteomics strategy for the rapid separation of monophosphorylated from multiply phosphorylated peptides. Mol. Cell. Proteomics **7**, 661–671

19 van Bentem, S.D., Anrather, D., Dohnal, I., Roitinger, E., Csaszar, E., Joore, J., Buijnink, J., Carreri, A., Forzani, C., Lorkovic, Z.J. et al. (2008) Site-specific phosphorylation profiling of *Arabidopsis* proteins by mass spectrometry and peptide chip analysis. J. Proteome Res. **7**, 2458–2470

20 Benschop, J.J., Mohammed, S., O'Flaherty, M., Heck, A.J.R., Slijper, M. and Menke, F.L.H. (2007) Quantitative phosphoproteomics of early elicitor signaling in *Arabidopsis*. Mol. Cell. Proteomics **6**, 1198–1214

21 Rudrabhatla, P., Reddy, M.M. and Rajasekharan, R. (2006) Genome-wide analysis and experimentation of plant serine/threonine/tyrosine-specific protein kinases. Plant Mol. Biol. **60**, 293–319

22 Sugiyama, N., Nakagami, H., Mochida, K., Daudi, A., Tomita, M., Shirasu, K. and Ishihama, Y. (2008) Large-scale phosphorylation mapping reveals the extent of tyrosine phosphorylation in *Arabidopsis*. Mol. Syst. Biol. **4**, 7

23 van Bentem, S.D. and Hirt, H. (2009) Protein tyrosine phosphorylation in plants: more abundant than expected? Trends Plant Sci. **14**, 71–76

24 Besant, P.G. and Attwood, P.V. (2009) Detection and analysis of protein histidine phosphorylation. Mol. Cell. Biochem. **329**, 93–106

25 Heazlewood, J.L., Durek, P., Hummel, J., Selbig, J., Weckwerth, W., Walther, D. and Schulze, W.X. (2008) PhosPhAt: a database of phosphorylation sites in *Arabidopsis thaliana* and a plant-specific phosphorylation site predictor. Nucleic Acids Res. **36**, D1015–D1021

26 Durek, P., Schmidt, R., Heazlewood, J.L., Jones, A., MacLean, D., Nagel, A., Kersten, B. and Schulze, W.X. (2010) PhosPhAt: the *Arabidopsis thaliana* phosphorylation site database. An update. Nucleic Acids Res. **38**, D828–D834

27 Gao, J., Agrawal, G.K., Thelen, J.J. and Xu, D. (2009) (PDB)-D-3: a plant protein phosphorylation database. Nucleic Acids Res. **37**, D960–D962

28 Yao, Q., Bollinger, C., Gao, J., Xu, D. and Thelen, J.J. (2012) P(3)DB: an integrated database for plant protein phosphorylation. Front. Plant Sci. **3**, 206–206

29 van Heusden, G.P. H. (2005) 14-3-3 proteins: regulators of numerous eukaryotic proteins. IUBMB Life **57**, 623–629

30 Heberle-Bors, E., Voronin, V., Touraev, A., Testillano, P.S., Risueno, M.C. and Wilson, C. (2001) MAP kinase signaling during pollen development. Sex. Plant Reprod. **14**, 15–19

31 Hrabak, E.M., Chan, C.W.M., Gribskov, M., Harper, J.F., Choi, J.H., Halford, N., Kudla, J., Luan, S., Nimmo, H.G., Sussman, M.R. et al. (2003) The *Arabidopsis* CDPK–SnRK superfamily of protein kinases. Plant Physiol. **132**, 666–680

32 Brewbaker, J.L. (1967) Distribution and phylogenetic significance of binucleate and trinucleate pollen grains in angiosperms. Am. J. Bot. **54**, 1069–1083

7.3. Souhrnný článek o vývoji samčího gametofytu

Hafidh, S., **Fíla, J.**, Honys, D. (2016). Male gametophyte development and function in angiosperms: a general concept. Plant Reproduction, *publikováno v režimu „on-line first"*, doi: 10.1007/s00497-015-0272-4. $IF_{2014} = 2{,}607$

V tomto přehledovém článku jsem analyzoval data potřebná pro tvorbu tabulky kináz identifikovaných v transkriptomu, proteomu a fosfoproteomu huseníčku rolního. Kromě toho jsem psal manuskript vybraných kapitol („Progamic phase: Catch me if you can" a „Reserves storage and mobilization: Shop till you drop").

CrossMark

REVIEW

Male gametophyte development and function in angiosperms: a general concept

Said Hafidh[1] · Jan Fíla[1] · David Honys[1,2]

Key message   Overview of pollen development.

Abstract   Male gametophyte development of angiosperms is a complex process that requires coordinated activity of different cell types and tissues of both gametophytic and sporophytic origin and the appropriate specific gene expression. Pollen ontogeny is also an excellent model for the dissection of cellular networks that control cell growth, polarity, cellular differentiation and cell signaling. This article describes two sequential phases of angiosperm pollen ontogenesis—developmental phase leading to the formation of mature pollen grains, and a functional or progamic phase, beginning with the impact of the grains on the stigma surface and ending at double fertilization. Here we present an overview of important cellular processes in pollen development and explosive pollen tube growth stressing the importance of reserves accumulation and mobilization and also the mutual activation of pollen tube and pistil tissues, pollen tube guidance and the communication between male and female gametophytes. We further describe the recent advances in regulatory mechanisms involved such as posttranscriptional regulation (including mass transcript storage) and posttranslational modifications to modulate protein function, intracellular metabolic signaling, ionic gradients such as Ca^{2+} and H^+ ions, cell wall synthesis, protein secretion and intercellular signaling within the reproductive tissues.

Communicated by Enrico Schleiff.

A contribution to the special issue 'Pollen development and stress response'.

✉   David Honys
    david@ueb.cas.cz

[1]   Institute of Experimental Botany ASCR, v.v.i., Rozvojová 263, 165 00 Prague 6, Czech Republic

[2]   Department of Experimental Plant Biology, Faculty of Science, Charles University in Prague, Viničná 5, 128 44 Prague 2, Czech Republic

Introduction

Reproduction is a characteristic feature of living organisms ensuring the continuity of life on earth through a series of successive generations. In plants, there is an alternation of sexual and asexual generations, sporophyte and gametophyte. In the sporophyte, the individuals consist of diploid cells and reproduce asexually through haploid spores generated by the meiotic division in sporogenous tissue. The spores germinate into the gametophyte, where specialized reproductive organs, female archegonia and male antheridia are formed in which haploid gametes of separate sexes arise. The fusion of male and female gametes leads to the formation of a diploid zygote, the first cell of the next sporophyte generation. In the evolutionary line of vascular plants (*Tracheophyta*), gametophytic reduction and increased functional dependence on the sporophyte is apparent. Angiosperms, which currently account for more than 280,000 species (reviewed by Scotland and Worltey 2003), constitute the overwhelming majority of plant species with maximum reduction of the gametophyte. This reduction together with protection of the reproductive organs within a flower and stringent selection of the fittest pollen to

reproduce is considered to be the main cause of the evolutionary success of angiosperms (Mulcahy 1979; Mulcahy et al. 1996). Most angiosperms form bisexual flowers containing anthers and pistils, where both male and female gametophytes develop. Both structures—pollen grain and ovule—are microscopic, consisting of only a few cells fully supported by the surrounding sporophytic tissues and organs for their development. The only time, when gametophytes of flowering plants exist independently of the sporophyte, is when mature pollen is shed from the anther and is carried to the stigma to undergo reproduction with female gametes.

In the past, the small size of the male gametophyte made its exploration—and even its discovery—very complicated. Therefore, the external appearance of pollen grains stood at the beginning of pollen research (Malpighi 1675, 1679; Purkyně 1830). Further knowledge of the pollen and pollen tube structure and function was gradually acquired together with the other basic phenomena associated with the sexual reproduction of angiosperms, such as the existence of bi- and tri-cellular pollen (Elfving 1879), differentiation of vegetative and generative cells (Strasburger 1884) and the double fertilization (Nawaschin 1898). Subsequent considerable progress in pollen research has been driven by the rapid development of cytological and molecular methods. Equally important was the introduction of in vitro, semi in vivo and in vivo techniques and in particular the onset of "high-throughput" technologies in the recent 20 years.

Male gametophyte

Male gametophyte development of angiosperms is a complex process that requires coordinated activity of different cell types and tissues of both gametophytic and sporophytic origin underlaid by specific gene expression patterns. Male gametophyte development is comprised of two consecutive phases, developmental and functional.

The developmental phase takes place in anther loculi and leads to the release of mature pollen grains from the anthers. It is characterized by the functional specialization of two cell types—vegetative cells and male gametes, the sperm cells, which together represent the male germline (reviewed by Berger and Twell 2011). This process is underpined by two successive cell divisions accompanied by remarkable morphological and physiological differentiation of both cell types including the synthesis of specialised pollen cell wall and the storage of protective substances and metabolic reserves.

The functional or progamic phase is initiated after the pollen grain lands on the stigma. Pollen is activated by rehydration, germinates and produces a long pollen tube that grows into the pistil tissues. Its growth ends with a double fertilization after reaching the ovule. It is not only the pollen tubes explosive growth that makes the progamic phase interesting but also the mutual activation of pollen tube and pistil tissues, pollen tube guidance and the communication between the two gametophytes (reviewed by Dresselhaus and Franklin-Tong 2013).

Unlike the sporophyte, the male gametophyte represents highly reduced, two- or three-celled model system providing a unique opportunity to study the developmental regulation of cell morphogenesis and differentiation at many levels as well as the functional interactions between different cell types (Berger and Twell 2011; Borg et al. 2009; Dresselhaus and Franklin-Tong 2013; Dresselhaus and Sprunck 2012; Hafidh et al. 2014; Kessler and Grossniklaus 2011; Ma 2005; Rutley and Twell 2015; Twell 2011).

Pollen maturation: get ready for the race!

Diploid microspore mother cells (microsporocytes) are encapsulated in the young anther loculi surrounded by four cell layers—tapetum, middle layer, endothecium and epidermis. The microsporocytes secrete cell wall materials consisting of β-1,3-glucan and callose. After two meiotic divisions, the microsporocytes divide into four haploid microspores forming a tetrad (Fig. 1). In Avena sativa, microspore mother cells communicate via cytoplasmic bridges enabling the synchronization of meiotic divisions throughout the loculus (Brett and Waldron 1990). The second meiotic division is followed by the synthesis of callose walls between the individual microspores within a tetrad. However, the timing of callose wall formation differs between different plant species (Chen and Kim 2009; De Storme and Geelen 2013; Lu et al. 2014).

During meiosis, the secretory tapetal cells differentiate into binuclear polar cells lacking the primary cell wall, especially at the loculi-facing side. These cells contain abundant ribosomes, mitochondria, endoplasmic reticulum, Golgi apparatus and specialized lipid-rich organelles, tapetosomes (Bedinger 1992; Hsieh and Huang 2005; Ting et al. 1998), close to the plasma membrane facing the anther loculi. The tapetal cells are interconnected by cytoplasmic bridges allowing the coordination of their activities. Transcriptomic studies of anther tissues in various plant species demonstrated the precise control of the activity and subsequent programmed cell death of tapetal cells and the tight coordination of these processes with pollen development (Huang et al. 2011).

Young microspores in tetrads undergo rapid development accompanied by synthesis of the cell wall consisting of an inner intine and outer exine. After the emergence of partially formed exine, microspores are released from tetrads in a synchronised manner (Fig. 1). The release of the microspores is prompted by the activity of an enzyme
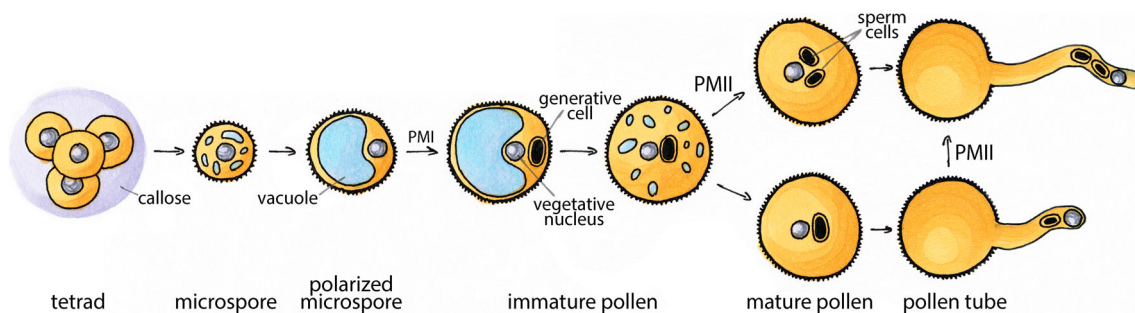
Fig. 1 Schematic diagram describing pollen development (adapted and simplified from Honys et al. 2006)

mixture secreted by tapetal cells, with callase (β-1,3-glu-canase) being its essential component responsible for the callose degradation (Lu et al. 2014; Scott et al. 2004). Callase synthesis was shown to be controlled by MYB-family transcription factor AtMYB80 that links pollen maturation with tapetum development resulting in pro-grammed cell death of tapetal cells (Phan et al. 2011; Zhang et al. 2007). Proper timing of callase secretion is one of the critical moments in microsporogenesis and its dis-tortion causes male sterility (Worrall et al. 1992). Free microspores rapidly enlarge and numerous small vacuoles eventually merge into one large vacuole pushing the microspore nucleus from its central position to the cell periphery. The actual microspore polarisation is not just a passive event caused by the growth of vacuoles but a highly dynamic process requiring the active participation of microtubules (Oh et al. 2010; Park et al. 1998; Twell 2011). During microsporogenesis, the tapetal cells remain highly metabolically active. They secrete proteins, lipids, carbohydrates and secondary metabolites to the loculi to be used by developing microspores to synthesize membranes, for exine formation and as a source of energy (Pacini 1990). Despite the obvious importance of tapetum, it is possible to achieve the proper maturation of functional pollen in vitro from uninuclear microspores in the presence of essential nutrients (Tupý et al. 1991).

The highly specialised biological role of angiosperm pollen is reflected by the unique composition of the sur-rounding cell wall. The sculptured pollen wall not only protects the male gametophyte and its precious cargo but facilitates the broad communication with the stigma surface (Scott et al. 2004). Its inner layer, intine, is of gametophytic origin whereas the outer layer, exine, is mostly sporophytic. The synthesis of pollen wall begins already in tetrads, immediately after the completion of meiosis. Microspores in tetrads first synthesize the pectin-cellulose primexine functioning as a matrix for the deposition of sporopollenin precursors preceding their subsequent polymerization. As a complex compound of fatty acids and phenylpropanoids, sporopollenin belongs among the toughest known

biopolymers and its role is the protection of the pollen internal environment (including genetic information) after pollen shedding from the anthers. Although the biochemical pathway of sporopollenin synthesis remains elusive, its synthesis requires close cooperation between microspores and tapetum (Ariizumi and Toriyama 2011; Dobritsa et al. 2009, 2010; Quilichini et al. 2015). The recalcitrant exine is not distributed evenly around pollen grains; it is not deposited or it is reduced in the apertures, where pollen tubes emerge (Furness and Rudall 2004). The number, size and distribution of apertures are an important classification factor that is under strict sporophytic control. In Ara-bidopsis, aperture marking depends on the prior localisation of INAPERTURATE POLLEN1 protein (Dobritsa and Coerper 2012; Dobritsa et al. 2011).

Formation of the pollen coat is completed in the later stages of microgametogenesis when the residues of the degenerating tapetum are deposited on the surface of pollen grains (Quilichini et al. 2015). Pollen coat determines the pollen adhesiveness, colour, taste and aroma. These prop-erties as well as the often highly elaborated structure of the pollen wall are species-specific. This is of key importance not only for pollen interaction with papillary cells on the stigma but also to facilitate its recognition by pollinators. Insect- and other animal-pollinated species shed pollen that can be decorated with extremely complex surface struc-tures facilitating its adhesion to the pollinators whereas in wind-pollinated species these structures are often absent (Fellenberg and Vogt 2015).

Polarised microspores undergo an asymmetric division during pollen mitosis I (PMI, Fig. 1) resulting in the for-mation of two unequal daughter cells with distinct cell fates, a large vegetative cell and a small generative cell. Both cells are present in the space bound by the microspore cell wall. The generative cell soon migrates into the veg-etative cell to form a unique "cell-within-a-cell" structure (Russell and Jones 2015; Russell et al. 1996). PMI repre-sents another critical moment in the male gametophyte development; it ensures the fixation of the ongoing male gametophytic developmental program, as demonstrated in

various plant species by transcriptomic (Bokvaj et al. 2015; Honys and Twell 2004; Wei et al. 2010) and proteomic studies (Chaturvedi et al. 2013; Grobei et al. 2009; Holmes-Davis et al. 2005; Ischebeck et al. 2014; Noir et al. 2005; Sheoran et al. 2006). Therefore the reversal from the gametophytic to the sporophytic development is achievable only with unicellular microspores but not with bicellular pollen grains (Gaillard et al. 1991). PMI also results in the initiation of the male germline; the generative cell retains its proliferative activity and divides once more during pollen mitosis II (PMII) to produce two male gametes, the sperm cells (Berger and Twell 2011; Twell 2011). The disruption of the asymmetry of PMI either by centrifugation (Terasaka and Niitsu 1987), by the application of microtubule-destabilizing agents, e.g. colchicine (Eady et al. 1995; Zaki and Dickinson 1991), or in particular pollen mutants, e.g. MOR1/GEM1 (Park et al. 1998), leads to the formation of two similar cells with the vegetative cell fate. Arabidopsis MOR1/GEM1 (Park et al. 1998; Twell et al. 2002) and its tobacco ortholog TMBP200 (Oh et al. 2010) encode microtubule-associated proteins, plant orthologs of the MAP215/Dis1 protein family. Phenotype defects resulting from the knock-out of the above genes clearly demonstrated the importance of microtubules in the establishment of cellular polarity preceding PMI, asymmetry of which is the key factor in the initiation of male germline (Twell 2011).

The generative cell undergoes yet another mitotic division—PMII—resulting in the formation of two sperm cells. The vegetative nucleus remains in a close physical connection with the two sperm cells after PMII forming the male germ unit (MGU). It plays the vital role not only in the delivery of sperm cells to the female gametophyte, but especially in direct communication between the cells and their nuclei of somatic origin and the germline (McCue et al. 2011) perhaps including the modulation of their gene expression (Slotkin et al. 2009).

The PMII can occur before or after pollen maturation and therefore the mature pollen grain can be shed as bicellular (in which the vegetative cell engulfs a single undivided generative cell) or as tricellular (where the vegetative cell is associated with two sperm cells) (Brewbaker 1967). From an evolutionary point of view, the bicellular pollen is a plesiomorphy trait whereas the tricellular pollen represents an advanced trait. However, it was postulated recently that a reverse transition from tricellular to bicellular pollen has also occurred (Williams et al. 2014). Thus, some species sheding bicellular pollen underwent two evolutionary changes rather than keeping the original trait permanently (Williams et al. 2014). The mature pollen grain has a dehydrated cytoplasm; bicellular pollen was usually shown to be in a more dehydrated and quiescent state than tricellular pollen. This assumption was based on the observation that tricellular pollen was usually quicker in the onset of pollen germination and subsequent tube growth (Brewbaker 1967). Furthermore, the basal angiosperm *Annona cherimola* was shown to shed both bicellular and tricellular pollen in different ratios according to the surrounding air temperature (Lora et al. 2009). In a higher temperature (30 °C), almost half of the pollen grains were tricellular whereas at lower temperature (20 °C), the bicellular pollen grains strongly prevailed. It was speculated that in warmer weather, a higher proportion of tricellular pollen was biologically relevant since it allowed faster germination and fertilization that was beneficial since stigma tissues were shorter-lived in a warmer climate. On the other hand, at lower temperature a higher proportion of bicellular pollen can successfully be more widely dispersed due to its higher dehydration and longer life span. This effect is further supported by a longer life span of pistils under milder temperatures around 20 °C (Lora et al. 2009).

Progamic phase: catch me if you can

As pollen grain reaches the papillary cells of the stigma, it is rehydrated and activated (Firon et al. 2012). Under in vitro conditions, Arabidopsis pollen does not increase in volume during the first 21 min of activation (Vogler et al. 2015). The period of no apparent pollen grain enlargement is even longer in more dehydrated bicellular pollen (Barnabas and Fridvalszky 1984). Then, the pollen tube emerges and starts growing with gradually increasing speed (Vogler et al. 2015). The pollen tubes growth rate reaches up to 1 cm per hour, placing them among the fastest-growing plant cells (Lim and Gumpil 1984). The pollen tube growth dynamics and its dependence on stored nutrition reserves differs between studied bicellular and tricellular pollen species (Mulcahy and Mulcahy 1988). Bicellular pollen tube growth consists of two phases—the first growth period is relatively slow with no formation of callose plugs. The second growth period showed more rapid growth characteristics accompanied by callose plugs formation (Fig. 2c). Growth during the first period consumed the reserves carried by the pollen grain itself whereas the second phase mostly relied on nutrition from the style. On the other hand, tricellular pollen started to grow quickly together with callose plug formation that relied on stylar nutrition from the beginning (Mulcahy and Mulcahy 1988).

Pollen tube growth is not isodiametric but together with root hairs, fungal hyphae and vertebrate axons represents an example of tip growth (Palanivelu and Preuss 2000; Šamaj et al. 2006). It is characterized by continuous elongation at one tip of the cell without any further

Fig. 2 Pollen tube apical region. **a** Scheme of the lily pollen tube tip showing actin cytoskeleton dynamics and pollen tube zonation (adapted from Hepler and Winship 2015); individual structures are not drawn to scale). **b** Ca^{2+} and H^+ gradients in lily pollen tube apex (adapted from Hepler and Winship 2015); individual structures are not drawn to scale). **c** Distribution of callose (*arrow*) in activated tobacco pollen grains and during pollen tube germination observed by aniline blue staining. Callose plugs are only visible >4 h post germination (Hafidh et al. unpublished data)
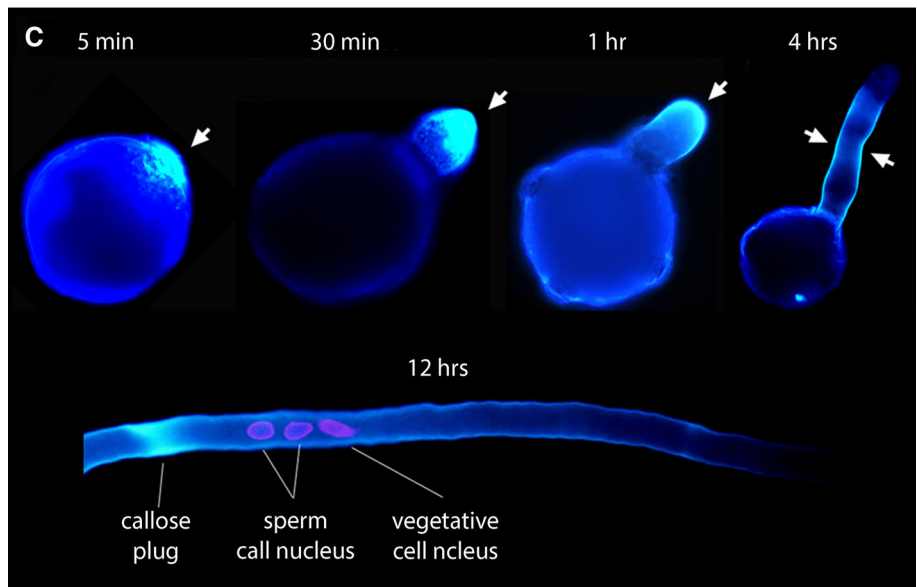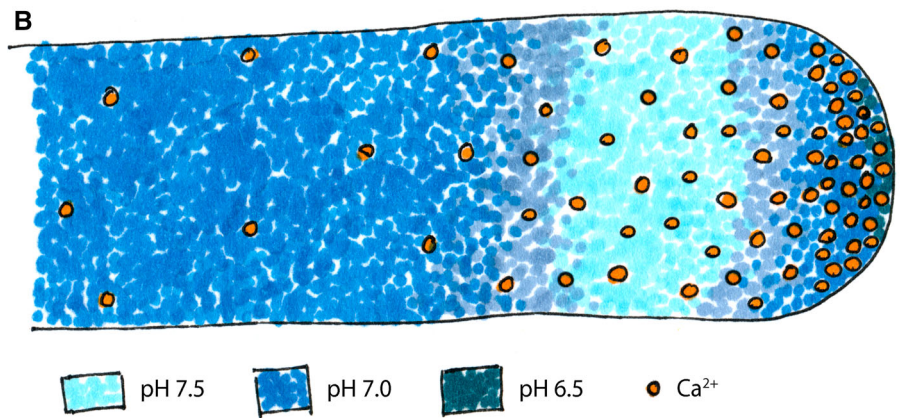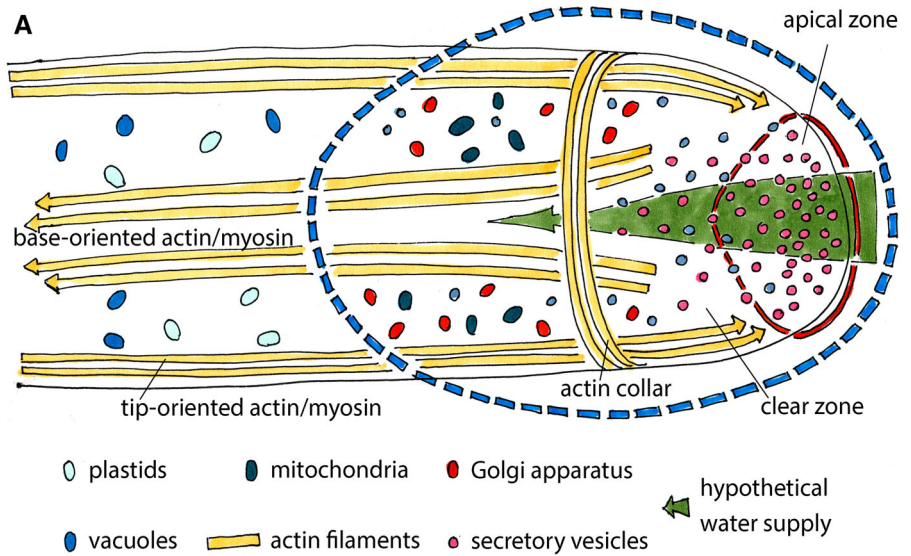
divisions of the vegetative cell. Pollen tubes can reach a maximum of 50 cm (Mascarenhas 1993) in plant species with long styles, for example maize. Tip growth requires several mechanisms that are evolutionary conserved in various tip-growing tissues of different organisms: cytoskeleton organization, vesicular trafficking, small GTPases signalling and ion gradient formation (Palanivelu and Preuss 2000; Šamaj et al. 2006). Moreover, novel formation of cell wall is required in the growing pollen tubes since they usually outgrow the diameter of the pollen grain several-fold. This is achieved by the formation of callose plugs in regular distances to maintain constant amount of cytoplasm required for filling the inside space of the pollen tube (Ferguson et al. 1998; Mogami et al. 2006).

From this point of view, pollen tube contains several zones. The tip-most zone is called clear zone as it looks "clear" under the microscope because the organelles present there have quite low refractivity—in particular, the starch-containing amyloplasts are missing from this part of pollen tube (Hepler and Winship 2015; Vidali et al. 2001). This clear zone comprises two distinct regions, apical and subapical (Fig. 2a). The apical region is typical for its inverted cone-shape, in which endoplasmic reticulum elements and vesicles are present. On the other hand, the subapical region of the clear zone contains also Golgi apparatus and mitochondria. Behind the clear zone, there are also larger organelles, such as amyloplasts and vacuoles (Lancelle and Hepler 1992). The refractivity of this region is also higher than that of the clear zone so its appearance is quite different in both light and electron microscopes (Hepler and Winship 2015).

Fast pollen tube growth and overall morphology is underlaid by the organization and function of the cytoskeleton. Starting behind the subapical zone of lily pollen, actin filaments are organized in parallel bundles (Staiger et al. 2010; Wilsen et al. 2006). The cortical filaments transport vesicles towards the tip whereas the central filaments are dedicated for the basipetal vesicular transport (Fig. 2a). Thus, the vesicular flow resembles a reversed fountain. Myosins, the motor molecules along the actin filaments, move towards the barbed ends of microfilaments. In order to allow the transport in the desired direction, the cortical and central filaments are oriented the opposite way: the central ones have their barbed ends facing the tube tip whereas the cortical filaments face the tip by their pointed ends (Lenartowska and Michalska 2008). Near the border between pollen tube apical and subapical regions an actin collar is formed and its position is likely to be regulated by a higher pH 7.5 and Ca^{2+} gradient. In comparison, pH at the very tip of the pollen tube reaches 6.5 (Feijó et al. 2004). These two factors (pH and Ca^{2+} concentration) control actin polymerization together with actin-binding proteins activity (see below). In the apical region, actin

filaments are randomly oriented so they are organized into a net structure. This tip-most region is shaped as a reversed cone and beside the net structure of actin filaments; it typically contains vesicles (Hepler and Winship 2015). The vital importance of this actin net structure in the apical zone was demonstrated by the application of latrunculin B that strongly impaired pollen tube growth and morphology (Vidali et al. 2001). Latrunculin B binds to the actin monomers and blocks them from polymerization whilst the stable actin filaments remain unimpaired by latrunculin B treatment. The role of microtubules in the growing pollen tubes was thought to be less important and originally it seemed that the organelles and vesicles were mainly transported along actin filaments since the colchicine application did not stop pollen tube growth (Heslop-Harrison et al. 1988). However, later, mitochondria were reported to be transported along microtubules in pollen tubes grown in vitro (Romagnoli et al. 2007) and tubulin was shown to be part of RNA storage particles (Honys et al. 2009). Recently, a more prominent role of microtubules in pollen tubes (for instance in vesicular transport) was reported (Onelli et al. 2015). Microtubules are therefore likely to attract more attention in the future pollen tube studies.

The distribution of pollen tube organelles as well as the organization of pollen tube growth rely also on ion fluxes and gradients. Among them, calcium ions (Ca^{2+}) and protons (H^+) are of a key importance (Michard et al. 2009). Ca^{2+} ions show a gradually increasing concentration towards the pollen tube tip, a distribution usually called "tip-focused gradient" (Fig. 2b). In the pollen tube apex, the Ca^{2+} concentration reaches 1–10 μM concentration, ten- to hundredfold higher than in the pollen tube shank with Ca^{2+} concentration ranging between 0.1 and 0.3 μM (Holdaway-Clarke et al. 1997). An increased Ca^{2+} concentration in the pollen tube apex can serve as a signal for Ca^{2+}/calmodulin protein kinases, some of which were identified in pollen trancriptome and/or proteome (Supplementary Table 1 and the section below). The Ca^{2+} gradient is also crucial for the regulation of actin cytoskeleton dynamics since Ca^{2+} ions activate villin/gelsolin, which promotes the destabilization of actin filaments (Ren and Xiang 2007). Moreover, the activity of profilin in monomer actin sequestration is promoted by Ca^{2+} (Kovar et al. 2000). Thus, these two proteins collectively destabilize actin filaments and prevent its re-polymerization in the tip-most region of the pollen tube. It should be stressed once more that the increased Ca^{2+} concentration is only at the pollen tube tip since further from the tip, the excessive Ca^{2+} ions are sequestered by endoplasmic reticulum and mitochondria and the Ca^{2+} concentration is kept at the normal physiological values (reviewed in Hepler and Winship 2015). Another process that is promoted by an

elevated Ca^{2+} concentration is exocytosis (Camacho and Malho 2003).

The proton gradient is formed in a similar way—protons enter the pollen tube cytoplasm via proton pumps at the tip where there is a slightly acidic pH (pH 6.5). The distal band in the clear zone remains, on the other hand, slightly alkaline (pH 7.5; Feijó et al. 2004) (Fig. 2b). Interestingly, this apical acidic pH area resembles the reverse-cone shape discussed above (Michard et al. 2008). Similar to calcium ions gradient, the pH variation contributes to the actin cytoskeleton dynamics via actin-binding proteins. The slightly alkaline pH in the subapical region promotes ADF/cofilin complex that cuts the actin filaments to more parts (Allwood et al. 2002; Chen et al. 2002; Lovy-Wheeler et al. 2006; Staiger et al. 2010) and thus promotes actin dynamics in the cortical region of pollen tube. In the shank and at the pollen tube tip, there is neutral pH 7.0 or slightly acidic pH 6.5, respectively, under which ADF/cofilin is inactive.

Taken together, the ion fluxes and gradients are not static in a growing pollen tube but exhibit regular oscillations (Feijó et al. 1999; Holdaway-Clarke et al. 1997; Shi et al. 2009). These gradient oscillations together with cytoskeleton dynamics are reflected in pollen tube growth. For example, growth rate of in vitro cultivated lily pollen tubes oscillates between 0.1 and 0.4 $\mu m \ s^{-1}$ within 15–50 s (Pierson et al. 1996). All of the above mentioned factors seem to be coordinated but a general pacemaker is still not known (Michard et al. 2009).

Both cytoskeleton dynamics and ion gradient oscillations tightly co-operate with the activity of small GTPases from the Rab, Arf and Rop/Rac families that play a key role during vesicular transport and other processes in the growing pollen tube (Šamaj et al. 2006). These small G-proteins have two states, the active form binding GTP and the inactive form bound to GDP (Bishop and Hall 2000). Moreover, the activity of the small GTPases is regulated by three main classes of protein factors—guanine nucleotide exchange factors (GEFs), GAFs and GDIs. GEFs promote the activity of small GTPases by exchanging GDP for GTP. The GTPases inactivate themselves by their GTPase activity, and this inactivation can be accelerated by GTPase accelerating factors (GAFs) that promote the GTPase activity of G-proteins. Finally, guanine nucleotide dissociation inhibitors (GDIs) conserve the G-protein in the GDP-bound form and thus block GTPase reactivation (Feher and Lajko 2015).

Arf GTPases are involved in the vesicular transport and localize to both endosomes and Golgi apparatus. Mutations directly affecting Arf GTPases themselves were not described in pollen tube functional studies. However, several experiments showed their roles during pollen tube growth by analysing *gnom* (Arf GEF) mutants or by application of brefeldin A that acts as a GNOM inhibitor (Zhang and McCormick 2010). Rab proteins are associated with endomembranes and show usual specificity to particular parts of the endomembrane system (Woollard and Moore 2008). RAB11B in tobacco and RABA4D in Arabidopsis were shown to be required for a correct pollen tube growth (de Graaf et al. 2005; Szumlanski and Nielsen 2009). Not surprisingly, these small GTPases were important for pollen tube growth since they are vital for exocytosis of various compounds such as cell wall precursors, membrane components and signalling molecules which promote pollen tube growth (Qin and Yang 2011). Rop GTPases with bound GTP are usually localized in the apical plasma membrane. They execute several important functions such as organization of the actin cytoskeleton. They generate reactive oxygen species, and mediate calcium-dependent signaling (Zheng and Yang 2000; Šamaj et al. 2006). ROP1 was discovered in apical membranes of tobacco and lily pollen tubes (Fu et al. 2001; Zhao and Ren 2006). Not only the GTPases themselves but also their regulating proteins such as RhoGDI were shown to play important roles in pollen tube growth (Klahre et al. 2006); they are integrated into the cellular signalling network of kinases acting both upstream and downstream the Rop GTPases (Feher and Lajko 2015).

Reserves storage and mobilization: shop till you drop

The vegetative cell of the immature pollen grain contains a dense cytoplasm with numerous organelles. The maturing pollen grain shows considerable metabolic activity and the vegetative cell accumulates a considerable amount of various metabolic reserves including carbohydrates, proteins and lipids necessary for the rapid growth of the pollen tube (Pacini 1996; Pacini et al. 2006). A specific portion of reserves comprises osmoprotectants, e.g. disaccharides, proline and glycinebetaine, protecting cellular membranes and proteins from damage caused by dehydration (Schwacke et al. 1999). The generative cell inherits from the microspore a very small portion of the cytoplasm and organelles. Whereas the generative nucleus contains highly condensed chromatin, the larger vegetative nucleus with numerous pores exits the cell cycle in G1 phase and contains decondensed chromatin. Therefore higher transcriptional activity of the vegetative nucleus in comparison to the generative cell can be assumed; however, that is not negligible either (Borges et al. 2008).

From PMI to the maturity, pollen accumulates both mRNA and proteins (Hafidh et al. 2011; Honys et al. 2009). In this period, pollen volume doubles, the amount of total RNA increases seven times and mRNA content increases

thirteen to twenty times (Schrauwen et al. 1990; Tupý 1982). Pioneering experiments using transcription and translation inhibitors in tobacco pollen tubes showed that transcription was detected only during the first several hours of the pollen tube growth, which led to the conclusion that pollen tube growth was mainly dependent on translation but virtually independent of transcription (Čapková et al. 1988). However, the introduction of high-throughput technologies led to the identification of numerous genes transcribed specifically after pollen germination in vitro in all species studied—Arabidopsis (Qin et al. 2009; Wang et al. 2008), rice (Wei et al. 2010) and tobacco (Hafidh et al. 2012a, b). Moreover, many transcripts were *de novo* synthesized even in the tobacco pollen tubes cultivated as long as 24 h (Hafidh et al. 2012a). Interestingly, the interaction of the pollen tube with the pistil tissues, during which pollen tubes gained the competence for fertilization (Higashiyama et al. 1998; Palanivelu and Preuss 2006), activated a specific set of 1254 genes that were not detected in in vitro cultivated pollen tubes (Qin et al. 2009). Moreover, 383 of these genes were pollen-enriched. De novo expression of genes involved predominantly in signal transduction, transcription and pollen tube growth in pistil-activated pollen tubes suggested the possibility of a female-responsive regulatory network orchestrating pollen tube gene expression upon growth through the pistil (Qin et al. 2009). A set of pistil-activated genes required for pollen tube differentiation and sperm cells release was later found to be controlled by three SIV pollen-tube expressed related MYB transcription factors—MYB97, MYB101 and MYB120 (Leydon et al. 2013).

In tobacco, stored transcripts were shown to be associated with large translationally silent ribonucleoprotein particles (EPP complexes; Honys et al. 2000). EPP complexes are associated with the cytoskeleton and contain small and large ribosomal subunits (Honys et al. 2009). Upon pollen activation and during subsequent pollen tube growth, the transcripts stored in EPPs are de-repressed and translated (Honys et al. 2009). Furthermore, EPP particles are likely to be transported towards the tip of the growing pollen tube and could represent a transport form of the transcripts originating from mature pollen. The translation itself leads to production of native polypeptides that undergo a plethora of possible post-translational modifications (PTMs) to form a functional mature protein product. These include phosphorylation, methylation, glycosylation, myristoylation, acetylation etc. (Knorre et al. 2009) that are usually essential for the proper protein structure and function. Here we will focus in more detail on protein glycosylation and phosphorylation since these modifications have been studied most intensely in the male gametophyte.

Protein glycosylation is a co-translational or post-translational covalent attachment of carbohydrate chains (glycans) to the polypeptide backbone. According to the atom, by which the carbohydrate residues are bound to the peptide, three types of glycosylation are recognized. *N*-glycosylated proteins bear the glycans on nitrogen atoms of asparagin in the Asn-X-Ser/Thr consensus sequence, where X is any amino acid except proline, serine, and threonine (Lerouge et al. 1998). *O*-glycosylation is executed on the oxygen atom of serine, threonine or hydroxyproline (Hanisch 2001). Finally, rare *S*-glycosylated proteins carry their glycan moiety on the sulphur atom of cysteine (Stepper et al. 2011).

Protein glycosylation usually increases protein stability and plays a role in protein–protein interactions (Ueda et al. 1996). Likewise, many pollen allergens are glycosylated (reviewed by Puc 2003). Glycoproteins or more heavily glycosylated proteoglycans are important components of cell walls and they are often found in association with membranes or as secreted proteins. In all these compartments, numerous members of a large family of the proline/hydroxyproline-rich glycoproteins are prominent. This family was originally classified into three separate classes: none or subtly glycosylated proline-rich proteins (PRPs), moderately glycosylated extensins and heavily glycosylated arabinogalactan-proteins (AGPs) (for review see Ellis et al. 2010; Wu et al. 2001). The latter two classes are defined by the presence of *O*-glycosylated hydroxyproline as hydroxyproline-rich glycoproteins (HRGPs) and their heterogeneity and abundance attributed them to multiple functions in plant growth and development, plant defence and signalling (Ellis et al. 2010). Recently, HRGPs were identified as a component of calcium signalling pathway (Lamport and Varnai 2013).

In Arabidopsis, a specific subset of AGPs was shown to be expressed in reproductive tissues with the majority of them being present in female tissues along the path taken by the growing pollen tube (Pereira et al. 2014). However, four AGPs, namely two classical AGPs (AGP6, AGP11) and two AG-peptides (AGP23 and AGP40) were specifically expressed in pollen and pollen tubes (Nguema-Ona et al. 2012). A subset of AGPs, namely those expressed in the male gametophyte, are attached to the plasma membrane by glycosylphosphatidylinositol (GPI) anchor (Lalanne et al. 2004). One function of these proteoglycans is the control of nexine formation (Jia et al. 2014) and subsequent pollen germination. Higher number of early germinating pollen tubes within the anthers was observed in *agl6/agl11* double and *agl6/agl11/agl40* triple mutants (Nguema-Ona et al. 2012). Accordingly, the knockout of pollen-expressed AGPs resulted in a reduced seed set. The expression pattern of male gametophytic AGPs is supposed to be balanced since the up-regulation of AGP40 and

AGP23 was observed in *agl6/agl11* double null mutant pollen tubes (Nguema-Ona et al. 2012). Recently it was reported that the expression of all four pollen-specific AGPs is directly controlled by the AT-hook nuclear localized (AHL) family DNA-binding TEK protein (Jia et al. 2014), which therefore indirectly controls nexine formation in the pollen wall (Lou et al. 2014).

Extensins (EXTs), the second large class of HRGPs, are also present in the cell wall where they are involved in the formation of crosslinking networks. Therefore their activity is predominantly observed in fast growing cells like root hairs and pollen tubes (Cannon et al. 2008; Lamport et al. 2011). Unlike AGPs, extensins do not show strict pollen-specific expression patterns and their co-expression in pollen tubes and root hairs was observed (Dupľáková et al. 2007; Hruz et al. 2008). This is also the case for EXT18, a classical extensin required for vegetative growth, reproductive development, pollen viability and fertility. Among other phenotypic defects, *ext18* mutants show significantly slower pollen tube growth and reduced seed set (Choudhary et al. 2015).

Although prominent, *O*-glycosylated HRGPs are not the only glycoproteins associated with male gametophyte function. In tobacco pollen tubes, two highly abundant cell wall *N*-glycoproteins of 66 and 69 kDa were identified (Čapková et al. 1997). The block of their *N*-glycosylation by tunicamycin caused reduction of the callose deposition into pollen tube cell wall and consequently impaired pollen tube growth. Glycoproteins of similar sizes were found also in several other angiosperm species (Fidlerová et al. 2001). In spite of the abundance and apparent important function of these *N*-glycoproteins, their exact molecular activity is still unknown. Moreover, protein *N*-glycosylation was demonstrated to be of vital importance in pollen tube perception (Lindner et al. 2015). The *EVAN* and *TURAN* genes encode putative uridine diphosphate (UDP)-glycosyltransferase superfamily protein and dolichol kinase, respectively. It is likely that proteins responsible for pollen tube perception in female organs are strongly glycosylated since mutations of these genes taking part in *N*-glycosylation pathway caused premature pollen tube burst (Lindner et al. 2015). Therefore membrane- and cell wall-associated glycoproteins are not only important for pollen tube growth through the pistil but are also good candidates to mediate male–female cross-talk during double fertilization.

Protein phosphorylation is rather fast, dynamic and transient PTM, and its reversible nature predestines it for a regulatory role. The switch from a metabolically quiescent pollen grain to a rapidly growing pollen tube has to be precisely regulated by several mechanisms including protein phosphorylation. In the past decade, plant phosphoproteomics evolved rapidly and nowadays, several protocols are available (Dunn et al. 2010; Fíla and Honys 2012). Some of these protocols deal with the challenges of protein extraction and phosphoprotein/phosphopeptide enrichment from very tough tissues such as mature pollen grain (Fíla et al. 2011, 2012; Mayank et al. 2012; Sheoran et al. 2009). Many phosphoproteomics studies have been performed in plants (Li et al. 2015; Meyer et al. 2012; van Bentem et al. 2008; Wolschin and Weckwerth 2005), however, none of these studies focused on pollen phosphoproteome.

The first male gametophytic phosphoproteomics study identified 962 phosphopeptides corresponding to 598 phosphoproteins in Arabidopsis mature pollen (Mayank et al. 2012). Notably, a high number of phosphoproteins (240 in particular) were newly identified. The most prevalent phosphoprotein categories were regulation of metabolism and protein function, signal transduction and cellular transport. Many kinases were identified, implying that kinases themselves were phosphorylated, for instance AGC protein kinases, calcium-dependent protein kinases, and SNF1-related protein kinases.

In tobacco, the protein phosphorylation dynamics during pollen activation was studied (Fíla et al. 2012). There, dry mature pollen grains and pollen suspension activated in vitro for 30 min were compared. In total, 139 phosphoprotein candidates carrying 52 phosphorylation sites were identified (Fíla et al. 2012). Most phosphoprotein candidates were associated with energy metabolism, a category that has to be precisely regulated after the pollen tube hydration. Other meaningful overrepresented protein categories were protein destination and storage, metabolism, cell structure and protein synthesis. Several phosphopeptides were found to be shared by both Arabidopsis and tobacco pollen (Fíla et al. 2014) pointing to the common nature of pollen activation in angiosperms. Pollen phosphoproteomics studies also significantly contributed to the public PhosPhAt database of *Arabidopsis thaliana* phosphorylation sites (Durek et al. 2010; Heazlewood et al. 2008). Many newly identified phosphorylated proteins were likely to be pollen-specific or -enriched as demonstrated by their transcription profiles (Dupľáková et al. 2007; Hruz et al. 2008; Mayank et al. 2012).

Interestingly, changes of the phosphoproteome in a gymnosperm *Picea wilsonii* pollen and pollen tubes were studied in response to nutrient depletion from pollen tube cultivation media (Chen et al. 2012). 42 phosphoproteins were found to be differentially regulated. Of them, phosphorylation of proteins involved in cytoskeleton dynamics was found to be specifically responsive to Ca^{2+} and sucrose deficiency (Chen et al. 2012). These three studies applied different phosphoproteomic approaches, and thus the data sets between them are not comparable since every protocol biases towards a different segment of phosphoproteome (Bodenmiller et al. 2007). However, together

they provided interesting input in the regulatory processes in male gametophyte.

Protein phosphorylation can be studied directly by phosphoproteomic approaches as mentioned above or alternatively, from the perspective of protein kinases (Supplementary Table 1). Several kinase motifs were reported amongst the phosphorylation sites both in Arabidopsis and tobacco male gametophytes (Fíla et al. 2012; Mayank et al. 2012) and few of them were shared by both species (Fíla et al. 2014). However, this in silico approach only revealed the presence of individual motifs but the actual link between a particular protein kinase and target proteins is still missing. To study the protein kinases activity themselves, several pollen-specific kinases were studied including mitogen-activated protein kinases (MAP kinases). MAP kinases represent a large family of Ser/Thr protein kinases common for all eukaryotes (Kultz 1998). They mediate the prolyl-directed phosphorylation on xxxxxxS*Pxxxxx, and xxxxxxT*Pxxxxx peptide motifs (Lee et al. 2011). However, a subset of these motifs is also recognized by cyclin-dependent protein kinases. Different MAP kinases play their roles in various phases of tobacco male gametophyte development. MAP kinase NTF4 was activated after pollen hydration but before the actual pollen tube emerged. Its role is likely in the activation of pollen metabolism (Wilson et al. 1997). In Arabidopsis, four MAP kinases were identified in the pollen shotgun proteome dataset—MPK6, MPK8, MPK9, and MPK15 (Grobei et al. 2009). Two of these (MPK8, and MPK15) were shown to be phosphorylated at the TDY motif (Mayank et al. 2012). However, their exact roles during male gametophyte development are not yet clear. The other motif over-represented in the Arabidopsis phosphoproteomic data set was a basophilic motif RxxS*xx, that is recognized by CaM-dependent protein kinase family (Lee et al. 2011). In pollen, three calmodulin protein kinases were identified (Honys and Twell 2003), one of which was present also in the pollen proteome and phosphoproteome (Grobei et al. 2009; Mayank et al. 2012). The kinases can also be functionally studied but this is intricate due to the complexity of protein kinases. However, a double homozygous mutant of two AGC protein kinases showed defects in pollen tube growth and their competitiveness but not in a full penetrance (Zhang et al. 2009); however, the connecting link with the signaling pathways is still missing.

Pollen tube guidance: show me the way

As the pollen tube grows through the pistil tissues, it is guided towards ovules to ensure delivery of two non-motile sperm cells for double fertilization. The guidance process involves both mechanical/physical orientation and chemotropic guidance of the pollen tube by the female reproductive tissues. The physical guidance is attributed to the organization of transmitting tract tissues (TT) as well as its secreted compounds. Some of the identified secreted compounds include sulfinylated azadecalin (S-azadecalin; Qin et al. 2011), γ-aminobutyric acid (GABA; Ling et al. 2013; Palanivelu et al. 2003; Yu et al. 2014), brassinosteroids (Vogler et al. 2014), as well as other hormones and metabolites that direct pollen tube growth towards the ovule. Whereas the chemotropic guidance is associated with secreted signals by the attractant (the ovules) either pre-laid along the pollen tube path towards micropylar entry or intensively secreted as diffusible signals ensuring successful ovule targeting by the pollen tube (Heslop-Harrison 1987; Heslop-Harrison and Heslop-Harrison 1986; Mascarenhas and Machlis 1962). The majority of these signals constitute small secreted peptides predominantly of the defensin-like cysteine rich subfamily (DEFL) secreted from the egg apparatus (reviewed by Bleckmann et al. 2014; Higashiyama 2015). Additionally, fail-safe mechanisms exist whereby undegenerated female synergid cell persist to attract additional pollen tube in a case of failed fertilization by the first pollen tube and ensure double fertilization of the female gametes (Kasahara et al. 2012).

This chapter will discuss (1) secreted peptides by the female reproductive tissues with role in pollen tube attraction, (2) factors of the pollen tube that could perceive female guidance signals directly or indirectly, (3) a brief discussion and transcriptomic analysis of the Arabidopsis DEFL subfamily, cysteine-rich receptor protein kinases (CRKs) and GPI-anchored proteins in Arabidopsis as potential factors likely to be involved in ovular attraction, signal perception and pollen tube guidance. Recent comprehensive reviews on pollen tube guidance are available, see Bleckmann et al. (2014) and Higashiyama (2015).

Ovular secreted peptides for pollen tube attraction

After successful pollination and penetration through the stigma, a compatible pollen tube grows through the extracellular matrix of the transmitting tract tissues with the aid of female guidance signals to reach and fertilize the female gametes (Maheshwari 1950; Yadegari and Drews 2004). This cell–cell communication has emerged as an important bottleneck for unfavourable fertilization and as a pre-zygotic barrier for interspecies hybridization. Techniques involving the use of single-cell laser ablation, use of genetic mutants and high-throughput genomic approaches such as tissue-specific transcriptomic studies have identified various transmitting tract and ovular secreted peptides

involved in pollen-pistil interactions and as ovular attractants with conserved roles across plant species (Márton et al. 2012; Okuda et al. 2009; Takeuchi and Higashiyama 2011). Among them are Arabinogalactan proteins, cysteine-rich polypeptides (CRP), defensin-like proteins (DEFL), S-RNases, transmitting tissue-specific proteins (TTS), class III pistil extensin-like proteins (PELPIII) and lipid transfer proteins (LTP) (Chae and Lord 2011; Dresselhaus and Franklin-Tong 2013; Hamamura et al. 2011). Characterisation and the continuous search for ovular secreted pollen tube attractants have spearheaded better understanding of the molecular dialogue during pollen tube-ovular attraction and successful fertilization.

To exit the transmitting tract and reorient towards target ovules, pollen tubes are attracted by secreted signals directly derived from the ovules. Genetic evidence have shown that functional female gametophyte plays an essential role in pollen tube attraction towards the ovule (Hulskamp et al. 1995; Ray et al. 1997; Shimizu and Okada 2000) by the secretion of ovular attractants (reviewed in Bleckmann et al. 2014; Higashiyama 2015). The ovular attractants for pollen tube guidance identified so far include LURE proteins from Torenia and Arabidopsis and ZmEA1 from maize. LURE proteins are short antifungal/antimicrobial polypeptides (typically 50–100 amino acids) belonging to the defensin-like subfamily of cysteine rich proteins first identified as secreted in *Torenia fourieri* synergid cells and termed LURE1 and LURE2 (Okuda et al. 2009). Through orthologous protein searches, other LURE proteins were identified in *Torenia concolor*, TcCRP1 (Kanaoka et al. 2011) and in *Arabidopsis thaliana* (AtLURE1.1–1.6) and *Arabidopsis lyrata* (AlLURE1.1–1.10) (Takeuchi and Higashiyama 2012). All LURE proteins were shown to be expressed and secreted by the synergid cells. Using semi in vitro assay and microfluidic device techniques (Agudelo et al. 2013; Arata and Higashiyama 2014; Horade et al. 2013; Sanati Nezhad et al. 2014), TfLURE1/2 and AtLURE1 proteins were confirmed as pollen tube attractants with long-range activities in a species-preferential manner (Horade et al. 2013). Antisense knockdown of TfLURE1 or TfLURE2 abolished pollen tube attraction and fertilization in *Torenia fourieri* (Okuda et al. 2009). Intriguingly, these identified LURE proteins are capable of cross-species activities and are sufficient to attract pollen tubes of distantly related species. This was elegantly demonstrated by the successful attraction and embryo sac entry of Arabidopsis pollen tubes by *Torenia fourieri* ovules expressing AtLURE1.2 peptides (Takeuchi and Higashiyama 2012). The range at which the LURE proteins are perceived by the approaching pollen tube is still unclear (see below).

Similar to LURE proteins, *Zea mays* egg apparatus 1 protein (ZmEA1), plays an essential role in pollen tube

ovular attraction (Fig. 3a) (Márton et al. 2005, 2012). ZmEA1 belongs to EAL family and is expressed in the egg apparatus predominantly in the synergid cells. ZmEA1 is specific to monocots. Heterologous expression of ZmEA1 in Arabidopsis ovules is sufficient to attract maize pollen tubes to the micropylar entry (Márton et al. 2005). These findings demonstrate that ovular secreted attractants are likely candidates to impose interspecific prezygotic barriers during pollen tube guidance.

One unresolved aspect of this cell–cell crosstalk event is the range at which the ovular attractants travel and are perceived by the pollen tubes. Clearly, the intercellular growth of the pollen tubes in transmitting tract happens basipetally and predominantly involves mechanical guidance by the female sporophytic tissues (Heslop-Harrison 1987; Heslop-Harrison and Heslop-Harrison 1986). Later, Sanders and Lord proposed the model that the pollen tubes are effectively dragged down the transmitting tract through interaction with the extracellular matrix of the transmitting tract tissues (Hulskamp et al. 1995; Sanders and Lord 1989, 1992). In lily and *Torenia* species, germinating pollen tubes emerge from opposite ends of the cut style (distal or proximal) or at both ends of cut style when germinated from a cut slit at the middle of the style (Higashiyama 2015). All above findings emphasise that mechanical guidance predominate intercellular pollen tube growth within the transmitting tract. Thereafter, deviation of the pollen tubes from the transmitting tract tissues onto the surface of the septum towards the target ovule requires additional independent signals (Schwemmie 1968). Precisely, this turning point marks the end of mechanical guidance and the beginning of ovular chemotropic attraction. Isolated sporophytic genetic mutations specifically affecting female gametogenesis (but not the sporophytic tissues) at various developmental stages are known to significantly reduce pollen tube-ovule targeting success including pollen tube emergence onto the surface of the septum (Hulskamp et al. 1995; Ray et al. 1997; Shimizu and Okada 2000). In support, secreted AtLURE1 peptides are detectable beyond the micropylar, at the surface of funiculus and septum (Higashiyama 2010, 2015), suggesting their likely involvement in pre-ovular guidance. Together, these results support the notion that ovular secreted peptides could have a long attraction/guidance range. Intuitively, it could be predicted that mutants affecting protein secretion in ovules would consequently impact on pollen tube guidance and attraction. Therefore, it is of great importance to further resolve the range through which ovular attraction signals operate and whether the transport of these signals involves diffusion or specific carrier molecules such as nanovesicles, carbohydrates moieties and/or encapsulated lipid molecules to reach their target cells, the pollen tube.

Fig. 3 Empirical model of pollen tube-pistil/ovule crosstalk. **a** A peptidome perspective of cell–cell communication during pollen tube-ovular guidance showing known and predicted secreted molecules involved. **b, c** Expression profile of Arabidopsis cysteine-rich polypeptide family proteins of <150 aa's and predicted GPI-anchored proteins outsourced from the UniProtKB and UniRef100 databases. LSP's are pollen tube Leaderless secreted proteins (without N-terminal signal peptide) that could be secreted via nanovesicles exosomes

Perception of female guidance signals by the pollen tube

Although to date there has not been a direct demonstration of female-secreted ligands binding to pollen tube surface receptors, with the exception of AtLURE1 that is indirectly perceived by LIP1/2 receptor kinases (Liu et al. 2013), the continuous efforts (including innovated techniques) are edging closer to reach such resolution of understanding. Several male mutants have been isolated that are defective in pollen tube-ovule targeting (reviewed in Bleckmann et al. 2014; Higashiyama 2015). Intriguingly, they include genes involved in cellular homeostasis, actin dynamics and those encoding membrane- and surface-anchored receptors.

Among them is Arabidopsis LOST IN POLLEN TUBE GUIDANCE 1 (LIP1) and LIP2. LIP1 and LIP2 are pollen-expressed membrane-anchored receptor-like kinases without extracellular domains and localize beneath the membrane at the pollen tube tip (Liu et al. 2013). Simultaneous knockdown of LIP1 and LIP2 results in reduced pollen tube ovule targeting ability and reduced attraction towards synthetic AtLURE1.2 peptides. This observation suggests an indirect perception of LURE ovular attractants by LIP1 and LIP2 pollen tube surface receptor proteins (Liu et al. 2013). Another pollen tube receptor identified is COBRA-LIKE 10 (COBL10). COBL10 is a GPI-anchored protein that localizes at the pollen tube tip through its C-terminal GPI-anchor sequence and is involved in the deposition of

apical pectin cap, cellulose microfibrils and functions in pollen tube guidance (Li et al. 2013). Its knock-out results in defects in ovule targeting that mimics those of *abnormal pollen tube guidance1* (*aptg1*), *seth1* and *seth2* knockdown mutants which all are involved in GPI biosynthetic pathway. These results suggest that GPI-mediated membrane anchoring of COBL10 is essential for pollen tube guidance (Li et al. 2013). Perception of ovular attraction signals by the pollen tube also involved proteins with a structural role. MICROTUBULE ASSOCIATE PROTEIN 18 (MAP18) and MICROTUBULE-DESTABILIZING PROTEIN 25 (MDP25), both possess actin filament severing activity and their mutants lack competence in perceiving ovule attraction signals but show normal pollen tube growth (Qin et al. 2014; Zhu et al. 2013). It is surprising that *map18* and *mdp25* mutants do not show defects in pollen tube growth as previously reported for other proteins involved in actin organization (Guan et al. 2013). Here they demonstrate that actin dynamics plays an exclusive role in directing the pollen tube towards the ovules (Higashiyama 2015). Two pollen tube potassium transporters, CHX21 and CHX23, were also identified as essential factors for pollen tube competence in ovule targeting (Lu et al. 2011). They are likely to regulate cytosolic cation dynamics rendering pollen tube competence in response to ovular attractants. Similar to secretion of ovular attractant peptides, pollen tube protein secretion and protein folding are also likely to play an important role in pollen tube competence to perceive ovular attractants (Hafidh, Potěšil, Fíla, Čapková, Zdráhal and Honys, unpublished). This was demonstrated for ER-localized POLLEN DEFECTIVE IN GUIDANCE 1 (POD1) protein, since *pod1* mutant pollen tubes were incompetent in ovular attraction response (Li et al. 2011). These findings suggests that ER-protein folding and likely secretion of membrane-associated and extracellular proteins from the ER are critical for pollen tube responsiveness towards female guidance signals. Moreover, genes involved in regulating secretory pathways are also likely to be essential in pollen tube guidance.

Similar to ovule-secreted peptides, the range of activities for pollen tube-secreted peptides also needs to be addressed. Cysteine-rich family protein LAT52 and Lipid transfer family protein LTP5 are the only known pollen tube-secreted ligand proteins that are perceived by pollen tube receptor like kinase, PRK2 (Zhao et al. 2013). Once secreted, LAT52 and LTP5 are believed to participate in an autocrine signalling involving RopGEFs to control polar tip growth of the pollen tube (Fig. 3a). It is not known whether LAT52 and LTP5 act as ligands to female receptors during pollen tube-pistil interaction. Furthermore, discovery of other pollen tube secreted proteins/peptides was hampered by the inaccessibility of the pollen tube "secretome" within the transmitting tract, however, current

developed techniques offer a compromised access to such molecules and have a potential to speed up the discovery of the pollen tube "peptidome" (Hafidh et al. 2014). The challenge ahead is to demonstrate the range of activities for LAT52, LTP5 and other pollen tube secreted peptides/proteins and how these secreted peptides reach their target receptors. An empirical model would be that short range intercellular signals might reach their targets by diffusion whereas long-range intercellular signals could be encapsulated within "carrier organelles/molecules" such as lipid bilayer capsules or secreted nanovesicles/exosomes (Prado et al. 2014) and either taken up or released by endocytosis upon contact with the target cell (Fig. 3a). With application of techniques such as microfluidic devices with live cell imaging capabilities (Cheung et al. 2010; Horade et al. 2013; Rotman et al. 2003; Uebler and Dresselhaus 2014), the intercellular dialogue between pollen tube ovular signal perception and ovular attraction will gain resolution to the molecular level and increase better understanding of the fertilization process and prezygotic interspecific barriers of flowering plants.

Cysteine-rich polypeptides and GPI-anchored proteins predicted as secreted in Arabidopsis

Ovular attractants that have been identified to date belong to the defensin-like DEFL subfamily of the cysteine-rich polypeptide group of proteins. The CRP proteins are present as isoforms and paralogs across species, whereas others are species-specific defensin-like proteins (Márton et al. 2005, 2012; Takeuchi and Higashiyama 2012). It is likely that other members of this family play an essential role in pollen tube guidance. We have surveyed the Arabidopsis genome using the proteome data from UniProt repository (http://www.uniprot.org/) and selected annotated CRP family peptides of <150 amino acids that were predicted as secreted (Supplementary Table 2). Transcriptomic analysis of publicly deposited dataset (Dupľáková et al. 2007; Hruz et al. 2008) followed by phylogenic classification using Euclidian distance algorithms and optimal leaf ordering based on co-expression and similar vector branching, highlighted two main groups of DEFL-like proteins and a small subset of "plant cysteine-rich small secretory family" of proteins (Fig. 3b). DEFL-like group I consisted of defensin-like peptides that showed consistent expression in male and female reproductive tissues but more strongly in pollen grains than in ovary (Fig. 3b). The DEFL-like group II on the other hand, displayed more variable expression patterns with much stronger expression in the female gametophyte and in dissected endospem (Fig. 3b). The subgroup of plant cysteine-rich small secretory family constituted exclusively of EPIDERMAL patterning factor-like proteins (EPFL).

EPFL's are <50 aa secreted peptides within the mesophyll cells and are known to increase stomatal formation through positive and negative protein–protein interaction and likely through their interaction with receptor-like proteins such as TMM receptor kinases (Lee et al. 2015). Their expression is uniform throughout plant development (Fig. 3b). Whether EPFL plays role also in pollen tube guidance remains to be demonstrated.

Another noteworthy subfamily is CRKs, cysteine-rich receptor-like kinases. CRKs are not secreted to the extracellular matrix but reside on the membrane with a single-pass transmembrane helix (Supplementary Table 2) and are likely to function as receptors for secreted ligands during pollen tube guidance. For majority, their expression in several plant tissues is also constitutive and shows no prominent specificity in particular tissues (Supplementary Fig.S1). However, five CRK genes showed exceptional profile; CRK42 (AT5G40380), CRK17 (AT4G23250), CRK33 (AT4G11490), CRK43 (AT4G28670) and CRK1 (AT1G19090), all appeared to be exclusively enriched in pollen and in sperm cells compared to any other tissues (Fig. S1). Their pattern hint towards possible role in kinase-mediated signalling in pollen tubes and in sperm cells during pollen-pistil interaction and during fertilization. To date, only one example of possible ligand-receptor interaction, LIP1/2–LUREs, has been reported (Li et al. 2013). Embedment of CRKs within the membrane places them as potential receptors that could link and transduce signals from cell surface receptors (such as GPI-anchored proteins, example COBL10) to inner receptors such as LIP1 and LIP2 (Fig. 3a). Therefore, understanding the role of these CRKs will pave way in the understanding the cascades of signal transduction during male–female crosstalk.

Similarly, GPI-anchored proteins are among the gene families identified as regulators of pollen tube guidance and reception. LLG1, a Lorelei-like GPI-anchored protein is expressed exclusively in synergid cells and could perceive signals secreted by the approaching pollen tube (Capron et al. 2008). Knockdown of LLG1 severely perturbs pollen tube reception resulting in pollen tube overgrowth, defective sperm cell release and embryo development (Capron et al. 2008; Tsukamoto et al. 2010). In pollen tubes, COBRA-like 10, is expressed and localized at the pollen tube tip through its C-terminal GPI-anchor (Li et al. 2013). Knockdown of CBL10 results in defects in pollen tube growth and ovule targeting. In mammals, GPI-anchored proteins are commonly deployed as cell sensors during cell–cell communications including during egg-sperm cell recognition. We have analysed expression of annotated secreted Arabidopsis GPI-anchored proteins in several tissues as potential candidate transient receptors during pollen-pistil interaction and pollen tube-ovule targeting

(Supplementary Table 3). The majority showed a general widespread expression pattern in all tissues including the gametophytes with the exception of COBL9 (AT5G49270), COBL8 (AT3G16860), COBL10 (AT3G20580), LLG3 (AT4G28280) and COBL11 (AT4G27110), which showed significantly higher expression levels in stamens, pollen grains and in sperm cells (Fig. 3c). Of them, only COBL10 has been reported to play critical role in pollen tube growth and in cell–cell crosstalk during pollen-pistil interaction and fertilization (Li et al. 2013). GPI-anchored proteins are likely to function as primary receptors in pollen tube and in synergid cell and the female gametophyte to perceive secreted signals. The aforementioned genes (as well as others on Table 3) are worth a detailed investigation to establish their role in pollen tube signal perception during male–female signaling and fertilization.

Termination of pollen tube guidance and attraction

Once the pollen tube successfully entered the embryo sac and released the two sperm cells, gamete fusions (both plasmogamy and karyogamy) of sperm cells with the egg cell and the central cells mark the end of pollen tube guidance and an ovule stops attracting any additional pollen tubes. This is preceded with induced programme cell death of the persistent synergid cell approximately 20 h post pollination (Beale et al. 2012). If plasmogamy or karyogamy fails with the first pollen tube, the persistent synergid cell is reactivated to attract additional pollen tubes and ensure double fertilization of both female gametes. Up to three pollen tubes can be attracted by a single ovule (Kasahara et al. 2012; Williams 2009). This phenomena is termed polytubey and ensures fertilization recovery. Polytubey can also lead to hetero-fertilization where male gametes involved in the fertilization are delivered by different pollen tubes (Maruyama et al. 2013). Ovule mutants defective in micropylar guidance such as *myb98* (Kasahara et al. 2005), *magatama* (Shimizu and Okada 2000), and *central cell guidance* (Chen et al. 2007), or those defective in pollen tube reception, such as *feronia/sirene* (Huck et al. 2003; Rotman et al. 2003) and *lorelei* (Capron et al. 2008; Tsukamoto et al. 2010), all show the polytubey phenotype. Similarly, male components that are required for gamete fusion and fertilization such as *GENERATIVE CELL SPECIFIC 1/HAPLESS 2* (*GCS1/HAP2*) which encodes a sperm cell plasma membrane protein and required for gamete fusion (Mori et al. 2005; von Besser et al. 2006), *cdka;1* (Hamamura et al. 2012), *duo1*, *duo3* (Beale et al. 2012; Kasahara et al. 2012) and *kokopeli* (Hamamura et al. 2012), which are all defective in producing two competent sperm cells, also display polytubey phenotypes suggesting that a cessation of pollen tube attraction is a direct consequence of the double fertilization event. For ovules that

have undergone successful fertilization, ethylene signalling is induced by ER localized ETHYLENE-INSENSITIVE 2 and 3 (EIN2 and EIN3) and perceived by the remaining synergid cell (Völz et al. 2013). Ethylene perception induces programmed cell death of the synergid cell and marks the end of pollen tube attraction and beginning of embryogenesis.

Conclusion

Unlike animals, the specification of specialized cells that give rise to gametes (the germline) happens much later and repeatedly during plant development. In angiosperms, the male gametogenesis takes place through coordinated activities of both gametophytic and sporophytic tissues and involves widespread dynamic changes in gene expression. Shed pollen grains constitute a vegetative cell (that forms a pollen tube and delivers two sperm cells for fertilization) and either undivided germ cell (bicellular species) or with two sperm cells (tricellular species). This process is underpinned by two successive cell divisions accompanied by morphological and physiological differentiation of both cell types (reviewed by Berger and Twell 2011). Tremendous efforts including genetic and transcriptomic approaches has led to the isolation of several mutants whose gene function regulates several steps of the male gametogenesis (reviewed by Borg et al. 2011). This has provided better understanding of male sterility and can be used to manipulate and improve male fitness.

A plethora of processes also regulates pollen tube growth, guidance competence and reception by the target ovule. They include posttranscriptional regulation (including mass transcript storage) and posttranslational modifications such as phosphorylation to modulate protein function, intracellular metabolic signalling, ionic gradients such as Ca^{2+} and H^+ ions, cell wall synthesis, protein secretion and intercellular signalling with the female reproductive tissues. Mechanisms regulating many of the above mentioned processes are being unravelled (reviewed by Dresselhaus and Franklin-Tong 2013). Current efforts have seen a big leap in the understanding of pollen tube guidance and ovular attraction with potential in understanding interspecies hybridization barriers (reviewed by Higashiyama 2015). Future challenges include the identification of other pollen tube guidance factors secreted from the female reproductive tissues, particularly those involved in ovular guidance. Equally critical, male factors involved in perceiving female guidance signals, including secreted receptors and ligands, will pave the way to better understanding of cell–cell communication between male and female gametophytes during pollen tube guidance and fertilization. Innovative techniques including microfluidic devices and live cell imaging will spearhead the discovery of molecules critical for fertilization, understanding pollen tube response towards female attraction signals as well as establish the range of activities through which female and male signalling molecules can be perceived by their target cell. Not to be underestimated, transcriptional approaches still offer a powerful tool to isolate such molecules and aid in the breakthroughs to understand mechanisms governing gametogenesis, fertilization and seed set.

References

Agudelo CG, Sanati Nezhad A, Ghanbari M, Naghavi M, Packirisamy M, Geitmann A (2013) TipChip: a modular, MEMS-based platform for experimentation and phenotyping of tip-growing cells. Plant J 73:1057–1068. doi:10.1111/tpj.12093

Allwood EG, Anthony RG, Smertenko AP, Reichelt S, Drobak BK, Doonan JH, Weeds AG, Hussey PJ (2002) Regulation of the pollen-specific actin-depolymerizing factor LIADF1. Plant Cell 14:2915–2927. doi:10.1105/tpc.005363

Arata H, Higashiyama T (2014) Poly(dimethylsiloxane)-based microdevices for studying plant reproduction. Biochem Soc Trans 42:320–324. doi:10.1042/bst20130258

Ariizumi T, Toriyama K (2011) Genetic regulation of sporopollenin synthesis and pollen exine development. In: Merchant SS, Briggs WR, Ort D (eds) Annual Review of Plant Biology, vol 62, pp 437–460

Barnabas B, Fridvalszky L (1984) Adhesion and germination of differently treated maize pollen grains on the stigma. Acta Bot Hung 30:329–332

Beale KM, Leydon AR, Johnson MA (2012) Gamete fusion is required to block multiple pollen tubes from entering an Arabidopsis ovule. Curr Biol 22:1090–1094. doi:10.1016/j.cub.2012.04.041

Bedinger P (1992) The remarkable biology of pollen. Plant Cell 4:879–887

Bendtsen JD, Jensen LJ, Blom N, von Heijne G, Brunak S (2004) Feature-based prediction of non-classical and leaderless protein secretion. Protein Eng Des Sel 17:349–356. doi:10.1093/protein/gzh037

Berger F, Twell D (2011) Germline specification and function in plants. Annu Rev Plant Biol 62:461–484. doi:10.1146/annurev-arplant-042110-103824

Bishop AL, Hall A (2000) Rho GTPases and their effector proteins. Biochem J 348:241–255. doi:10.1042/0264-6021:3480241

Bleckmann A, Alter S, Dresselhaus T (2014) The beginning of a seed: regulatory mechanisms of double fertilization. Front Plant Sci 5:452. doi:10.3389/fpls.2014.00452

Bodenmiller B, Mueller LN, Mueller M, Domon B, Aebersold R (2007) Reproducible isolation of distinct, overlapping segments of the phosphoproteome. Nat Methods 4:231–237. doi:10.1038/nmeth1005

Bokvaj P, Hafidh S, Honys D (2015) Transcriptome profiling of male gametophyte development Nicotiana tabacum. Genom Data 3:106–111

Borg M, Brownfield L, Twell D (2009) Male gametophyte development: a molecular perspective. J Exp Bot 60:1465–1478. doi:10.1093/jxb/ern355

Borg M, Brownfield L, Khatab H, Sidorova A, Lingaya M, Twell D (2011) The R2R3 MYB transcription factor DUO1 activates a male germline-specific regulon essential for sperm cell differentiation in Arabidopsis. Plant Cell 23:534–549. doi:10.1105/tpc.110.081059

Borges F, Gomes G, Gardner R, Moreno N, McCormick S, Feijó JA, Becker JD (2008) Comparative transcriptomics of Arabidopsis sperm cells. Plant Physiol 148:1168–1181. doi:10.1104/pp.108.125229

Brett C, Waldron K (1990) Physiology and biochemistry of plant cell walls. Unwin Hyman, London

Brewbaker JL (1967) Distribution and phylogenetic significance of binucleate and trinucleate pollen grains in angiosperms. Am J Bot 54:1069–1083. doi:10.2307/2440530

Camacho L, Malho R (2003) Endo/exocytosis in the pollen tube apex is differentially regulated by Ca^{2+} and GTPases. J Exp Bot 54:83–92. doi:10.1093/jxb/erg043

Cannon MC, Terneus K, Hall Q, Tan L, Wang Y, Wegenhart BL, Chen L, Lamport DT, Chen Y, Kieliszewski MJ (2008) Self-assembly of the plant cell wall requires an extensin scaffold. Proc Natl Acad Sci USA 105:2226–2231. doi:10.1073/pnas.0711980105

Čapková V, Hrabětová E, Tupý J (1988) Protein synthesis in pollen tubes: preferential formation of new species independent of transcription. Sex Plant Reprod 1:150–155

Čapková V, Fidlerová A, van Amstel T, Croes AF, Mata C, Schrauwen JAM, Wullems GJ, Tupý J (1997) Role of N-glycosylation of 66 and 69 kDa glycoproteins in wall formation during pollen tube growth in vitro. Eur J Cell Biol 72:282–285

Capron A, Gourgues M, Neiva LS, Faure JE, Berger F, Pagnussat G, Krishnan A, Alvarez-Mejia C, Vielle-Calzada JP, Lee YR, Liu B, Sundaresan V (2008) Maternal control of male-gamete delivery in Arabidopsis involves a putative GPI-anchored protein encoded by the LORELEI gene. Plant Cell 20:3038–3049. doi:10.1105/tpc.108.061713

Chae K, Lord EM (2011) Pollen tube growth and guidance: roles of small, secreted proteins. Ann Bot 108:627–636. doi:10.1093/aob/mcr015

Chaturvedi P, Ischebeck T, Egelhofer V, Lichtscheidl I, Weckwerth W (2013) Cell-specific analysis of the tomato pollen proteome from pollen mother cell to mature pollen provides evidence for developmental priming. J Proteome Res 12:4892–4903. doi:10.1021/pr400197p

Chen XY, Kim JY (2009) Callose synthesis in higher plants. Plant Signal Behav 4:489–492

Chen CY, Wong EI, Vidali L, Estavillo A, Hepler PK, Wu HM, Cheung AY (2002) The regulation of actin organization by actin-depolymerizing factor in elongating pollen tubes. Plant Cell 14:2175–2190. doi:10.1105/tpc.003038

Chen YH, Li HJ, Shi DQ, Yuan L, Liu J, Sreenivasan R, Baskar R, Grossniklaus U, Yang WC (2007) The central cell plays a critical role in pollen tube guidance in Arabidopsis. Plant Cell 19:3563–3577. doi:10.1105/tpc.107.053967

Chen Y, Liu P, Hoehenwarter W, Lin J (2012) Proteomic and phosphoproteomic analysis of Picea wilsonii pollen development

under nutrient limitation. J Proteome Res 11:4180–4190. doi:10.1021/pr300295m

Cheung AY, Boavida LC, Aggarwal M, Wu HM, Feijó JA (2010) The pollen tube journey in the pistil and imaging the in vivo process by two-photon microscopy. J Exp Bot 61:1907–1915. doi:10.1093/jxb/erq062

Choudhary P, Saha P, Ray T, Tang Y, Yang D, Cannon MC (2015) EXTENSIN18 is required for full male fertility as well as normal vegetative growth in Arabidopsis. Front Plant Sci 6:553. doi:10.3389/fpls.2015.00553

de Graaf BHJ, Cheung AY, Andreyeva T, Levasseur K, Kieliszewski M, Wu HM (2005) Rab11 GTPase-regulated membrane trafficking is crucial for tip-focused pollen tube growth in tobacco. Plant Cell 17:2564–2579. doi:10.1105/tpc.105.033183

De Storme N, Geelen D (2013) Cytokinesis in plant male meiosis. Plant Signal Behav 8:e23394. doi:10.4161/psb.23394

Dobritsa AA, Coerper D (2012) The novel plant protein INAPERTURATE POLLEN1 marks distinct cellular domains and controls formation of apertures in the Arabidopsis pollen exine. Plant Cell 24:4452–4464. doi:10.1105/tpc.112.101220

Dobritsa AA, Shrestha J, Morant M, Pinot F, Matsuno M, Swanson R, Moller BL, Preuss D (2009) CYP704B1 is a long-chain fatty acid omega-hydroxylase essential for sporopollenin synthesis in pollen of Arabidopsis. Plant Physiol 151:574–589. doi:10.1104/pp.109.144469

Dobritsa AA, Lei Z, Nishikawa S, Urbanczyk-Wochniak E, Huhman DV, Preuss D, Sumner LW (2010) LAP5 and LAP6 encode anther-specific proteins with similarity to chalcone synthase essential for pollen exine development in Arabidopsis. Plant Physiol 153:937–955. doi:10.1104/pp.110.157446

Dobritsa AA, Geanconteri A, Shrestha J, Carlson A, Kooyers N, Coerper D, Urbanczyk-Wochniak E, Bench BJ, Sumner LW, Swanson R, Preuss D (2011) A large-scale genetic screen in Arabidopsis to identify genes involved in pollen exine production. Plant Physiol 157:947–970. doi:10.1104/pp.111.179523

Dresselhaus T, Franklin-Tong N (2013) Male–female crosstalk during pollen germination, tube growth and guidance, and double fertilization. Mol Plant 6:1018–1036. doi:10.1093/mp/sst061

Dresselhaus T, Sprunck S (2012) Plant fertilization: maximizing reproductive success. Curr Biol 22:R487–R489. doi:10.1016/j.cub.2012.04.048

Dunn JD, Reid GE, Bruening ML (2010) Techniques for phosphopeptide enrichment prior to analysis by mass spectrometry. Mass Spectrom Rev 29:29–54. doi:10.1002/mas.20219

Dupľáková N, Reňák D, Hovanec P, Honysová B, Twell D, Honys D (2007) Arabidopsis Gene Family Profiler (aGFP): user-oriented transcriptomic database with easy-to-use graphic interface. BMC Plant Biol 7:39. doi:10.1186/1471-2229-7-39

Durek P, Schmidt R, Heazlewood JL, Jones A, MacLean D, Nagel A, Kersten B, Schulze WX (2010) PhosPhAt: the Arabidopsis thaliana phosphorylation site database: an update. Nucleic Acids Res 38:D828–D834. doi:10.1093/nar/gkp810

Eady C, Lindsey K, Twell D (1995) The significance of microspore division and division symmetry for vegetative cell-specific transcription and generative cell differentiation. Plant Cell 7:65–74. doi:10.1105/tpc.7.1.65

Eisenhaber B, Wildpaner M, Schultz CJ, Borner GH, Dupree P, Eisenhaber F (2003) Glycosylphosphatidylinositol lipid anchoring of plant proteins. Sensitive prediction from sequence- and genome-wide studies for Arabidopsis and rice. Plant Physiol 133:1691–1701. doi:10.1104/pp.103.023580

Elfving F (1879) Studien über die Pollenkörner der Angiospermen. Jenaische Zeitschrift für Naturwissenschaft 13:1–28

Ellis M, Egelund J, Schultz CJ, Bacic A (2010) Arabinogalactan-proteins: key regulators at the cell surface? Plant Physiol 153:403–419. doi:10.1104/pp.110.156000

Feher A, Lajko DB (2015) Signals fly when kinases meet Rho-of-plants (ROP) small G-proteins. Plant Sci 237:93–107. doi:10.1016/j.plantsci.2015.05.007

Feijó JA, Sainhas J, Hackett GR, Kunkel JG, Hepler PK (1999) Growing pollen tubes possess a constitutive alkaline band in the clear zone and a growth-dependent acidic tip. J Cell Biol 144:483–496. doi:10.1083/jcb.144.3.483

Feijó JA, Costa SS, Prado AM, Becker JD, Certal AC (2004) Signalling by tips. Curr Opin Plant Biol 7:589–598. doi:10.1016/j.pbi.2004.07.014

Fellenberg C, Vogt T (2015) Evolutionarily conserved phenylpropanoid pattern on angiosperm pollen. Trends Plant Sci 20:212–218. doi:10.1016/j.tplants.2015.01.011

Ferguson C, Teeri TT, Siika-aho M, Read SM, Bacic A (1998) Location of cellulose and callose in pollen tubes and grains of Nicotiana tabacum. Planta 206:452–460. doi:10.1007/s004250050421

Fidlerová A, Smýkal P, Tupý J, Čapková V (2001) Glycoproteins 66 and 69 kDa of pollen tube wall: properties and distribution in angiosperms. J Plant Physiol 158:1367–1374. doi:10.1078/0176-1617-00562

Fíla J, Honys D (2012) Enrichment techniques employed in phosphoproteomics. Amino Acids 43:1025–1047. doi:10.1007/s00726-011-1111-z

Fíla J, Čapková V, Fecikova J, Honys D (2011) Impact of homogenization and protein extraction conditions on the obtained tobacco pollen proteomic patterns. Biol Plant 55:499–506. doi:10.1007/s10535-011-0116-5

Fíla J, Matros A, Radau S, Zahedi RP, Čapková V, Mock H-P, Honys D (2012) Revealing phosphoproteins playing role in tobacco pollen activated in vitro. Proteomics 12:3229–3250. doi:10.1002/pmic.201100318

Fíla J, Čapková V, Honys D (2014) Phosphoproteomic studies in Arabidopsis and tobacco male gametophytes. Biochem Soc Trans 42:383–387. doi:10.1042/bst20130249

Firon N, Nepi M, Pacini E (2012) Water status and associated processes mark critical stages in pollen development and functioning. Ann Bot 109:1201–1213. doi:10.1093/aob/mcs070

Fu Y, Wu G, Yang ZB (2001) Rop GTPase-dependent dynamics of tip-localized F-actin controls tip growth in pollen tubes. J Cell Biol 152:1019–1032. doi:10.1083/jcb.152.5.1019

Furness CA, Rudall PJ (2004) Pollen aperture evolution: a crucial factor for eudicot success? Trends Plant Sci 9:154–158. doi:10.1016/j.tplants.2004.01.001

Gaillard A, Vergne P, Beckert M (1991) Optimization of maize microspore isolation and culture conditions for reliable plant regeneration. Plant Cell Rep 10:55–58. doi:10.1007/BF00236456

Grobei MA, Qeli E, Brunner E, Rehrauer H, Zhang R, Roschitzki B, Basler K, Ahrens CH, Grossniklaus U (2009) Deterministic protein inference for shotgun proteomics data provides new insights into Arabidopsis pollen development and function. Genome Res 19:1786–1800. doi:10.1101/gr.089060.108

Guan Y, Guo J, Li H, Yang Z (2013) Signaling in pollen tube growth: crosstalk, feedback, and missing links. Mol Plant 6:1053–1064. doi:10.1093/mp/sst070

Hafidh S, Čapková V, Honys D (2011) Safe keeping the message: mRNP complexes tweaking after transcription. Adv Exp Med Biol 722:118–136. doi:10.1007/978-1-4614-0332-6_8

Hafidh S, Breznenová K, Honys D (2012a) De novo post-pollen mitosis II tobacco pollen tube transcriptome. Plant Signal Behav 7:918–921. doi:10.4161/psb.20745

Hafidh S, Breznenová K, Růžička P, Fecikova J, Čapková V, Honys D (2012b) Comprehensive analysis of tobacco pollen transcriptome unveils common pathways in polar cell expansion and underlying heterochronic shift during spermatogenesis. BMC Plant Biol 12:24. doi:10.1186/1471-2229-12-24

Hafidh S, Potěšil D, Fíla J, Fecikova J, Čapková V, Zdráhal Z, Honys D (2014) In search of ligands and receptors of the pollen tube: the missing link in pollen tube perception. Biochem Soc Trans 42:388–394. doi:10.1042/BST20130204

Hamamura Y, Saito C, Awai C, Kurihara D, Miyawaki A, Nakagawa T, Kanaoka MM, Sasaki N, Nakano A, Berger F, Higashiyama T (2011) Live-cell imaging reveals the dynamics of two sperm cells during double fertilization in Arabidopsis thaliana. Curr Biol 21:497–502. doi:10.1016/j.cub.2011.02.013

Hamamura Y, Nagahara S, Higashiyama T (2012) Double fertilization on the move. Curr Opin Plant Biol 15:70–77. doi:10.1016/j.pbi.2011.11.001

Hanisch FA (2001) O-glycosylation of the mucin type. Biol Chem 382:143–149. doi:10.1515/bc.2001.022

Heazlewood JL, Durek P, Hummel J, Selbig J, Weckwerth W, Walther D, Schulze WX (2008) PhosPhAt: a database of phosphorylation sites in Arabidopsis thaliana and a plant-specific phosphorylation site predictor. Nucleic Acids Res 36:D1015–D1021. doi:10.1093/nar/gkm812

Hepler PK, Winship LJ (2015) The pollen tube clear zone: clues to the mechanism of polarized growth. J Integr Plant Biol 57:79–92. doi:10.1111/jipb.12315

Heslop-Harrison J (1987) Pollen germination and pollen-tube growth. In: Giles KL, Prakash J (eds) Pollen: cytology and development. Academic Press, London, pp 1–78

Heslop-Harrison J, Heslop-Harrison Y (1986) Pollen-tube chemotropism: fact or delusion? In: Cresti M, Romano D (eds) In biology of reproduction and cell motility in plants and animals. University of Sienna Press, Siena, pp 169–174

Heslop-Harrison J, Heslop-Harrison Y, Cresti M, Tiezzi A, Moscatelli A (1988) Cytoskeletal elements, cell shaping and movement in the angiosperm pollen tube. J Cell Sci 91:49–60

Higashiyama T (2010) Peptide signaling in pollen–pistil interactions. Plant Cell Physiol 51:177–189. doi:10.1093/pcp/pcq008

Higashiyama T (2015) The mechanism and key molecules involved in pollen tube guidance. Annu Rev Plant Biol 2015:393–413

Higashiyama T, Kuroiwa H, Kawano S, Kuroiwa T (1998) Guidance in vitro of the pollen tube to the naked embryo sac of Torenia fournieri. Plant Cell 10:2019–2032

Holdaway-Clarke TL, Feijó JA, Hackett GR, Kunkel JG, Hepler PK (1997) Pollen tube growth and the intracellular cytosolic calcium gradient oscillate in phase while extracellular calcium influx is delayed. Plant Cell 9:1999–2010

Holmes-Davis R, Tanaka CK, Vensel WH, Hurkman WJ, McCormick S (2005) Proteome mapping of mature pollen of Arabidopsis thaliana. Proteomics 5:4864–4884. doi:10.1002/pmic.200402011

Honys D, Twell D (2003) Comparative analysis of the Arabidopsis pollen transcriptome. Plant Physiol 132:640–652. doi:10.1104/pp.103.020925

Honys D, Twell D (2004) Transcriptome analysis of haploid male gametophyte development in Arabidopsis. Genome Biol. doi:10.1186/gb-2004-5-11-r85

Honys D, Combe JP, Twell D, Čapková V (2000) The translationally repressed pollen-specific ntp303 mRNA is stored in non-polysomal mRNPs during pollen maturation. Sex Plant Reprod 13:135–144

Honys D, Reňák D, Twell D (2006) Male gametyphyte development and function. In: da Silva JT (ed) Floriculture, ornamental and plant biotechnology: advances and topical issues, vol 1. Global Science Books, London, pp 76–87

Honys D, Reňák D, Fecikova J, Jedelský PL, Nebesářová J, Dobrev P, Čapková V (2009) Cytoskeleton-associated large RNP complexes in tobacco male gametophyte (EPPs) are associated with ribosomes and are involved in protein synthesis, processing, and

localization. J Proteome Res 8:2015–2031. doi:10.1021/pr8009897

Horade M, Kanaoka M, Kuzuya M, Higashiyama T, Kaji N (2013) A microfluidic device for quantitative analysis of chemoattraction in plants. RSC Adv 3:22301–22307

Hruz T, Laule O, Szabo G, Wessendorp F, Bleuler S, Oertle L, Widmayer P, Gruissem W, Zimmermann P (2008) Genevestigator v3: a reference expression database for the meta-analysis of transcriptomes. Adv Bioinform 2008:420747. doi:10.1155/2008/420747

Hsieh K, Huang AH (2005) Lipid-rich tapetosomes in Brassica tapetum are composed of oleosin-coated oil droplets and vesicles, both assembled in and then detached from the endoplasmic reticulum. Plant J 43:889–899. doi:10.1111/j.1365-313X.2005.02502.x

Huang MD, Hsing YI, Huang AH (2011) Transcriptomes of the anther sporophyte: availability and uses. Plant Cell Physiol 52:1459–1466. doi:10.1093/pcp/pcr088

Huck N, Moore JM, Federer M, Grossniklaus U (2003) The Arabidopsis mutant *feronia* disrupts the female gametophytic control of pollen tube reception. Development 130:2149–2159

Hulskamp M, Schneitz K, Pruitt RE (1995) Genetic evidence for a long-range activity that directs pollen tube guidance in Arabidopsis. Plant Cell 7:57–64. doi:10.1105/tpc.7.1.57

Ischebeck T, Valledor L, Lyon D, Gingl S, Nagler M, Meijon M, Egelhofer V, Weckwerth W (2014) Comprehensive cell-specific protein analysis in early and late pollen development from diploid microsporocytes to pollen tube growth. Mol Cell Proteomics 13:295–310. doi:10.1074/mcp.M113.028100

Jia Q-S, Zhu J, Xu XF, Lou Y, Zhang ZL, Zhang ZP, Yang ZN (2014) Arabidopsis AT-hook protein TEK positively regulates the expression of arabinogalactan proteins for Nexine formation. Mol Plant 8:251–260

Kanaoka MM, Kawano N, Matsubara Y, Susaki D, Okuda S, Sasaki N, Higashiyama T (2011) Identification and characterization of TcCRP1, a pollen tube attractant from *Torenia concolor*. Ann Bot 108:739–747. doi:10.1093/aob/mcr111

Kasahara RD, Portereiko MF, Sandaklie-Nikolova L, Rabiger DS, Drews GN (2005) MYB98 is required for pollen tube guidance and synergid cell differentiation in Arabidopsis. Plant Cell 17:2981–2992. doi:10.1105/tpc.105.034603

Kasahara RD, Maruyama D, Hamamura Y, Sakakibara T, Twell D, Higashiyama T (2012) Fertilization recovery after defective sperm cell release in Arabidopsis. Curr Biol 22:1084–1089. doi:10.1016/j.cub.2012.03.069

Kessler SA, Grossniklaus U (2011) She's the boss: signaling in pollen tube reception. Curr Opin Plant Biol 14:622–627. doi:10.1016/j.pbi.2011.07.012

Klahre U, Becker C, Schmitt AC, Kost B (2006) Nt-RhoGDI2 regulates Rac/Rop signaling and polar cell growth in tobacco pollen tubes. Plant J 46:1018–1031. doi:10.1111/j.1365-313X.2006.02757.x

Knorre DG, Kudryashova NV, Godovikova TS (2009) Chemical and functional aspects of posttranslational modification of proteins. Acta Nat 1:29–51

Kovar DR, Drobak BK, Staiger CJ (2000) Maize profilin isoforms are functionally distinct. Plant Cell 12:583–598

Kultz D (1998) Phylogenetic and functional classification of mitogen- and stress-activated protein kinases. J Mol Evol 46:571–588. doi:10.1007/pl00006338

Lalanne E, Honys D, Johnson A, Borner GH, Lilley KS, Dupree P, Grossniklaus U, Twell D (2004) SETH1 and SETH2, two components of the glycosylphosphatidylinositol anchor biosynthetic pathway, are required for pollen germination and tube growth in Arabidopsis. Plant Cell 16:229–240. doi:10.1105/tpc.014407

Lamport DT, Varnai P (2013) Periplasmic arabinogalactan glycoproteins act as a calcium capacitor that regulates plant growth and development. N Phytol 197:58–64. doi:10.1111/nph.12005

Lamport DT, Kieliszewski MJ, Chen Y, Cannon MC (2011) Role of the extensin superfamily in primary cell wall architecture. Plant Physiol 156:11–19. doi:10.1104/pp.110.169011

Lancelle SA, Hepler PK (1992) Ultrastructure of freeze-substituted pollen tubes of *Lilium longiferum*. Protoplasma 167:215–230. doi:10.1007/bf01403385

Lee TY, Bretana NA, Lu CT (2011) PlantPhos: using maximal dependence decomposition to identify plant phosphorylation sites with substrate site specificity. BMC Bioinform 12:13. doi:10.1186/1471-2105-12-261

Lee JS, Hnilova M, Maes M, Lin YC, Putarjunan A, Han SK, Avila J, Torii KU (2015) Competitive binding of antagonistic peptides fine-tunes stomatal patterning. Nature 522:439–443. doi:10.1038/nature14561

Lenartowska M, Michalska A (2008) Actin filament organization and polarity in pollen tubes revealed by myosin II subfragment 1 decoration. Planta 228:891–896. doi:10.1007/s00425-008-0802-5

Lerouge P, Cabanes-Macheteau M, Rayon C, Fischette-Laine AC, Gomord V, Faye L (1998) N-glycoprotein biosynthesis in plants: recent developments and future trends. Plant Mol Biol 38:31–48. doi:10.1023/a:1006012005654

Leydon AR, Beale KM, Woroniecka K, Castner E, Chen J, Horgan C, Palanivelu R, Johnson MA (2013) Three MYB transcription factors control pollen tube differentiation required for sperm release. Curr Biol 23:1209–1214. doi:10.1016/j.cub.2013.05.021

Li HJ, Xue Y, Jia DJ, Wang T, Hi DQ, Liu J, Cui F, Xie Q, Ye D, Yang WC (2011) POD1 regulates pollen tube guidance in response to micropylar female signaling and acts in early embryo patterning in Arabidopsis. Plant Cell 23:3288–3302. doi:10.1105/tpc.111.088914

Li S, Ge FR, Xu M, Zhao XY, Huang GQ, Zhou LZ, Wang JG, Kombrink A, McCormick S, Zhang XS, Zhang Y (2013) Arabidopsis COBRA-LIKE 10, a GPI-anchored protein, mediates directional growth of pollen tubes. Plant J 74:486–497. doi:10.1111/tpj.12139

Li Y, Ye Z, Nie Y, Zhang J, Wang G-L, Wang Z (2015) Comparative phosphoproteome analysis of *Magnaporthe oryzae*-responsive proteins in susceptible and resistant rice cultivars. J Proteomics 115:66–80. doi:10.1016/j.jprot.2014.12.007

Lim ES, Gumpil JS (1984) The flowering, pollination and hybridization of groundnuts (*Arachis hypogaea* L.). Pertanika 7:61–66

Lindner H, Kessler SA, Muller LM, Shimosato-Asano H, Boisson-Dernier A, Grossniklaus U (2015) TURAN and EVAN mediate pollen tube reception in Arabidopsis synergids through protein glycosylation. PLoS Biol. doi:10.1371/journal.pbio.1002139

Ling Y, Chen T, Jing Y, Fan L, Wan Y, Lin J (2013) γ-Aminobutyric acid (GABA) homeostasis regulates pollen germination and polarized growth in *Picea wilsonii*. Planta 238:831–843. doi:10.1007/s00425-013-1938-5

Liu J, Zhong S, Guo X, Hao L, Wei X, Huang Q, Hou Y, Shi J, Wang C, Gu H, Qu LJ (2013) Membrane-bound RLCKs LIP1 and LIP2 are essential male factors controlling male–female attraction in Arabidopsis. Curr Biol 23:993–998. doi:10.1016/j.cub.2013.04.043

Lora J, Herrero M, Hormaza JI (2009) The coexistence of bicellular and tricellular pollen in *Annona cherimola* (*Annonaceae*): implications for pollen evolution. Am J Bot 96:802–808. doi:10.3732/ajb.0800167

Lou Y, Xu XF, Zhu J, Gu JN, Blackmore S, Yang ZN (2014) The tapetal AHL family protein TEK determines nexine formation in the pollen wall. Nat Commun 5:3855. doi:10.1038/ncomms4855

Lovy-Wheeler A, Kunkel JG, Allwood EG, Hussey PJ, Hepler PK (2006) Oscillatory increases in alkalinity anticipate growth and may regulate actin dynamics in pollen tubes of lily. Plant Cell 18:2182–2193. doi:10.1105/tpc.106.044867

Lu Y, Chanroj S, Zulkifli L, Johnson MA, Uozumi N, Cheung A, Sze H (2011) Pollen tubes lacking a pair of K^+ transporters fail to target ovules in Arabidopsis. Plant Cell 23:81–93. doi:10.1105/tpc.110.080499

Lu P, Chai M, Yang J, Ning G, Wang G, Ma H (2014) The Arabidopsis CALLOSE DEFECTIVE MICROSPORE1 gene is required for male fertility through regulating callose metabolism during microsporogenesis. Plant Physiol 164:1893–1904. doi:10.1104/pp.113.233387

Ma H (2005) Molecular genetic analyses of microsporogenesis and micro grametogenesis in flowering plants. Annu Rev Plant Biol 2005:393–434

Maheshwari P (1950) An introduction to embryology of angiosperms. McGraw-Hill, New York

Malpighi M (1675, 1679) Die Anatomie der Pflanzen. I und II Theil. London 1675 und 1679. Engelmann, Leipzig, 1901

Márton ML, Cordts S, Broadhvest J, Dresselhaus T (2005) Micropylar pollen tube guidance by egg apparatus 1 of maize. Science 307:573–576. doi:10.1126/science.1104954

Márton ML, Fastner A, Uebler S, Dresselhaus T (2012) Overcoming hybridization barriers by the secretion of the maize pollen tube attractant ZmEA1 from Arabidopsis ovules. Curr Biol 22:1194–1198. doi:10.1016/j.cub.2012.04.061

Maruyama D, Hamamura Y, Takeuchi H, Susaki D, Nishimaki M, Kurihara D, Kasahara RD, Higashiyama T (2013) Independent control by each female gamete prevents the attraction of multiple pollen tubes. Dev Cell 25:317–323. doi:10.1016/j.devcel.2013.03.013

Mascarenhas JP (1993) Molecular mechanisms of pollen tube growth and differentiation. Plant Cell 5:1303–1314. doi:10.1105/tpc.5.10.1303

Mascarenhas JP, Machlis L (1962) The hormonal control of the directional growth of pollen tubes. Vitam Horm 20:347–372

Mayank P, Grossman J, Wuest S, Boisson-Dernier A, Roschitzki B, Nanni P, Nühse T, Grossniklaus U (2012) Characterization of the phosphoproteome of mature Arabidopsis pollen. Plant J 72:89–101. doi:10.1111/j.1365-313X.2012.05061.x

McCue AD, Cresti M, Feijó JA, Slotkin RK (2011) Cytoplasmic connection of sperm cells to the pollen vegetative cell nucleus: potential roles of the male germ unit revisited. J Exp Bot 62:1621–1631. doi:10.1093/jxb/err032

Meyer LJ, Gao J, Xu D, Thelen JJ (2012) Phosphoproteomic analysis of seed maturation in Arabidopsis, rapeseed, and soybean. Plant Physiol 159:517–528. doi:10.1104/pp.111.191700

Michard E, Dias P, Feijó JA (2008) Tobacco pollen tubes as cellular models for ion dynamics: improved spatial and temporal resolution of extracellular flux and free cytosolic concentration of calcium and protons using pHluorin and YC3.1 CaMeleon. Sex Plant Reprod 21:169–181. doi:10.1007/s00497-008-0076-x

Michard E, Alves F, Feijó JA (2009) The role of ion fluxes in polarized cell growth and morphogenesis: the pollen tube as an experimental paradigm. Intern J Dev Biol 53:1609–1622. doi:10.1387/ijdb.072296em

Mogami N, Miyamoto M, Onozuka M, Nakamura N (2006) Comparison of callose plug structure between dicotyledon and monocotyledon pollen germinated in vitro. Grana 45:249–256. doi:10.1080/00173130600726687

Mori T, Kuroiwa H, Higashiyama T, Kuroiwa T (2005) GENERATIVE CELL SPECIFIC 1 is essential for angiosperm fertilization. Nat cell biol 8:64–71

Mulcahy DL (1979) The rise of the angiosperms: a genecological factor. Science 206:20–23. doi:10.1126/science.206.4414.20

Mulcahy GB, Mulcahy DL (1988) The effect of supplemented media on the growth in vitro of binucleate and trinucleate pollen. Plant Sci 55:213–216

Mulcahy DL, Sari Gorla M, Mulcahy GB (1996) Pollen selection: past, present and future. Sex Plant Reprod 9:353–356

Nawaschin S (1898) Resultate einer Revision der Befruchtungsvorgänge bei Lilium martagon und Fritillaria tenella. Bulletin de l'Académie Impériale des Sciences 9:377–382

Nguema-Ona E, Coimbra S, Vicre-Gibouin M, Mollet J-C, Driouich A (2012) Arabinogalactan proteins in root and pollen-tube cells: distribution and functional aspects. Ann Bot 110:383–404. doi:10.1093/aob/mcs143

Noir S, Bräutigam A, Colby T, Schmidt J, Panstruga R (2005) A reference map of the Arabidopsis thaliana mature pollen proteome. Biochem Biophys Res Commun 337:1257–1266. doi:10.1016/j.bbrc.2005.09.185

Oh SA, Pal MD, Park SK, Johnson JA, Twell D (2010) The tobacco MAP215/Dis1-family protein TMBP200 is required for the functional organization of microtubule arrays during male germline establishment. J Exp Bot 61:969–981. doi:10.1093/jxb/erp367

Okuda S, Tsutsui H, Shiina K, Sprunck S, Takeuchi H, Yui R, Kasahara RD, Hamamura Y, Mizukami A, Susaki D, Kawano N, Sakakibara T, Namiki S, Itoh K, Otsuka K, Matsuzaki M, Nozaki H, Kuroiwa T, Nakano A, Kanaoka MM, Dresselhaus T, Sasaki N, Higashiyama T (2009) Defensin-like polypeptide LUREs are pollen tube attractants secreted from synergid cells. Nature 458:357–361. doi:10.1038/nature07882

Onelli E, Idilli AI, Moscatelli A (2015) Emerging roles for microtubules in angiosperm pollen tube growth highlight new research cues. Front Plant Sci. doi:10.3389/fpls.2015.00051

Pacini E (1990) Tapetum and microspore function. In: Blackmore S, Knox RB (eds) Microspores: evolution and ontogeny. Academic Press, London, pp 213–237

Pacini E (1996) Types and meaning of pollen carbohydrate reserves. Sex Plant Reprod 9:362–366

Pacini E, Guarnieri M, Nepi M (2006) Pollen carbohydrates and water content during development, presentation, and dispersal: a short review. Protoplasma 228:73–77. doi:10.1007/s00709-006-0169-z

Palanivelu R, Preuss D (2000) Pollen tube targeting and axon guidance: parallels in tip growth mechanisms. Trends Cell Biol 10:517–524. doi:10.1016/s0962-8924(00)01849-3

Palanivelu R, Preuss D (2006) Distinct short-range ovule signals attract or repel Arabidopsis thaliana pollen tubes in vitro. BMC Plant Biol 6:7. doi:10.1186/1471-2229-6-7

Palanivelu R, Brass L, Edlund AF, Preuss D (2003) Pollen tube growth and guidance is regulated by POP2, an Arabidopsis gene that controls GABA levels. Cell 114:47–59

Park SK, Howden R, Twell D (1998) The Arabidopsis thaliana gametophytic mutation gemini pollen1 disrupts microspore polarity, division asymmetry and pollen cell fate. Development 125:3789–3799

Pereira AM, Masiero S, Nobre MS, Costa ML, Solis MT, Testillano PS, Sprunck S, Coimbra S (2014) Differential expression patterns of arabinogalactan proteins in Arabidopsis thaliana reproductive tissues. J Exp Bot 65:5459–5471

Petersen TN, Brunak S, von Heijne G, Nielsen H (2011) SignalP 4.0: discriminating signal peptides from transmembrane regions. Nat Methods 8:785–786. doi:10.1038/nmeth.1701

Phan HA, Iacuone S, Li SF, Parish RW (2011) The MYB80 transcription factor is required for pollen development and the regulation of tapetal programmed cell death in Arabidopsis thaliana. Plant Cell 23:2209–2224. doi:10.1105/tpc.110.082651

Pierloni A, Martelli PL, Casadio R (2008) PredGPI: a GPI-anchor predictor. BMC Bioinform 9:392. doi:10.1186/1471-2105-9-392

Pierson ES, Miller DD, Callaham DA, van Aken J, Hackett G, Hepler PK (1996) Tip-localized calcium entry fluctuates during pollen tube growth. Dev Biol 174:160–173. doi:10.1006/dbio.1996.0060

Prado N, de Dios Alche J, Casado-Vela J, Mas S, Villalba M, Rodriguez R, Batanero E (2014) Nanovesicles are secreted during pollen germination and pollen tube growth: a possible role in fertilization. Mol Plant 7:573–577. doi:10.1093/mp/sst153

Puc M (2003) Characterisation of pollen allergens. Ann Agric Environ Med 10:143–149

Purkyně JE (1830) De cellulis antherarum fibrosis nec non de granorum pollinarium formis: commentatio phytomica. Sumtibus J. D. Gruesonii, Breslau, Vratislaviae

Qin Y, Yang ZBA (2011) Rapid tip growth: insights from pollen tubes. Semin Cell Dev Biol 22:816–824. doi:10.1016/j.semcdb.2011.06.004

Qin Y, Leydon AR, Manziello A, Pandey R, Mount D, Denic S, Vasic B, Johnson MA, Palanivelu R (2009) Penetration of the stigma and style elicits a novel transcriptome in pollen tubes, pointing to genes critical for growth in a pistil. PLoS Genet. doi:10.1371/journal.pgen.1000621

Qin Y, Wysocki RJ, Somogyi A, Feinstein Y, Franco JY, Tsukamoto T, Dunatunga D, Levy C, Smith S, Simpson R, Gang D, Johnson MA, Palanivelu R (2011) Sulfinylated azadecalins act as functional mimics of a pollen germination stimulant in Arabidopsis pistils. Plant J 68:800–815. doi:10.1111/j.1365-313X.2011.04729.x

Qin T, Liu X, Li J, Sun J, Song L, Mao T (2014) Arabidopsis microtubule-destabilizing protein 25 functions in pollen tube growth by severing actin filaments. Plant Cell 26:325–339. doi:10.1105/tpc.113.119768

Quilichini TD, Grienenberger E, Douglas CJ (2015) The biosynthesis, composition and assembly of the outer pollen wall: a tough case to crack. Phytochemistry 113:170–182. doi:10.1016/j.phytochem.2014.05.002

Ray SM, Park SS, Ray A (1997) Pollen tube guidance by the female gametophyte. Development 124:2489–2498

Ren HY, Xiang Y (2007) The function of actin-binding proteins in pollen tube growth. Protoplasma 230:171–182. doi:10.1007/s00709-006-0231-x

Romagnoli S, Cai G, Faleri C, Yokota E, Shimmen T, Cresti M (2007) Microtubule- and actin filament-dependent motors are distributed on pollen tube mitochondria and contribute differently to their movement. Plant Cell Physiol 48:345–361. doi:10.1093/pcp/pcm001

Rotman N, Rozier F, Boavida L, Dumas C, Berger F, Faure JE (2003) Female control of male gamete delivery during fertilization in Arabidopsis thaliana. Curr Biol 13:432–436

Russell SD, Jones DS (2015) The male germline of angiosperms: repertoire of an inconspicuous but important cell lineage. Front Plant Sci 6:173. doi:10.3389/fpls.2015.00173

Russell SD, Strout GW, Stramski AK, Mislan TW, Thompson RA, Schoemann LM (1996) Development polarization and morphogenesis of the generative and sperm cells of Plumbago zeylanica. 1. Descriptive cytology and three-dimensional organization. Am J Bot 83:1435–1453

Rutley N, Twell D (2015) A decade of pollen transcriptomics. Plant Reprod 28:73–89. doi:10.1007/s00497-015-0261-7

Šamaj J, Muller J, Beck M, Böhm N, Menzel D (2006) Vesicular trafficking, cytoskeleton and signalling in root hairs and pollen tubes. Trends Plant Sci 11:594–600. doi:10.1016/j.tplants.2006.10.002

Sanati Nezhad A, Packirisamy M, Geitmann A (2014) Dynamic, high precision targeting of growth modulating agents is able to trigger pollen tube growth reorientation. Plant J 80:185–195. doi:10.1111/tpj.12613

Sanders LC, Lord EM (1989) Directed movement of latex particles in the gynoecia of three species of flowering plants. Science 243:1606–1608

Sanders LC, Lord EM (1992) A dynamic role for the stylar matrix during pollen tube extension. Int Rev Cytol 140:297–318

Schrauwen JA, de Groot PF, van Herpen MM, van der Lee T, Reynen WH, Weterings KA, Wullems GJ (1990) Stage-related expression of mRNAs during pollen development in lily and tobacco. Planta 182:298–304. doi:10.1007/BF00197125

Schwacke R, Grallath S, Breitkreuz KE, Stransky E, Stransky H, Frommer WB, Rentsch D (1999) LeProT1, a transporter for proline, glycine betaine, and gamma-amino butyric acid in tomato pollen. Plant Cell 11:377–392

Schwemmie J (1968) Selective fertilization in Oenothera. Adv Genet 14:225–324

Scotland RW, Worltey AH (2003) How many species of seed plants are there? Taxon 52:101–104

Scott RJ, Spielman M, Dickinson HG (2004) Stamen structure and function. Plant Cell 16(Suppl):S46–S60. doi:10.1105/tpc.017012

Sheoran IS, Sproule KA, Olson DJH, Ross ARS, Sawhney VK (2006) Proteome profile and functional classification of proteins in Arabidopsis thaliana (Landsberg erecta) mature pollen. Sex Plant Reprod 19:185–196. doi:10.1007/s00497-006-0035-3

Sheoran IS, Ross ARS, Olson DJH, Sawhney VK (2009) Compatibility of plant protein extraction methods with mass spectrometry for proteome analysis. Plant Sci 176:99–104. doi:10.1016/j.plantsci.2008.09.015

Shi YY, Tao WJ, Liang SP, Lu YT, Zhang L (2009) Analysis of the tip-to-base gradient of CaM in pollen tube pulsant growth using in vivo CaM-GFP system. Plant Cell Rep 28:1253–1264. doi:10.1007/s00299-009-0725-z

Shimizu KK, Okada K (2000) Attractive and repulsive interactions between female and male gametophytes in Arabidopsis pollen tube guidance. Development 127:4511–4518

Slotkin RK, Vaughn M, Borges F, Tanurdzic M, Becker JD, Feijo JA, Martienssen RA (2009) Epigenetic reprogramming and small RNA silencing of transposable elements in pollen. Cell 136:461–472. doi:10.1016/j.cell.2008.12.038

Staiger CJ, Poulter NS, Henty JL, Franklin-Tong VE, Blanchoin L (2010) Regulation of actin dynamics by actin-binding proteins in pollen. J Exp Bot 61:1969–1986. doi:10.1093/jxb/erq012

Stepper J, Shastri S, Loo TS, Preston JC, Novak P, Man P, Moore CH, Havlicek V, Patchett ML, Norris GE (2011) Cysteine S-glycosylation, a new post-translational modification found in glycopeptide bacteriocins. FEBS Lett 585:645–650. doi:10.1016/j.febslet.2011.01.023

Strasburger E (1884) Neue Untersuchungen uber den Befruchtungsvorgang bei den Phanerogamen als Grundlage fur eine Theorie der Zeugung. Gustav Fischer, Jena

Szumlanski AL, Nielsen E (2009) The Rab GTPase RabA4d regulates pollen tube tip growth in Arabidopsis thaliana. Plant Cell 21:526–544. doi:10.1105/tpc.108.060277

Takeuchi H, Higashiyama T (2011) Attraction of tip-growing pollen tubes by the female gametophyte. Curr Opin Plant Biol 14:614–621. doi:10.1016/j.pbi.2011.07.010

Takeuchi H, Higashiyama T (2012) A species-specific cluster of defensin-like genes encodes diffusible pollen tube attractants in Arabidopsis. PLoS Biol 10:e1001449. doi:10.1371/journal.pbio.1001449

Terasaka O, Niitsu T (1987) Unequal cell division and chromatin differentiation in pollen grain cells I. Centrifugal, cold and caffeine treatment. Bot Mag (Tokyo) 100:205–216

Ting JT, Wu SS, Ratnayake C, Huang AH (1998) Constituents of the tapetosomes and elaioplasts in Brassica campestris tapetum and their degradation and retention during microsporogenesis. Plant J 16:541–551

Tsukamoto T, Qin Y, Huang Y, Dunatunga D, Palanivelu R (2010) A role for LORELEI, a putative glycosylphosphatidylinositol-anchored protein, in *Arabidopsis thaliana* double fertilization and early seed development. Plant J 62:571–588. doi:10.1111/j.1365-313X.2010.04177.x

Tupý J (1982) Alterations in polyadenylated RNA during pollen maturation and germination. Biol Plant 24:331–340

Tupý J, Říhová L, Žárský V (1991) Production of fertile tobacco pollen from microspores in suspension culture and its storage for in situ pollination. Sex Plant Reprod 4:284–287

Twell D (2011) Male gametogenesis and germline specification in flowering plants. Sex Plant Reprod 24:149–160. doi:10.1007/s00497-010-0157-5

Twell D, Park SK, Hawkins TJ, Schubert D, Schmidt R, Smertenko A, Hussey PJ (2002) MOR1/GEM1 has an essential role in the plant-specific cytokinetic phragmoplast. Nat Cell Biol 4:711–714. doi:10.1038/ncb844

Uebler S, Dresselhaus T (2014) Identifying plant cell-surface receptors: combining 'classical' techniques with novel methods. Biochem Soc Trans 42:395–400. doi:10.1042/bst20130251

Ueda T, Iwashita H, Hashimoto Y, Imoto T (1996) Stabilization of lysozyme by introducing *N*-glycosylation signal sequence. J Biochem 119:157–161

van Bentem SD, Anrather D, Dohnal I, Roitinger E, Csaszar E, Joore J, Buijnink J, Carreri A, Forzani C, Lorkovic ZJ, Barta A, Lecourieux D, Verhounig A, Jonak C, Hirt H (2008) Site-specific phosphorylation profiling of Arabidopsis proteins by mass spectrometry and peptide chip analysis. J Proteome Res 7:2458–2470. doi:10.1021/pr8000173

Vidali L, McKenna ST, Hepler PK (2001) Actin polymerization is essential for pollen tube growth. Mol Biol Cell 12:2534–2545

Vogler F, Schmalzl C, Englhart M, Bircheneder M, Sprunck S (2014) Brassinosteroids promote Arabidopsis pollen germination and growth. Plant Reprod 27:153–167. doi:10.1007/s00497-014-0247-x

Vogler F, Konrad SSA, Sprunck S (2015) Knockin' on pollen's door: live cell imaging of early polarization events in germinating Arabidopsis pollen. Front Plant Sci. doi:10.3389/fpls.2015.00246

Völz R, Heydlauff J, Ripper D, von Lyncker L, Groß-Hardt R (2013) Ethylene signaling is required for synergid degeneration and the establishment of a pollen tube block. Dev Cell 25:310–316. doi:10.1016/j.devcel.2013.04.001

von Besser K, Frank AC, Johnson MA, Preuss D (2006) Arabidopsis HAP2 (GCS1) is a sperm-specific gene required for pollen tube guidance and fertilization. Development 133:4761–4769. doi:10.1242/dev.02683

Wang Y, Zhang W-Z, Song L-F, Zou J-J, Su Z, Wu W-H (2008) Transcriptome analyses show changes in gene expression to accompany pollen germination and tube growth in Arabidopsis. Plant Physiol 148:1201–1211. doi:10.1104/pp.108.126375

Wei LQ, Xu WY, Deng ZY, Su Z, Xue Y, Wang T (2010) Genome-scale analysis and comparison of gene expression profiles in developing and germinated pollen in *Oryza sativa*. BMC Genomics 11:338. doi:10.1186/1471-2164-11-338

Williams JH (2009) *Amborella trichopoda* (Amborellaceae) and the evolutionary developmental origins of the angiosperm progamic phase. Am J Bot 96:144–165. doi:10.3732/ajb.0800070

Williams JH, Taylor ML, O'Meara BC (2014) Repeated evolution of tricellular (and bicellular) pollen. Am J Bot 101:559–571. doi:10.3732/ajb.1300423

Wilsen KL, Lovy-Wheeler A, Voigt B, Menzel D, Kunkel JG, Hepler PK (2006) Imaging the actin cytoskeleton in growing pollen tubes. Sex Plant Reprod 19:51–62. doi:10.1007/s00497-006-0021-9

Wilson C, Voronin V, Touraev A, Vicente O, Heberle Bors E (1997) A developmentally regulated MAP kinase activated by hydration in tobacco pollen. Plant Cell 9:2093–2100

Wolschin F, Weckwerth W (2005) Combining metal oxide affinity chromatography (MOAC) and selective mass spectrometry for robust identification of in vivo protein phosphorylation sites. Plant Methods 1(1):9

Woollard AAD, Moore I (2008) The functions of Rab GTPases in plant membrane traffic. Curr Opin Plant Biol 11:610–619. doi:10.1016/j.pbi.2008.09.010

Worrall D, Hird DL, Hodge R, Paul W, Draper J, Scott R (1992) Premature dissolution of the microsporocyte callose wall causes male sterility in transgenic tobacco. Plant Cell 4:759–771. doi:10.1105/tpc.4.7.759

Wu H, de Graaf BHJ, Mariani C, Cheung AY (2001) Hydroxyproline-rich glycoproteins in plant reproductive tissues: structure, functions and regulation. Cell Mol Life Sci 58:1418–1429

Yadegari R, Drews GN (2004) Female gametophyte development. Plant Cell 16:S133–S141. doi:10.1105/tpc.018192

Yu GH, Zou J, Feng J, Peng XB, Wu JY, Wu YL, Palanivelu R, Sun MX (2014) Exogenous γ-aminobutyric acid (GABA) affects pollen tube growth via modulating putative Ca^{2+}-permeable membrane channels and is coupled to negative regulation on glutamate decarboxylase. J Exp Bot 65:3235–3248. doi:10.1093/jxb/eru171

Zaki MAM, Dickinson H (1991) Microspore-derived embryos in Brassica: the significance of division asymmetry in pollen mitosis I to embryogenic development. Sex Plant Reprod 4:48–55

Zhang Y, McCormick S (2010) The regulation of vesicle trafficking by small GTPases and phospholipids during pollen tube growth. Sex Plant Reprod 23:87–93. doi:10.1007/s00497-009-0118-z

Zhang ZB, Zhu J, Gao JF, Wang C, Li H, Li H, Zhang HQ, Zhang S, Wang DM, Wang QX, Huang H, Xia HJ, Yang ZN (2007) Transcription factor AtMYB103 is required for anther development by regulating tapetum development, callose dissolution and exine formation in Arabidopsis. Plant J 52:528–538. doi:10.1111/j.1365-313X.2007.03254.x

Zhang Y, He J, McCormick S (2009) Two Arabidopsis AGC kinases are critical for the polarized growth of pollen tubes. Plant J 58:474–484. doi:10.1111/j.1365-313X.2009.03792.x

Zhao HP, Ren HY (2006) Rop1Ps promote actin cytoskeleton dynamics and control the tip growth of lily pollen tube. Sex Plant Reprod 19:83–91. doi:10.1007/s00497-006-0024-6

Zhao XY, Wang Q, Li S, Ge FR, Zhou LZ, McCormick S, Zhang Y (2013) The juxtamembrane and carboxy-terminal domains of Arabidopsis PRK2 are critical for ROP-induced growth in pollen tubes. J Exp Bot 64(18):5599–5610. doi:10.1093/jxb/ert323

Zheng ZL, Yang ZB (2000) The Rop GTPase: an emerging signaling switch in plants. Plant Mol Biol 44:1–9. doi:10.1023/a:1006402628948

Zhu L, Zhang Y, Kang E, Xu Q, Wang M, Rui Y, Liu B, Yuan M, Fu Y (2013) MAP18 regulates the direction of pollen tube growth in Arabidopsis by modulating F-actin organization. Plant Cell 25:851–867. doi:10.1105/tpc.113.110528

7.4. Sekretom pylových láček tabáku virginského

Hafidh, S., Potěšil, D., **Fíla, J.**, Čapková, V., Zdráhal, Z., Honys, D. (2016). Direct quantification of the pollen tube secretome identifies novel pollen tube guidance proteins following its interaction with the pistil. Genome Biology 17, 81. doi: 10.1186/s13059-016-0928-x. $IF_{2014} = 10,810$

U této původní práce jsem se podílel na klonování vybraných konstruktů a na analýze sekretomických dat.

Genome Biology

CrossMark

Quantitative proteomics of the tobacco pollen tube secretome identifies novel pollen tube guidance proteins important for fertilization

Said Hafidh[1*], David Potěšil[2,3], Jan Fíla[1], Věra Čapková[1^], Zbyněk Zdráhal[2,3] and David Honys[1*]

Abstract

Background: As in animals, cell–cell communication plays a pivotal role in male–female recognition during plant sexual reproduction. Prelaid peptides secreted from the female reproductive tissues guide pollen tubes towards ovules for fertilization. However, the elaborate mechanisms for this dialogue have remained elusive, particularly from the male perspective.

Results: We performed genome-wide quantitative liquid chromatography–tandem mass spectrometry analysis of a pistil-stimulated pollen tube secretome and identified 801 pollen tube-secreted proteins. Interestingly, *in silico* analysis reveals that the pollen tube secretome is dominated by proteins that are secreted unconventionally, representing 57 % of the total secretome. In support, we show that an unconventionally secreted protein, translationally controlled tumor protein, is secreted to the apoplast. Remarkably, we discovered that this protein could be secreted by infiltrating through the initial phases of the conventional secretory pathway and could reach the apoplast via exosomes, as demonstrated by co-localization with Oleisin1 exosome marker. We demonstrate that translationally controlled tumor protein-knockdown *Arabidopsis thaliana* plants produce pollen tubes that navigate poorly to the target ovule and that the mutant allele is poorly transmitted through the male. Further, we show that regulators of the endoplasmic reticulum–trans-Golgi network protein secretory pathway control secretion of *Nicotiana tabacum* Pollen tube-secreted cysteine-rich protein 2 and Lorelei-like GPI-anchor protein 3 and that a regulator of endoplasmic reticulum–trans-Golgi protein translocation is essential for pollen tube growth, pollen tube guidance and ovule-targeting competence.

Conclusions: This work, the first study on the pollen tube secretome, identifies novel genome-wide pollen tube-secreted proteins with potential functions in pollen tube guidance towards ovules for sexual reproduction. Functional analysis highlights a potential mechanism for unconventional secretion of pollen tube proteins and reveals likely regulators of conventional pollen tube protein secretion. The association of pollen tube-secreted proteins with marker proteins shown to be secreted via exosomes in other species suggests exosome secretion is a possible mechanism for cell–cell communication between the pollen tube and female reproductive cells.

Keywords: Protein secretion, Pollen tube guidance, Cell-cell signaling, Double fertilization

* Correspondence: hafidh@ueb.cas.cz; david@ueb.cas.cz
^Deceased
[1]Laboratory of Pollen Biology, Institute of Experimental Botany ASCR, Rozvojová 263, 165 02 Prague 6, Czech Republic
Full list of author information is available at the end of the article

Hafidh *et al. Genome Biology* (2016) 17:81

Page 2 of 29

Background

The cell apoplast and the extracellular matrix provide a hub for cell–cell communication in plants. These inter-spaces relay secreted peptide-mediated signals to neighboring cells. In flowering plant reproduction, the pollen tubes carrying two non-motile sperm cells (male gametes) grow through the extracellular matrix of the transmitting tract tissues (TT) with the aid of female guidance signals to reach and fertilize deeply embedded female gametes [1, 2]. This molecular dialog between the pollen tube and pollen tube attractants has emerged as an important bottleneck for unfavorable fertilization and a pre-zygotic barrier for interspecies hybridization; however, its mechanism has so far remained unknown. Studies using single-cell laser ablation and genetic techniques have identified various female secreted peptides involved in pollen–pistil interactions with conserved roles across plant species [3–5]. Predominantly, they are arabinogalactan proteins, cysteine-rich polypeptides, defensin-like (DEFL) proteins, S-RNases, hydroxyproline-rich proteins, transmitting tissue-specific (TTS) proteins, class III pistil extensin-like proteins (PELPIII) and lipid transfer proteins (LTPs) [6–8]. Recently, CENTRAL CELL GUIDANCE (CCG) protein together with its interacting partners, CCG BINDING PROTEIN1 (CBP1), mediator complex (MED), and central cell-specific AGAMOUS-transcription factors, was shown to co-regulate a subset of cysteine-rich proteins (CRPs), including pollen tube attractant LURE1, that mediate pollen tube attraction [9].

A handful of proteins are known to be secreted by the male gametophyte. They include LAT52, a pollen tube-secreted ligand from tomato [10, 11]; lipid transfer protein 5 (LTP5), a homolog of Lily SCA protein [9]; thionin [12]; and HAP2 as a sperm-specific factor required for gamete fusion and blocking polytubey [13].

The discovery of pollen tube-secreted proteins that perceive female-secreted signals has been hampered by the inaccessibility of the pollen tubes within pistils and the likelihood of contamination from surrounding female tissues. We have therefore improvised a semi-in vivo technique (SIV) for tobacco pollen tube growth through the pistil to allow capture and detection of proteins secreted by the pollen tube following its penetration through the stigma and style [14]. In contrast to in vitro grown pollen tubes, SIV pollen tubes have been shown to have unique transcriptomes [15] as well as the ability to respond to synthetic pollen tube attractant peptides (LUREs) secreted by female synergid cells of *Torenia fournieri* [3, 16]. These findings emphasize the necessity for research into pollen tube–pistil interaction, specifically on the mechanisms of protein secretion and the identity of secreted factors that render pollen tubes competent for ovule-targeting, pollen tube reception, and fertilization. We used a high-throughput gel-free and label-free workflow utilizing nanoscale liquid chromatography (LC) and tandem mass spectrometry (MS/MS) to identify proteins of the *Nicotiana tabacum* semi-in vivo pollen tube secretome (SIV-PS). We observed an unprecedented bias towards unconventional protein secretion by the pollen tube. This type of secretion could be partly mediated by secreted nanovesicles (exosomes), suggesting for the first time a possible mechanism for long distance signaling by the pollen tube. Further, our results revealed a critical role for the endoplasmic reticulum (ER)–trans-Golgi network (TGN)–plasma membrane secretory components YIP4a,b and ECHIDNA on protein secretion, pollen tube growth, and competence of pollen tube targeting to the ovule, as well as fertilization. We show that this pathway can be hijacked by unconventionally secreted pollen tube proteins such as Translationally controlled tumor protein (TCTP), which could eventually be secreted to the extracellular matrix via exosomes and play a critical role in pollen tube–pistil signaling, fertilization, and seed production.

Results

A SIV method for high-throughput detection of pollen tube-secreted proteins following penetration through the pistil

Previously, we optimized a technique for tobacco pollen tube growth through the female stylar explant to detect pollen tube-secreted proteins following penetration through the female reproductive tissues. We termed this technique the semi-in vivo pollen tube-secretome (SIV-PS) assay [14]. In this study, we have coupled the SIV-PS assay with a gel-free and label-free semi-quantitative LC-MS/MS workflow to detect and quantify pollen tube-secreted proteins using minimum quantities of 2 μg of the pollen tube total secretome (Additional file 1: Figure S1). Our gel- and label-free strategy maximized detection of naturally low-abundant small secreted proteins by more than four orders of magnitude (relative to in-gel protein detection) and enabled us to detect proteins at concentrations as low as 0.45 parts per million (ppm), demonstrating the feasibility of the SIV-PS technique coupled with gel-free LC-MS/MS. Using the SIV-PS method, we have observed remarkable reproducibility with regard to pollen tube physiology, including growth, viability and intactness, cytoplasmic streaming, uniform tip morphology, callose wall and callose plug formation, and sperm cell production (Additional file 1: Figure S1). To test the purity of the secretome samples, we used alcohol dehydrogenase (ADH) as the most abundant cytosolic protein and performed an ADH assay to estimate cytosolic contamination (Additional file 1: Figure S1 and Additional file 2: Figure S2). Our results show that SIV-PS samples are pure

Hafidh *et al. Genome Biology* (2016) 17:81

Page 3 of 29

with minimal cytosolic contamination relative to whole protein extracts from pollen tubes (15-fold less ADH activity in SIV-PS samples relative to control). The SIV-PS modifications maximized the identification of pistil-dependent pollen tube-secreted proteins induced following crosstalk with the female reproductive tissues compared with those secreted by in vitro germinated pollen tubes.

Quantification of pollen tube-secreted proteins

To detect pollen tube-secreted proteins, we used label-free LC-MS/MS on two control samples (excised, unpollinated pistils, C1 and C2), four SIV-PS samples (SIV-PS1–4), four in vitro germinated pollen tube secretome samples after 24 h growth (PT24-PS1-4), four semi-in vivo whole proteome (SIV-PP1-4) samples, and four in vitro germinated pollen tube whole proteome samples (PT24-PP1-4). We used the Top3 label-free algorithm [17, 18] to determine approximate relative and absolute protein abundances from LC-MS/MS data, which allowed categorization of true secreted proteins over false positives for the SIV-PS samples as well as comparison of secretion dynamics across sample replicates and sample types. We identified an average of 1003 (2916 protein accessions) and 339 (1173 protein accessions) protein groups in individual SIV-PS and control samples, respectively. Protein relative quantification using the Top3 algorithm (up-regulated three-fold or more and up-regulated in at least two SIV-PS samples and at the same time identified using three or more peptides) showed an average of 341 protein groups (801 protein accessions) to be likely pollen tube-secreted proteins following penetration through stigma and style (Additional file 3: Table S1). Our results show that quantitative LC-MS/MS can distinguish between secreted proteins and false negatives, particularly in cases where the same protein accessions were also detected in control unpollinated pistils. We provide three examples to demonstrate the resolution of our quantitative data with regard to determining true protein secretion (Additional file 4: Figure S3).

Raw peptide counts revealed that protein identification was predominantly based on two to ten peptides (65 %), followed by singletons (20 %) and those with more than ten total peptide counts (15 %) (Fig. 1a). Comparison of pollen tube secretome replicates based on absolute quantification of protein abundances in parts per million (see "Methods") revealed that pollen tube protein secretion is consistent but also relatively dynamic, as observed from limited overlap of protein accessions between SIV-PS sample replicates (Fig. 1b). Protein size distribution showed a high frequency of secreted proteins of ≤20 kDa (Fig. 1c and Additional file 5: Table S2). Classification of protein families and domains highlighted glycoside-hydrolase family 16, proteinase

inhibitor II, Cu-oxidase, LRR 1/4/6/8, and fasciclin as among the most overrepresented conventionally secreted proteins (Fig. 1d and Additional file 6: Table S3). In the unconventionally secreted protein group, histone, RNA-binding (RRM_1), HSP70, and proteasome families were the most frequent activities (Fig. 1d and Additional file 6: Table S3). Using the Top3 algorithm, the absolute abundance of pollen tube-secreted proteins was comparable regardless of the pathway of secretion utilized (Fig. 1e). Mapping of the identified pollen tube-secreted proteins to a tobacco microarray [19, 20] revealed a significant enrichment in gametophytic expression and, in some instances, specificity to the gametophyte (Fig. 1f). We conclude that: (1) the sensitivity of the gel-free sample preparation coupled with label-free LC-MS/MS analysis readily allowed quantitative evaluation and determination of pollen tube-secreted protein abundances; and (2) the pollen tube secretome is dominated by small secreted proteins with elevated hydrolase activities.

The secretome of pollen tubes grown through the pistil is unique from that of in vitro cultured pollen tubes

To establish the unique physiology of the SIV pollen tube secretome following growth through the pistil, we compared it (SIV-PS) and the SIV proteome (SIV-PP) with the 24 h in vitro pollen tube secretome (PT24-PS) and its proteome (PT24-PP). Three-dimensional principal component analysis distinctively separated the samples into two groups, "secretome" and "proteome", and spatially sub-grouped them further into "semi in vivo" and "in vitro" (Fig. 2a). These results clearly demonstrate that the pollen tube secretome is distinct from its proteome and that the SIV-PS is unique compared with PT24-PS. Comparison of protein supergroups (see materials and methods) from each sample type further emphasized the limited overlap between SIV and in vitro sample types (Fig. 2b). Pairwise comparison between the SIV-PS and PT24-PS using protein supergroups that constitute only accessions identified with three or more peptides and present in at least one replicate identified 414 protein supergroups that are unique to the SIV-PS (Fig. 2c, Additional file 7: Table S4). We observed only 36.3 % (586 protein groups) overlap between the SIV-PS and PT24-PS (Fig. 2c). Gene Ontology (GO) analysis revealed that the most overrepresented GO categories in the SIV-PS included ATP binding, defense response, and cellulase activities (Fig. 2c), all of which have been previously implicated in pollen tube growth and fertilization [4, 6]. The unique set of SIV-PS proteins secreted by pollen tubes grown through the pistil (Additional file 7: Table S4) represent some of the potential factors responsible for pollen tube guidance and ovule-targeting competence. They are candidates for further understanding how
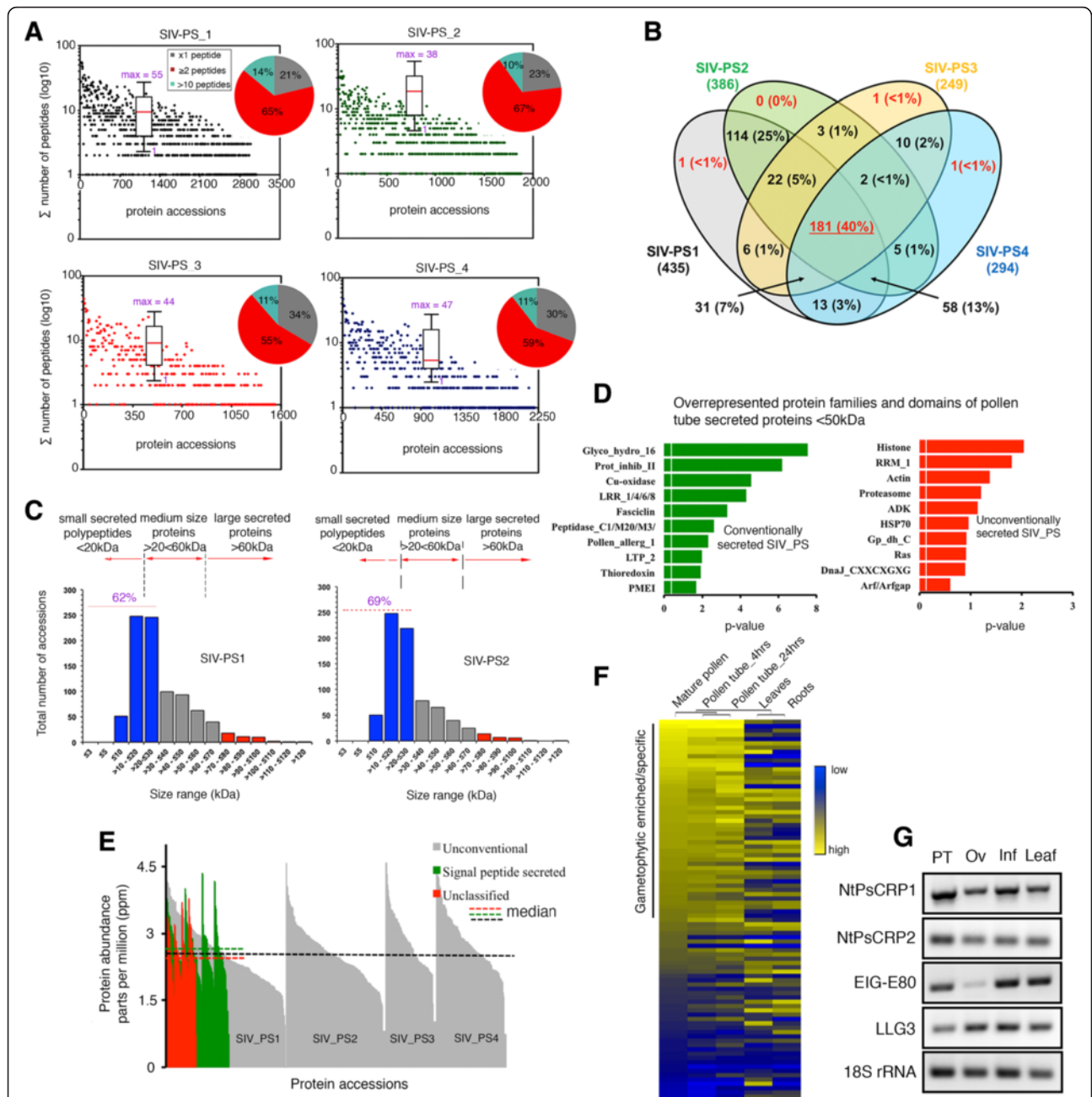
Hafidh *et al. Genome Biology* (2016) 17:81

Page 4 of 29

Fig. 1 Label-free, high-throughput LC-MS/MS quantification of the SIV pollen tube secretome. **a** Numbers of peptides identified by LC-MS/MS. Box plots summarize peptide number distribution per protein accession within a single sample replicate with the median value designated by the *solid red line*. Appended pie charts show the distribution of peptide counts in arbitrary bins. **b** SIV-PS samples showing the reproducibility and dynamics of the secreted protein groups (threefold or more abundant in at least two SIV-PS samples relative to unpollinated controls and identified by at least three or more peptides). **c** Size distribution of pollen tube-secreted proteins, showing predominant bias towards small secreted proteins. SIV-PS1–2 are used as representatives of all four replicates. **d** In silico analysis of pollen tube-secreted proteins using SMART and Pfam databases of overrepresented protein families and domains. The v*ertical white line* indicates significance cutoff ($p < 0.05$). **e** Classified pollen tube-secreted proteins based on the Top3 algorithm showing the dominant presence of unconventionally secreted proteins, although these have comparable protein abundance to conventionally secreted proteins. **f** Heatmap derived from the Agilent tobacco microarray [19, 20] of transcripts encoding identified pollen tube-secreted proteins showing predominantly gametophytic enrichment. **g** Validated expression profile by semi-quantitative RT-PCR of selected pollen tube-secreted proteins assessed in this study. All samples analyzed were from *N. tabacum*. *NtPsCRP1/2 Nicotiana tabacum* cysteine-rich polypeptide protein 1 and 2, *EIG-E80* elicitor inducible gene subE80, *LLG3* Lorelei-like GPI-anchored protein 3, *PT* semi in vivo pollen tubes, *Ov* unfertilized ovules, *Inf* inflorescence
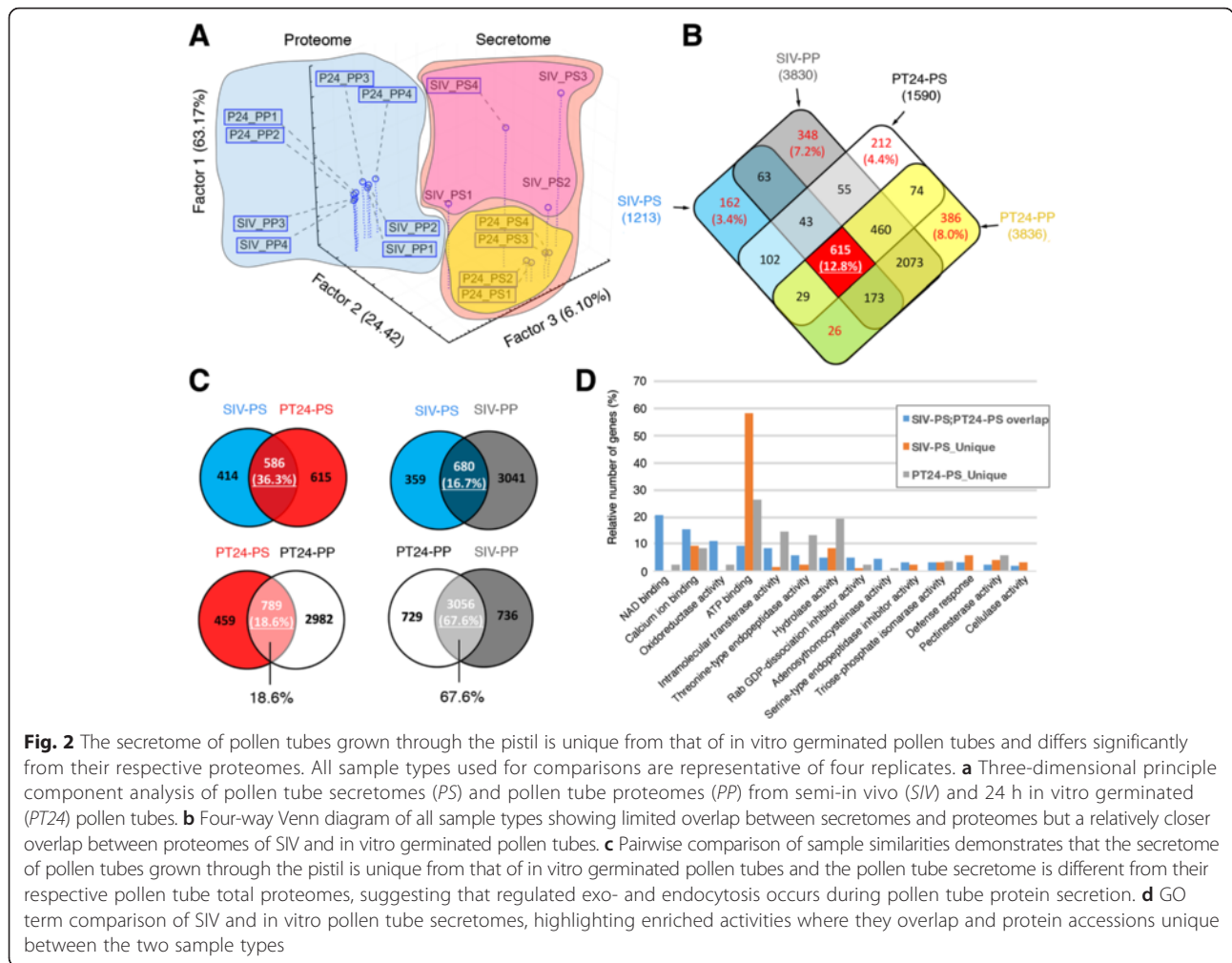
Hafidh *et al. Genome Biology* (2016) 17:81

Page 5 of 29

Fig. 2 The secretome of pollen tubes grown through the pistil is unique from that of in vitro germinated pollen tubes and differs significantly from their respective proteomes. All sample types used for comparisons are representative of four replicates. **a** Three-dimensional principle component analysis of pollen tube secretomes (*PS*) and pollen tube proteomes (*PP*) from semi-in vivo (*SIV*) and 24 h in vitro germinated (*PT24*) pollen tubes. **b** Four-way Venn diagram of all sample types showing limited overlap between secretomes and proteomes but a relatively closer overlap between proteomes of SIV and in vitro germinated pollen tubes. **c** Pairwise comparison of sample similarities demonstrates that the secretome of pollen tubes grown through the pistil is unique from that of in vitro germinated pollen tubes and the pollen tube secretome is different from their respective pollen tube total proteomes, suggesting that regulated exo- and endocytosis occurs during pollen tube protein secretion. **d** GO term comparison of SIV and in vitro pollen tube secretomes, highlighting enriched activities where they overlap and protein accessions unique between the two sample types

the pollen tube communicates with and is guided through the female reproductive tissues to achieve successful double fertilization.

Quantitative analysis of protein groups revealed that, despite the pollen tube secretome being dominated by unconventionally secreted proteins, both conventionally and unconventionally secreted proteins were secreted at comparable abundances (Fig. 1f). To establish whether the presence of a large number of unconventionally secreted proteins in the SIV-PS is a result of regulated secretion or is a consequence of a non-selective extrusion of cytoplasmic proteins due to extremely dynamic exocytosis and endocytosis in pollen tubes, a phenomena observed in tip growing cell types (Additional file 2: Figure S2) [21, 22], we compared the SIV-PS and PT24-PS samples with their respective total proteomes. Our results showed a limited overlap (16.7 % and 18.6 %, respectively) between the secretome and total proteome, suggesting that the observed dominant unconventional protein secretion

of the SIV-PS is a result of a regulated process and not a consequence of extreme exocytosis and endocytosis (Fig. 2b, c).

More interestingly, the pollen tube proteomes from SIV and in vitro grown pollen tubes showed a much bigger overlap (67.6 %) than their respective secretomes (Fig. 2c). These results suggest that distinct pistil factors (for instance, the female-secreted pollen tube guidance signals) might affect the pollen tube secretome independently of other pistil factors that influence the SIV pollen tube proteome or transcriptome.

Correlation of the tobacco SIV-PS with the *Arabidopsis* SIV transcriptome

To understand tobacco pollen tube secretion dynamics, we studied the correlation between the tobacco SIV-PS and transcript profiles from *Arabidopsis* SIV microarray data [15]. Mapping of a subset of the tobacco pollen tube-secreted proteins (only those identified in the UniProt database) to close homologs from the *Arabidopsis*

Hafidh *et al. Genome Biology* (2016) 17:81

Page 6 of 29

SIV pollen tube transcriptome revealed an astonishing 90.65 % (681/739) overlap, of which 372 genes (50.34 %) showed reliable expression in all three microarray replicates (Additional file 8: Table S5). These results suggest that the 681 genes expressed in *Arabidopsis* SIV pollen tubes are also detected in the tobacco SIV-PS. The near-complete overlap between the two datasets also suggests that the physiological response of pollen tubes following growth through the stigma and style is strongly conserved

at the transcriptome level as well as at the secretome level in both plant species.

When we compared transcript profiles with the corresponding secreted protein abundances, we found that, for the bulk of the dataset, the pollen tube protein secretion was uncoupled from gene expression profiles (Fig. 3). The relative abundances of secreted proteins showed no linear correlations with the transcript levels, although we did observe moderate positive (R1 = 0.375, p = 0.013; R2 = 0.486,
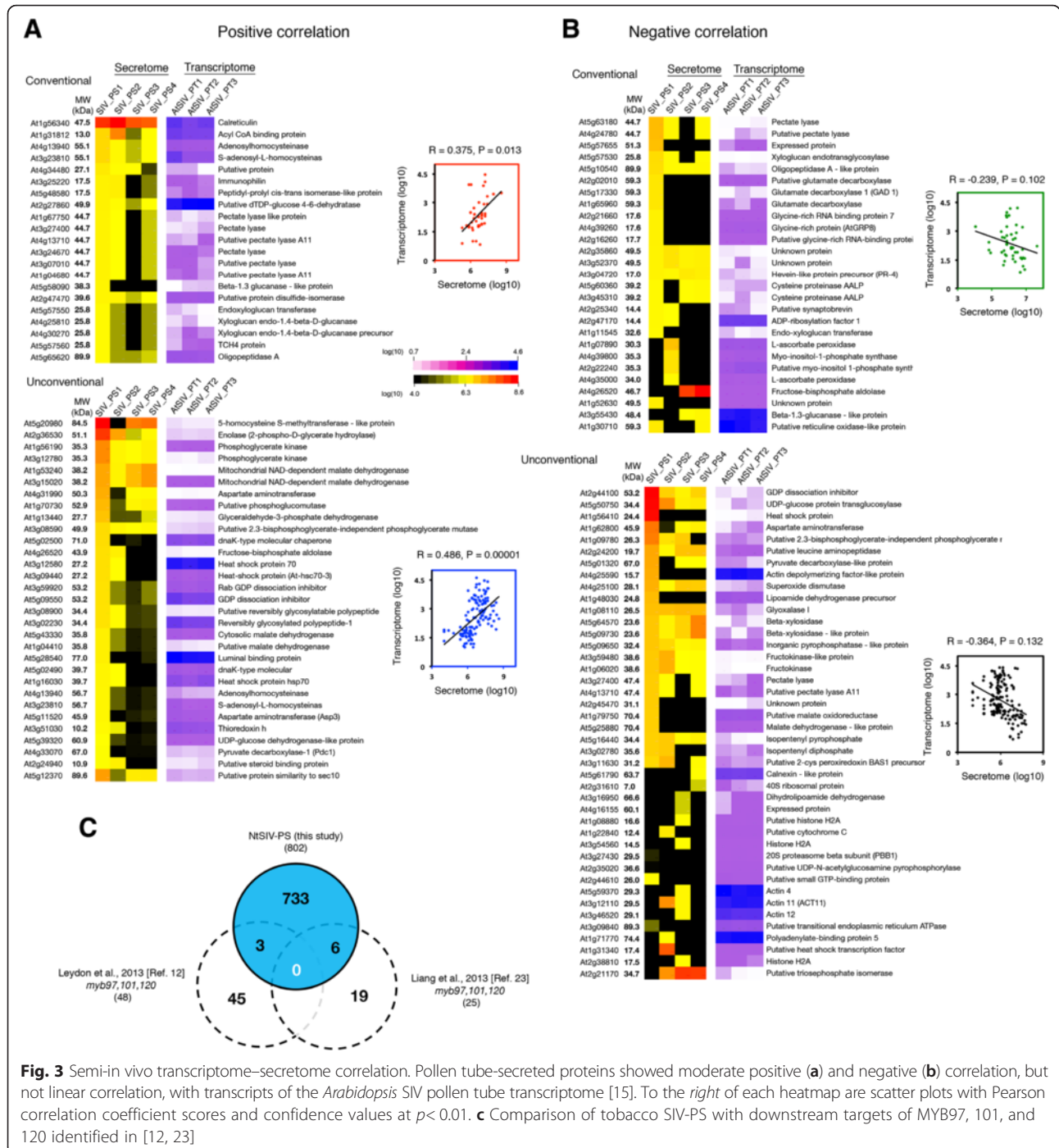

Fig. 3 Semi-in vivo transcriptome–secretome correlation. Pollen tube-secreted proteins showed moderate positive (**a**) and negative (**b**) correlation, but not linear correlation, with transcripts of the *Arabidopsis* SIV pollen tube transcriptome [15]. To the *right* of each heatmap are scatter plots with Pearson correlation coefficient scores and confidence values at p< 0.01. **c** Comparison of tobacco SIV-PS with downstream targets of MYB97, 101, and 120 identified in [12, 23]

Hafidh *et al. Genome Biology* (2016) 17:81

Page 7 of 29

$p = 0.00001$) and negative (R1 = −0.239, $p = 0.102$; R2 = −0.364, $p = 0.132$) correlations based on Pearson correlation coefficient scores (Fig. 3a, b). These data suggest that the pollen tube secretome is a specialized subset of the male gametophyte signaling repertoire and cannot be predicted from transcriptional profiling alone.

Moreover, two previous studies by Leydon et al. [12] and Liang et al. [23] have shown that simultaneous knockdown of pollen-expressed MYB transcription factors (*MYB97, MYB101*, and *MYB120*) in SIV pollen tubes led to the down-regulation of target genes, some of which were essential for pollen tube guidance, reception, and fertility [12, 23]. Comparison of these MYB97/101/120 targets, 48 genes from Leydon et al. and 25 genes from Liang et al., with the tobacco SIV-PS identified overlaps of 3/48 (6 %) and 6/25 (24 %), respectively (Fig. 3c). These overlapping proteins include galactokinase 2 (ATGALK2), cellulase 3 (CEL3) with hydrolase activity, and myo-inositol-1-phosphate synthase 2 (MIPS) from the Leydon et al. study and CC (carboxylate clamp)-TPR (tetratricopeptide repeat) protein (AT5G48570), similar to endo-xyloglucan transferase (AT4G30270), histone H2A protein (AT1G51060), HSP70B (HEAT SHOCK PROTEIN 70B; AT1G16030), HSP20-like chaperones superfamily protein (AT1G07400) and HSP70 (DG4; AT3G12580) from the Liang et al. study. The minimum overlap observed between the tobacco SIV-PS and potential downstream targets of MYB97/101/120 transcription factors could be due to tobacco genes encoding pollen tube-secreted proteins not being predominant targets of the *MYB97;MYB101;MYB120* transcription unit. This implies possible activities of multiple transcriptional pathways are involved in coordinating pollen tube-secreted protein transcriptional activation in tobacco. It is also possible that MYB97/101/120 transcriptional regulation of pollen tube-secreted proteins could be species-specific. The lack of positive correlation between secreted protein abundance and their corresponding transcripts could imply that transcriptional activation and protein secretion are regulated independently, which might influence protein/transcript detection and hence lack of correlation.

Further, a comparison with the protein families of the MYB97/101/120 downstream target genes classified as potentially secreted proteins [12] identified that three-quarters of them were in common with the tobacco SIV-PS. These include alpha carbonic anhydrase (in tobacco we identified beta carbonic anhydrase, Nt_000566), thionin (in tobacco cysteine-rich family proteins Nt_017951, *Q9SDN7-NtPs CRP2* (characterized in this study), Nt_013502) and GDSL-motif lipase/hydrolase (in tobacco we also identified GDSL-motif lipase/hydrolases Nt_021542, Nt_066702, Nt_015437, and Nt_001237). We did not detect a self-incompatibility (SI)-related protein identified in *Arabidopsis* but instead we identified two highly abundant secreted RNases (discussed in section "SP-containing proteins secreted following pollen tube– pistil interaction) that are also involved in self-incompatibility during pollen tube growth through the pistil. The identification of these common protein families between the tobacco pollen tube secretome and the downstream targets of *Arabidopsis* MYB97/101/120 in SIV pollen tubes suggests that pollen tube perception of female guidance signals, recognition of pollen tube arrival by the female, and the ability of pollen tubes to respond to these signals is likely conserved in both species.

In silico classification of pollen tube-secreted proteins and their post-translational modifications

Conventionally secreted proteins contain a short N-terminal signal peptide (SP) [24] and are secreted through the ER–Golgi–TGN pathway. In silico analysis using the SignalP-TM prediction database [25] of protein groups with three or more peptides and up-regulated by threefold or more relative to the median of the two control samples, revealed that 15.69 % of the pollen tube-secreted proteins possessed an N-terminal SP (Additional file 9: Figure S4a). Analysis using the SecretomeP server [26] further supported that > 85 % of the SIV secretome likely constitutes true secreted proteins (Additional file 9: Figure S4a). To rule out their possible retention on the ER membrane system, we manually scanned for the presence of ER-retention motifs (HDEL/KDEL) using ProSite scan [27]. None of the accessions were found to possess likely functional HDEL/KDEL core motifs, signifying their secretion towards the plasma membrane and the extracellular matrix. Analysis of the remaining non-SP-containing proteins intriguingly highlighted > 57.18 % as potential unconventionally secreted pollen tube proteins (Additional file 9: Figure S4a) [28]. This high proportion of unconventionally secreted proteins suggests that the unconventional protein secretion pathways could be the predominant mechanism for pollen tube protein secretion.

Next, we assessed the possibility of post-translational modifications of the identified secreted proteins. ER–Golgi–TGN-secreted proteins are known to commonly undergo post-translational N-linked glycosylation within the tripeptide Asp-Xaa-Ser/Thr sequon [29]. Using the NetNGlyc v1.0 [29] and GPP [30] databases, we revealed that 81.33 % of the conventionally secreted proteins and, unexpectedly, 41.30 % of the unconventionally secreted proteins were predicted to be N-glycosylated (Additional file 9: Figure S4a). We confirmed glycosylation of pollen tube secreted proteins by concavalin A glycoprotein staining, which demonstrated that a subset of the pollen tube secretome underwent N-glycosylation (Additional file 9: Figure S4e).

We then investigated post-translational palmitoylation of the pollen tube-secreted proteins. Palmitoylation is the

Hafidh et al. Genome Biology (2016) 17:81

Page 8 of 29

covalent attachment of palmitic acid, most frequently at a cysteine residue, to enhance protein hydrophobicity and affinity for the plasma membrane. Interestingly, 71.76 % of conventionally and 40.12 % of unconventionally secreted proteins were predicted to be palmitoylated (Additional file 9: Figure S4a). Additionally, 14.75 % of the conventionally secreted proteins were predicted to be post-translationally modified at the C-terminal ω-site for glycophosphatidylinositol (GPI)-anchoring (Additional file 9: Figure S4b). Surprisingly, the majority (61 %) of the predicted GPI-anchored proteins (GAPs) were also predicted to undergo palmitoylation. One possible explanation for this unexpected observation is that a subset of proteins destined to the plasma membrane but lack transmembrane helices (TMHs) could be palmitoylated to enhance their affinity for the lateral plasma membrane and thereafter anchored to the plasma membrane potentially with the GPI motif. We therefore investigated whether pollen tube-secreted proteins possess class I or class II TMHs. Using TMHMM v2.0 algorithms, our analysis revealed no reliable prediction for the presence of TMHs in both conventionally (average of 11.03 amino acids in TMHs) and unconventionally secreted proteins (average of 1.23 amino acids in TMHs) (Additional file 10: Figure S5a). In comparison, TMH prediction with known pollen tube plasma membrane signaling proteins (ACA9, PRK2, PRK4, ANX1, and ANX2) revealed an average score of 70.49, verifying confidence in the algorithms used for prediction of TMHs (Additional file 10: Figure S5a). A similar test with LIP1/2 (Loss in pollen tube guidance 1/2 receptor kinases) [31], which localizes to the pollen tube plasma membrane only through palmitoylation, showed an average score of zero (Additional file 10: Figure S5a). We concluded that pollen tube-secreted proteins are less likely to posses TMHs; instead, putative pollen tube receptor proteins could function through transient anchors on the plasma membrane following post-translational modification and secretion.

Subcellular localization of pollen tube-secreted proteins

We used LocTree2 prediction algorithms with a precomputed kernel matrix in support vector machine learning (SVM) and implemented tree-like hierarchy subcellular protein sorting to assess the subcellular localization of the pollen tube-secreted proteins [32]. Approximately 68.5 % of SP-containing proteins were classified as secreted and a further 16.5 % as localizing in secretory compartments, including the ER lumen, Golgi apparatus, vacuole, and plasma membrane, accounting for a total of 85 % as secreted with a reliability index score of 60.1 (Additional file 9: Figure S4c). Intriguingly, LocTree2 predicted 13.7 % of the unconventionally secreted proteins as secreted and an additional 7.1 % that were destined to be in or transported through

secretory compartments (Additional file 9: Figure S4c). The majority of the unconventionally secreted proteins (> 42.9 %) were predicted to localize to the cytoplasm (Additional file 9: Figure S4). However, the term "cytoplasm" was secondarily associated with GO terms secretory granules, extracellular space, Golgi intermediate, membrane bound vesicles, mitochondrion, nucleus, and protein complexes, among others. Independent analysis using TargetP1.1 [33] showed that over 94 % of the SP-containing proteins were predicted as secreted (p > 0.95; Additional file 10: Figure S5b). Only 6.5 % of unconventionally secreted proteins were classified as secreted. Nonetheless, 58.5 % of the unconventionally secreted proteins were classified as "ambiguous localization" (Additional file 10: Figure S5b). The "ambiguous" domain is derived from the lack of significant differences between the specificity scores for different subcellular compartments [33]. Therefore, our observation suggests that the identified unconventionally secreted proteins are less likely to be truly retained cytosolic proteins; instead, they could utilize as yet unknown features for their secretion.

Analysis of enriched GO terms associated with the predicted subcellular localization revealed predominant protein secretion by the pollen tube to the extracellular space and less frequently protein retention in secretory pathways, the ER, and vacuoles (Additional file 10: Figure S5c). These results support our earlier observations that the identified secreted proteins lack ER-retention signals and transmembrane domains (Additional file 10: Figure S5a).

GO-slim term enrichment analysis revealed the terms signaling, post-translational protein modification, response to stimulus, small molecule metabolic process, GTPase activity, calcium and copper ion binding, endopeptidase activity, hydrolase and redox activities, as well as intracellular membrane transport to be enriched in the pollen tube secretome (Additional file 11: Figure S6a). Interestingly, the categories "proteins anchored to membrane" and "serine-type endopeptidase inhibitor activity" were the most enriched in conventionally secreted proteins, whereas defense response, L-ascorbate peroxidase activity, cell redox homeostasis, and calcium ion binding were the most enriched terms of the unconventionally secreted protein subgroup. A full list of pollen tube secretome enriched GO terms is presented in Additional file 8: Table S5.

Identification of predicted palmitoylated and GPI-anchored secreted proteins as potential pollen tube transient receptors

We searched our pollen tube secretome for putative pollen tube-secreted receptors. Since secreted proteins should not possess transmembrane helices, we searched for secreted proteins predicted to be palmitoylated and

Hafidh *et al. Genome Biology* (2016) 17:81

Page 9 of 29

those with a plasma membrane GPI anchor and ω-site with a cutoff false discovery rate (FDR) of 0.1 %; 14.75 % were predicted to be bona fide GAPs (Additional file 9: Figure S4b). Among the reliably predicted secreted GAPs were LORELEI-like GPI anchored protein 3 (LLG3, 97 ppm), lipid transfer protein (18 kDa LTP, Nt_005942, 4590 ppm), a 24 kDa unknown protein (Nt_002352, 24 ppm), 19 kDa nsGRP-2 (Nt_058890, 198 ppm), 29 kDa plasmodesmata callose-binding protein 3 (29 kDa PDCB3, Nt_004725, 258 ppm), 26 kDa glycosyl hydro-lase family 17 protein (Nt_031990, 954 ppm), glycosyl phosphatidylinositol-anchored lipid protein transfer 1 (LTPG1, Nt_003387-2, 397 ppm) and 20 kDa NtEPc-like protein (Nt_051987, 578 ppm). Notably, NtEPa–c were previously purified as markers for the embryo-genic dedifferentiation of immature tobacco pollen grains cultivated in vitro [34].

Intriguingly, we observed that 61.7 % of the predicted GAPs were also predicted to be palmitoylated. The pal-mitoylation could increase affinity for the plasma mem-brane and the GPI modification is likely to mediate anchoring to the outer face of the plasma membrane. We cautiously propose that some of these predicted pal-mitoylated GAPs are potential pollen tube transient re-ceptors that could facilitate signal perception by binding ligands secreted by female reproductive tissues.

Pollen tube-secreted kinases and cysteine-rich proteins as putative carbohydrate modifiers and signal transducers

We searched for kinases among the pollen tube-secreted proteins as putative modifiers of carbohydrates in the extracellular matrix. Modified carbohydrates could function as ligands for some protein receptors. The most abundant kinases identified were phospho-glycerate kinases, hexokinases, fructokinases, adenylate kinases, and pyruvate kinases. Three phosphoglycerate kinases, Q42962 (2354 ppm), Nt_011032 (2130 ppm) and Nt_008716 (1948 ppm) containing the phosphoglyc-erate kinase domain at the C-terminus were predicted to be secreted through the unconventional secretion path-way. Other kinases included a PfkB-type carbohydrate kinase family protein (Nt_054946, 498 ppm), UMP-CMP cytidylate kinase (PYR6; Nt_001852; 497 ppm), SHV3-like 4 glycerolphosphodiester kinase (Nt_053416, 162 ppm) and adenosine kinase (Nt_046116, 24 ppm). The PfkB kin-ase contains the PfkB domain and ribokinase domain whereas PYR6 contains a P-loop NTPase domain and cytidylate kinase domain.

Cysteine-rich proteins (CRPs) have also been discovered to function as ligands during signal transduction. Some of the CRPs detected in SIV-PS samples included OTU-like cysteine protease family protein (Nt_006421, 104 ppm), cysteine-rich proteins (Nt_017951, 396 ppm and Nt_013502, 57 ppm), NRCL4 (Nt_029302, 76 ppm), and a

cysteine proteinase inhibitor (Nt_051779, 97 ppm). The full list is searchable in Additional file 3: Table S1.

SP-containing proteins secreted following pollen tube–pistil interaction

Approximately 16 % of the pollen tube secretome is comprised of SP-containing proteins (Additional file 9: Figure S4a). These include two highly abundant RNases belonging to the RNase T2 family. The T2 family S-RNases are female determinants of self-incompatibility in the Solanaceae, Rosaceae, and Scrophulariaceae, whereas S-locus F-box (SLF)/S-haplotype-specific F-box proteins are male determinants of self-incompatibility within these families [35]. Pollen tube-secreted RNase NE (Q40382, 234 ppm) and RNase1 (Q9MB71, 317 ppm) were both detected in both pollinated and unpollinated pistils but convincingly absent in SIV pollen tube total proteomes. More interestingly, both RNases were not present in the in vitro pollen tube secretome or total pollen tube pro-teomes (Additional file 3: Table S1 and Additional file 7: Table S4). NtRNase1 shares 99.53 % identity with *Nicoti-ana tomentosiformis* extracellular ribonuclease LE-like (XM_009627901.1) and RNase NE shares 83.5 % identity with *Solanum lycopersicum* extracellular ribonuclease LE of the T2 family. Moreover, NtRNase1 and RNase EN show 62.3 % similarity with PD1, an S-like ribonuclease from *Prunus dulcis* (Additional file 12: Figure S7a). To establish the origin of the detected pollen tube-secreted RNases, we performed semi-quantitative RT-PCR analysis and observed that both NtRNase1 and RNase EN were specifically expressed in unpollinated and pollinated stig-mas and style of *N. tabacum* (14 h post-pollination) but absent in in vitro grown pollen tubes 24 h after germin-ation (Additional file 12: Figure S7b). Since *N. tabacum* is a self-compatible species, our results indicate that pollen tubes grown through the pistil uptake secreted RNases [36, 37] from transmitting tract extracellular matrix and secrete them out in cases of matching S-allele haplotypes, supporting the inhibitory model of self-compatibility/in-compatibility [36, 37].

Another conventionally secreted protein identified was 11.7 kDa tobacco cysteine-rich defensin-like protein, here annotated as *N. tabacum* Pollen tube-secreted cyst-eine rich protein 1 (NtPsCRP1). NtPsCRP1 belongs to the subgroup of the DEFL family with CSαβ and γ-core motifs, similar to TfCRP1 (LURE1), TfCRP2, and TfCRP3 (LURE 2) identified in *T. fournieri* [3]. NtPsCRP1 is closely related to TfCRP1 and TfCRP3, with eight conserved cysteine residues and an N-terminal signal peptide (Additional file 12: Figure S7c, d). Moreover, NtPsCRP1 was only detected in the SIV-PS samples and not in unpollinated pistil controls. Further, NtPsCRP1 expression is enriched in SIV pollen tubes but also occurs in unfertilized ovules as verified by

Hafidh *et al. Genome Biology* (2016) 17:81

Page 10 of 29

semi-quantitative RT-PCR analysis (Fig. 1g). We also detected secretion of another CRP of 8.3 kDa (Q9SDN7, 295 ppm) that possessed six conserved cysteine residues in its mature form and was specifically secreted in pollinated pistils. It belongs to the pollen allergen Ole-e-6 superfamily and has 98.6 % homology to NtP-CysR, a *N. tabacum* pollen CRP corresponding to a 63 amino acid secreted protein precursor enriched in olive pollen [38]. We annotated this protein as *N. tabacum* Pollen tube-secreted cysteine rich protein 2 (NtPsCRP2). Semi-quantitative RT-PCR analysis revealed a slightly higher expression of NtPsCRP2 in pollen tubes relative to unfertilized ovules (Fig. 1g).

Other conventionally secreted proteins detected were enzymes involved in carbohydrate metabolism predicted to be involved in cell wall modification. These include beta-expansin-like protein (Nt_065866 422 ppm), pectinesterase (K4AWN9, 1084 ppm), and P18 with putative pectinesterase activity (O65849, 1769 ppm). Detected cell wall proteoglycans, arabinogalactan proteins (AGPs), included fasciclin-like arabinogalactan protein 14 (FLA14; Nt_005615; 3478 ppm), FLA3 (Nt_016813, 3115 ppm), FLA2 (Nt_002342, 116 ppm), FLA8 (Nt_002342, 257 ppm), and UDP-arabinopyranose mutase 2-like (UPI00032A57BC, 590 ppm) as unconventionally secreted proteins. Several extensin-like proteins were also identified, including pollen-specific leucine-repeats extensin-like protein (UPI0002339BC6, 155 ppm) and 120 kDa pistil-extensin-like proteins (PELP, Q49I34, 115 ppm). Pistils-extensin-like proteins were classified as major components of the transmitting tract extracellular matrix [39, 40]. PELPIII was recently demonstrated to be essential for interspecific incompatibility in *N. tabacum* by inhibiting interspecific pollen tube growth [41], whereas Pex1 was identified as a pollen-specific extensin in *Zea mays* that is secreted and glycosylated [42] and functions as a male factor in pollen tube growth through the transmitting tract [43].

Conventionally secreted proteins predicted to function in pollen tube guidance and directional growth were also detected, in particular members of the plant lipid transfer protein (LTP) family. These include non-specific lipid-transfer proteins NtLTP1 (Q42952, 660 ppm), NtLTP3 (F2ZAM0, 142 ppm), and NtLTP5 (Q6E0U9, 142 ppm) (Additional file 3: Table S1). Plant LTPs and LTP-like proteins were implicated in diverse extracellular functions, including anti-fungal and anti-microbial activities, cuticular wax deposition, and cell wall loosening [44]. We have also detected lipid-binding proteins such as the annexin calcium-dependent phospholipid binding protein AN2 (Nt_004158, 134 ppm). Other novel conventionally secreted proteins with potential roles as pollen tube-guidance proteins included luminal binding protein 5 (Q03685, 525 ppm), peptidyl-prolyl cis-trans isomerase (B2BF99, 227 ppm), endoplasmic reticulum HSC70-cognate binding protein (685 ppm), proteinase inhibitor (Q84L56, 58 ppm), and tobacco NTS1 protein (Q9FV64, 1405 ppm).

The LAT52-PRK2/PRK4 receptor kinase module could function late in pollen tube signal perception

We detected secretion of the CRP LAT52 (Nt_005952; 21394 ppm; a representative accession) from the Ole e I family in SIV-PS samples 48 h post-pollination and *Lb*LAT52-like small protein (H6VN37, 88 ppm) from *Lycium barbarum* (91 % identity) in the unpollinated pistil control (Additional file 3: Table S1 and Additional file 13: Figure S8e–g). The detection of *Lb*LAT52-like small protein in unpollinated pistils is likely due to peptide homology (detected as a single unique peptide that shared homology with LAT52 from *S. lycopersicum*) rather than true secretion from the pistil tissues. The interaction of LAT52 with its plasma membrane receptor kinases, the PRK2 and PRK4 ligand–receptor complex, is known as an essential endocrine module that promotes pollen germination and pollen tube growth [10]. LAT52 was detected in all four replicates of both SIV and in vitro pollen tube secretomes as well as in their respective total proteomes (Additional file 3: Table S1 and Additional file 7: Table S4). Contrarily, PRK2 and PRK4 were not detected in any of the secretome samples nor in the total proteome samples, verifying the high purity of the secretome samples. Lack of their detection in the total proteomes is likely due to a generic protocol used for total protein extraction rather than a membrane protein enrichment protocol. Analysis of their expression using microarray data and by RT-PCR revealed abundant expression of PRK2 and PRK4 receptor kinases specifically in mature pollen grains, in vitro cultivated pollen tubes after 4 h and 24 h, as well as SIV pollen tubes of *Arabidopsis* and tobacco (Additional file 13: Figure S8f,g). We could not detect expression of PRK2 or PRK4 in unfertilized ovules of *N. tabacum*, implying conserved male gametophyte-specific expression (Additional file 13: Figure S8g); both genes were also not expressed in the sporophyte (Additional file 13: Figure S8F,G). We propose that the detection of pollen tube-secreted LAT52 ligands and expression of PRK2/4 receptors (Additional file 13: Figure S8h) late during tobacco pollen tube growth suggests a likely continuous function of the LAT52–PRK2/4 complex module, either to quench or to establish homeostasis with PRK-RopGEF-promoted activities or to perform an as yet unknown role in male–female signal perception.

Hindrance of the N-terminal SP impairs secretion of pollen tube EIG-E80 protein to the apoplast of leaf epidermal cells

To demonstrate utilization of the N-terminal SP motif for the conventional secretion of pollen tube proteins in

Hafidh *et al. Genome Biology* (2016) 17:81

Page 11 of 29

a heterologous system, we selected NtPsCRP2 and elicitor-induced protein E80 (EIG-E80) to assess their subcellular localization with a blocked N-terminal SP (Fig. 4). Transient expression in tobacco leaf epidermal cells revealed unambiguous secretion of NtPsCRP2 to the proximity of the plasma membrane and EIG-E80 to the apoplast (Fig. 4a, b, g, h). We verified their respective localizations by plasmolysis and co-expression of viral apoplastic protein AVR2-mCherry (Fig. 4c–f, l–o). We then restructured the EIG-E80 protein conformation by masking its N-terminal SP through C-terminal green fluorescent protein (GFP) fusion (Fig. 4i). Protein topology analysis predicted extracellular localization for both conformations of the EIG-E80 protein (Fig. 4g, i). Remarkably, the restructured GFP–EIG-E80 chimeric protein failed to be secreted effectively to the apoplast, instead predominantly accumulated into the nucleus (Fig. 4j, k). These results demonstrate the significance of the SP position in directing protein entry into the secretory pathway. A weak signal was still observed in the apoplast, suggesting partial secretion. The ectopic expression of selected pollen tube-secreted proteins in leaves of *Nicotiana benthamiana* was verified by western blot analysis (Fig. 4t). We concluded that these identified proteins posses functional SP and are likely to utilize the ER–TGN secretion pathway, providing indirect evidence for their secretion from the pollen tubes during a crosstalk with the female reproductive tissues.

NtPsCRP2 is associated with dynamic Golgi-derived vesicles in close proximity of the plasma membrane

The near-plasma membrane localization of NtPsCRP2-GFP in leaf epidermal cells prompted us to investigate the exact pathway for its secretion. We co-expressed NtPsCRP2-GFP in leaf epidermal cells with an ER retention marker, HDEL-mCherry, under the CaMV 35S promoter. NtPsCRP2-GFP distinctly decorated the ER lumen and co-localized with the HDEL-mCherry, supporting NtPsCRP2 ER localization (Fig. 5a, a-i). Additionally, NtPsCRP2-GFP formed GFP foci that did not co-localize with the ER retention marker (Fig. 5a a-ii,). When we co-expressed NtPsCRP2-GFP with an early ER–Golgi marker, GmMan1-mCherry derived from soybean [45], a clear overlap of 77 % ($n = 340$ confocal slices) was observed, suggesting NtPsCRP2 is translocated from the ER to the Golgi and TGN (Fig. 5b, b-i). Furthermore, NtPsCRP2-GFP;GmMan1-mCherry-associated Golgi-derived vesicles showed stop-and-go, unidirectional, non-zigzag, cycling movements along the proximity of the plasma membrane (Fig. 5f). We observed dynamic GmMan1-labeled vesicles alone as well as NtPsCRP2-GFP-loaded GmMan1-mCherry vesicles (Fig. 5f). Our observations suggest a common route for NtPsCRP2 delivery via Golgi-derived vesicles to the plasma membrane and recycling of unloaded vesicles. We have identified similar NtPsCRP2 stop-and-go cycling movements in root epidermal cells of *Arabidopsis thaliana* (Additional file 14: Figure S9a, b, Additional file 15: Movie S1, and Additional file 16: Movie S2). The rationale for such NtPsCRP2-GFP;GmMan1-mCherry vesicle movements is still unclear, and whether actin and microtubule dynamics are involved in implementing such movements.

Unconventionally secreted proteins are the dominant class of pollen tube-secreted proteins following pollen tube–pistil interaction

In our SIV-PS, 57 % of the secreted proteins identified were predicted to be unconventionally secreted proteins. Secreted proteins without the canonical N-terminal SP have been identified in animals and yeast but very few have been reported in plants [28, 46, 47]. In *Arabidopsis*, 18 % of its total proteome is predicted to be secreted and 40–70 % of the proteins identified in secretome studies do not contain the N-terminal SP [48]. We identified unconventionally secreted pollen tube proteins with sizes ranging between 5.4 and 138 kDa, with the most predominant class being 20–50 kDa (50.2 %), followed by proteins of < 20 kDa (24 %) (Additional file 3: Table S1, Additional file 8: Table S5, and Additional file 17: Table S6). In comparison, the size of conventionally secreted proteins ranged between 8.4 and 105 kDa and were also predominately 20–50 kDa (40.1 %) and those < 20 kDa (9.1 %) (Additional file 3: Table S1, Additional file 8: Table S5, and Additional file 17: Table S6). Some selected unconventionally secreted pollen tube proteins identified included glyceraldehyde 3-phosphate dehydrogenase (H9U034, 312 ppm), dihydrolipoyl dehydrogenase from *S. lycopersicum* (Q6QJL7, 2401 ppm), elicitor inducible (EIG-I24) tobacco gene (Q9FXS7, 235 ppm), ubiquitin fold-modifier (G7K8X5, 237 ppm), and pollen-specific actin-depolymerizing factor 1 (Q8H2B7, 104 ppm); for the complete list see Additional file 3: Table S1 and Additional file 8: Table S5. Our observations imply that unconventional secretion might be a default or dominant secretory pathway in growing pollen tubes. We hypothesize that some of the major pathways for unconventional protein secretion (including soluble cytosolic proteins) in pollen tubes is through multivesicular bodies and translocation into exosomes to reach the plasma membrane, apoplast, and the extracellular matrix.

Unconventionally secreted pollen tube protein TCTP remarkably finds entry into the ER and Golgi and co-localizes with the Ole1 exosome marker

The multiple pathways for unconventional protein secretion have largely remained undefined. To demonstrate unconventional protein secretion and define the pathway
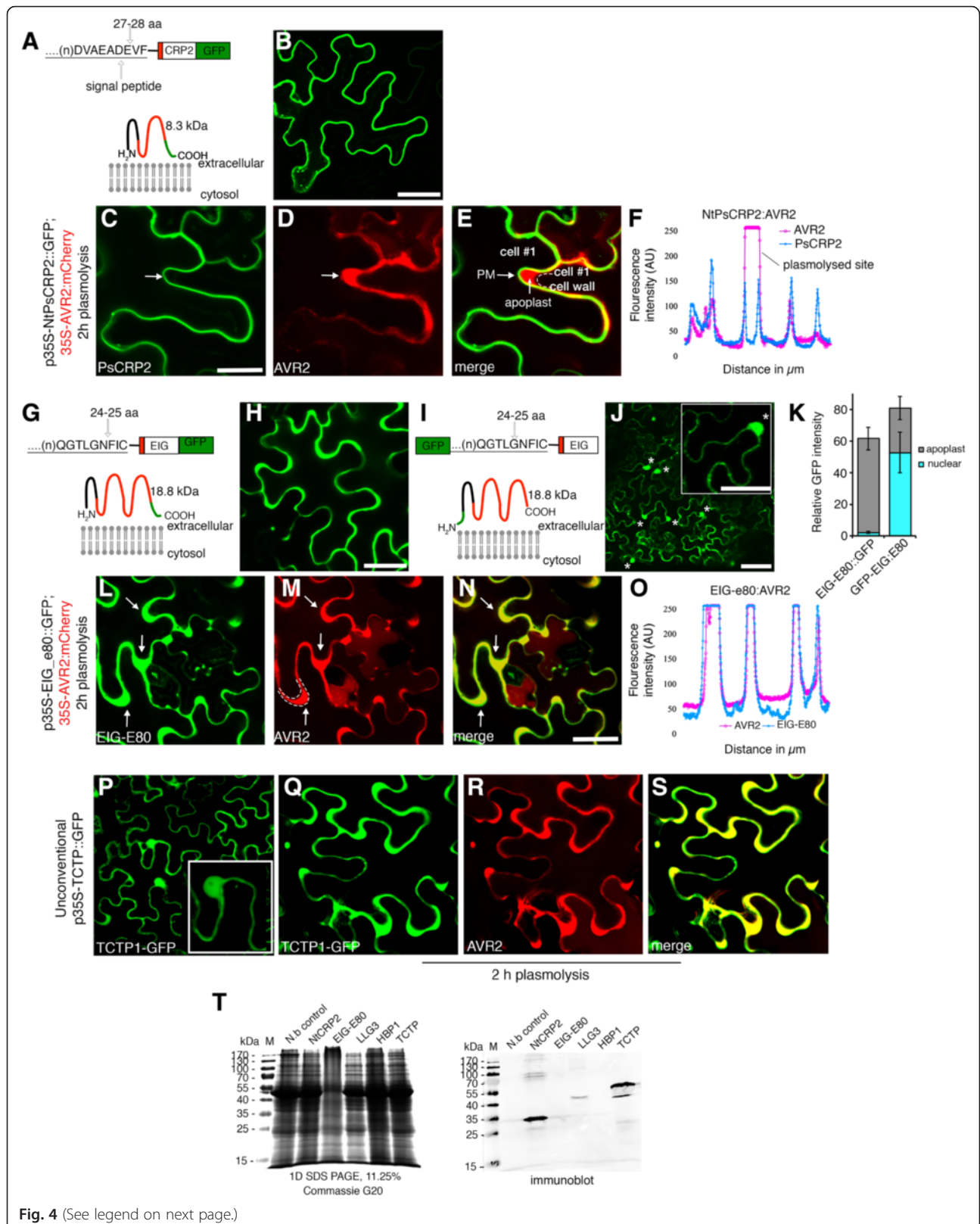
Hafidh *et al. Genome Biology* (2016) 17:81

Page 12 of 29

Fig. 4 (See legend on next page.)

Hafidh *et al. Genome Biology* (2016) 17:81

Page 13 of 29

(See figure on previous page.)

Fig. 4 Interference of the N-terminal signal peptide compromises apoplastic localization of the EIG-E80 pollen tube-secreted protein. Secretion of pollen tube-secreted proteins to the proximity of the plasma membrane and the apoplast of tobacco leaf epidermal cells is signal peptide-dependent. **a, b** Chimeric construct of pollen tube-secreted cysteine-rich polypeptide protein 2 (NtPsCRP2) and its predicted topology showing extracellular localization. **c–e** Verification of NtPsCRP2 localization near the plasma membrane (*PM*) by plasmolysis of tobacco epidermal cells co-infiltrated with apoplastic viral AVR2-mCherry. The *arrow* shows plasmolyzed regions with detached plasma membrane and apoplastic localized PR1a-AVR2-mCherry. **f** Two-channel confocal laser scan profile during co-localization of NtPsCRP2 with apoplastic marker AVR2-mCherry following plasmolysis. *AU* arbitrary units. **g, h** Chimeric construct of elicitor-induced protein E80 (EIG-E80) and its predicted topology showing apoplastic/extracellular localization. **i, j** Reconstituted GFP:EIG-E80 chimeric construct with blocked signal peptide resulted in partial apoplastic localization and predominant nuclear localization instead. **k** Subcellular quantification of the modified GFP:EIG-E80 expression. Error bars represent ± standard deviation. **l–o** Verification of EIG-E80:GFP apoplastic localization by plasmolysis with viral AVR2 apoplastic marker. *Arrows* indicate plasmolysed regions. **p** Localization of the unconventionally secreted tobacco pollen tube protein Translationally controlled tumor protein (TCTP) showing nucleoplasm, cytosol, and apoplastic localization. **q–s** Verification of TCTP apoplastic localization. **t** Immunodetection verification of ectopically expressed GFP chimeric pollen tube-secreted proteins with rat anti-GFP monoclonal antibodies in tobacco epidermal cells. Commassie G250 stain of total protein extract (*left*) and immunoblot (*right*) 48 h post-infiltration. Scale bars = 10 μM. *N.b* untransformed Nicotiana benthamiana

of secretion, we chose a leaderless secreted protein, translationally controlled tumor protein (NtTCTP), based on its lack of a predicted N-terminal SP, its ambiguous localization prediction, the prediction that it is secreted by secretomeP (neural network (NN) score = 0.6), its absence of transmembrane helices, and the prediction that it resides "outside" with highly hydrophobic residues (Additional file 13: Figure S8). NtTCTP is an 18.7 kDa protein containing a pfam TCTP domain that is similar to *Arabidopsis* TCTP/TCTP2 (Additional file 13: Figure S8). Using an in silico approach, TCTP was predicted to localize in the cytosol and be associated with the GO terms multivesicular bodies and extracellular space. We expressed NtTCTP-GFP under the CaMV 35S promoter and observed that NtTCTP localizes to the apoplast as well as the cytosol and the nucleoplasm of tobacco leaf epidermal cells (Fig. 4p–s). We verified the apoplastic localization by plasmolysis and co-expression with viral AVR2-RFP apoplastic protein (Fig. 4p–s). Next, we co-expressed NtTCTP with ER and ER–TGN markers. Remarkably, we observed that NtTCTP partially co-localized with the ER retention marker HDEL-mCherry in the ER lumen and ER lamina (Fig. 5c, c-i, d). Subsequently, NtTCTP co-expression with the soybean Golgi vesicle marker GmMan1-mCherry showed over 89 % co-localization (*n* = 296 confocal slices), suggesting that NtTCTP is translocated from the ER to Golgi vesicles (Fig. 5e, ei). These unexpected observations imply the existence of a non-canonical motif within the NtTCTP sequence (or the presence of an ER TCTP chaperon protein) that enables TCTP to enter the ER and progress through the Golgi and TGN secretory pathway.

We then assessed how NtTCTP could reach the apoplast. In mammals, TCTP accumulation is regulated at the transcriptional and translational levels through reciprocal repression with p53 [49]. In humans, TSAP6 facilitates the unconventional secretion of TCTP outside the cell to participate in inflammatory responses

[50]. Its secretion was not affected by brefeldin A (BFA) or monesin treatment and it localized in secreted nanovesicle exosomes [50]. We have used the Oleisin 1 (Ole1) protein from *Arabidopsis* as an exosome marker, a homolog of which was detected in secreted exosomes of olive pollen tubes [51]. Co-expression of NtTCTP-GFP with Ole1-mRFP in *N. benthamiana* leaf epidermal cells revealed a remarkable average overlap of > 75 % between NtTCTP-GFP-labeled granules and Ole1-mRFP-labeled granules (Fig. 5g, h). The identified exosome-like aggregates showed diverse morphological features, suggesting several levels of likely aggregation (Fig. 5g). Although independent verification of the NtTCTP association with exosomes will be necessary, our initial results nevertheless imply that NtTCTP could reach the apoplast via secreted nanovesicle exosomes. Remarkably, when we compared the proteome of secreted exosomes from olive pollen tubes [51] with our tobacco SIV secretome, we observed a significant 68.8 % (35/51) overlap, of which 94.3 % were unconventionally secreted proteins (Additional file 18: Table S7). It will be critical to confirm whether NtTCTP secretion to the apoplast is indeed mediated by nanovesicles and whether its infiltration into the conventional secretion pathway is a phenomenon shared with other unconventionally secreted proteins.

Secretion of NtPsCRP2 is partially compromised in TGN *yip4a-1;4b* double mutants

To provide genetic evidence of the pathway for NtPsCRP2 secretion as well as establish whether conventionally secreted pollen tube proteins follow a conserved pathway of secretion in the sporophyte, we ectopically expressed NtPsCRP2-GFP in *Arabidopsis yip4a-1;4b* double mutant plants. YIP4A and YIP4B are conserved YPT/RAB GTPase-interacting proteins that form a complex with ECHIDNA (ECH) at the TGN and participate in the recycling of RAB-GDP during retrograde vesicle assembly
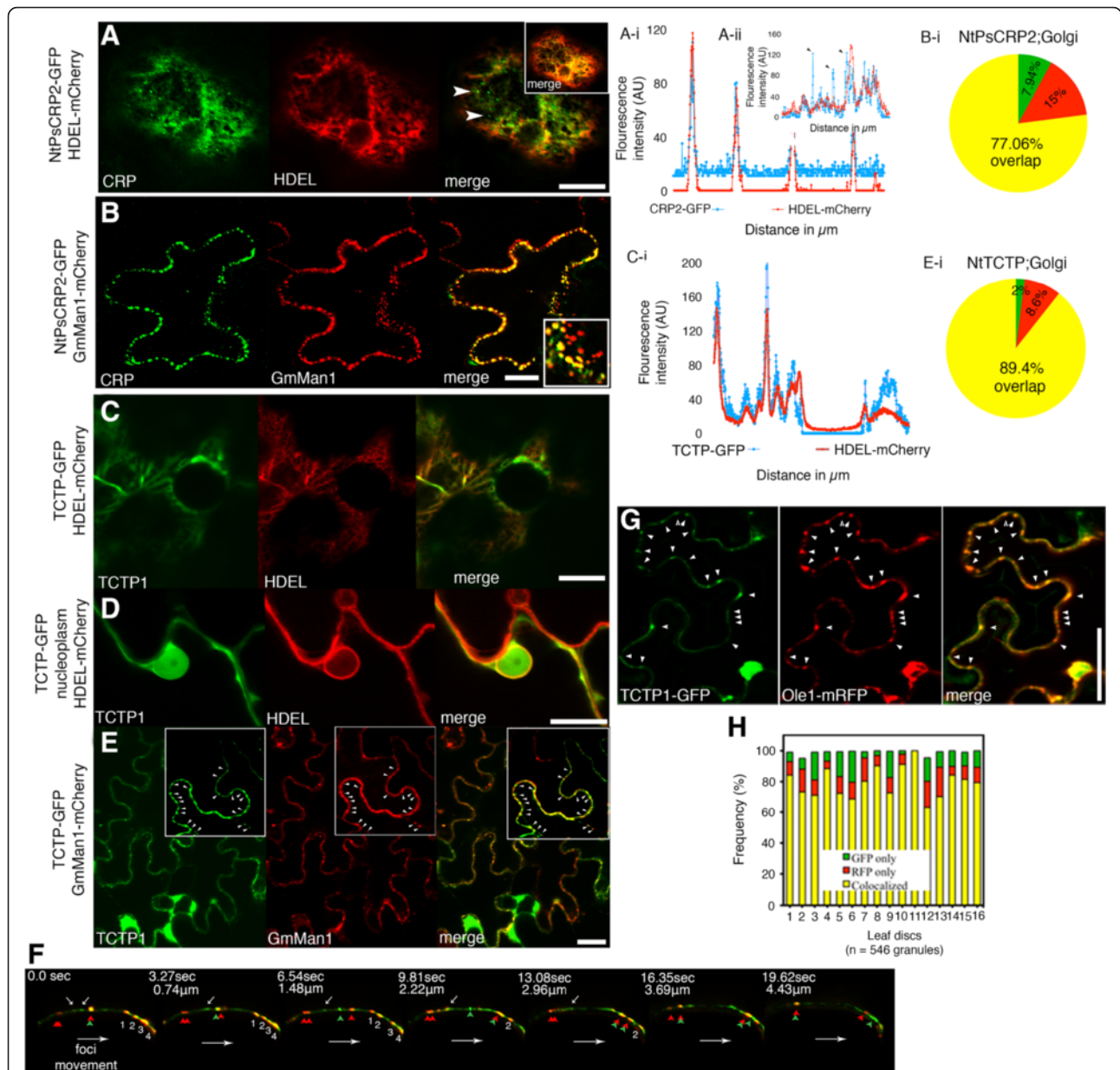
Fig. 5 NtPsCRP2 and unconventionally secreted NtTCTP enter the ER and co-localize with the Golgi marker GmMan1 and exosome marker Ole1. **a** Confocal micrographs showing co-localization NtPsCRP2-GFP with the ER retention marker HDEL-mCherry with the exception of GFP foci (*white arrowheads*). Two-channel profile overlap (*a-i*). Emphasis on the lack of complete overlap (*black arrowheads*) of ER-HDEL with NtPsCRP2-GFP foci (*a-ii*). **b** NtPsCRP2 co-localization with the ER–Golgi vesicle marker GmMan1-mCherry from soybean. Frequency of co-localization (29 confocal slices, n = 340) (*b-i*). **c** Co-localization of unconventionally secreted NtTCTP with ER HDEL-mCherry. Visualization of ER co-localization of NtTCTP by two-channel pixel-intensity profiling (*c-i*). **d** NtTCTP also co-localizes with the ER–nuclear lamina and is present in the nucleoplasm. **e** NtTCTP co-localization with the Golgi vesicle marker GmMan1-mCherry. *Arrowheads* indicate granules formed by TCTP-GFP and those by GmMan1-mCherry. **e–i** Frequency of overlapping foci observed in 32 confocal slices (n = 292). **f** Dynamics of NtPsCRP2-GFP foci (*green*) and Golgi-derived vesicles (*red*) in the proximity of the plasma membrane. The *top white arrows* point to tethered NtPsCRP2-GFP foci over time, the *red arrowheads* Golgi vesicles alone, the *green arrowheads* NtPsCRP2-GFP foci alone, and the *red-green arrowheads* co-localized NtCRP1-Golgi signals, and foci *1–4* are additional NtCRP1-Golgi co-localized vesicles migrating clockwise towards the membrane horizon over time. Note the appearance and disappearance of co-localized NtPsCRP2-Golgi vesicles as well as NtPsCRP2-GFP foci alone. Scale bars = 20 μM. **g** NtTCTP co-localized with Ole1 in potential nanovesicle exosomes. Co-expression of NtTCTP-GFP with AtOle1-mRFP in tobacco leaf epidermal cells revealed granular co-localizations (marked with *arrowheads*). **h** Frequency of co-localizations observed from multiple leaf discs. Scale bars = 10 μM, *RFP* red fluorescent protein

Hafidh *et al. Genome Biology* (2016) 17:81

Page 15 of 29

and plasma membrane vesicle tethering [52]. Knock-down of both isoforms perturbs ER–TGN protein secretion and causes severe defects in plant development [52]. At the root-hair maturation zone, NtPsCRP2-GFP localized in mature root hairs and rarely in root hair initials, both in wild type and in *yip4a-1;yip4b* seedlings (Fig. 6a–c). In hypocotyl epidermal cells of 4-day-old etiolated wild-type seedlings, secreted NtPsCRP2-GFP formed uniform spherically shaped aggregates likely derived from endomembrane compartments that were restricted at the stem–root junction (Fig. 6d, e). Conversely, in *yip4a-1;yip4b* double mutants, NtPsCRP2-GFP was localized in deformed, rod-shaped endomembrane compartments instead of the spherical endomembrane aggregates observed in the wild type (Fig. 6f–h). Further, at the stem–root junction, NtPsCRP2-GFP showed diffuse localization and non-uniform protein aggregates (Fig. 6g, arrowheads) that were not observed in wild-type seedlings. In roots, NtPsCRP2-GFP localized predominantly in the epidermal cell layer in uniform endomembrane/secretory vesicles at the root apex, root elongation zone, and root hair zone (Fig. 6i, j). Interestingly, in the epidermal cell layer at the root apical zone, NtPsCRP2-GFP localized in spindle-shaped ER-body-like structures (Fig. 6j, inset). Live cell imaging of epidermal cells at the root elongation zone at 16.7 and 2.7 seconds per frame revealed that NtPsCRP2-GFP-labeled vesicles displayed three main types of dynamic behaviour: (1) quiescent or permanently membrane-tethered vesicles; (2) membrane-tethered vesicles that re-initiated mobility; and (3) mobile vesicles followed by membrane tethering (Additional file 14: Figure S9). In *yip4a-1;yip4b* roots, NtPsCRP2-GFP localized in endomembrane aggregates that were not uniformly distributed and formed larger aggregates in epidermal cells that resembled BFA compartments (Fig. 6k, l). However, the NtPsCRP2 localization in spindle ER-body-like structures (Fig. 6k, arrow) was maintained. We independently observed similar secretion defects of NtPsCRP2-GFP in roots following 2-h treatment of 4–5-day-old seedlings with BFA or wortmannin drugs (Fig. 6m–o). Our observations emphasize that NtPsCRP2-GFP is secreted through the ER–TGN pathway in vegetative tissues and that the recycling of NtPsCRP2 secretion to the proximity of the plasma membrane and endocytic secretory vesicles is perturbed in *yip4a-1,4b* double mutant plants. Since NtPsCRP2 posses an N-terminal SP and is secreted by the pollen tubes, this suggests that the conventional pathway is conserved between the gametophytic and sporophytic tissues. Further, it is likely that NtPsCRP2 is maintained in the secretory pathway until the appropriate signal (likely derived from the female reproductive tissues) is perceived for its secretion to the extracellular matrix.

Secretion of LORELEI-like GPI-anchored protein 3 (LLG3) is perturbed in *yip4a-1;yip4b* pollen tubes

To provide evidence for pollen tube protein secretion among the identified candidate secreted proteins, we analyzed the subcellular localization of GPI-anchor protein LLG3 and its likely secretion pathway. We fused a genomic fragment (AT4G28280) of the *Arabidopsis* ortholog of *N. tabacum* LLG3, including its putative promoter, with red fluorescent protein (RFP) inserted 12 amino acids upstream of the predicted GPI-anchor site. Microarray analysis [53] identified *Arabidopsis* LLG3 to be predominantly expressed in pollen and pollen tubes with elevated expression in pistils 8 h after pollination (Additional file 19: Figure S10). Semi-quantitative RT-PCR results showed tobacco LLG3 to be expressed in SIV pollen tubes as well as in unfertilized ovules of *N. tabacum* (Fig. 1g). It is not clear if this differential expression of LLG3 between the two species is significant. Expression of chimeric proLLG3-LLG3:RFP-GPI anchor in *Arabidopsis* showed localization in distinct compartments in the cytosol of mature *Arabidopsis* pollen grains partially resembling the ER network (Fig. 7a). In *yip4a-1;4b* mature pollen grains, LLG3-RFP distribution showed a distinct vegetative cell "bird cage-like" polarised localization, suggesting perturbed secretion or localization of LLG3 (Fig. 7b). After 12 h of in vitro wild type pollen tube growth, LLG3-RFP-GPI localized in secretory vesicles, in the vegetative cell cytosol, and partially in the likely ER network (Fig. 7c). In contrast, in *yip4a-1;4b* mutant pollen tubes, LLG3-RFP-GPI distinctively localized in non-uniform, aggregated endomembrane-derived vesicles of variable sizes (Fig. 7c). However, the ER localization was not affected in the mutant background (Fig. 7c). Further, LLG3-RFP-GPI accumulated at the sub-apical domain, both in wild-type and in *yip4a-1;4b* mutant pollen tubes, but we could not observe localization at the pollen tube tip and the plasma membrane (Fig. 7d). In tobacco pollen tubes, LLG3-RFP-GPI as well as LLG3-GFP-GPI occasionally showed exclusive tip localization as well as granular formation in likely secretory vesicles (Fig. 7e). In the *Arabidopsis* female gametophyte, we could not detect LLG3-RFP-GPI expression in unfertilized ovules, although we rarely observed weak signal at the embryo-proper region approximately 18 h after pollination. Our results verify secretion by the pollen tube of candidate pollen tube-secreted proteins identified in this study and provide evidence for the requirement for YIP4A/4B isoforms for proper LLG3 secretion through the ER–TGN pathway during pollen tube growth.

The ER–TGN secretory mutant *echidna* is severely infertile, partly attributable to a lack ovule-targeting competence in the pollen tube

Since 15.95 % of the pollen tube secretome comprises proteins secreted through a conventional ER–TGN pathway, we investigated whether loss of ECHIDNA function, an
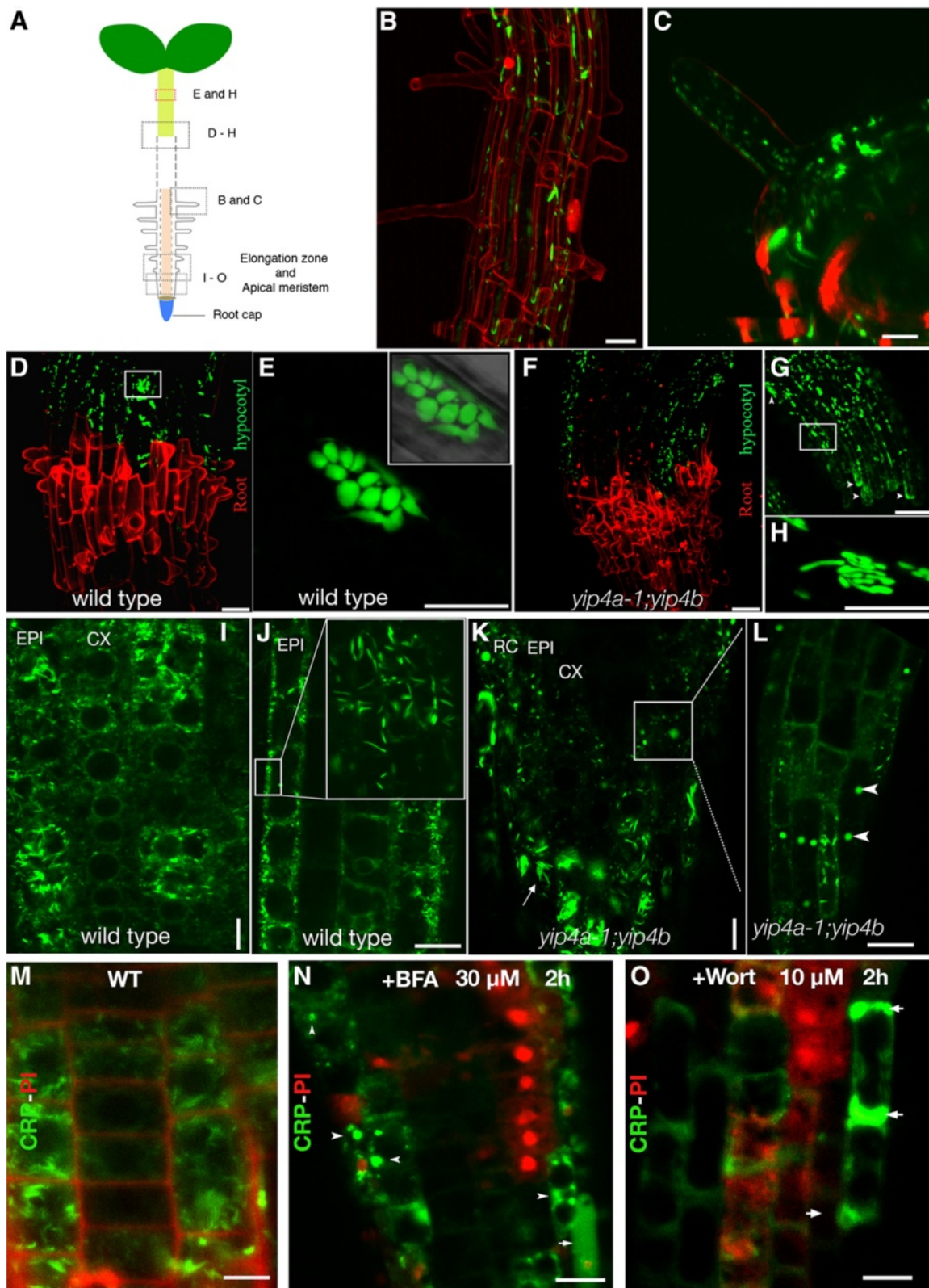
Hafidh *et al. Genome Biology* (2016) 17:81

Page 16 of 29

Fig. 6 (See legend on next page.)

Hafidh *et al. Genome Biology* (2016) 17:81

Page 17 of 29

(See figure on previous page.)

Fig. 6 Simultaneous knockdown of YIP4A/B perturbed NtPsCRP2 secretion in seedlings. **a** An *Arabidopsis* seedling showing regions analyzed in this study. **b, c** NtPsCRP2-GFP localized less frequently in young root hairs but more frequently in mature root hairs, both in the wild type and in the *yip4a-1;yip4b* double mutant. **d** NtPsCRP2 secretion in 4-day-old etiolated wild-type seedlings showing localization in epidermal cells of the hypocotyl. The secretion was restricted at the hypocotyl–root junction. Propidium iodide (*red*) marks the beginning of the root. **e** Close-up of NtPsCRP2-GFP in elongated epidermal cells of the hypocotyl showing accumulation in spherical, aggregated endosomal-like vesicles. **f, g** Conversely, in *yip4a-1;yip4b* seedlings, NtPsCRP2 secretion was severely distorted, showing diffuse localization and non-uniform protein aggregates (*arrowheads*). **h** The spherical marked endosomal aggregates observed in the wild type were substituted with rod-like labeled organelles in *yip4a-1;yip4b* hypocotyl. **i** NtPsCRP2 localization at the root tip of wild-type seedlings marking secretory organelles. *EPI* epidermis, *CX* cortex. **j** Magnified root epidermal cells from wild type showing NtPsCRP2-marked organelles constrained to the vicinity of the plasma membrane (*white rectangle*) and also localized in ER-body-like organelles (*inset*). **k, l** In *yip4a-1;yip4b*, NtPsCRP2-GFP localization in secretory organelles at the root apical meristem appeared largely disorganized, showing severe organelle aggregations resembling BFA-like compartments (*arrowheads*). The ER-body-like localization (*arrow*) was maintained, suggesting no effect on ER-body biogenesis in *yip4a-1;yip4b* mutants. **m–o** Perturbed secretion of NtPsCRP2-GFP was also recapitulated following BFA or wortmannin treatment. *Arrowheads* show NtPsCRP2-GFP BFA compartments, *arrows* point to diffusely aggregated NtPsCRP2-GFP aberrant secretion. *RC* lateral root cap *PI* propidium iodide stain, *WT* wild type. Scale bars = 10 μM
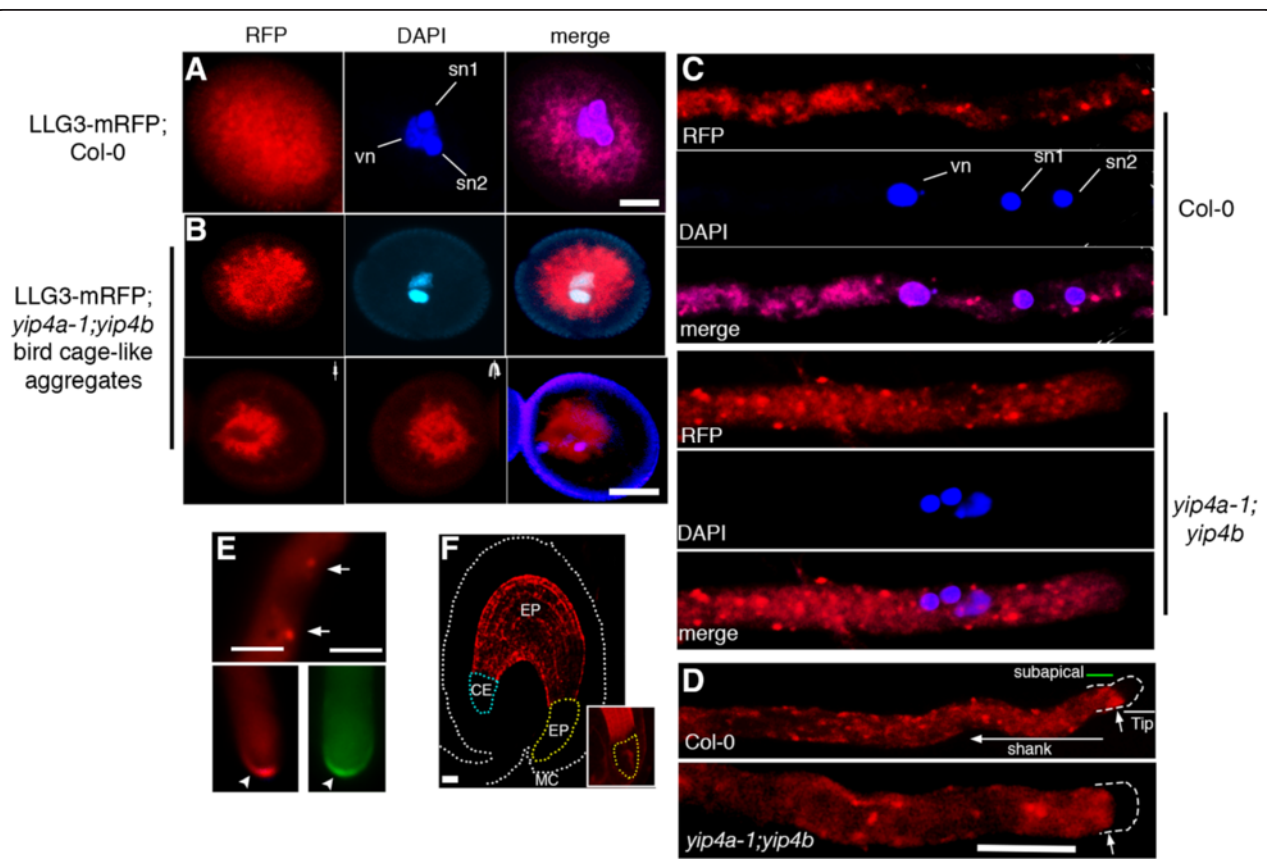

Fig. 7 LLG3 secretion is compromised in *yip4a-1;yip4b* mutant pollen and pollen tubes. **a** Subcellular localization of LLG3-mRFP under native promoter showing cytosolic foci-like aggregates. *vn* vegetative cell nucleus, *sn* sperm cell nuclei. **b** *Top*: in the *yip4a-1;yip4b* mutant, the majority of the pollen grains displayed distinct cytosolic aggregates different from those observed in the wild type. *Bottom*: z-stack projection of 25 confocal slices showing distinct vegetative cell "bird cage-like" localization that was not observed in wild-type pollen grains. **c** Localization of LLG3-mRFP in wild-type pollen tubes grown in vitro for 16 h showing localization in likely secretory vesicles of uniform size and partially in the pollen tube ER (*top three panels*). In contrast, *yip4a-1;yip4b* mutant pollen tubes displayed a significantly higher frequency of LLG3-mRFP-marked endomembrane aggregated vesicles of variable sizes (*bottom three panels*). However, the ER localization was not greatly affected. **d** LLG3-mRFP also specifically accumulated at the subapical domain (*top panel, arrow*). This accumulation was also not significantly affected in *yip4a-1;yip4b* mutant pollen tubes (*bottom panel*). **e** In tobacco pollen tubes, similar localization in secretory vesicles was also observed (*top panel, arrows*) and occasionally LLG3-mRFP as well as LLG3-sGFP showed pollen tube tip-specific localization (*bottom panels, arrowheads*). **f** Absence of LLG3-mRFP protein in *Arabidopsis* unfertilized ovules and embryos soon after fertilization (18 h after pollination). Rarely, LLG3-mRFP could be detected at the embryo proper (*EP*) zone in some fertilized ovules. *MC* micropylar, *EP* endosperm proper, *CE* chalaza end endosperm. Scale bars for **a** and **b** = 30 μM and for **c–e** = 10 μM

Hafidh *et al. Genome Biology* (2016) 17:81

Page 18 of 29

interaction partner of YIP4A/4B [54], would also compromise pollen tube–ovule crosstalk and ovule-targeting competence. Earlier observations revealed that *ech-/-* plants are male semi-sterile, producing only a handful of pollen grains with reduced viability and ability to grow pollen tubes [55]. Despite this, the study showed that >42 % of the tetrads from *ech-/-* plants had three to four viable pollen grains.

Moreover, *echidna* mutation can be propagated as homozygous, indicating that some *echidna* pollen grains can germinate a pollen tube and undergo fertilization with *echidna* mutant ovules. Here, we have also shown that *ech-/-* pollen grains can germinate pollen tubes in vitro as well as semi-in vivo, although at a reduced growth rate compared with wild-type pollen tubes (Fig. 8a, b). We have independently
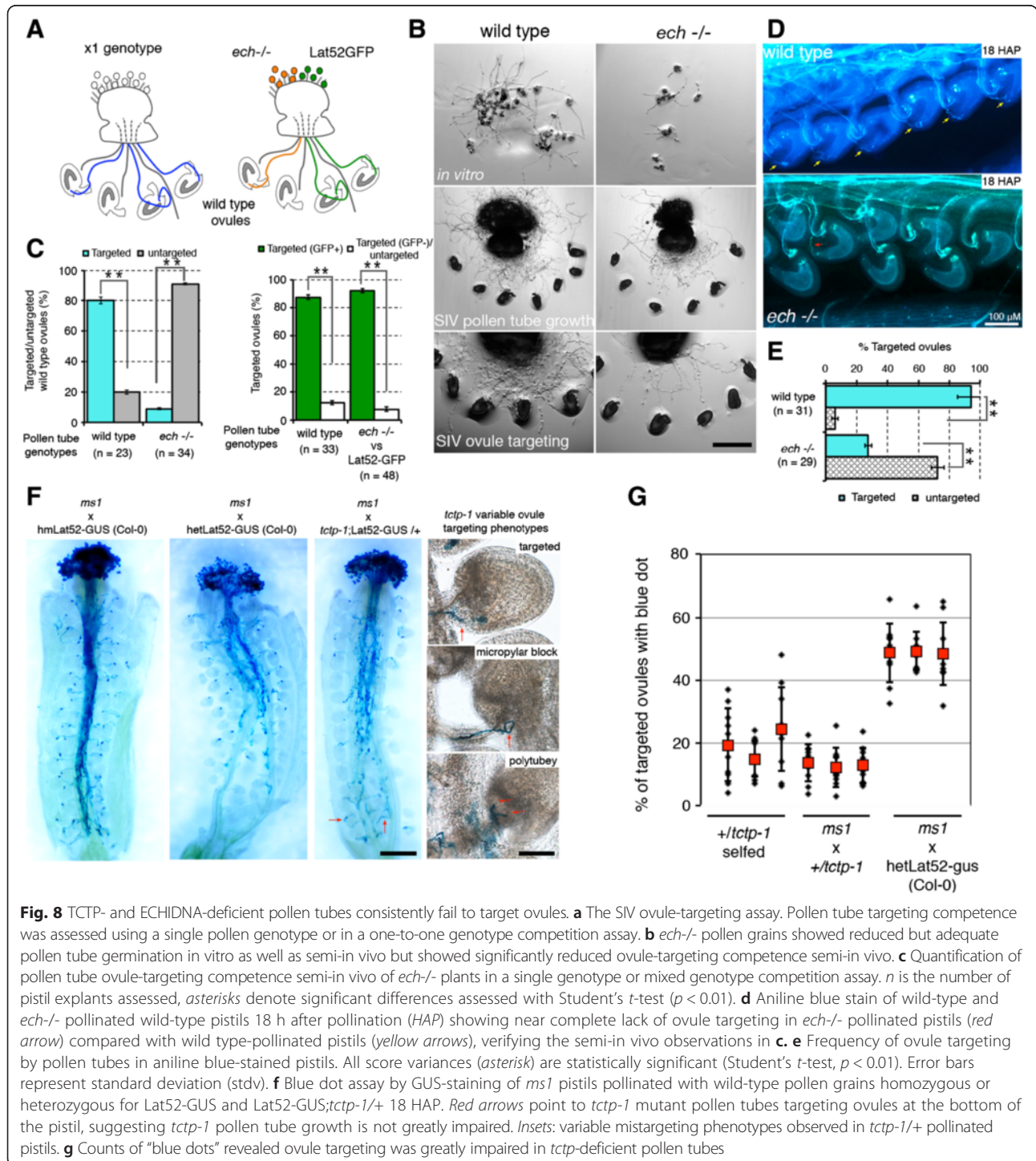

Fig. 8 TCTP- and ECHIDNA-deficient pollen tubes consistently fail to target ovules. **a** The SIV ovule-targeting assay. Pollen tube targeting competence was assessed using a single pollen genotype or in a one-to-one genotype competition assay. **b** *ech-/-* pollen grains showed reduced but adequate pollen tube germination in vitro as well as semi-in vivo but showed significantly reduced ovule-targeting competence semi-in vivo. **c** Quantification of pollen tube ovule-targeting competence semi-in vivo of *ech-/-* plants in a single genotype or mixed genotype competition assay. *n* is the number of pistil explants assessed, *asterisks* denote significant differences assessed with Student's *t*-test (*p* < 0.01). **d** Aniline blue stain of wild-type and *ech-/-* pollinated wild-type pistils 18 h after pollination (*HAP*) showing near complete lack of ovule targeting in *ech-/-* pollinated pistils (*red arrow*) compared with wild type-pollinated pistils (*yellow arrows*), verifying the semi-in vivo observations in **c**. **e** Frequency of ovule targeting by pollen tubes in aniline blue-stained pistils. All score variances (*asterisk*) are statistically significant (Student's *t*-test, *p* < 0.01). Error bars represent standard deviation (stdv). **f** Blue dot assay by GUS-staining of *ms1* pistils pollinated with wild-type pollen grains homozygous or heterozygous for Lat52-GUS and Lat52-GUS;*tctp-1/+* 18 HAP. *Red arrows* point to *tctp-1* mutant pollen tubes targeting ovules at the bottom of the pistil, suggesting *tctp-1* pollen tube growth is not greatly impaired. *Insets*: variable mistargeting phenotypes observed in *tctp-1/+* pollinated pistils. **g** Counts of "blue dots" revealed ovule targeting was greatly impaired in *tctp*-deficient pollen tubes

shown that pollination of wild-type pistils by *ech-/-* pollen grains produced adequate amounts of viable seeds that are able to germinate into plantlets; these amounts were greater than from *ech-/-* selfing plants, suggesting that the *echidna* mutant has reduced fertility in both gametophytes. These results provide evidence that *echidna* mutation can be transmitted through the male (albeit at very low frequency), supporting the ability of *ech-/-* pollen grains to grow a pollen tube and occasionally target ovules for successful fertilization.

To emphasize the fertility defects of *ech-/-* plants, we investigated the guidance and ovule-targeting ability of the viable *echidna* pollen tubes. We used *ech-/-* pollen grains to hand-pollinate pistils and score their ovule-targeting competence 18 h after pollination (HAP) (Fig. 8a–e). Critically, we used the SIV assay to score only pollen tubes that emerged from the cut pistils on their ability to target wild-type ovules (Fig. 8a, b). This way, we eliminated the non-viable population of *ech-/-* pollen grains and dealt only with the pollen grains that could germinate and grow pollen tubes through the cut pistil (Fig. 8b). Of the handful of viable *ech-/-* pollen grains produced and able to germinate, we noticed that they were vastly outcompeted by wild-type pollen tubes labeled with LAT52-GFP in targeting ovules for fertilization in a mixed genotype competition assay or were poorly targeting in self-pollinated *ech-/-* pistils (Fig. 8c–e). The *ech-/-* pollen tube ovule-targeting incompetence was further emphasized by the fertility defects and lack of ovule fertilization observed in dissected mature *ech-/-* siliques (Fig. 9e). On average, only 10 % of the ovules in *ech-/-* plants were fertilized and able to develop into "wild-type-like" seeds (Fig. 9e–g). Moreover, nearly 50 % of the self-fertilized *ech-/-* ovules showed embryo developmental defects, the majority of the embryos arresting at the heart and torpedo stages (Fig. 9h). The penetrance of this infertility was greatly variable between siliques as well as between individual plants, with some siliques producing almost no seeds (Fig. 9h). ECHIDNA protein is required for the secretion of secGFP but not BR11 or PIN2 auxin efflux carrier and the *ech-/-* mutant effect phenocopied concanamycin A defective secretion [54]. Earlier, we showed that the secretion of both the pollen tube proteins NtPsCRP2 and LLG3 was perturbed in *yip4a-1;4b* double mutants (Figs. 6 and 7). Since ECH forms a complex with YIP4A/B in the TGN, both *ech* and *yip4a/yip4b* double mutants could widely affect secretion of several pollen tube-secreted proteins essential for pollen tube growth, pollen tube–ovule crosstalk, fertilization, as well as embryogenesis in flowering plants, contributing to the infertility observed in *echidna* mutant plants.

Secreted TCTP protein is required for pollen tube guidance and ovule targeting

Loss of function of TCTP was previously reported to impact on pollen tube growth [56] and plant fertility [57]

in *Arabidopsis*. Here, we have incorporated our findings on NtTCTP secretion by the pollen tube following stylar penetration and independently investigated the phase of TCTP function during fertilization. We analyzed a T-DNA knockout line of the tobacco TCTP homolog (74 % identity, e-value 2.0E-85; Additional file 13: Figure S8) from *Arabidopsis* (AT3G16640, SAIL_28_C03, *tctp-1*) and investigated the ovule-targeting ability of its pollen tube and its seed production. Surprisingly, we did not observe the pollen tube growth defects reported by Berkowitz et al. [56] (Additional file 13: Figure S8). We exploited the GUS marker that co-segregates with the T-DNA insertion and performed a blue dot assay by GUS staining in pistils 18 HAP. We observed that *tctp-1* mutant pollen tubes from *+/tctp-1* plants poorly target ovules for fertilization (Fig. 8f). We noticed that *tctp-1* mutant pollen tubes can grow normally to the bottom of the pistil and occasionally target ovules, suggesting pollen tube growth in the *tctp-1* mutant is normal (Fig. 8f, arrow) Up to 35 % targeting variability was observed between pistils and between individual plants, suggesting variable *tctp-1* phenotypic penetrance (Fig. 8g). Transmission analysis confirmed that *tctp-1* mutation is poorly transmitted through the male (8.9 % transmission efficiency) but is normally transmitted through the female (Fig. 9a). Further, reciprocal pollination revealed that the mutant embryo lethal phenotype is exclusively induced by mutant pollen tubes at low penetrance (two weeks post-pollination) but not by the *tctp-1* mutant ovules (Fig. 9). Collectively, these results suggest that TCTP is essential for proper pollen tube guidance and ovule targeting as well as embryogenesis.

Dissected mature siliques from self-fertilized *+/tctp-1* plants revealed severe infertility and reduced seed set (Fig. 9b–d). The appearance of mutant seeds was randomized in siliques, suggesting equal competitiveness between the mutant and wild-type pollen tube growth (Fig. 9c). We observed an average of 12.3 % aborted ovules early post-fertilization and additionally 10.9 % of seeds were aberrantly chlorotic (Fig. 9d). In total, 44.5 % of the embryos with chlorotic seeds were arrested at the heart stage, with 37 % terminating at the torpedo stage and 18.5 % at the premature cotyledon stage (Fig. 9d). Our results suggest a critical role of TCTP in pollen tube guidance, ovule targeting, the events leading to fertilization, and the early stages of embryogenesis.

Discussion

Navigation of the pollen tube through several female sporophytic tissues to reach the ovule for fertilization (pre-ovular guidance) relies on guidance mediated by proteins, peptides, and other chemoattractants secreted by the female reproductive tissues [58]. This molecular dialog has emerged as an important bottleneck for
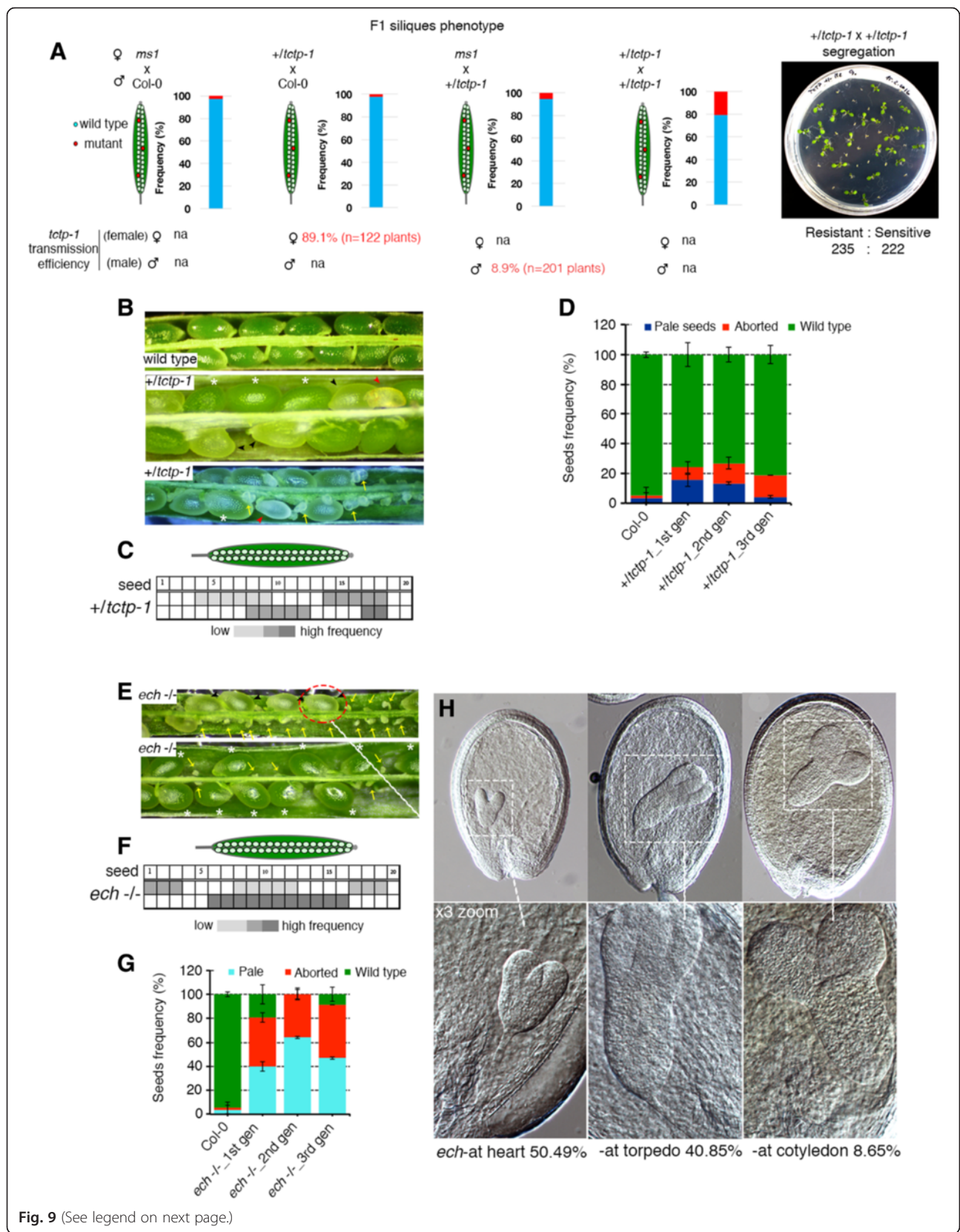
Hafidh *et al. Genome Biology* (2016) 17:81

Page 20 of 29

Fig. 9 (See legend on next page.)

Hafidh *et al. Genome Biology* (2016) 17:81

Page 21 of 29

Fig. 9 Loss of TCTP and ECHIDNA functions also impairs post-fertilization events. **a** Reciprocal test crosses of the *tctp-1* mutation showing low penetrance male-specific phenotypic induction in F1 siliques as well as significantly reduced male transmission efficiency scored by PCR genotyping as well as GUS-staining of LAT52-GUS-tagged T-DNA insertion. The micrograph on the *far right* shows seedling segregation of self-fertilized +/*tctp-1* plants, supporting the near complete block of *tctp-1* allele transmission through the male. **b** Dissected siliques of wild-type and self-fertilized +/*tctp-1* plants. *Asterisks* indicate wild-type-like seeds, *black arrowheads* indicate underdeveloped chlorotic mutant seeds, *red arrowheads* and *yellow arrows* show arrested embryos with failed embryogenesis soon after fertilization as well as unfertilized ovules. **c** Frequency and positioning of mutant seeds within dissected siliques. The random distribution of mutant seeds within +/*tctp-1* siliques suggests *tctp-1* mutant pollen tube growth is competent. **d** Frequency of *tctp-1* mutant seed phenotypic classes observed (n = 25 siliques per line). Error bars represent standard deviation (stdv). **e** Dissected siliques of self-fertilized *ech-/-* plants showing the high frequency of failed fertilization, defective embryogenesis, as well as "wild-type-like" seeds (*asterisks*). **f** Frequency and random positioning of *ech* mutant embryos/unfertilized ovules within *ech-/-* self-fertilized siliques implying *ech* pollen tubes can grow to the base of the pistil and target ovules for fertilization. **g** Frequency of mutant seed phenotypic classes observed (n = 25 siliques per line). Error bars represent standard deviation (stdv). **h** Embryogenesis lethality in ECHIDNA-deficient embryos showing stages and frequency of embryo arrest. Scale bars = 10 μM. *gn* germ cell nuclei, *na* not applicable, *sn* sperm cell nuclei, *vn* vegetative cell nuclei, *wt* wild type

unfavorable fertilization and as a pre-zygotic barrier for interspecies hybridization. A compendium of recent studies have identified a handful of secreted peptides from female synergid cells of *T. fournieri*, *Z. mays*, and *Arabidopsis* as pollen tube attractants [3–5, 59]. Another recent study also reported that CENTRAL CELL GUIDANCE protein (CCG) together with its interaction partners, CCG BINDING PROTEIN 1 (CBP1), mediator complex (MED), and central cell-specific AGAMOUS-transcription factors, co-regulate a subset of cysteine-rich proteins (CRPs), including pollen tube attractant LURE1 [9]. Only two pollen tube receptor proteins have been identified so far as playing a role in pollen tube guidance, LIP1 and COBL10 [31, 60]. Such slow progress has been attributed to the lack of accessibility of the pollen tubes within the pistil to capture and identify proteins secreted by the pollen tubes during their interaction with pistil tissues. In vitro approaches are feasible but pollen tubes grown in vitro do not acquire the competence to respond to female guidance signals [16] and develop different pollen tube physiology [12, 15, 61–63]. In this study we have successfully demonstrated the application of a previously developed pollen tube semi-in vivo technique (SIV-PS) [14] combined with gel- and label-free quantitative LC-MS/MS as a powerful assay for the genome-wide characterization of pollen tube-secreted proteins following its penetration through stigma and style. The SIV-PS tool offers access to pistil-stimulated pollen tube-secreted proteins with minimal contamination. We show that by coupling SIV-PS with gel- and label-free LC-MS/MS together with a structured bioinformatics workflow, one could quantitatively identify known pollen tube-secreted proteins as well as establish novel proteins with previously unknown extracellular functions. Using this technique, we demonstrate that the SIV-PS is unique from that of in vitro germinated pollen tubes (36.3 % overlap), emphasizing the requirement of pistil factors in rendering pollen tubes competent to target the ovule.

We have demonstrated the efficacy of the SIV-PS-identified proteins through subcellular localization prediction and *in planta* demonstration and investigated the undertaken secretory pathways and the involvement of key regulators of secretory pathways and pollen tube-secreted proteins in plant fertility and seed setting (Figs. 8 and 9). Among the identified secreted proteins are supposed ligands and receptors of the pollen tube that could facilitate cell–cell communication with the female reproductive and gametophytic tissues during ovule targeting by the pollen tube and fertilization. These include the plant defensin subfamily, CRPs, LORELEI-like GPI-anchored 3 (LLG3), thionin-like protein, RNases, lipid transfer proteins (LTPs), pollen Ole-e-allergen, arabinogalactans, pectinases, and invertases. Correlation analysis between the pollen tube secretome and transcript abundance revealed the two processes are uncoupled, as shown by the lack of linearity (Fig. 3). These observations clearly indicate that secreted proteins are subjected to multiple regulatory mechanisms at the post-transcriptional level prior to their secretion to the extracellular matrix. This lack of correlation has been reported in secretome studies of various human cancer types that deploy secretome techniques in search of biomarkers and cancer therapeutic targets ([64] and references therein). Therefore, in silico prediction alone for protein secretion provides only a rough guideline; instead, direct quantitative proteomic analysis of secreted proteins is necessary to identify and evaluate true protein secretion.

Further, we have demonstrated that conventional pathways play an essential role in pollen tube protein secretion. This was underscored by the defective secretion of the pollen tube proteins NtPsCRP2 and LLG3 in *yip4a-1;yip4b* double mutants, lack of pollen tube guidance and ovule-targeting competence in an *echidna* loss-of-function mutant, and the broader expression of several conventional pathway regulatory genes in tobacco SIV

Hafidh *et al. Genome Biology* (2016) 17:81

Page 22 of 29

pollen tubes (Additional file 10: Figure S5). A similar role was previously demonstrated for the POD1 protein involved in ER protein folding [65] as well as CHX21 and CHX23, which maintain ER potassium homeostasis [66], both exclusively affecting pollen tube guidance.

We have shown that, despite the significance of conventional protein secretion (Additional file 20: supplementary text), the bulk of pollen tube-secreted proteins utilize unconventional secretory pathways [48, 67]. We propose that one pathway for unconventional secretion of pollen tube proteins is via bioactive nanovesicle exosomes. In animals, several cell types secrete exosomes and other types of vesicles (ectosomes and shedding microvesicles) for intercellular communication with neighboring cells, affecting gene expression and overall cell physiology [68, 69]. Similarly, exosome secretion was recently reported in olive pollen tubes [51]. Of great interest, our comparison of the proteome from the secreted exosome of olive pollen tubes with the tobacco pollen tube secretome revealed a significant 68.6 % (35/51) overlap (Additional file 18: Table S7). Astonishingly, 94.3 % of these shared proteins are secreted unconventionally and only 5.7 % were signal peptide (SP)-containing proteins. These include proteins involved in cell wall expansion, stress/defense, membrane transport, metabolism, signaling, and protein synthesis and processing. In support, we have demonstrated that TCTP is secreted to the apoplast and strongly co-localized with the exosome marker Ole1 from *Arabidopsis* (Figs. 4p–s and 5g–h). Our results suggest that pollen tube-secreted exosomes could account for the secretion of the majority of unconventionally secreted pollen tube proteins to the extracellular matrix. In animals, Notch ligand Delta-like 4 is secreted via exosomes and was shown to impact on neighboring cells without the conventional cell–cell contact and potentially at a longer range [70]. We propose that pollen tube-secreted exosomes could facilitate a latent mechanism for pollen tube long-distance signaling with the female reproductive tissues, possibly including crosstalk with ovules. We have shown that secretion of NtTCTP seems to follow the ER–TGN route, as shown by co-localization with ER and Golgi markers (Fig. 5c–e). This phenomenon has so far not been reported for unconventionally secreted proteins [28]. Secretion of unconventional proteins is known to be insensitive to BFA treatments, suggesting a Golgi apparatus bypass [71]. Perhaps it is questionable to base the absolute localization of NtTCTP in Golgi on co-localization with the Golgi marker GmMan1 alone. In *Arabidopsis*, the secretion of the unconventionally secreted protein hygromycin phosphotransferase (HYG^R) is BFA-insensitive; however, it still requires the participation of a Golgi-localized synaptotagmin homolog, SYT2 [72]. Moreover, SYT2's role in HYG^R unconventional secretion has been compared with the Golgi-localized GRASP

function in the unconventional secretion of AcbA in *Dictyostelium* and alpha-integrin in *Drosophila* [71]. Therefore, the co-localization of NtTCTP with GmMan1 could suggest either that NtTCTP is not strictly localized in the Golgi apparatus or that GmMan1 is instead involved in the unconventional secretion of NtTCTP. Alternatively, NtTCTP could be truly localized in the Golgi apparatus and its unconventional secretion does not bypass the Golgi as in other examples of unconventionally secreted plant proteins. Future experiments will confirm precisely which route NtTCTP follows for its final phase of secretion to the apoplast.

A parallel pathway that could also facilitate unconventional protein secretion, particularly of soluble cytosolic proteins, is via secretory lysosomes [73]. Cofactors such as plant orthologs of animal caspases could facilitate secretion through lysosome membrane fusion and microvesicle shedding [73]. Another exciting proposal for an unconventional protein secretion pathway in plants is via a recently discovered exocyst positive organelle, EXPO [74]. Although EXPO co-localized with Exo70E2, a marker of the exocyst complex, its role in conventional protein secretion was ruled out based on the fact that EXPOs are not influenced by BFA or wortmannin and are unable to uptake the endocytotic marker FM4-64 [28]. EXPOs role in mediating unconventional protein secretion was demonstrated in the secretion of SAMS2 (S-adenosyl methionine synthetase 2) from the cytosol to punctate organelles that co-localized with Exo70E2 in the protoplast [74]. Further, EXPOs have been identified as double membrane organelles and fuse with plasma membrane to expel a single membrane vesicle to the apoplast [74]. It will be of great interest to establish whether EXPOs are also involved in unconventional secretion of pollen tube proteins alongside exosomes during male–female communication.

The bioinformatics analysis of the SIV-PS dataset also revealed unexpected phenomena. Proteins predicted to be palmitoylated at cysteine residues showed an extensive overlap with proteins predicted to undergo GPI-anchoring modification. This might be explained by the fact that cysteine palmitoylation of putative GPI-anchored proteins (GAPs) could facilitate increased affinity of GAPs for the plasma membrane prior to their secretion. Indeed, both COBRA-like 10, a pollen tube receptor protein, and Lorelei-like GPI-anchored 3 (LLG3, this study) were predicted to be palmitoylated at amino acids Cys206, 336, 337, and 433 for COBRA-like 10 and amino acids Cys7, 74, and 75 for LLG3. Furthermore, in animals, cysteine palmitoylation was shown to regulate raft affinity for the majority of the raft integral proteins, including GAPs [75, 76]. Because of the low proportion (14 %) and very low abundance of GAPs identified in this study, it will be important to perform GPI-protein

Hafidh *et al. Genome Biology* (2016) 17:81

Page 23 of 29

enrichment of the pollen tube fractions to identify other potential pollen tube GPI-anchored receptors.

Using gel- and label-free quantitative LC-MS/MS at the genome-wide scale, our study has revealed for the first time the pollen tube proteins secreted in response to pollen tube interaction with the female reproductive tissues. These secreted proteins represent potential ligands and receptors for cell–cell signaling during pollen tube–pistil interaction. Most significantly, we speculate that pollen tubes might deploy exosome nanovesicles as a mechanism to facilitate long distance cell–cell communication with the female reproductive tissues. We have shown the utilization of ER–TGN pathways by pollen tube-secreted proteins in both the sporophyte and male gametophyte and demonstrated that perturbation of this pathway is detrimental for their secretion. Using the unconventionally secreted pollen tube protein NtTCTP, we have demonstrated that pollen tube secreted proteins are indispensable for pollen tube guidance and ovule targeting as well as for embryogenesis. We have emphasized the significance of pollen tube protein secretion activities by showing defective pollen tube guidance and ovule targeting ability and near-complete sterility following the knockdown of ECHIDNA. Identified secreted proteins from this study offer a direct demonstration of species-specific candidate ligand–receptor interaction partners with an emphasis on cell–cell signaling mechanisms during successful plant reproduction.

Conclusions

We have identified 801 genome-wide pollen tube secreted proteins following pollen tube penetration through female reproductive tissues. Bioinformatics analysis revealed that the vast majority of the pollen tube secretome comprises unconventionally secreted proteins, predominantly small proteins of < 20 kDa. They are predominantly expressed in the male gametophyte and include glycoside-hydrolase, copper binding, RNA-binding, and proteolysis among the most frequent associated activities. Tagging of selected candidate proteins with fluorophores verified localization in secretory pathways and secretion to the extracellular matrix. Further functional analysis revealed pollen tube-secreted proteins as well as regulators of ER–TGN protein translocation as crucial players for proper pollen tube protein secretion, guidance of pollen tubes to the ovule, and embryogenesis. Our study has provided new insights into alternative pathways for unconventional protein secretion involving nanovesicle exosomes and for the first time provided access to newly identified pollen tube secreted proteins that could perceive guidance signals from the female reproductive tissues during cell–cell communication and plant sexual reproduction.

Methods

Preparation of tobacco pollen tube secretome using the SIV-PS approach

To capture pollen tube-secreted proteins following penetration through the pistil, we developed the following procedure. On day 1, flowers were emasculated one day before anthesis and netted for 24 h. On day 2, pollen grains stored at –20 °C were acclimatized to room temperature for 5 min and used for limited pollination of half of the emasculated flowers. On day 3, both pollinated and unpollinated (control) pistils were collected and excised at approximately 22 mm from the stigma shoulders (Additional file 1: Figure S1). Pistils were arranged in a "germination cup" (5 × 4 cm radius × height) filled with SMM-MES pollen germination media (0.175 M sucrose, 1.6 mM H_3BO_3, 3 M $Ca(NO_3)_2.4H_2O$, 0.8 mM $MgSO_4.7H_2O$, 1 M KNO_3, 23 mM MES, pH 5.9). Pollen tube germination was performed at 28 °C in a 70 % humid chamber for 24 h (Additional file 1: Figure S1). Proteins secreted into media were concentrated using a Millipore filter (Amicon, USA Ultra-2 Pre-Launch 10 K and 3 K), and final samples were stored at –80 °C. Final protein concentrations were measured by 2D-Quant kit (GE Healthcare, USA). Pistils with protruding pollen tubes were used for viability tests and microscopic analysis and the remaining pollen tubes were excised for RNA extraction. For a stepwise description, see [14]. A list of primers used for semi quantitative RT-PCR analysis is provided in Additional file 21: Table S8.

FASP processing

Biological replicates of concentrated SIV-PS media (including negative controls from unpollinated pistils) were subjected to filter-aided sample preparation (FASP) [77, 78]. Samples containing about 5 μg of total protein were mixed with UA buffer (8 M urea in 100 mM Tris-HCl, pH 8.5), loaded onto the Vivacon 500 device with MWCO 10 kDa (Sartorius Stedim Biotech, Germany), and centrifuged at 14,000× g for 30 min at 20 °C. Before sample application, 5 μl of 1 % (w/v) polyethylene glycol 20,000 (PEG) was added onto the membrane. The retained proteins were washed with 400 μl UA buffer. The final protein concentrates kept in the Vivacon 500 device were mixed with 100 μl of UA buffer containing 50 mM dithiothreitol and incubated for 30 min at room temperature. After additional centrifugation, the samples were mixed with 100 μl of UA buffer containing 50 mM iodoacetamide and incubated in the dark for 30 min. After the next centrifugation step, the samples were washed three times with 400 μl UA buffer and three times with 200 μl of 50 mM $NaHCO_3$. Trypsin (sequencing grade, Promega, USA) was added onto the filter and the mixture (total volume about 50 μl, PEG concentration about 0.1 % (w/v)) was incubated for 14 h at 37 °C. The tryptic peptides were finally eluted by

Hafidh *et al. Genome Biology* (2016) 17:81

Page 24 of 29

centrifugation followed by two additional elutions with 50 μl of 50 mM NaHCO$_3$. The final eluate was concentrated using a SpeedVac concentrator (Thermo Fisher Scientific) down to about 20 μl and transferred into a LC-MS vial containing 2.5 μl of 0.01 % PEG, with additional acidic "extraction" of peptides from FASP eluate test tube walls by 50 % acetonitrile (ACN) containing 2.5 % formic acid (v/v) and by 100 μl of 100 % ACN (each extraction step was done twice with 50 and 100 μl of the solution, respectively). The final solution was concentrated in a SpeedVac concentrator to < 25 μl and refilled to 25 μl with water.

LC-MS/MS analysis of peptides from FASP

LC-MS/MS analyses of the peptide mixture were done using a RSLCnano system connected to an Orbitrap Elite hybrid spectrometer (Thermo Fisher Scientific, Waltham, MA, USA). Prior to LC separation, tryptic digests were online concentrated and desalted using a trapping column (100 μm × 30 mm) filled with 3.5 μm X-Bridge BEH 130 C18 sorbent (Waters, Milford, MA, USA). After washing the trapping column with 0.1 % formic acid , the peptides were eluted (flow 300 nl/min) from the trapping column onto an Acclaim Pepmap100 C18 column (2 μm particles, 75 μm × 250 mm; Thermo Fisher Scientific, Waltham, MA, USA) using the following gradient program (mobile phase A, 0.1 % FA in water; mobile phase B, ACN:methanol:2,2,2-trifluoroethanol (6:3:1; v/v/v) containing 0.1 % FA). The gradient elution started at 1 % of mobile phase B and increased from 1 to 56 % during the first 100 min (1 % in the first, 14 % in the 30th, 30 % in the 60th, and 56 % in 100th min), then increased linearly to 80 % of mobile phase B in the next 5 min, remaining at this state for the next 15 min. Equilibration of the trapping column and the column was done prior to sample injection into the sample loop. The analytical column outlet was directly connected to the Nanospray Flex Ion Source (Thermo Fisher Scientific, Waltham, MA, USA).

MS data were acquired in a data-dependent strategy selecting up to the top 20 precursors based on precursor abundance in the survey scan (350 – 1700 m/z). The resolution of the survey scan was 120,000 (400 m/z) with a target value of 1×10^6 ions, one microscan and maximum injection time of 200 ms. Low resolution CID MS/MS spectra were acquired with a target value of 10,000 in rapid CID scan mode with the m/z range adjusted according to actual precursor mass and charge. MS/MS acquisition in the linear ion trap was carried out in parallel to the survey scan in the Orbitrap analyzer by using the preview mode. The maximum injection time for MS/MS was 150 ms. Dynamic exclusion was enabled for 45 s after one MS/MS spectra acquisition and early expiration was disabled. The isolation window for MS/MS fragmentation was set to 2 m/z.

Two LC-MS/MS analyses in total were done for each sample (using 10 out of the 25 μl of the final solution). The second LC-MS/MS analysis was done with exclusion of m/z masses already assigned to peptides from the target database (FDR < 1 %) based on the first LC-MS/MS analysis. Mass tolerance for m/z exclusion was set to 10 ppm and the retention time window to 2 min. The two resulting raw files for each sample were searched as a single data set to obtain complete identification results for each sample.

The analysis of the mass spectrometric RAW data files was carried out using the Proteome Discoverer software (Thermo Fisher Scientific; version 1.4) with in-house Mascot (Matrixscience, London, UK; version 2.4.1) and Sequest search engines. Mascot MS/MS ion searches were done against the concatenated UniRef100 protein database for Solanaceae, Brassicaceae, and Fabaceae taxonomies (downloaded on 2014-02-26 from http://www.uniprot.org/) and an in-house tobacco protein database based on sequencing data (total number of protein sequences 624,436). A modified cRAP database (downloaded from http://www.thegpm.org/crap/) was searched in parallel for detection of contaminants. Mass tolerance for peptides and MS/MS fragments was 5 ppm and 0.5 Da, respectively. Oxidation of methionine and deamidation (N, Q) as an optional modification, carbamidomethylation of C as a fixed modification, and two enzyme miscleavages were set for all searches. Percolator was used for post-processing of database search results. Peptides with a FDR (q-value) <1 %, rank 1, and with at least six amino acids were considered. Label-free quantification using protein group area calculation in Proteome Discoverer was used (Top3 protein quantification) [17, 18]. Parts per million (ppm) values for all or potentially secreted proteins were calculated as protein group area divided by the sum of areas of all or potentially secreted protein groups (molar ratio; expected to be directly proportional to protein amount in the original samples) multiplied by 10^6, respectively.

Following label-free quantitative LC-MS/MS, protein groups were considered secreted based on Top3 protein algorithms stipulating that (1) the ratio of the calculated median of a protein group in a sample to the average median of the two control unpollinated samples was > 3 (cell "CP1" of Additional file 3: Table S1) and (2) the number of peptides was, at a minimum, 3 and that the protein group must be up-regulated in at least two SIV-PS samples (column "CS, U > 2). For comparison, individual protein accessions from replicates of all sample types were combined into supergroups (SGs) and reported in SG column Additional file 7: Table S4. Proteins were put into the same SG if they were reported in sample type replicate report as alternative proteins. For more information see actual reports and comments

Hafidh *et al. Genome Biology* (2016) 17:81

Page 25 of 29

within tabs. To compare in vitro secreted proteins and the respective in vitro total proteomes, only protein groups with a minimum of three peptides and present in at least one replicate were used. All accessions from the respective groups that fulfill the above criteria are provided in Additional file 7: Table S4 with separate group columns for each pairwise comparison and accessions that are unique or intersect with the paired sample.

Alcohol dehydrogenase enzyme assay

Endogenous ADH activity was measured in unpollinated controls, SIV-PS samples and in SIV pollen tubes total extract (SIV-PP) to estimate the extent of cytosolic protein contamination. As a control, the total soluble protein fraction from the respective pollen tubes was extracted using RIPA extraction buffer (Tris 50 mM, pH 8.0, 150 mM NaCl, 0.1 % SDS, 0.5 % sodium deoxycholate, Triton X-100, 1 mM PMSF) and protein concentrations were quantified using a 2D-Quant kit (GE Healthcare, USA). The reaction mixture for the ADH assay was composed of 50 mM Tris, pH 9.0, 0.867 mM NADþ, 20 % ethanol (Sigma, USA), and equal aliquots of protein extracts from each samples. The assay was repeated with three biological replicates. The increase in absorbance at 450 nm was monitored every 5 min for 45 min. The ADH activity was expressed as nmole/min/ml (milliunits/ml) for 1.0 µmole NAD^+ to NADH reduction per minute at pH 8.0 and 37 °C, per aliquot of protein.

Immunoblot protein detection

Total proteins from transiently transformed *N. benthamiana* leaves 48 h post-transfection or those from SIV and in vitro tobacco pollen tubes were extracted using RIPA extraction buffer (50 mM Tris pH7.4, 150 mM NaCl, 0.5 % Na-deoxycholate, 1.0 % Triton X-100). Protein samples were quantified using a 2D-Quant kit (GE Healthcare, USA), resolved by one-dimensional SDS-PAGE and blotted using the semi dry technique (e-blot, GeneScript) onto nitrocellulose membranes (GE Healthcare, USA). After 30 min blocking, blots were probed with a 1:1000 dilution of rabbit monoclonal anti-GFP antibody raised against sGFP (ChromoTek, Germany) overnight at 4 °C followed by a 1:30,000 dilution of rat anti-rabbit IgG conjugated to alkaline phosphatase (Sigma USA). Chemiluminescence was developed using BCIP (5-bromo-4-chloro-3-indolyl-phosphate, final concentration 165 ng/ml) and NBT (nitro blue tetrazolium chloride, final concentration 33 ng/ml) developing solutions in AP buffer (100 mM Tris-Cl pH 9.5, 100 mM NaCl, 5 mM $MgCl_2$). Blot images were captured and analyzed using a Syngene G:Box EF imaging system (Syngene, UK).

Concavalin A-coupled horseradish-peroxidase N-glycosylation test

Total proteins (40 µg per sample) were resolved by one-dimensional SDS-PAGE in quadruple replicates. Proteins were transferred onto nitrocellulose membrane and stained with Ponceau Red stain (Sigma, USA) for visualizing protein loading control. Membranes were de-stained, washed in TTBS buffer (500 mM NaCl, 80 mM Tris.HCl, pH 7.6, 0.1 % Tween 20) for 1 h and incubated in TTBS buffer supplemented with 25 µg/ml concavalin A for 1 h. Membranes were then washed for 30 min in TTBS and incubated for 30 min in TTBS with 50 µg/ml horseradish peroxidase before being washed again in TTBS for 45 min. N-glycosylated protein bands were visualized with detection buffer (45 mg 4-chloro-1-naftol, 15 ml methyalcohol, and 60 ml 10 mM Tris-HCl pH 6.8) by drop-wise addition of a 25 µl aliquot of hydrogen peroxide (H_2O_2, up to 100 µl) until membrane saturation.

Microscopy

Pollen tube bundles from excised pistils were mounted directly on a glass slide and visualized by bright field microscopy with Hoffman modulation contrast (Nikon, Japan). For aniline blue staining (callose stain), pistils were collected 18 HAP and fixed in 9:1 ethanol:acetic acid (v/v) for 24 h. Samples were washed in an ethanol series and then alkaline-treated in 1.0 M NaOH for ~16 h. Samples were stained in aniline blue stain solution (0.1 % (w/v) aniline blue, 108 mM K_3PO_4 (pH 11)) for 12 h. To investigate the competence of pollen tubes to target the ovule by blue dot GUS-staining assay, pistils pollinated with +/*tctp-1* SAIL_28_C03 or Lat52-GUS-marked wild-type control pollen were collected at 18 HAP and dissected along the septum to remove carpel walls. Exposed fertilized ovules were stained for GUS activity with a solution containing 50 mM sodium phosphate buffer, pH 7, 0.2 % Triton X-100, 10 mM potassium ferrocyanide, 10 mM potassium ferricyanide, and 1 mM X-Gluc (5-bromo-4-chloro-3-indolyl-D-glucoronic acid). Samples were vacuum-infiltrated for 10 min and stained overnight at 37 °C.

For the pollen tube viability test using Alexander staining, pollen tubes were placed on a microscopic slide with a few drops of Alexander stain solution (10 ml 95 % ethanol, 1 ml Malachite green (1 % in 95 % ethanol), 5 ml Fuchsin acid (1 % in water), 0.5 ml Orange G (1 % in water), 5 g phenol, 5 g chloral hydrate, 2 ml glacial acetic acid, 25 ml glycerol, and distilled water to 50 ml). Stained samples were visualized by bright field microscopy with Hoffman modulation contrast (Nikon, Japan). Callose stain distribution was analyzed with NIS-Element software following fixed UV exposure under cyan filter (460 – 500 nm bandwidth, Nikon, Japan). For propidium iodide staining, tissues were incubated in

Hafidh *et al. Genome Biology* (2016) 17:81

Page 26 of 29

10 µg/ml propidium iodide for 20 s, rinsed in deionized water, and visualized under a RFP filter (560–615 nm, Nikon, Japan).

For protein subcellular localization, samples were visualized with a Zeiss LSM 5 DUO laser scanning confocal microscope (CLSM) equipped with an argon laser and a Zeiss C-Apochromat × 40 9/1.2 water-corrected objective. For co-localization, dual fluorescence channels and differential interference contrast (DIC) were used simultaneously for live cell imaging. A Nikon Eclipse Ti confocal microscope with a CSU-X1 spinning disk module and Andor iXon3 EMCCD camera was used to verify vesicle dynamics as well as subcellular localization in pollen tubes. Images were analyzed and assembled with ImageJ (http://imagej.net), Adobe Photoshop CS6 (http://www.adobe.com/) and Ink-scape (https://inkscape.org/en/) software.

Availability of supporting raw data

The mass spectrometry proteomics data sets supporting the results of this article are available at the ProteomeXchange Consortium via the PRIDE partner repository with the dataset identifier PXD002215 (http://www.ebi.ac.uk/pride/archive/projects/PXD002215).

Additional files

Additional file 1: Figure S1. Semi-in vivo pollen tube secretome (SIV-PS) approach for identification and quantification of pollen tube-secreted proteins. a An improvised SIV-PS technique setup from *in planta* (steps 1–3) to in vitro incubation of the pollen tubes (step 4–5). The *inset* shows emerging pollen tubes from excised pistils. Scale bars = 2 mm. b Schematic representation of the SIV-PS workflow. c Micrographs of SIV pollen tubes showing normal pollen tube growth in bright field with streaming organelles (*top panel*), sperm cell formation (*second panel*), callose deposition and callose plugs (*asterisk, third panel*), and pollen tube viability assessed by Alexander stain (*bottom panel*). *sn* sperm cell nucleus, *VN* vegetative cell nucleus. Scale bar = 40 µM. d A tobacco pollinated pistil showing the site of stylar excision and the presumed peptide signaling flow from male and female gametophytes. (TIF 714 kb)

Additional file 2: Figure S2. Assessment of pollen tube integrity, secretome purity using an alcohol-dehydrogenase (ADH) assay, and secretion activities in pollen tubes. a *Top panels*: pollen tube penetration (*left*) and exit (*right*) through the transmitting tract of the style visualized with aniline blue. *Bottom panels*: excised stylar ends visualized by DAPI stain marking cell nuclei (*asterisk, left*) and by toluidine blue (*right*) outlining cell wall boundaries. Excised ends of pistils are marked with the *dashed line*; *red* and *white arrowheads* mark the upper border of pistil broken cells following excision; and *yellow arrowheads* mark the upper and lower borders of intact cells. Scale bars = 5 µM. b Frequency of viable and non-viable semi-in vivo pollen tubes as well as integrity following 48 h growth through stylar tissues and in vitro. Error bars represent ± standard error; *asterisks* indicate statistical significance by Student's *t*-test with *p* values indicated. c Purity assessment using an ADH assay of the secretome samples. ADH activities were calculated as nmole/min/ml. *SIV-PS1–3* SIV-pollen tube secretome samples 1–3. d–f Live-cell imaging of endocytic tracer FM4-64 uptake and recycling in tobacco in vitro germinated pollen tubes co-localized with ER tracer in the absence (d) or presence (e, f) of brefeldin A (*BFA*), an inhibitor of protein secretion. Addition of BFA resulted in aggregation of endocytic vesicles and formation of BFA compartments (*arrows*), evidence of a defective conventional protein secretion pathway. BFA-treated pollen tubes showed specific defects only in

FM4-64 labeled vesicles and not in the ER network. Scale bars = 5 µM. (TIF 1554 kb)

Additional file 3: Table S1. List of protein accessions identified from semi-in vivo pollen tube secretome and semi-in vivo total proteomes by gel-free LC/MS/MS. (XLSX 53714 kb)

Additional file 4: Figure S3. Evaluation of true pollen tube-secreted proteins using quantitative LC-MS/MS. Depicted are three examples of proteins categorized as pollen tube-secreted proteins or predominantly secreted by the pollen tube following peptide mapping and quantitative peptide area evaluation to compute protein abundances relative to control. With subtractive approaches, these proteins would normally be eliminated from analysis as they were also identified in unpollinated pistil controls (most likely due to peptide homology with pistil proteins); however, using absolute quantitative analysis, their true source of secretion could clearly be demonstrated. (TIF 415 kb)

Additional file 5: Table S2. Tobacco semi-in vivo pollen tube secreted proteins of ≤ 20 kDa. (XLSX 306 kb)

Additional file 6: Table S3. Identified protein families and domains of semi-in vivo pollen tube-secreted proteins. (XLSX 515 kb)

Additional file 7: Table S4. List of protein accessions derived from protein supergroup (see materials and methods) pairwise comparison listing unique and common protein accessions between SIV-PS and in vitro pollen tube secretomes and proteomes. The data file also includes individual replicates of in vitro pollen tube-secreted proteins and identified total proteomes. (XLSX 30434 kb)

Additional file 8: Table S5. Pollen tube secretome protein accessions mapped to the Arabidopsis semi-in vivo transcriptome. (XLSX 178 kb)

Additional file 9: Figure S4. Bioinformatic workflow and detection of N-glycosylation of secreted proteins by concavalin A staining. a In silico classification of secreted proteins into conventionally and unconventionally secreted proteins based on the presence or absence of an N-terminal signal peptide (SP) using SignalP v4.1 prediction algorithms. Each protein class was further analyzed for its potential secretion using the secretomeP database and putative post-translational modifications as indicated. b Prediction of plasma membrane GPI-anchoring using FragAnchor. The reliability of the implemented prediction algorithms was tested by independently analyzing Uniprot-derived accessions (*upper column*) and in-house *Nicotiana tabacum* protein sequences (*lower column*) with limited sequence annotation. c Subcellular localization prediction using the LocTree prediction database. Independent prediction with the targetP database (Additional file 10: Figure S5) emphasized secretion of SP-containing proteins and largely ambiguous localization of unconventionally secreted pollen tube proteins. d One-dimensional SDS-PAGE profiling of pollen tube-secreted proteins. *Right*: banding patterns show the distinct profile of SIV secreted proteins (SIV-PS1, SIV-PS3) relative to unpollinated pistil control. e Concavalin A glycosylated protein detection of pollen tube-secreted proteins. A subfraction of SIV-PS is postranslationally glycosylated (*red rectangle*). (TIF 896 kb)

Additional file 10: Figure S5. Prediction of transmembrane helices (TMHs) in pollen tube-secreted proteins and LocTree-associated GO terms. a Analysis of TMHs of pollen tube-secreted proteins using TMHMM algorithms. *Right*: validation of TMHMM algorithms using sequences from known Arabidopsis pollen tube plasma membrane proteins (ACA9, ANX1, ANX2, KRP2, KRP4) and non-TMH-containing pollen tube palmitoylated plasma membrane proteins LIP1 and LIP2 as controls. The absence of TMHs in pollen tube-secreted proteins also supports their potential secretion to the apoplast and extracellular matrix. b Independent prediction of pollen tube-secreted protein subcellular localization using the TargetP database. c Representative GO terms associated with the corresponding LocTree-predicted localization (Additional file 9: Figure S4) derived from PSI-Blast of pollen tube-secreted proteins. (TIF 780 kb)

Additional file 11: Figure S6. Pollen tube secretome GO-slim term enrichment and expression profiling of secretory pathway genes. a Enriched GO-slim term comparison. The color scale indicates comparative enrichment and overlaid bar charts show GO term enrichment within protein subgroups; numbers represent associated accessions (*p* < 0.05).

Hafidh *et al. Genome Biology* (2016) 17:81

Page 27 of 29

b Unique GO-slim terms of the unconventionally secreted pollen tube protein subset. A full list of GO terms is provided in Additional file 8: Table S5. c Plant secretory pathways with annotated genes derived from genetic studies [79–81]. d Microarray profiling of secretory pathway genes during tobacco pollen tube growth. e Semi-RT-PCR validation of selected secretory pathway genes in tobacco semi-in vivo pollen tubes and unfertilized ovules. A list of primers is provided in Additional file 20: Table S8. (TIF 610 kb)

Additional file 12: Figure S7. Assessment of pollen tube secreted RNases and defensin subgroup protein homology. a PD1 RNase family protein alignment with tobacco-derived NtRNase1 and RNase NE proteins. b RT-PCR analysis of pollen tube-secreted RNases showing specific expression in female reproductive tissues alone in unpollinated as well as pollinated samples (14 hours post-pollination). *PT24* 24 h cultivated in vitro pollen tubes. c Alignment of *Torenia fournieri* CRP1–3 with NtPsCRP1. *Pink highlighting* indicates the predicted signal peptide of NtPsCRP1 and the *green highlighting* shows the six conserved cysteine residues of the defensin subfamily. Amino acids conserved in at least two sequences are shaded. d Neighbor-joining phylogenetic tree using percentage identity and node values showing closer association of NtPsCRP1 with TfCRP1 and TfCRP3. A list of primers used is provided in Additional file 20: Table S8. (TIF 546 kb)

Additional file 13: Figure S8. Pairwise alignment of *Arabidopsis* and tobacco TCTP proteins and expression profile of LAT52 and PRK2/4 receptor kinases. a Amino acid conservation between the *Arabidopsis* and *N. tabacum* TCTP protein. *Blue highlighting* indicates mismatches. b A hydropathy plot of NtTCTP hydrophobicity prediction based on the Kyte Doolitle method showing GRAVY score (*red line*) and overall hydrophobic nature of NtTCTP. c In vitro pollen tube growth assay of +/*Attctp-1* tetrad pollen showing normal pollen tube germination. d Aniline blue staining of self-fertilized +/*Attctp-1* pistils 18 h after pollination, independently verifying normal pollen tube growth *in planta*. e Pairwise alignment of pollen tube-secreted *L. barbarum* LAT52-like and *S. lycopersicum* LAT52 proteins. Alignment showing the predicted 23 amino acid N-terminal signal peptide (*blue highlighting*), the conserved eight cysteine residues (*boxed*), and N-glycosylation sites (*grey highlighting*). f Expression profiles of pollen receptor kinase 2 (PRK2) and pollen receptor kinase 4 (PRK4) derived from Agilent 44 K Tobacco Genome Array [19] and Arabidopsis Affymetrix ATH1 microarray [53] data. g Semi-RT-PCR verification of PRK2 and PRK4 expression in tobacco mature pollen (*MP*), 4 h (*PT4*) and 24 h (*PT24*) in vitro pollen tubes, leaves (*LF*), roots (*RT*), SIV pollen tubes, and unfertilized ovules. h Topology of the receptor modules, PRK2 and PRK4, and the ligand module LAT52. We speculate that detection of both modules after 24 h of pollen tube growth implies a later function of the complex leading to successful fertilization. (TIF 953 kb)

Additional file 14: Figure S9. Secreted NtPsCRP2 displays "stop-and-go" movements in root epidermal cells. a A 2'30" span confocal time-series and b a close-up 0'55" of the junction of two root epidermal cells showing NtPsCRP2-GFP localized activities at the root elongation zone. Three classes of activities could be deduced: "a", plasma membrane tethered or dormant (static) vesicles; "b", tethered at first followed by active movements; and "c", mobile at first followed by tethering. Scale bars = 5 μM. (TIF 1515 kb)

Additional file 15: Movie 1. The "stop-and-go" cycling movements of NtPsCRP2-GFP in *Arabidopsis* roots. (AVI 17600 kb)

Additional file 16: Movie 2. A close-up of NtPsCRP2-GFP "stop-and-go" movements at the junction of two epidermal cells at the root elongation zone. (AVI 3679 kb)

Additional file 17: Table S6. GO terms enriched in the semi-in vivo pollen tube secretome. (XLSX 472 kb)

Additional file 18: Table S7. Overlap between the tobacco semi-in vivo pollen tube secretome and the proteome of olive pollen tube-secreted nanovesicle exosomes. (XLSX 17 kb)

Additional file 19: Figure S10. Microarray expression profiling of AtLLG3 pre- and post-pollination. a High abundance of AtLLG3 in mature pollen relative to whole flower expression. b A near twofold increase of AtLLG3 expression in pollinated pistils 8 h after pollination relative to 3.5 h post-pollination. Expression data were derived from the Affymetrix Arabidopsis ATH1 Genome Array at Genevestigator [53]. c Predicted NtLLG3 25 amino acid N-terminal signal peptide motif (*red*) as well as protease cleavage site (*arrow*). At the C-terminus is the predicted

GPI-anchor site (*blue*) and cleavage site (serine, *red underlined S*) for anchor release. (TIF 402 kb)

Additional file 20. Supplementary text. Expression profiling of core genes of the classic secretory pathways in semi-in vivo pollen tubes and unfertilized ovules. (DOC 23 kb)

Additional file 21: Table S8. List of primers used in this study. (XLSX 12 kb)

Abbreviations
ADH: alcohol dehydrogenase; BFA: brefeldin A; CRP: cysteine-rich protein; DEFL: defensin-like; ER: endoplasmic reticulum; FDR: false discovery rate; GAP: GPI-anchored protein; GFP: green fluorescent protein; GO: Gene Ontology; GPI: glycophosphatidylinositol; HAP: hours after pollination; LC: liquid chromatography; LLG3: Lorelei-like GPI-anchored protein 3; LTP: lipid transfer protein; MS: mass spectrometry; MS/MS: tandem mass spectrometry; PEG: polyethylene glycol; ppm: parts per million; PT24-PP: 24 h in vitro pollen tube proteome; PT24-PS: 24 h in vitro pollen tube secretome; RFP: red fluorescent protein; SIV: semi in vivo; SIV-PS: semi-in vivo pollen tube secretome; SP: signal peptide; TCTP: Translationally controlled tumor protein; TGN: trans-Golgi network; TMH: transmembrane helix; YIP4a/b: YPT/RAB GTPase interacting protein 4a/b.

Competing interests
The authors declare that they have no competing interests.

Authors' contributions
SH and VC conceived this study. SH performed the experiments. DP and ZZ performed the LC-MS/MS analysis. SH analyzed the data with help from JF and DH. SH and DH wrote the manuscript. All authors read and approved the final manuscript.

Author details
[1]Laboratory of Pollen Biology, Institute of Experimental Botany ASCR, Rozvojová 263, 165 02 Prague 6, Czech Republic. [2]Research group Proteomics, CEITEC-MU, Masaryk University, Kamenice 5, 625 00 Brno, Czech Republic. [3]Laboratory of Functional Genomics and Proteomics, National Centre for Biomolecular Research, Faculty of Science, Masaryk University, Kamenice 5, 625 00 Brno, Czech Republic.

References
1. Maheshwari P. An introduction to embryology of angiosperms. New York: McGraw-Hill; 1950.
2. Yadegari R, Drews GN. Female gametophyte development. Plant Cell. 2004; 16:S133–41.
3. Okuda S, Tsutsui H, Shiina K, Sprunck S, Takeuchi H, Yui R, et al. Defensin-like polypeptide LUREs are pollen tube attractants secreted from synergid cells. Nature. 2009;458:357–61.

Hafidh *et al. Genome Biology* (2016) 17:81

Page 28 of 29

4. Takeuchi H, Higashiyama T. Attraction of tip-growing pollen tubes by the female gametophyte. Curr Opin Plant Biol. 2011;14:614–21.

5. Marton ML, Fastner A, Uebler S, Dresselhaus T. Overcoming hybridization barriers by the secretion of the maize pollen tube attractant ZmEA1 from Arabidopsis ovules. Curr Biol. 2012;22:1194–8.

6. Dresselhaus T, Franklin-Tong N. Male-female crosstalk during pollen germination, tube growth and guidance, and double fertilization. Mol Plant. 2013;6:1018–36.

7. Hamamura Y, Saito C, Awai C, Kurihara D, Miyawaki A, Nakagawa T, et al. Live-cell imaging reveals the dynamics of two sperm cells during double fertilization in Arabidopsis thaliana. Curr Biol. 2011;21:497–502.

8. Chae K, Lord EM. Pollen tube growth and guidance: roles of small, secreted proteins. Ann Bot. 2011;108:627–36.

9. Hong-Ju L, Shan-Shan Z, Meng-Xia Z, Tong W, Liang L, Yong X, et al. Arabidopsis CBP1 is a novel regulator of transcription initiation in central cell-mediated pollen tube guidance. Plant Cell. 2015. doi:10.1105/tpc.15.00370.

10. Tang WH, Ezcurra I, Muschietti J, McCormick S. A cysteine-rich extracellular protein, LAT52, interacts with the extracellular domain of the pollen receptor kinase LePRK2. Plant Cell. 2002;14:2277–87.

11. Zhang D, Wengier D, Shuai B, Gui C-P, Muschietti J, McCormick S, et al. The pollen receptor kinase LePRK2 mediates growth-promoting signals and positively regulates pollen germination and tube growth. Plant Physiol. 2008;148:1368–79.

12. Leydon AR, Beale KM, Woroniecka K, Castner E, Chen J, Horgan C, et al. Three MYB transcription factors control pollen tube differentiation required for sperm release. Curr Biol. 2013;23:1209–14.

13. Beale KM, Leydon AR, Johnson MA. Gamete fusion is required to block multiple pollen tubes from entering an Arabidopsis ovule. Curr Biol. 2012;22:1090–4.

14. Hafidh S, Potesil D, Fila J, Fecikova J, Capkova V, Zdrahal Z, et al. In search of ligands and receptors of the pollen tube: the missing link in pollen tube perception. Biochem Soc Trans. 2014;42:388–94.

15. Qin Y, Leydon AR, Manziello A, Pandey R, Mount D, Denic S, et al. Penetration of the stigma and style elicits a novel transcriptome in pollen tubes, pointing to genes critical for growth in a pistil. PLoS Genet. 2009;5: e1000621.

16. Kanaoka MM, Kawano N, Matsubara Y, Susaki D, Okuda S, Sasaki N, et al. Identification and characterization of TcCRP1, a pollen tube attractant from Torenia concolor. Ann Bot. 2011;108:739–47.

17. Silva JC, Gorenstein MV, Li GZ, Vissers JP, Geromanos SJ. Absolute quantification of proteins by LCMSE: a virtue of parallel MS acquisition. Mol Cell Proteomics. 2006;5:144–56.

18. Ahrné E, Molzahn L, Glatter T, Schmidt A. Critical assessment of proteome-wide label-free absolute abundance estimation strategies. Proteomics. 2013;13:2567–78.

19. Hafidh S, Breznenova K, Ruzicka P, Fecikova J, Capkova V, Honys D. Comprehensive analysis of tobacco pollen transcriptome unveils common pathways in polar cell expansion and underlying heterochronic shift during spermatogenesis. BMC Plant Biol. 2012;12.

20. Hafidh S, Breznenova K, Honys D. De novo post-pollen mitosis II tobacco pollen tube transcriptome. Plant Signaling Behav. 2012;7:918–21.

21. Qin Y, Yang Z. Rapid tip growth: insights from pollen tubes. Semin Cell Dev Biol. 2011;22:816–24.

22. Žárský V, Cvrcková F, Potocký M, Hála M. Exocytosis and cell polarity in plants–exocyst and recycling domains. New Phytol. 2009;183:255–72.

23. Liang Y, Tan ZM, Zhu L, Niu QK, Zhou JJ, Li M, et al. MYB97, MYB101 and MYB120 function as male factors that control pollen tube-synergid interaction in Arabidopsis thaliana fertilization. PLoS Genet. 2013;9(11):e1003933.

24. Nielsen H, Engelbrecht J, Brunak S. vonHeijne G. Identification of prokaryotic and eukaryotic signal peptides and prediction of their cleavage sites. Protein Eng. 1997;10:1–6.

25. Petersen TN, Brunak S, von Heijne G, Nielsen H. SignalP 4.0: discriminating signal peptides from transmembrane regions. Nat Methods. 2011;8:785–6.

26. Bendtsen JD, Jensen LJ, Blom N, von Heijne G, Brunak S. Feature-based prediction of non-classical and leaderless protein secretion. Protein Eng Design Selection. 2004;17:349–56.

27. Sigrist CJA, Cerutti L, de Castro E, Langendijk-Genevaux PS, Bulliard V, Bairoch A, et al. PROSITE, a protein domain database for functional characterization and annotation. Nucleic Acids Res. 2010;38:D161–6.

28. Ding Y, Wang J, Stierhof YD, Robinson DG, Jiang L. Unconventional protein secretion. Trends Plant Sci. 2012;17:606–15.

29. Blom N, Sicheritz-Ponten T, Gupta R, Gammeltoft S, Brunak S. Prediction of post-translational glycosylation and phosphorylation of proteins from the amino acid sequence. Proteomics. 2004;4:1633–49.

30. Hamby SE, Hirst JD. Prediction of glycosylation sites using random forests. BMC Bioinformatics. 2008;9:500.

31. Liu J, Zhong S, Guo X, Hao L, Wei X, Huang Q, et al. Membrane-bound RLCKs LIP1 and LIP2 are essential male factors controlling male-female attraction in Arabidopsis. Curr Biol. 2013;23:993–8.

32. Goldberg T, Hamp T, Rost B. LocTree2 predicts localization for all domains of life. Bioinformatics. 2012;28:l458–65.

33. Emanuelsson O, Brunak S, von Heijne G, Nielsen H. Locating proteins in the cell using TargetP, SignalP and related tools. Nat Protocols. 2007;2:953–71.

34. Kyo M, Miyatake H, Mamezuka K, Amagata K. Cloning of cDNA encoding NtEPc, a marker protein for the embryogenic dedifferentiation of immature tobacco pollen grains cultured in vitro. Plant Cell Physiol. 2000;41:129–37.

35. Higashiyama T. Peptide signaling in pollen-pistil interactions. Plant Cell Physiol. 2010;51:177–89.

36. Luu DT, Qin X, Morse D, Cappadocia M. S-RNase uptake by compatible pollen tubes in gametophytic self-incompatibility. Nature. 2000;407:649–6510.

37. McClure B, Cruz-García F, Romero C. Compatibility and incompatibility in S-RNase-based systems. Ann Bot. 2011;179:1–12.

38. Cheung AY, Wu HM, Di Stilio V, Glaven R, Chen C, Wong E, et al. Pollen-pistil interactions in Nicotiana tabacum. Ann Bot. 2000;85:29–37.

39. de Graaf BHJ, Knuiman BA, Derksen J, Mariani C. Characterization and localization of the transmitting tissue-specific PELPIII proteins of Nicotiana tabacum. J Exp Bot. 2003;54:55–63.

40. Bosch M, Knudsen JS, Derksen J, Mariani C. Class III pistil-specific extensin-like proteins from tobacco have characteristics of arabinogalactan proteins. Plant Physiol. 2001;125:2180–8.

41. Eberle CA, Anderson NO, Clasen BM, Hegeman AD, Smith AG. PELPIII: the class III pistil-specific extensin-like Nicotiana tabacum proteins are essential for interspecific incompatibility. Plant J. 2013;74:805–14.

42. Stratford S, Barnes W, Hohorst DL, Sagert JG, Cotter R, Golubiewski A, et al. A leucine-rich repeat region is conserved in pollen extensin-like (Pex) proteins in monocots and dicots. Plant Mol Biol. 2001;46:43–56.

43. Amy R, Jesús M, Maria S-C, Patricia B. Extensin-like glycoproteins in the maize pollen tube wali. Plant Cell. 1995a;7:2211–25.

44. Chae K, Kieslich CA, Morikis D, Kim S-C, Lord EM. A gain-of-function mutation of Arabidopsis lipid transfer protein 5 disturbs pollen tube tip growth and fertilization. Plant Cell. 2009;21:3902–14.

45. Nelson BK, Cai X, Nebenfuehr A. A multicolored set of in vivo organelle markers for co-localization studies in Arabidopsis and other plants. Plant J. 2007;51:1126–36.

46. Cheng F-y, Zamski E, Guo W-W, Pharr DM, Williamson JD. Salicylic acid stimulates secretion of the normally symplastic enzyme mannitol dehydrogenase: a possible defense against mannitol-secreting fungal pathogens. Planta. 2009;230:1093–103.

47. Cheng F-y, Williamson JD. Is there leaderless protein secretion in plants? Plant Signaling Behav. 2010;5:129–31.

48. Alexandersson E, Ali A, Resjö S, Andreasson E. Plant secretome proteomics. Front Plant Sci. 2013;4:9.

49. Amson R, Pece S, Lespagnol A, Vyas R, Mazzarol G, Tosoni D, et al. Reciprocal repression between P53 and TCTP. Nat Med. 2012;18:91–9.

50. Amzallag N, Passer BJ, Allanic D, Segura E, Thery C, Goud B, et al. TSAP6 facilitates the secretion of translationally controlled tumor protein/histamine-releasing factor via a nonclassical pathway. J Biol Chem. 2004;279:46104–12.

51. Prado N, de Dios AJ, Casado-Vela J, Mas S, Villalba M, Rodriguez R, et al. Nanovesicles are secreted during pollen germination and pollen tube growth: a possible role in fertilization. Mol Plant. 2014;7:573–7.

52. Gendre D, McFarlane HE, Johnson E, Mouille G, Sjodin A, Oh J, et al. Trans-Golgi network localized ECHIDNA/Ypt interacting protein complex is required for the secretion of cell wall polysaccharides in Arabidopsis. Plant Cell. 2013;25:2633–46.

53. Zimmermann P, Hirsch-Hoffmann M, Hennig L, Gruissem W. Genevestigator: an Arabidopsis thaliana microarray database and analysis toolbox. Plant Biol. 2004;2004:186–6.

54. Gendre D, Oh J, Boutte Y, Best JG, Samuels L, Nilsson R, et al. Conserved Arabidopsis ECHIDNA protein mediates trans-Golgi-network trafficking and cell elongation. Proc Natl Acad Sci U S A. 2011;108:8048–53.

55. Fan X, Yang C, Klisch D, Ferguson A, Bhaellero RP, Niu X, et al. ECHIDNA protein impacts on male fertility in Arabidopsis by mediating trans-Golgi network secretory trafficking during anther and pollen development. Plant Physiol. 2014;164:1338–49.

56. Berkowitz O, Jost R, Pollmann S, Masle J. Characterization of TCTP, the translationally controlled tumor protein, from Arabidopsis thaliana. Plant Cell. 2008;20:3430–47.

Hafidh *et al. Genome Biology* (2016) 17:81

Page 29 of 29

57. Brioudes F, Thierry A-M, Chambrier P, Mollereau B, Bendahmane M. Translationally controlled tumor protein is a conserved mitotic growth integrator in animals and plants. Proc Natl Acad Sci U S A. 2010;107:16384–9.

58. Higashiyama T. The mechanism and key molecules involved in pollen tube guidance. Annu Rev Plant Biol; 2015;66:393-413.

59. Márton ML, Cordts S, Broadhvest J, Dresselhaus T. Micropylar pollen tube guidance by egg apparatus 1 of maize. Science. 2005;307:573–6.

60. Li S, Ge FR, Xu M, Zhao XY, Huang GQ, Zhou LZ, et al. Arabidopsis COBRA-LIKE 10, a GPI-anchored protein, mediates directional growth of pollen tubes. Plant J. 2013;74:486–97.

61. Higashiyama T, Kuroiwa H, Kawano S, Kuroiwa T. Guidance in vitro of the pollen tube to the naked embryo sac of Torenia fournieri. Plant Cell. 1998;10:2019–31.

62. Palanivelu R, Preuss D. Distinct short-range ovule signals attract or repel Arabidopsis thaliana pollen tubes in vitro. BMC Plant Biol. 2006;6:7.

63. Kasahara RD, Maruyama D, Hamamura Y, Sakakibara T, Twell D, Higashiyama T. Fertilization recovery after defective sperm cell release in Arabidopsis. Curr Biol. 2012;22:1084–9.

64. Blanco MA, LeRoy G, Khan Z, Aleckovic M, Zee BM, Garcia BA, et al. Global secretome analysis identifies novel mediators of bone metastasis. Cell Res. 2012;22:1339–55.

65. Li H-J, Xue Y, Jia D-J, Wang T, Shi D-Q, Liu J, et al. POD1 regulates pollen tube guidance in response to micropylar female signaling and acts in early embryo patterning in Arabidopsis. Plant Cell. 2011;23:3288–302.

66. Lu Y, Chanroj S, Zulkifli L, Johnson MA, Uozumi N, Cheung A, et al. Pollen tubes lacking a pair of K+ transporters fail to target ovules in Arabidopsis. Plant Cell. 2011;23:81–93.

67. Drakakaki G, Dandekar A. Protein secretion: how many secretory routes does a plant cell have? Plant Sci. 2013;203–204:74–8.

68. Thery C. Exosomes: secreted vesicles and intercellular communications. F1000 Biol Rep. 2011;3:15–5.

69. Raposo G, Stoorvogel W. Extracellular vesicles: exosomes, microvesicles, and friends. J Cell Biol. 2013;200:373–83.

70. Sheldon H, Heikamp E, Turley H, Dragovic R, Thomas P, Oon CE, et al. New mechanism for Notch signaling to endothelium at a distance by Delta-like 4 incorporation into exosomes. Blood. 2010;116:2385–94.

71. Miki B, McHugh S. Selectable marker genes in transgenic plants: applications, alternatives and biosafety. J Biotechnol. 2004;107:193–232.

72. Zhang H, Zhang L, Gao B, Fan H, Jin J, Botella MA, et al. Golgi apparatus-localized synaptotagmin 2 is required for unconventional secretion in *Arabidopsis*. PLoS One. 2011;6(11):e26477. doi:10.1371/journal.pone.0026477.

73. Nickel W. Rabouille. Mechanisms of regulated unconventional protein secretion. Nat Rev Mol Cell Biol. 2019;10:148–55.

74. Wang J, Ding Y, Wang J, Hillmer S, Miao Y, Wan SL, et al. EXPO, an exocyst-positive organelle distinct from multivesicular endosomes and autophagosomes, mediates cytosol to cell wall exocytosis in *Arabidopsis* and tobacco cells. Plant Cell. 2010;22(12):4009–30.

75. Simons K, Toomre D. Lipid rafts and signal transduction. Nat Rev Mol Cell Biol. 2000;1:31–9.

76. Levental I, Lingwood D, Grzybek M, Coskun U, Simons K. Palmitoylation regulates raft affinity for the majority of integral raft proteins. Proc Natl Acad Sci U S A. 2010;107:22050–4.

77. Wiśniewski JR, Zougman A, Nagaraj N, Mann M. Universal sample preparation method for proteome analysis. Nat Methods. 2009;6:359–62.

78. Wiśniewski JR, Ostasiewicz P, Mann M. High recovery FASP applied to the proteomic analysis of microdissected formalin fixed paraffin embedded cancer tissues retrieves known colon cancer markers. J Proteome Res. 2011;10:3040–9.

79. Vitale A, Denecke J. The endoplasmic reticulum–gateway of the secretory pathway. Plant Cell. 1999;11:615–28.

80. Jouhet J, Marechal E, Block MA. Glycerolipid transfer for the building of membranes in plant cells. Prog Lipid Res. 2007;46:37–55.

81. Rojo E, Denecke J. What is moving in the secretory pathway of plants? Plant Physiol. 2008;147:1493–503.

8. Seznam literatury

Arabidopsis Genome Initiative. (2000). Analysis of the genome sequence of the flowering plant *Arabidopsis thaliana*. Nature **408,** 796–815.

Aryal, U.K., Ross, A.R.S. (2010). Enrichment and analysis of phosphopeptides under different experimental conditions using titanium dioxide affinity chromatography and mass spectrometry. Rapid Commun Mass Sp **24,** 219–231.

Attwood, P.V., Piggott, M.J., Zu, X.L., Besant, P.G. (2007). Focus on phosphohistidine. Amino Acids **32,** 145–156.

Baláž, V., Balážová, A., Fíla, J., Kolář, F., Mikát, M. (2012). Láska sex a něžnosti v říši živočichů a rostlin. Česká zemědělská univerzita v Praze, Praha. ISBN 978-80-213-2288-2

Balážová, A., Kolář, F., Fíla, J., Mikát, M., Baláž, V. (2016). Rozmnožování z pohledu evoluce. Academia, Praha. *V tisku.*

Bashan, A., Zarivach, R., Schluenzen, F., Agmon, I., Harms, J., Auerbach, T., Baram, D., Berisio, R., Bartels, H., Hansen, H.A.S., Fucini, P., Wilson, D., Peretz, M., Kessler, M., Yonath, A. (2003). Ribosomal crystallography: Peptide bond formation and its inhibition. Biopolymers **70,** 19–41.

Bauer, P.M., Fulton, D., Boo, Y.C., Sorescu, G.P., Kemp, B.E., Jo, H., Sessa, W.C. (2003). Compensatory phosphorylation and protein–protein interactions revealed by loss of function and gain of function mutants of multiple-serine phosphorylation sites in endothelial nitric-oxide synthase. J Biol Chem **278,** 14841–14849.

Beausoleil, S.A., Jedrychowski, M., Schwartz, D., Elias, J.E., Villen, J., Li, J.X., Cohn, M.A., Cantley, L.C., Gygi, S.P. (2004). Large-scale characterization of HeLa cell nuclear phosphoproteins. P Natl Acad Sci USA **101,** 12130–12135.

Beckers, G.J., Hoehenwarter, W., Röhrig, H., Conrath, U., Weckwerth, W. (2014). Tandem metal-oxide affinity chromatography for enhanced depth of phosphoproteome analysis. Methods Mol Biol **1072,** 621–632.

Benschop, J.J., Mohammed, S., O'Flaherty, M., Heck, A.J.R., Slijper, M., Menke, F.L.H. (2007). Quantitative phosphoproteomics of early elicitor signaling in Arabidopsis. Mol Cell Proteomics **6,** 1198–1214.

Besant, P.G., Attwood, P.V. (2009). Detection and analysis of protein histidine phosphorylation. Mol Cell Biochem **329,** 93–106.

Bodenmiller, B., Mueller, L.N., Mueller, M., Domon, B., Aebersold, R. (2007). Reproducible isolation of distinct, overlapping segments of the phosphoproteome. Nat Methods **4,** 231–237.

Boisson-Dernier, A., Roy, S., Kritsas, K., Grobei, M.A., Jaciubek, M., Schroeder, J.I., Grossniklaus, U. (2009). Disruption of the pollen-expressed FERONIA homologs ANXUR1 and ANXUR2 triggers pollen tube discharge. Development **136,** 3279–3288.

Bonhomme, L., Valot, B., Tardieu, F., Zivy, M. (2012). Phosphoproteome dynamics upon changes in plant water status reveal early events associated with rapid growth adjustment in maize leaves. Mol Cell Proteomics **11,** 957–972.

Borg, M., Twell, D. (2010). Life after meiosis: patterning the angiosperm male gametophyte. Biochem Soc T **38,** 577–582.

Brewbaker, J.L. (1967). Distribution and phylogenetic significance of binucleate and trinucleate pollen grains in angiosperms. Am J Bot **54,** 1069–1083.

Carson, J.H., Barbarese, E. (2005). Systems analysis of RNA trafficking in neural cells. Biol Cell **97,** 51–62.

Collins, M.O., Yu, L., Coba, M.P., Husi, H., Campuzano, L., Blackstock, W.P., Choudhary, J.S., Grant, S.G.N. (2005). Proteomic analysis of *in vivo* phosphorylated synaptic proteins. J Biol Chem **280,** 5972–5982.

Čapková, V., Hrabětová, E., Tupý, J. (1988). Protein synthesis in pollen tubes: preferential formation of new species independent of transcription. Sex Plant Reprod **1,** 150–155.

Darewicz, M., Dziuba, J., Minkiewicz, P. (2005). Some properties of beta-casein modified via phosphatase. Acta Aliment **34,** 403–415.

Dissanayake, K., Castillo, C., Takasaki, T., Nakanishi, T., Norioka, N., Norioka, S. (2004). Molecular cloning, functional expression and characterization of two serine/threonine-specific protein kinases from *Nicotiana tabacum* pollen. Sex Plant Reprod **17,** 165–175.

Drews, G.N., Yadegari, R. (2002). Development and function of the angiosperm female gametophyte. Annu Rev Genet **36,** 99–124.

Dunn, J.D., Reid, G.E., Bruening, M.L. (2010). Techniques for phosphopeptide enrichment prior to analysis by mass spectrometry. Mass Spectrom Rev **29,** 29–54.

Edmead, C., Kanthou, C., Benzakour, O. (1999). Thrombin activates transcription factors Sp1, NF-kappa B, and CREB: Importance of the use of phosphatase inhibitors during nuclear protein extraction for the assessment of transcription factor DNA-binding activities. Anal Biochem **275,** 180–186.

Enaleeva, N. (1997). A tobacco mutant with a reduced cell number in embryo sacs; 1. Expression of the mutation in plants of different generations at the mature gametophyte stage. Sex Plant Reprod **10,** 300–304.

Feng, S., Ye, M.L., Zhou, H.J., Jiang, X.G., Jiang, X.N., Zou, H.F., Gong, B.L. (2007). Immobilized zirconium ion affinity chromatography for specific enrichment of phosphopeptides in phosphoproteome analysis. Mol Cell Proteomics **6,** 1656–1665.

Fíla, J., Čapková, V., Honys, D. (2014). Phosphoproteomic studies in Arabidopsis and tobacco male gametophytes. Biochem Soc T **42,** 383–387.

Fíla, J., Čapková, V., Feciková, J., Honys, D. (2011). Impact of homogenization and protein extraction conditions on the obtained tobacco pollen proteomic patterns. Biol Plantarum **55,** 499–506.

Fíla, J., Honys, D. (2012). Enrichment techniques employed in phosphoproteomics. Amino Acids **43,** 1025–1047.

Fíla, J., Matros, A., Radau, S., Zahedi, R.P., Čapková, V., Mock, H.-P., Honys, D. (2012). Revealing phosphoproteins playing role in tobacco pollen activated *in vitro*. Proteomics **12,** 3229–3250.

Fíla, J., Radau, S., Matros, A., Hartmann, A., Scholz, U., Feciková, J., Mock, H.-P., Čapková, V., Zahedi, R.P., Honys, D. (2016). Phosphoproteomics profiling of tobacco mature pollen and pollen activated *in vitro*. Mol Cell Proteomics **15,** 1338–1350.

Garnak, M., Reeves, H.C. (1979). Phosphorylation of isocitrate dehydrogenase of *Escherichia coli*. Science **203,** 1111–1112.

Groban, E.S., Narayanan, A., Jacobson, M.P. (2006). Conformational changes in protein loops and helices induced by post-translational phosphorylation. PLOS Comput Biol **2,** 238–250.

Grobei, M.A., Qeli, E., Brunner, E., Rehrauer, H., Zhang, R., Roschitzki, B., Basler, K., Ahrens, C.H., Grossniklaus, U. (2009). Deterministic protein inference for shotgun proteomics data provides new insights into Arabidopsis pollen development and function. Genome Res **19,** 1786–1800.

Hafidh, S., Breznenová, K., Honys, D. (2012a). *De novo* post-pollen mitosis II tobacco pollen tube transcriptome. Plant Signal Behav **7,** 918–921.

Hafidh, S., Breznenová, K., Růžička, P., Feciková, J., Čapková, V., Honys, D. (2012b). Comprehensive analysis of tobacco pollen transcriptome unveils common pathways in polar cell expansion and underlying heterochronic shift during spermatogenesis. BMC Plant Biol **12,** 24.

Hafidh, S., Fíla, J., Honys, D. (2016a). Male gametophyte development and function in angiosperms: a general concept. Plant Reprod. *doi: 10.1007/s00497-015-0272-4*

Hafidh, S., Potěšil, D., Fíla, J., Čapková, V., Zdráhal, Z., Honys, D. (2016b). Direct quantification of the pollen tube secretome identifies novel pollen tube guidance proteins following its interaction with the pistil. Genome Biol **17,** 81.

Hafidh, S., Potěšil, D., Fíla, J., Feciková, J., Čapková, V., Zdráhal, Z., Honys, D. (2014). In search of ligands and receptors of the pollen tube: the missing link in pollen tube perception. Biochem Soc T **42,** 388–394.

Haig, D. (2010). What do we know about Charophyte (Streptophyta) life cycles? J Phycol **46,** 860–867.

Hoehenwarter, W., Thomas, M., Nukarinen, E., Egelhofer, V., Röhrig, H., Weckwerth, W., Conrath, U., Beckers, G.J.M. (2013). Identification of novel *in vivo* MAP kinase substrates in *Arabidopsis thaliana* through use of tandem metal oxide affinity chromatography. Mol Cell Proteomics **12,** 369–380.

Holdaway-Clarke, T.L., Feijó, J.A., Hackett, G.R., Kunkel, J.G., Hepler, P.K. (1997). Pollen tube growth and the intracellular cytosolic calcium gradient oscillate in phase while extracellular calcium influx is delayed. Plant Cell **9,** 1999–2010.

Holdaway-Clarke, T.L., Hepler, P.K. (2003). Control of pollen tube growth: role of ion gradients and fluxes. New Phytol **159,** 539–563.

Holmes-Davis, R., Tanaka, C.K., Vensel, W.H., Hurkman, W.J., McCormick, S. (2005). Proteome mapping of mature pollen of *Arabidopsis thaliana*. Proteomics **5,** 4864–4884.

Honys, D., Combe, J.P., Twell, D., Čapková, V. (2000). The translationally repressed pollen-specific ntp303 mRNA is stored in non-polysomal mRNPs during pollen maturation. Sex Plant Reprod **13,** 135–144.

Honys, D., Reňák, D., Feciková, J., Jedelský, P.L., Nebesářová, J., Dobrev, P., Čapková, V. (2009). Cytoskeleton-associated large RNP complexes in tobacco male gametophyte

(EPPs) are associated with ribosomes and are involved in protein synthesis, processing, and localization. J Proteome Res **8,** 2015–2031.

Huang, B.Q., Russell, S.D. (1992). Female germ unit – organization, isolation, and function. Int Rev Cytol **140,** 233–293.

Huang, X.Y., Niu, J., Sun, M.X., Zhu, J., Gao, J.F., Yang, J., Zhou, Q., Yang, Z.N. (2013). CYCLIN-DEPENDENT KINASE G1 is associated with the spliceosome to regulate CALLOSE SYNTHASE 5 splicing and pollen wall formation in Arabidopsis. Plant Cell **25,** 637–648.

Huck, N., Moore, J.M., Federer, M., Grossniklaus, U. (2003). The Arabidopsis mutant feronia disrupts the female gametophytic control of pollen tube reception. Development **130,** 2149–2159.

Hultquist, D.E. (1968). The preparation and characterization of phosphorylated derivatives of histidine. Biochim Biophys Acta **153,** 329–340.

Chang, Y., Graham, S.W. (2011). Inferring the higher-order phylogeny of mosses (Bryophyta) and relatives using a large, multigene plastid data set. Am J Bot **98,** 839–849.

Chen, Y., Liu, P., Hoehenwarter, W., Lin, J. (2012). Proteomic and phosphoproteomic analysis of *Picea wilsonii* pollen development under nutrient limitation. J Proteome Res **11,** 4180–4190.

Chou, M.F., Schwartz, D. (2011). Biological sequence motif discovery using motif-x. Curr Protoc Bioinformatics **13,** 15–24.

Christensen, C.A., Subramanian, S., Drews, G.N. (1998). Identification of gametophytic mutations affecting female gametophyte development in Arabidopsis. Dev Biol **202,** 136–151.

Ischebeck, T., Valledor, L., Lyon, D., Gingl, S., Nagler, M., Meijon, M., Egelhofer, V., Weckwerth, W. (2014). Comprehensive cell-specific protein analysis in early and late pollen development from diploid microsporocytes to pollen tube growth. Mol Cell Proteomics **13,** 295–310.

Ito, J., Taylor, N.L., Castleden, I., Weckwerth, W., Millar, A.H., Heazlewood, J.L. (2009). A survey of the *Arabidopsis thaliana* mitochondrial phosphoproteome. Proteomics **9,** 4229–4240.

Janek, K., Wenschuh, H., Bienert, M., Krause, E. (2001). Phosphopeptide analysis by positive and negative ion matrix-assisted laser desorption/ionization mass spectrometry. Rapid Commun Mass Sp **15,** 1593–1599.

Jensen, S.S., Larsen, M.R. (2007). Evaluation of the impact of some experimental procedures on different phosphopeptide enrichment techniques. Rapid Commun Mass Sp **21,** 3635–3645.

Kim, J., Shen, Y., Han, Y.J., Park, J.E., Kirchenbauer, D., Soh, M.S., Nagy, F., Schafer, E., Song, P.S. (2004). Phytochrome phosphorylation modulates light signaling by influencing the protein–protein interaction. Plant Cell **16,** 2629–2640.

Kokubu, M., Ishihama, Y., Sato, T., Nagasu, T., Oda, Y. (2005). Specificity of immobilized metal affinity-based IMAC/C18 tip enrichment of phosphopeptides for protein phosphorylation analysis. Anal Chem **77,** 5144–5154.

Krebs, E.G., Beavo, J.A. (1979). Phosphorylation–dephosphorylation of enzymes. Annu Rev Biochem **48,** 923–959.

Kweon, H.K., Håkansson, K. (2006). Selective zirconium dioxide-based enrichment of phosphorylated peptides for mass spectrometric analysis. Anal Chem **78,** 1743–1749.

Lapko, V.N., Wells, T.A., Song, P.S. (1996). Protein kinase A-catalyzed phosphorylation and its effect on conformation in phytochrome A. Biochemistry **35,** 6585–6594.

Lee, T.Y., Bretana, N.A., Lu, C.T. (2011b). PlantPhos: using maximal dependence decomposition to identify plant phosphorylation sites with substrate site specificity. BMC Bioinformatics **12,** 13.

Lee, T.Y., Lin, Z.Q., Hsieh, S.J., Bretana, N.A., Lu, C.T. (2011a). Exploiting maximal dependence decomposition to identify conserved motifs from a group of aligned signal sequences. Bioinformatics **27,** 1780–1787.

Lenman, M., Sorensson, C., Andreasson, E. (2008). Enrichment of phosphoproteins and phosphopeptide derivatization identify universal stress proteins in elicitor-treated Arabidopsis. Mol Plant Microbe In **21,** 1275–1284.

Lindner, H., Muller, L.M., Boisson-Dernier, A., Grossniklaus, U. (2012). CrRLK1L receptor-like kinases: not just another brick in the wall. Curr Opin Plant Biol **15,** 659–669.

Liu, Y., Cox, C.J., Wang, W., Goffinet, B. (2014). Mitochondrial phylogenomics of early land plants: Mitigating the effects of saturation, compositional heterogeneity, and codon-usage bias. Syst Biol **63,** 862–878.

Luo, X., Chen, Z., Gao, J., Gong, Z. (2014). Abscisic acid inhibits root growth in Arabidopsis through ethylene biosynthesis. Plant J **79,** 44–55.

Machida, M., Kosako, H., Shirakabe, K., Kobayashi, M., Ushiyama, M., Inagawa, J., Hirano, J., Nakano, T., Bando, Y., Nishida, E., Hattori, S. (2007). Purification of phosphoproteins by immobilized metal affinity chromatography and its application to phosphoproteome analysis. FEBS J **274,** 1576–1587.

Mascarenhas, J.P. (1993). Molecular mechanisms of pollen tube growth and differentiation. Plant Cell **5,** 1303–1314.

Mayank, P., Grossman, J., Wuest, S., Boisson-Dernier, A., Roschitzki, B., Nanni, P., Nuehse, T., Grossniklaus, U. (2012). Characterization of the phosphoproteome of mature Arabidopsis pollen. Plant J **72,** 89–101.

McCormick, S. (1993). Male gametophyte development. Plant Cell **5,** 1265–1275.

McCoy, C.E., Campbell, D.G., Deak, M., Bloomberg, G.B., Arthur, J.S.C. (2005). MSK1 activity is controlled by multiple phosphorylation sites. Biochem J **387,** 507–517.

McNulty, D.E., Annan, R.S. (2008). Hydrophilic interaction chromatography reduces the complexity of the phosphoproteome and improves global phosphopeptide isolation and detection. Mol Cell Proteomics **7,** 971–980.

Mithoe, S.C., Menke, F.L.H. (2011). Phosphoproteomics perspective on plant signal transduction and tyrosine phosphorylation. Phytochemistry **72,** 997–1006.

Molina, H., Horn, D.M., Tang, N., Mathivanan, S., Pandey, A. (2007). Global proteomic profiling of phosphopeptides using electron transfer dissociation tandem mass spectrometry. P Natl Acad Sci USA **104,** 2199–2204.

Mulcahy, G.B., Mulcahy, D.L. (1988). The effect of supplemented media on the growth *in vitro* of binucleate and trinucleate pollen. Plant Sci **55,** 213–216.

Myers, C., Romanowsky, S.M., Barron, Y.D., Garg, S., Azuse, C.L., Curran, A., Davis, R.M., Hatton, J., Harmon, A.C., Harper, J.F. (2009). Calcium-dependent protein kinases regulate polarized tip growth in pollen tubes. Plant J **59,** 528–539.

Nakagami, H., Sugiyama, N., Mochida, K., Daudi, A., Yoshida, Y., Toyoda, T., Tomita, M., Ishihama, Y., Shirasu, K. (2010). Large-scale comparative phosphoproteomics identifies conserved phosphorylation sites in plants. Plant Physiol **153,** 1161–1174.

Negroni, L., Claverol, S., Rosenbaum, J., Chevet, E., Bonneu, M., Schmitter, J.-M. (2012). Comparison of IMAC and MOAC for phosphopeptide enrichment by column chromatography. J Chromatogr B **891,** 109–112.

Neville, D.C.A., Rozanas, C.R., Price, E.M., Gruis, D.B., Verkman, A.S., Townsend, R.R. (1997). Evidence for phosphorylation of serine 753 in CFTR using a novel metal-ion affinity resin and matrix-assisted laser desorption mass spectrometry. Protein Sci **6,** 2436–2445.

Nito, K., Wong, C.C.L., Yates, J.R., Chory, J. (2013). Tyrosine phosphorylation regulates the activity of phytochrome photoreceptors. Cell Rep **3,** 1970–1979.

Noir, S., Bräutigam, A., Colby, T., Schmidt, J., Panstruga, R. (2005). A reference map of the *Arabidopsis thaliana* mature pollen proteome. Biochem Bioph Res Co **337,** 1257–1266.

Nühse, T.S., Stensballe, A., Jensen, O.N., Peck, S.C. (2004). Phosphoproteomics of the Arabidopsis plasma membrane and a new phosphorylation site database. Plant Cell **16,** 2394–2405.

Obaya, A.J., Sedivy, J.M. (2002). Regulation of cyclin-Cdk activity in mammalian cells. Cell Mol Life Sci **59,** 126–142.

Oh, M.H., Wang, X.F., Kota, U., Goshe, M.B., Clouse, S.D., Huber, S.C. (2009). Tyrosine phosphorylation of the BRI1 receptor kinase emerges as a component of brassinosteroid signaling in Arabidopsis. P Natl Acad Sci USA **106,** 658–663.

Oh, S.A., Johnson, A., Smertenko, A., Rahman, D., Park, S.K., Hussey, P.J., Twell, D. (2005). A divergent cellular role for the FUSED kinase family in the plant-specific cytokinetic phragmoplast. Curr Biol **15,** 2107–2111.

Olsen, J.V., Blagoev, B., Gnad, F., Macek, B., Kumar, C., Mortensen, P., Mann, M. (2006). Global, *in vivo*, and site-specific phosphorylation dynamics in signaling networks. Cell **127,** 635–648.

Palanivelu, R., Preuss, D. (2000). Pollen tube targeting and axon guidance: parallels in tip growth mechanisms. Trends Cell Biol **10,** 517–524.

Pandey, A., Podtelejnikov, A.V., Blagoev, B., Bustelo, X.R., Mann, M., Lodish, H.F. (2000). Analysis of receptor signaling pathways by mass spectrometry: Identification of Vav-2 as a substrate of the epidermal and platelet-derived growth factor receptors. P Natl Acad Sci USA **97,** 179–184.

Park, S.K., Howden, R., Twell, D. (1998). The *Arabidopsis thaliana* gametophytic mutation gemini pollen1 disrupts microspore polarity, division asymmetry and pollen cell fate. Development **125,** 3789–3799.

Pinkse, M.W.H., Uitto, P.M., Hilhorst, M.J., Ooms, B., Heck, A.J.R. (2004). Selective isolation at the femtomole level of phosphopeptides from proteolytic digests using 2D-nanoLC–ESI–MS/MS and titanium oxide precolumns. Anal Chem **76,** 3935–3943.

Plimmer, R.H.A. (1941). Esters of phosphoric acid: Phosphoryl hydroxyamino-acids. Biochem J **35,** 461–469.

Poovaiah, B.W., Xia, M., Liu, Z.H., Wang, W.Y., Yang, T.B., Sathyanarayanan, P.V., Franceschi, V.R. (1999). Developmental regulation of the gene for chimeric calcium/calmodulin-dependent protein kinase in anthers. Planta **209,** 161–171.

Posewitz, M.C., Tempst, P. (1999). Immobilized gallium(III) affinity chromatography of phosphopeptides. Anal Chem **71,** 2883–2892.

Qiu, Y.L., Li, L.B., Wang, B., Chen, Z.D., Knoop, V., Groth-Malonek, M., Dombrovska, O., Lee, J., Kent, L., Rest, J., Estabrook, G.F., Hendry, T.A., Taylor, D.W., Testa, C.M., Ambros, M., Crandall-Stotler, B., Duff, R.J., Stech, M., Frey, W., Quandt, D., Davis, C.C. (2006). The deepest divergences in land plants inferred from phylogenomic evidence. P Natl Acad Sci USA **103,** 15511–15516.

Qiu, Y.L., Taylor, A.B., McManus, H.A. (2012). Evolution of the life cycle in land plants. J Syst Evol **50,** 171–194.

Raghavan, V. (2003). Some reflections on double fertilization, from its discovery to the present. New Phytol **159,** 565–583.

Reiser, L., Fischer, R.L. (1993). The ovule and the embryo sac. Plant Cell **5,** 1291–1301.

Rocchetti, M.T., Alfarano, M., Varraso, L., Di Paolo, S., Papale, M., Ranieri, E., Grandaliano, G., Gesualdo, L. (2014). Two dimensional gel phosphoproteome of peripheral blood mononuclear cells: comparison between two enrichment methods. Proteome Sci **12,** 46.

Röhrig, H., Colby, T., Schmidt, J., Harzen, A., Facchinelli, F., Bartels, D. (2008). Analysis of desiccation-induced candidate phosphoproteins from *Craterostigma plantagineum* isolated with a modified metal oxide affinity chromatography procedure. Proteomics **8,** 3548–3560.

Röhrig, H., Schmidt, J., Colby, T., Bräutigam, A., Hufnagel, P., Bartels, D. (2006). Desiccation of the resurrection plant *Craterostigma plantagineum* induces dynamic changes in protein phosphorylation. Plant Cell Environ **29,** 1606–1617.

Roos, A., Boron, W.F. (1981). Intracellular pH. Physiol Rev **61,** 296–434.

Rush, J., Moritz, A., Lee, K.A., Guo, A., Goss, V.L., Spek, E.J., Zhang, H., Zha, X.M., Polakiewicz, R.D., Comb, M.J. (2005). Immunoaffinity profiling of tyrosine phosphorylation in cancer cells. Nat Biotechnol **23,** 94–101.

Sabotič, J., Kos, J. (2012). Microbial and fungal protease inhibitors – current and potential applications. Appl Microbiol Biot **93,** 1351–1375.

Sheoran, I.S., Ross, A.R.S., Olson, D.J.H., Sawhney, V.K. (2009). Compatibility of plant protein extraction methods with mass spectrometry for proteome analysis. Plant Sci **176,** 99–104.

Sheoran, I.S., Sproule, K.A., Olson, D.J.H., Ross, A.R.S., Sawhney, V.K. (2006). Proteome profile and functional classification of proteins in *Arabidopsis thaliana* (Landsberg erecta) mature pollen. Sex Plant Reprod **19,** 185–196.

Schulz, C., Little, D.P., Stevenson, D.W., Bauer, D., Moloney, C., Stutzel, T. (2010). An overview of the morphology, anatomy, and life cycle of a new model species: the lycophyte *Selaginella apoda* (L.) SPRING. Int J Plant Sci **171,** 693–712.

Schwartz, D., Gygi, S.P. (2005). An iterative statistical approach to the identification of protein phosphorylation motifs from large-scale data sets. Nat Biotechnol **23,** 1391–1398.

Sierro, N., Battey, J.N.D., Ouadi, S., Bakaher, N., Bovet, L., Willig, A., Goepfert, S., Peitsch, M.C., Ivanov, N.V. (2014). The tobacco genome sequence and its comparison with those of tomato and potato. Nat Commun **5,** 3833.

Smith, M.A., Coupland, G., Dolan, L., Harberd, N., Jones, J., Martin, C., Sablowski, R., Amey, A. (2010). Plant biology. Garland Science, New York a Abingdon. ISBN 978-0815340256

Spirin, A.S., Nemer, M. (1965). Messenger RNA in early sea urchin embryos – cytoplasmic particles. Science **150,** 214–216.

Stewart, W.D.P., Rodgers, G.A. (1977). Cyanophyte-hepatic symbiosis: 2. Nitrogen fixation and interchange of nitrogen and carbon. New Phytol **78,** 459–471.

Sugiyama, N., Nakagami, H., Mochida, K., Daudi, A., Tomita, M., Shirasu, K., Ishihama, Y. (2008). Large-scale phosphorylation mapping reveals the extent of tyrosine phosphorylation in Arabidopsis. Mol Syst Biol **4,** 7.

Šamaj, J., Muller, J., Beck, M., Böhm, N., Menzel, D. (2006). Vesicular trafficking, cytoskeleton and signalling in root hairs and pollen tubes. Trends Plant Sci **11,** 594–600.

Thingholm, T.E., Jensen, O.N., Robinson, P.J., Larsen, M.R. (2008). SIMAC (sequential elution from IMAC), a phosphoproteomics strategy for the rapid separation of monophosphorylated from multiply phosphorylated peptides. Mol Cell Proteomics **7,** 661–671.

Tian, Z., Wang, Y., Zhao, C., Wang, T., Hou, E., Sun, N. (2014). Qualitative and quantitative analysis of phosphoproteomic experimental workflow based on phosphoprotein enrichment strategy and two-dimensional difference gel electrophoresis (2D–DIGE) techniques. Curr Proteomics **11,** 252–263.

Tsai, C.F., Wang, Y.T., Chen, Y.R., Lai, C.Y., Lin, P.Y., Pan, K.T., Chen, J.Y., Khoo, K.H., Chen, Y.J. (2008). Immobilized metal affinity chromatography revisited: pH/acid control toward high selectivity in phosphoproteomics. J Proteome Res **7,** 4058–4069.

Uno, Y.C., Milla, M.A.R., Maher, E., Cushman, J.C. (2009). Identification of proteins that interact with catalytically active calcium-dependent protein kinases from Arabidopsis. Mol Genet Genomics **281,** 375–390.

van Bentem, S.D., Hirt, H. (2009). Protein tyrosine phosphorylation in plants: more abundant than expected? Trends Plant Sci **14,** 71–76.

van Bentem, S.D., Anrather, D., Dohnal, I., Roitinger, E., Csaszar, E., Joore, J., Buijnink, J., Carreri, A., Forzani, C., Lorkovic, Z.J., Barta, A., Lecourieux, D., Verhounig, A., Jonak, C., Hirt, H. (2008). Site-specific phosphorylation profiling of Arabidopsis proteins by mass spectrometry and peptide chip analysis. J Proteome Res **7,** 2458–2470.

Villarreal, J.C., Renzaglia, K.S. (2015). The hornworts: important advancements in early land plant evolution. J Bryol **37,** 157–170.

Vogler, F., Konrad, S.S.A., Sprunck, S. (2015). Knockin' on pollen's door: live cell imaging of early polarization events in germinating Arabidopsis pollen. Front Plant Sci **6,** 246.

Wagner, I., Musso, H. (1983). New naturally occurring amino acids. Angew Chem Int Edit **22,** 816–828.

Wang, X.M., Paulin, F.E.M., Campbell, L.E., Gomez, E., O'Brien, K., Morrice, N., Proud, C.G. (2001). Eukaryotic initiation factor 2B: identification of multiple phosphorylation sites in the epsilon-subunit and their functions *in vivo*. EMBO J **20,** 4349–4359.

Wickett, N.J., Mirarab, S., Nam, N., Warnow, T., Carpenter, E., Matasci, N., Ayyampalayam, S., Barker, M.S., Burleigh, J.G., Gitzendanner, M.A., Ruhfel, B.R., Wafula, E., Der, J.P., Graham, S.W., Mathews, S., Melkonian, M., Soltis, D.E., Soltis, P.S., Miles, N.W., Rothfels, C.J., Pokorny, L., Shaw, A.J., De Gironimo, L., Stevenson, D.W., Surek, B., Villarreal, J.C., Roure, B., Philippe, H., dePamphilis, C.W., Chen, T., Deyholos, M.K., Baucom, R.S., Kutchan, T.M., Augustin, M.M., Wang, J., Zhang, Y., Tian, Z., Yan, Z., Wu, X., Sun, X., Wong, G.K.-S., Leebens-Mack, J. (2014). Phylotranscriptomic analysis of the origin and early diversification of land plants. P Natl Acad Sci USA **111,** E4859–E4868.

Williams, J.H., Taylor, M.L., O'Meara, B.C. (2014). Repeated evolution of tricellular (and bicellular) pollen. Am J Bot **101,** 559–571.

Wilson, C., Voronin, V., Touraev, A., Vicente, O., Heberle-Bors, E. (1997). A developmentally regulated MAP kinase activated by hydration in tobacco pollen. Plant Cell **9,** 2093–2100.

Wolschin, F., Weckwerth, W. (2005). Combining metal oxide affinity chromatography (MOAC) and selective mass spectrometry for robust identification of *in vivo* protein phosphorylation sites. Plant Methods **1,** 9.

Wolschin, F., Wienkoop, S., Weckwerth, W. (2005). Enrichment of phosphorylated proteins and peptides from complex mixtures using metal oxide/hydroxide affinity chromatography (MOAC). Proteomics **5,** 4389–4397.

Ye, J.Y., Zhang, X.M., Young, C., Zhao, X.L., Hao, Q., Cheng, L., Jensen, O.N. (2010). Optimized IMAC–IMAC protocol for phosphopeptide recovery from complex biological samples. J Proteome Res **9,** 3561–3573.

Ye, J.Y., Zhang, Z.B., Long, H.F., Zhang, Z.M., Hong, Y., Zhang, X.M., You, C.J., Liang, W.Q., Ma, H., Lu, P.L. (2015). Proteomic and phosphoproteomic analyses reveal

extensive phosphorylation of regulatory proteins in developing rice anthers. Plant J **84,** 527–544.

Zhang, Y., He, J., McCormick, S. (2009). Two Arabidopsis AGC kinases are critical for the polarized growth of pollen tubes. Plant J **58,** 474–484.

Zhao, L.N., Shen, L.K., Zhang, W.Z., Zhang, W., Wang, Y., Wu, W.H. (2013). Ca^{2+}-dependent protein kinase 11 and 24 modulate the activity of the inward rectifying K^+ channels in Arabidopsis pollen tubes. Plant Cell **25,** 649–661.

Zhou, H.J., Ye, M.L., Dong, J., Han, G.H., Jiang, X.N., Wu, R.N., Zou, H.F. (2008). Specific phosphopeptide enrichment with immobilized titanium ion affinity chromatography adsorbent for phosphoproteome analysis. J Proteome Res **7,** 3957–3967.

Zhou, L.M., Lan, W.Z., Jiang, Y.Q., Fang, W., Luan, S. (2014). A calcium-dependent protein kinase interacts with and activates a calcium channel to regulate pollen tube growth. Mol Plant **7,** 369–376.

Zhu, S.Y., Yu, X.C., Wang, X.J., Zhao, R., Li, Y., Fan, R.C., Shang, Y., Du, S.Y., Wang, X.F., Wu, F.Q., Xu, Y.H., Zhang, X.Y., Zhang, D.P. (2007). Two calcium-dependent protein kinases, CPK4 and CPK11, regulate abscisic acid signal transduction in Arabidopsis. Plant Cell **19,** 3019–3036.

Zi, H.J., Xiang, Y., Li, M., Wang, T., Ren, H.Y. (2007). Reversible protein tyrosine phosphorylation affects pollen germination and pollen tube growth via the actin cytoskeleton. Protoplasma **230,** 183–191.